# BERICHTE

## aus dem Fachbereich Geowissenschaften der Universität Bremen

No. 95

Bleil, U., A. Benthien, W. Böke, H. Buschhoff, B. Donner, B. Dorschel, K. Enneking, T. Frederichs, M. Giese, C. Hensen, C. Hilgenfeldt, S. Hinrichs, O. Holby, C. Hübscher, A. Janke, S. Kasten, A. Meyer, S. Meyer, B. Meyer-Schack, S. Mulitza, U. Rosiak, B. Schlünz, F. Schmieder, A. Schmidt, V. Spieß, G. Uenzelmann-Neben, A. Vink, F. Wenzhöfer, L. Zühlsdorff

# REPORT AND PRELIMINARY RESULTS OF METEOR CRUISE 38/2 RECIFE - LAS PALMAS, 04.03.-14.04.1997

Berichte, Fachbereich Geowissenschaften, Universität Bremen, No. 95, 126 pages, Bremen 1998

ISSN 0931-0800

The "Berichte aus dem Fachbereich Geowissenschaften" are issued at irregular intervals by the Department of Geosciences, University of Bremen.
Publications include Ph.D. theses, scientific studies and contributions from research projects accomplish in the department.

The reports are available from:

Mrs. Gisela Boelen
Sonderforschungsbereich 261
Universität Bremen
Postfach 330 440
D 28334 BREMEN
Telefon: (+49) 421 218-4124
Fax: (49) 421 218-3116

Reference:
Bleil, U. and cruise participants
Report and Preliminary Results of METEOR Cruise M 38/2, Recife - Las Palmas, 04.03. - 14.04.1997.
Berichte, Fachbereich Geowissenschaften, Universität Bremen, No. 95, Bremen, 1998.

ISSN 0931-0800

## Table of Contents

## 1 Participants

| Name | Research Field | Institution |
|---|---|---|
| Bleil, Ulrich, Prof. Dr. (Chief Scientist) | Geophysics | GeoB |
| Benthien, Albert, Dipl.-Geol. | Geology | GeoB |
| Böke, Wolfgang, Technician | Geophysics | GeoB |
| Buschhoff, Hella, Technician | Geology | GeoB |
| Donner, Barbara, Dr. | Geology | GeoB |
| Dorschel, Boris, Student | Geology | GeoB |
| Enneking, Karsten, Technician | Geochemistry | GeoB |
| Frederichs, Thomas, Dr. | Geophysics | GeoB |
| Giese, Martina, Dr. | Geology | GeoB |
| Hensen, Christian, Dr. | Geochemistry | GeoB |
| Hilgenfeldt, Christian, Dipl.-Ing. | Geophysics | GeoB |
| Hinrichs, Sigrid, Technician | Geochemistry | GeoB |
| Holby, Ola, Dr. | Biogeochemistry | MPI |
| Hübscher, Christian, Dr. | Geophysics | GeoB |
| Janke, André, Dipl.-Geophys. | Geophysics | GeoB |
| Kasten, Sabine, Dr. | Geochemistry | GeoB |
| Meyer, Anne, Technician | Paleobiology | GeoB |
| Meyer, Stephan, Technician | Biogeochemistry | MPI |
| Meyer-Schack, Birgit, Technician | Geology | GeoB |
| Mulitza, Stefan, Dr. | Geology | GeoB |
| Rosiak, Uwe, Technician | Geophysics | GeoB |
| Schlünz, Birger, Dipl.-Geol. | Geology | GeoB |
| Schmieder, Frank, Dipl.-Geophys. | Geophysics | GeoB |
| Schmidt, Andrea, Dipl.-Geophys. | Geophysics | GeoB |
| Spieß, Volkhard, Prof. Dr. | Geophysics | GeoB |
| Uenzelmann-Neben, Gabriele, Dr. | Geophysics | AWI |
| Vink, Annemiek, Dipl.-Geol. | Paleobiology | GeoB |
| Wenzhöfer, Frank, Dipl.-Ing. | Biogeochemistry | MPI |
| Zühlsdorff, Lars, Dipl.-Geophys. | Geophysics | GeoB |

AWI Alfred-Wegener-Institut für Polar- und Meeresforschung
Columbus Straße, 27515 Bremerhaven, Germany

GeoB Fachbereich Geowissenschaften
Universität Bremen
Klagenfurter Straße, 28344 Bremen, Germany

MPI Max-Planck-Institut für Marine Mikrobiologie
Celsius Straße 1, 28359 Bremen, Germany

## 2 Research Program

Summary

The "Geo Bremen South Atlantic 1997" Expedition was programmed to continue a long-term study aimed at reconstructing the mass budget and current systems of the South Atlantic during the late Quaternary. It started with METEOR Cruise M6/6 in 1988 and was established as a Special Research Project (Sonderforschungsbereich 261) in July 1989 at the University of Bremen and Alfred-Wegener-Institute, Bremerhaven.

During Leg M38/2 the depositional processes in the western equatorial Atlantic off the Amazon River mouth and on the Ceará Rise were prime objectives of investigation. They are controlled by complex relationships between downslope transport into the Amazon Fan, dispersion of suspended matter from the river and pelagic biogenic sedimentation. The regional sediment distribution is further modified by surface and deep water currents about parallel to the coast as well as by carbonate dissolution effects.

The geological and geophysical operations concentrated on the lower Amazon Fan, the Ceará Rise and the various adjacent abyssal plains. Specifically the transitional facies zones were targeted for surveying and coring to take advantage of dilution effects by terrigenous material in high sedimentation rate, but continuously deposited and undisturbed late Quaternary sedimentary sequences. Data sets of previous METEOR cruises (M16/2, M34/4) and results of drilling activities of the Ocean Drilling Program (ODP) in the Amazon Fan (Leg 155) and on the Ceará Rise (Leg 154) gave valuable hints for the detailed planning. Large and small scale multichannel seismic and sediment echosounder profiles provided a regional stratigraphic framework and allowed to identify the predominant depositional processes and sediment distribution patterns. The selection of appropriate locations for geologic sampling further relied on stratigraphic marker horizons discerned in ODP drill sites.

At several locations deployments of the *in situ* equipments of the Max-Planck-Institute for Marine Microbiology, Bremen, were arranged. They are designed to perform high-resolution measurements of oxygen and other relevant parameters in the water / sediment boundary layer at the ocean floor.

### Geophysics

Geophysical activities during METEOR Cruise M38/2 particularly focused on regional seismic and echographic surveys. A new high-resolution multichannel seismic gear allowed to image even small scale sedimentary structures and provided a superior vertical resolution of closely spaced layers which formerly could not be recognized as individual reflectors. By applying larger volume GI airguns in alternate mode with a small chamber watergun, simultaneously also seismic sections of deeper penetration could be acquired giving insight into the structural context of the near surface depositional processes.

An integrated processing of reflection seismic data with PARASOUND sediment echosounder and HYDROSWEEP swath bathymetry sounder profiles optimizes the structural resolution at all depth levels of the sedimentary column. Both echographic shipboard systems were permanently operated during a 24-hour watch keeping and routinely utilized on site as basis for an appropriate selection and positioning of all sediment sampling locations. Furthermore, the digital PARASOUND records can directly be compared to sedimentological observations and quantitatively be related to sediment physical properties core logs through synthetic seismograms.

The main working areas were located between 42° and 52° western longitude at the South American continental margin off Brazil (Fig. 2). They centered on those regions, where significant variations in sediment supply should have a major impact on the seismic signature as in the southern and northern Amazon Fan, on the flanks of the Ceará Rise and in the Pará Abyssal Plain. Seismic and acoustic lines across selected ODP drill sites served as references for the seismostratigraphic framework. Supplementary gravity cores will specifically improve information about the late Quaternary evolution of depositional processes. A series of profiles over the northeastern flanks of the Ceará Rise were planned to particularly reveal specific the impact of carbonate dissolution on the seismic characteristics.

Marine Geology

For paleoceanographic purposes and to supplement core material recovered 1991 during METEOR Cruise M16/2, sediment sampling at the Ceará Rise focused on water depths between about 4200 and 4600 m, the boundary layer between Antarctic Bottom Water (AABW) and North Atlantic Deep Water (NADW). In addition to gravity cores multicorer casts were especially intended to establish a reliable correlation to the modern hydrology of the region. Analyses of the deposits will provide further constrains on deep water variabilities using carbonate dissolution indices and the stable isotopic composition of benthic foraminifera. To reconstruct changes in the western equatorial Atlantic surface current pattern, coring locations were also arranged on the mid-Atlantic Ridge near 17°N in the North Equatorial Current domain. Combined with already existing data sets from the Ceará Rise, the isotopic composition of deep-dwelling planktic foraminifera should be very well suited to unravel fluctuations of the equatorial surface circulation system during the late Quaternary.

Along the entire cruise track living planktic foraminifera were collected from the surface waters to acquire species specific ecological data (e.g., their temperature sensitivity). The plankton samples should give important new information about the surface water foraminiferal assamblage which is finally preserved in deep-sea sediments. Furthermore, detailed isotope geochemical studies will reveal effects of the hydrographic conditions in the photic zone on the stable isotopic composition of foraminiferal shells. These results are of substantial importance for the paleoceanographic interpretation of late Quaternary foraminiferal assemblages and their isotopic compositions.

Paleobiology

In the Amazon deep-sea fan area and on the Ceará Rise surface sediments were sampled using the multicorer at a various locations, to study the recent and sub-recent distribution of organic walled and calcareous dinoflagellate cysts. These data sets are of principal interest as they will substantially improve the interpretation of variable dinoflagellate cyst assemblages through glacial and interglacial periods and should also provide more insight into changing South Atlantic current systems.

Geochemistry

Geochemical activities during this cruise focused on sampling and analyses of sedimentary deposits of the Amazon deep-sea fan and the Ceará Rise expanding work on sample material collected on METEOR Cruise M16/2 (1991). Prime aim was at recovering supplementary sediment series as well as at quantifying additional geochemical parameters which have not been available so far. The sediments retrieved at the former station GeoB 1514 (Amazon Fan) were conserved under argon atmosphere. Below sediment depths of 5 m analysis for methane was intended to prove that sulphate reduction taking place here in a narrow depth interval between 5 and 6 m is essentially driven by anaerobic oxidation of methane. Sediments at station GeoB 1523 (Ceará Rise) were re-sampled to determine relevant pore water constituents to complement already existing high resolution solid phase data sets. These measurements on pore water and also on fresh sediment material should give conclusive evidence for the mode of formation and origin of characteristic barium enrichments found at glacial / interglacial transitions in these deposits. Finally, surface sediment samples were planned to retrieve at the ESTOC station using the multicorer for studies in the scope of the interdisciplinary BIGSET program to examine seasonal changes in benthic reaction rates and related variations in trace element distributions.

Biogeochemistry

The working group from the Max-Planck-Institute for Marine Microbiology followed three different research topics during this cruise, (i) mineralization processes and sediment / water exchange rates of dissolved inorganic compounds, (ii) calcite dissolution, and (iii) oxygen penetration in deep-sea areas.

These objectives were studied *in situ* by deployment of two lander systems; Elinor, a benthic flux chamber lander and Profilur, a microsensor profiling lander. Mineralization processes and sediment / water exchanges have also been examined in the laboratory by incubation of multicorer sediment cores. The total oxygen consumption and the exchange rates of different mineralization products were determined by incubating sediment *in situ* using the lander Elinor. At the same time a pre-programmed electronic unit allows to collected water samples which are later analyzed to evaluate the benthic processes. By comparing the results of Elinor with those of Profilur effects of benthic organisms and the rates of different exchange processes can be estimated.

The dynamics of the benthic carbonate system are of critical importance for the understanding of the global carbon cycle. Calcite dissolution is mainly affected by two processes, dissolution through pressure and pH lowering caused by benthic mineralization. *In situ* pH and carbonate measurements have been designed to study these processes in the sediments. Profilur was equipped with pH electrodes and newly developed carbonate electrodes for this purpose. To obtain the calcite dissolution degree $\Omega$ and for calibration of the electrodes, water samples were taken with a Niskins bottle mounted on the frame of the lander.

Oxygen is the energetically best electron acceptor in sediments and depleted before other electron acceptors are utilized. The penetration depths of oxygen essentially depends on the amount easy degradable organic carbon available, and has therefore often been used as an indicator of productivity / activity in an area. In deep-sea environment the penetration depth of oxygen is mostly deeper than the reach of conventional glass electrodes (about 10 cm). For this reason a newly developed optrode system was operated on Profilur during this cruise with a capacity to measure oxygen concentration profiles down to around 50 cm in the sediment column.

## 3 Narrative of the Cruise

As several times before in recent years, the German research vessel METEOR sailed from the Brazilian seaport Recife for a scientific expedition on March 4, 1997. Prime objectives of this second leg of her 38th cruise were geophysical, geological, geochemical and microbiological studies in the southern and northern realm of the Amazon deep-sea fan and in the Ceará Rise region. In addition to bathymetric, sediment acoustic and seismic profiling, main interests were a sampling of the water column and the sedimentary deposits at the sea floor. Altogether 28 scientists from the University of Bremen, the Alfred-Wegener-Institute for Polar and Marine Research, Bremerhaven and the Max-Planck-Institute for Marine Microbiology, Bremen, took part in the cruise making use of the total capacity of R/V METEOR.

Following the exchange of a number of containers with scientific equipment in Recife, the various laboratories were set up during transit to the first working area. Only after leaving the Brazilian 200 nm zone on March 7, the shipboard hydroacoustic systems were activated and also a systematic sampling of the surface waters could be started. With completing comprehensive and altogether favorable tests of the entire gear, the first seismic profile along around 184 nm (Fig. 1) was recorded on a northeasterly course from the abyssal plain onto the Ceará Rise passing over the former Ocean Drilling Program Site 925 (ODP Leg 154).

The initial station work at the end of this seismic transect gave very encouraging results on March 9. Handling of the water sampler down to depths of 3000 m could be accomplished without any problems, the multicorer recovered a full set of samples and

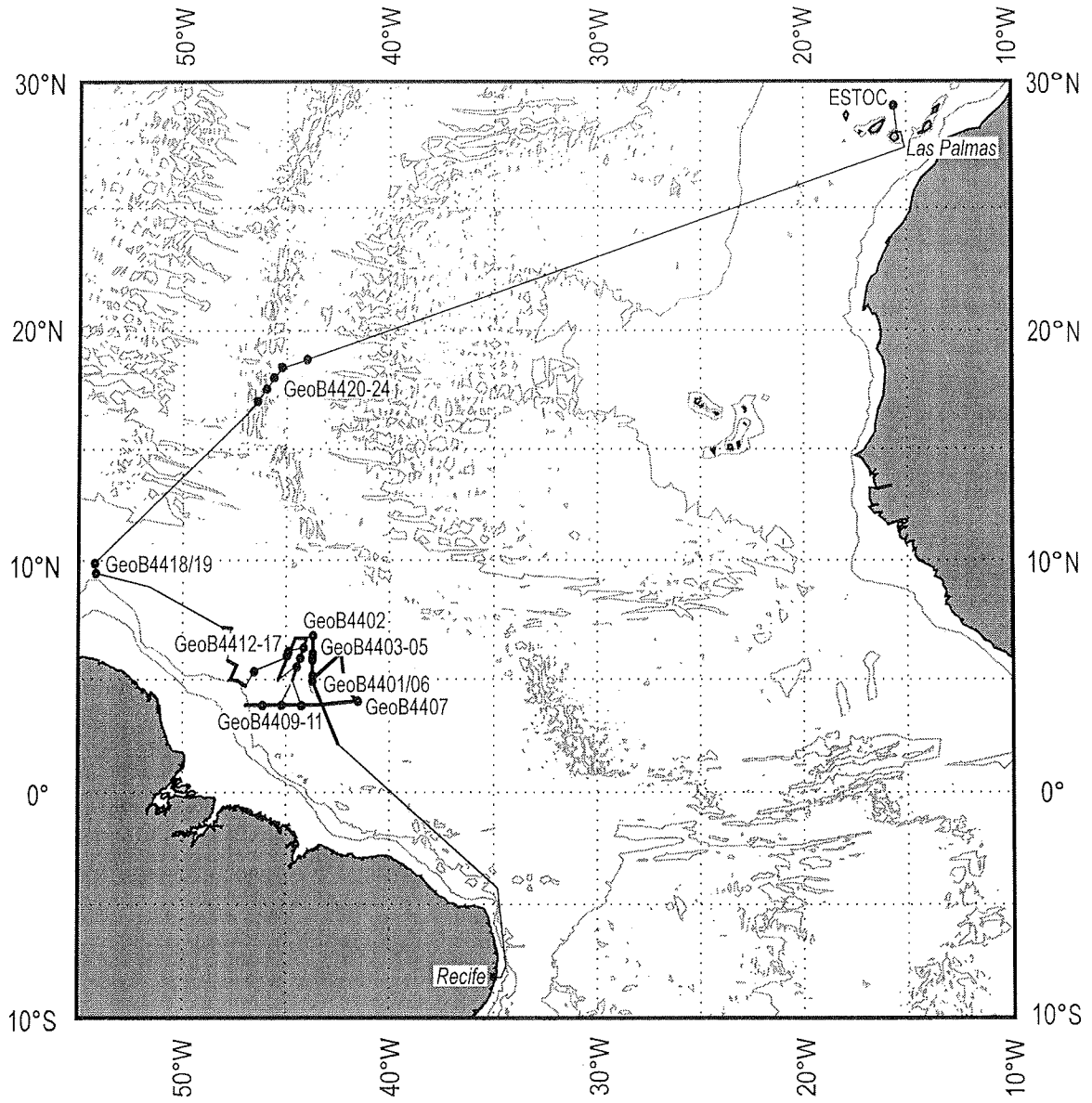


Figure 1 METEOR Cruise M38/2 - route and station map. Thick lines indicate seismic, thin lines echographic profiles. Bathymetry from GEBCO.

the gravity corer retrieved almost 7 m of sediments. After deployment of the twolander units Elinor and Profilur, subsequent seismic multichannel measurements concentrated on the northeastern flanks of the Ceará Rise. With further testing of the streamer and its depth control during this survey, it was possible to substantially improve the quality of the records. As seismic sources a small volume (0.16 l) water gun and a two chamber air gun (0.4 l, GI-Gun) were alternatively operated every second shot. They allow a detailed assessment of the sedimentary structures to several hundred meters sub-bottom depth. The transition from the Ceará Rise to the Pará Abyssal Plain with water depths of more than 4600 m is characterized by a progressive carbonate dissolution which was clearly identified in all seismic and acoustic data sets. Various crossings of previous ODP drill sites should provide a basic chrono- and lithostratigraphic framework for these sediment sequences.

The seismic and acoustic observations were then used for an optimum selection of a series of coring stations along this bathymetric transect. All multicorers came back with sufficient recoveries. Gravity core lengths between some 6.5 and 8.5 m matched about the results of the 1991 R/V METEOR Cruise M16/2 in the same area. On March 12, the ship reached again the position of the two landers, as planned after 65 hours. Repetitious attempts to release Elinor and Profilur acoustically failed, unfortunately. Also more intensified efforts during the following night - after completing a nearby supplementary coring station - did not result in any definite achievement. The only hope left in this situation was a discovery of the landers by the ARGOS satellite as soon as they would become afloat. In the meantime the other scientific program had to be continued.

For the remaining days of this second week at sea it mainly consisted of seismo-acoustic profiling in the eastern and southern parts of the Ceará Rise. Over the following weekend the at present most celebrated station of the Bremen SFB (GeoB 1523, METEOR Cruise M16/2) was re-sampled. All operations were successful and the two gravity cores obtained, which exceeded those of 1991 by up to 25% in length, should offer new opportunities for a variety of exciting analyses.

Early on Monday morning, March 17, the long awaited news finally arrived. The ARGOS satellite had located the lander Profilur more than 60 nm off its original deployment location. Later received new information indicated that the device was drifting with more than 0.5 knots in southwesterly direction and that it must have been at the sea surface for a couple of days already. The current seismic profile was therefore interrupted during the following night. R/V METEOR headed towards the actual lander position and recovered Profilur safely on deck at daybreak. Until the end of the cruise, no sign of Elinor has been found, though.

Divers major research goals could be accomplished later this week. First, an about 320 nm long seismic line led from the top region of the Ceará Rise across the Ceará Abyssal Plain to the lower terraces of the Amazon Fan. Sediments recovered with the gravity corer at 3 stations on the western half of this traverse were predominantly com-

posed of terrigenous constituents, reflecting an important fluvial influx from the South American continent. To the excitement of the geochemists on board, quite noticeable methane gas concentrations could be detected in the deeper layers of these deposits. Valuable sample materials were also obtained from multicorer and water sampler casts. In the immediate vicinity of one of the stations the lander Profilur was deployed once more to the sea floor and, on this turn, came back in time with an almost complete set of measurements.

Working conditions, in particular on deck, were often rather unpleasant in these days as regular massive rain showers impressively illustrated the fact that R/V METEOR was operating right in the center of the Intertropical Convergence Zone for a longer period. In addition, an active frontal system farther to the north sent a relatively high swell further intensified by the local trade winds. Notwithstanding this adverse situation, all laboratories pursued their activities with the usual routine.

The reflection seismic program was continued with a two days survey along 3 profiles in the northern Ceará Rise region. A relatively rough topography results there in an unusual relationship between pelagic sediments and distal Amazon Fan deposits. Afterwards an efficient sampling of the Quaternary sediment series could be achieved at 3 stations on each of the 2 main seismic lines and also at the former SFB site GeoB 1514 (METEOR Cruise M16/2, 1991). Likewise, several deployments of the water sampler to a maximum depth of 3000 m and the remaining lander system were entirely successful. The latter provided high-resolution (0.1 mm spacing) electrochemical analyses of oxygen and pH across the sediment / water interface. For the first time also the deep penetration module of Profilur could be activated which quantifies oxygen *in situ* down to 50 cm sub-bottom by means of optical sensors (optrodes).

Final seismic measurements focused on the surroundings of different ODP drill sites in the Amazon Fan. For some 24 hours prime data were collected over heterogeneous channel / levee systems. Together with the PARASOUND records they reveal a wealth of details about the channel evolution from the upper down to the lowermost deep-sea fan. On March 28, the streamer and guns were retrieved for the last time on deck terminating the projected seismic operations of this cruise. All components of the new equipment performed fairly reliable for more than 75000 shots along a total of 2300 km of lines. Making use of the full range of resolution of the watergun and the GI-Gun an altogether 375 GigaByte data set was accumulated.

The last station work at the South American continental margin in the westernmost study area on the lower Guyana Plateau was to adequately supplemented the sample collection of the 1996 METEOR Cruise M34/4. On March 30, the eve of the Easter holidays, R/V METEOR set course to the mid-Atlantic Ridge, near 17°N / 45°W, where, until April 4, a series of 5 stations was located on a bathymetric transect between 2600 and 4800 m water depth from the top to the eastern ridge flanks. The sediment and water samples recovered fill a regional gap of critical importance for the Bremen SFB.

During the about 1700 nm journey to port, all laboratories were busy to finish the shipboard examinations and analyses of core and sample materials and the various working groups began to summarize their preliminary findings. Particularly for the Ceará Rise sediments measurements of the magnetic susceptibility already allowed to define fairly detailed age models. They indicate unexpectedly high sedimentation rates which increase to deeper waters. These sediment series should specifically be suited to resolve the present controversial discussion about the tropical climate variability during oxygen isotope stage 3. With the transition to the abyssal plains, distinctly higher numbers of turbidites occur. They produce mostly strong anomalies in all physical property core logs. A diagenetic remineralization of magnetite within those layers is likely to explain the typical rise in magnetic susceptibility. Various turbidites could convincingly be correlated between the different coring sites.

Plankton samples, which were collected daily from the surface waters on the entire cruise, provided some attractive insights into the life rhythm of calcareous dinoflagellates and foraminifers. Species of the shallow dwelling dinoflagellate *Thoracosphaera heimii,* an organism of specific interest for the micropaleontologists on board, was cultivated for later shore based investigations. Also new data could be obtained about the reproduction cycle of the planktic foraminifer *Globigerinoides sacculifer.* Highest concentrations caught from the surface waters in the full moon period and the subsequent week remarkably declined thereafter. These observations strongly support the previous hypothesis that *G. sacculifer* effectively synchronizes its reproduction sequence with the moon phases.

Against expectation and former experience, very favorable wind and sea states accompanied the whole transit from the working areas to the Canary Islands. R/V METEOR thus arrived in Las Palmas one day early, on April 11 and most all of the scientific team disembarked.

The following day the ship sailed to the ESTOC station around 60 nm north of Gran Canaria for an oceanographic, chemical and biological sampling of the water column. New working groups from the German Universities of Bremen, Hamburg, Kiel and Oldenburg were on board for this purpose. Of their European partners of cooperation, experts from Spanish institutions and the University of Edinburgh took part in the research activities. During an about 30 hours program various devices to collect water samples down to a maximum depth of 3500 m, the multinet and also a free floating sediment trap were deployed. A number of experiments which had failed because of adverse weather conditions and technical problems during METEOR Cruise M37 could now successfully be accomplished. Late on April 13, R/V METEOR returned to Las Palmas, where Cruise M38 ended the next morning as scheduled.

# 4 Multichannel Reflection Seismic and Sediment Acoustic Profiling

*V. Spieß, W. Böke, C. Hilgenfeld, C. Hübscher, A. Janke, U. Rosiak, G. Uenzelmann-Neben, L. Zühlsdorff and all PARASOUND Watchkeepers*

## 4.1 Introduction

The depositional processes in the western equatorial Atlantic off the Amazon River and on the Ceará Rise are controlled by complex relationships between downslope transport into the Amazon Fan, distribution of suspended matter from the river andbiogenic sedimentation. Strong surface and deep water currents parallel to the coast line and associated carbonate dissolution modify the sedimentary pattern.

A major portion of the scientific program of R/V METEOR Cruise M38/2 was assigned to swath sounder, sediment echosounder and multichannel reflection seismic profiling to document the Quaternary and Neogene sedimentation history. Working areas were the transitional region from the lower Amazon Fan to the Ceará Abyssal Plain, on the northern flanks of the Ceará Rise bordering the pathway of Antarctic Bottom Water and in the central Amazon Fan. Several drill sites of ODP Legs 154 and 155 have been crossed to constrain the seismostratigraphic interpretation.

Acoustic systems in 4 different frequency domains were operated to optimize the resolution in different sub-bottom levels. The HYDROSWEEP system provides topographic information across a width of twice the water depth. The PARASOUND sediment echosounder with frequencies of around 4 kHz allows a signal penetration between 10 and 100 m depending on sediment composition and grain size. Digital echosounder data were collected on a 24-hour watchkeeping routine.

Multichannel seismic measurements were performed with the new instrumentation of the Geoscience Department, University of Bremen, using two seismic sources of different volumes in alternating mode. A water gun with a frequency range from 200 to 2000 Hz provides information about the upper 100 to 300 m of the sediment column, whereas a GI-Gun with signal energy to 500 Hz yields deeper penetrations. A total of 2290 km of multichannel data were recorded along 14 seismic lines (Fig. 2; Table 1).

## 4.2 Methods and Instruments

### 4.2.1 PARASOUND

The PARASOUND system operates both as low-frequency sediment echosounder and as high-frequency narrow beam sounder to determine the water depth. It makes use of the parametric effect producing additional frequencies through nonlinear acoustic interaction of finite amplitude waves. If two sound waves of similar frequency (here, 18 kH

Table 1 Statistics of METEOR M38/2 multichannel seismic lines.

| Line | Start | | | | End | | | | Shot | Length |
|---|---|---|---|---|---|---|---|---|---|---|
| | Latitude | Longitude | Date | Time | Latitude | Longitude | Date | Time | Points | (km) |
| 97-001 | 1°55.80'N | 42°25.10'W | 07.03.97 | 12:49 | 4°50.00'N | 43°46.60'W | 09.03.97 | 04:58 | 11774 | 356.1 |
| 97-002 | 4°47.60'N | 43°45.90'W | 09.03.97 | 16:13 | 6°38.28'N | 43°43.48'W | 10.03.97 | 14:32 | 6639 | 205.0 |
| 97-003 | 4°48.00'N | 43°45.80'W | 13.03.97 | 02:35 | 5°49.40'N | 42°20.20'W | 14.03.97 | 15:29 | 7990 | 194.5 |
| 97-004 | 5°49.40'N | 42°20.20'W | 14.03.97 | 15:29 | 4°40.60'N | 42°13.10'W | 15.03.97 | 05:15 | 4074 | 128.1 |
| 97-005 | 4°40.60'N | 42°13.10'W | 15.03.97 | 05:15 | 3°49.64'N | 41°37.45'W | 15.03.97 | 18:10 | 3676 | 115.1 |
| 97-006 | 3°49.64'N | 41°37.45'W | 16.03.97 | 05:52 | 3°40.00'N | 47°00.00'W | 19.03.97 | 13:30 | 19273 | 596.4 |
| 97-007 | 5°00.00'N | 44°41.60'W | 21.03.97 | 15:27 | 6°30.00'N | 44°00.00'W | 22.03.97 | 10:25 | 5654 | 183.5 |
| 97-008 | 6°30.00'N | 44°00.00'W | 22.03.97 | 10:25 | 6°30.00'N | 44°35.00'W | 22.03.97 | 17:28 | 2070 | 64.4 |
| 97-009 | 6°30.00'N | 44°35.00'W | 22.03.97 | 17:28 | 5°00.00'N | 45°30.00'W | 23.03.97 | 14:00 | 6084 | 195.1 |
| 97-010 | 4°31.09'N | 47°04.30'W | 26.03.97 | 23:39 | 4°42.34'N | 47°23.82'W | 27.03.97 | 04:10 | 1211 | 41.6 |
| 97-011 | 4°42.34'N | 47°23.82'W | 27.03.97 | 04:10 | 4°46.10'N | 47°43.80'W | 27.03.97 | 08:13 | 1193 | 37.5 |
| 97-012 | 4°46.10'N | 47°43.80'W | 27.03.97 | 08:13 | 5°21.14'N | 47°24.85'W | 27.03.97 | 16:16 | 2360 | 73.7 |
| 97-013 | 5°21.14'N | 47°24.85'W | 27.03.97 | 16:16 | 5°35.90'N | 47°52.30'W | 27.03.97 | 23:16 | 1914 | 57.5 |
| 97-014 | 6°55.90'N | 47°44.80'W | 28.03.97 | 07:19 | 6°58.10'N | 48°06.90'W | 28.03.97 | 11:44 | 1324 | 40.8 |
| | | | | | | | | Total | 75236 | 2289.3 |

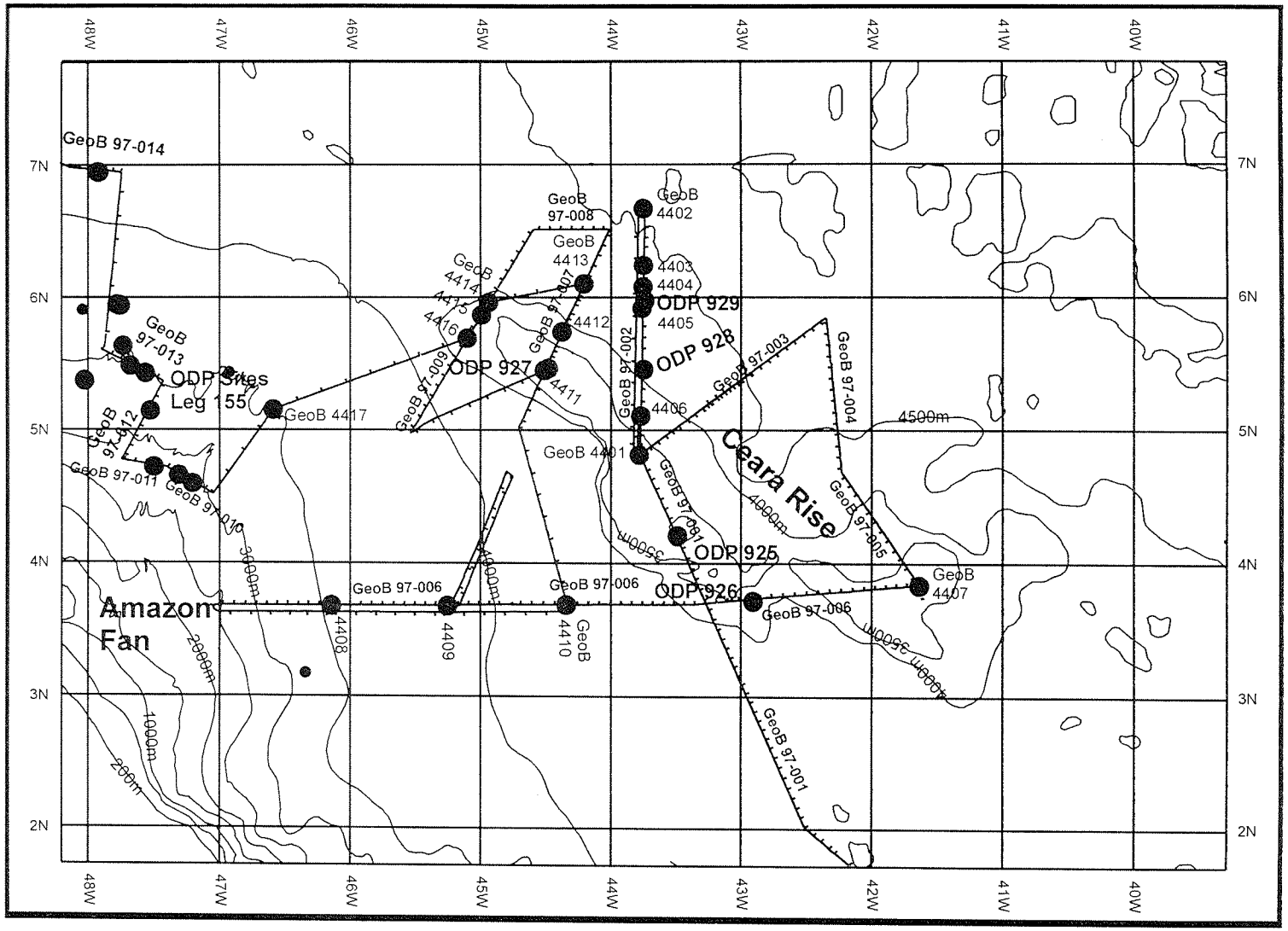


Figure 2 Cruise track, seismic lines and sampling stations of METEOR Cruise M38/2 at the Brazilian continental margin. Also shown are ODP drill sites on Ceará Rise (Leg 154) and in the Amazon Fan (Leg 155). Bathymetry from GEBCO.

and, e.g., 22 kHz) and sufficiently high primary amplitude are emitted simultaneously, a signal of the difference frequency (4 kHz) is generated. The new component travels within the emission cone of the original high-frequency waves limited to an angle of only 4° for the PARASOUND system. Therefore, the footprint size is much smaller than for conventional echosounders and both vertical and lateral resolution are significantly improved.

The PARASOUND system is permanently installed on the ship. Its hull-mounted transducer array has 128 elements on an area of ~1 $m^2$. Due to the low degree of efficiency of the parametric effect, it requires up to 70 kW of electric power. In 2 electronic cabinets beamforming, signal generation and the separation of primary (18, and, e.g., 22 kHz) and secondary frequencies (e.g., 4 kHz) are performed. Via a third electronic cabinet in the echosounder control room the system is operated on a 24-hour watch schedule.

Since the two-way travel time is long in the deep sea compared to the length of the reception window (up to 266 ms), the PARASOUND System sends out a burst of pulses at 400 ms intervals until the first echo returns. The coverage of this discontinuous mode depends on the water depth and produces non-uniform time spans between bursts. On average, one seismogram is recorded every second yielding a spatial resolution of a few meters at 4.9 knots along the seismic profiles.

Main tasks of the operators are to adjust the reception window as well as system and quality control. Because of the limited penetration of the echosounder signal into the sediment, only a small window close to the sea floor is recorded. The excellent depth resolution on the order of a few tens of centimeters provides a very high information density.

In addition the analog recording device DESO 25 PARASOUND is equipped with the digital data acquisition system ParaDigMA developed at the University of Bremen (Spieß, 1993). The data were stored directly on 6250 bpi, 1/2" magnetic tapes in the standard, industry compatible SEGY format. The 486-processor based PC allows the buffering, transfer and storage of the digital seimograms at very high repetition rates. Of the emitted series of pulses usually every second pulse was digitized and stored, resulting in recording intervals of 800 ms within a pulse sequence. The seismograms were sampled at a frequency of 40 kHz with a typical registration length of 266 ms for a depth window of ~200 m. The source signal was a band limited, 2 - 6 kHz sinusoidal wavelet of 4 kHz dominant frequency and 2 periods duration (~500 µs total length).

Already during acquisition of the data an online processing was carried out. For all profiles seismic sections were plotted on a vertical scale of several hundred meters. Most of the changes in window depth could thereby be eliminated. These plots give a first impression of variations in sea floor morphology, sediment coverage and sedimentary patterns along the ship's track. To improve the signal-to-noise ratio, the echo-

gram sections were filtered with a wide bandpass and also normalized to a constant value much smaller than the maximum average amplitude to exaggerate in particular deeper and weaker reflections.

To study the influence of frequency and length of the source signal on the reflection pattern, the parameters were systematically varied at all sites, where gravity cores have been recovered ('source signal test'). The frequency of the source signal was changed in 0.5 kHz steps over the available frequency range from 2.5 to 5.5 kHz, the pulse length set to 1, 2 and 4 sinus periods. Every combination was kept unchanged for a time span of 2 minutes to enable signal stacking and an evaluation of the seismogram variability at each location. In order to quantify interference phenomena, seismograms recorded with different frequencies will later be analyzed in detail and compared to physical property logs of the core materials.

### 4.2.2 HYDROSWEEP

The multibeam swath sounder HYDROSWEEP of R/V METEOR was routinely operated during Cruise M38/2 on a 24-hour watch by the scientific crew without technical problems. The system provided a complete coverage of the sea floor topography over a width of twice the water depth along the ship's track. The generally adequate data quality at times deteriorated at higher sea states.

### 4.2.3 Very High-Resolution Multichannel Reflection Seismics

Seismic Sources

During seismic surveying two different seismic sources, a GI-Gun and a watergun, were triggered in alternating mode at an interval of 12 s between the two devices. With an average ship's speed of 4.9 kn the shot distance amounted to approximately 30 m between different sources and 60 m for the same source. Each gun was driven by air pressure of 150 bar and shot more than 38000 times without failure. A broken weld at the air exhausting pipe of the watergun had no impact on the source signature. The configuration of the guns during measurements is shown in Figure 3. For high-pressure air supply 4 JUNKERS compressors built into a 10 ft container were made available by the Institute of Geophysics, University of Hamburg. They performed without major failures for a total survey time of about 11 days.

The 2 x 0.41 l volume GI-Gun (Generator-Injector-Gun; SODERA) was towed portside 18 m behind the ship's stern at a wire led through a drum hanging directly beneath the A-crane. An elongated buoy connected via two rope loops stabilized the GI-Gun to horizontal position in about 1 m water depth. To efficiently eliminate a bubble signal, the injector was triggered with a delay of 31 ms after the generator.

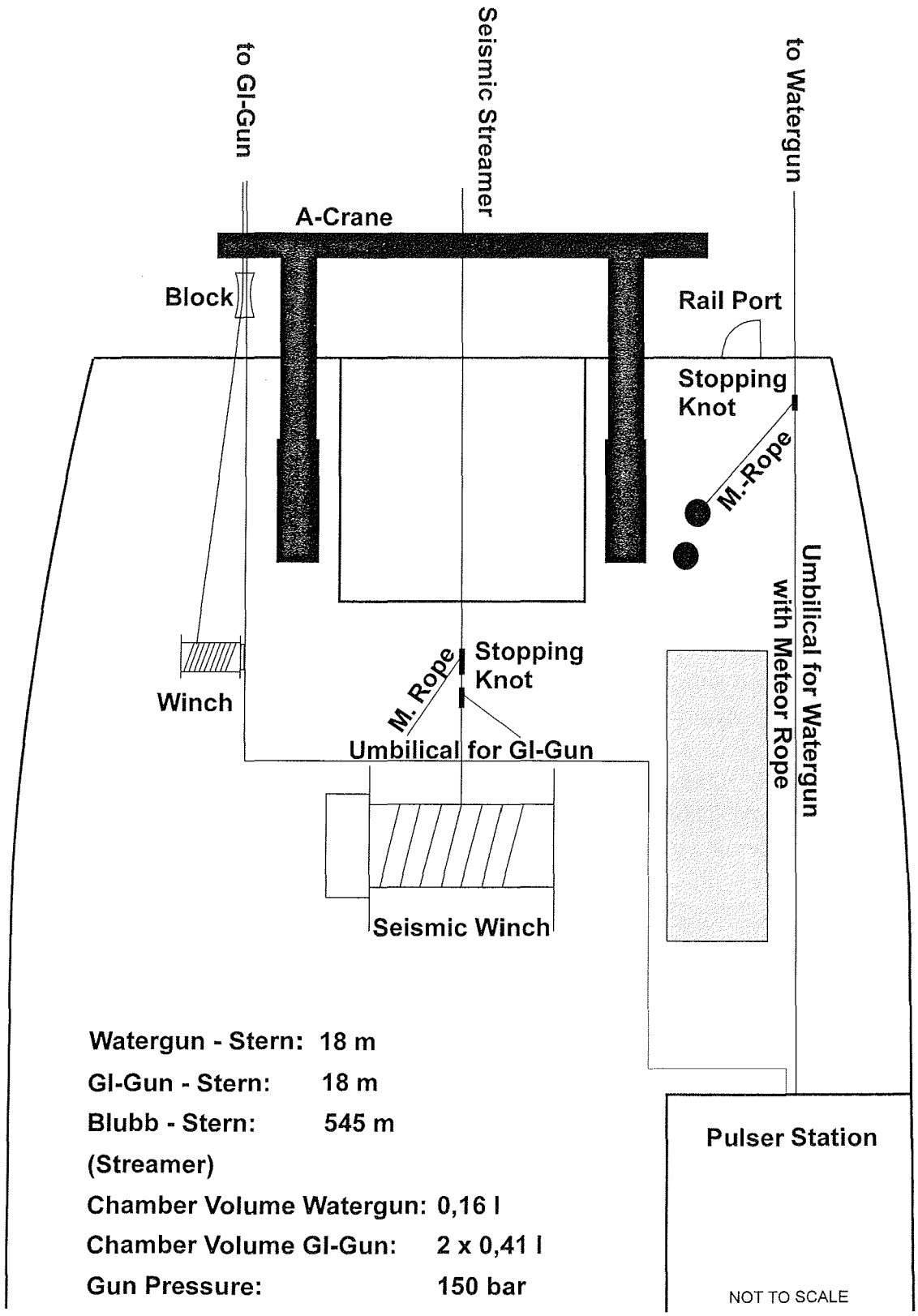


Figure 3 Set up of seismic equipment on the working deck during METEOR Cruise M38/2 (not to scale).

The second source was a S-15 watergun (SODERA) of 0.16 l volume towed with a METEOR rope 18 m behind the ship at starboard side (Fig. 3). A steel frame held the watergun in steady position parallel to an elongated buoy in approximately 0.7 m water depth. To prevent corrosion, a zinc plate was attached to the frame. Frequency characteristics of both sources, measured under optimum conditions, are displayed in Figure 4. During operations, the seismic watchkeeper routinely checked the near field source signature of both guns on a digital scope.

Streamer

The multichannel seismic streamer (SYNTRON) consisted of a tow lead, one stretch section and three active sections of 100 m length each. The 4th active section could not be used due to crooked connector shells. A 100 m long METEOR rope with a buoy at the end was attached to the tail swivel, a deck cable connected the streamer to the recording system. The winch position on the working deck is shown in Figure 3. During operations, the tow lead was fixed with two METEOR ropes and paid out ~55 m giving 45 m distance between ship and stretch section. During deployment and retrieval of the guns and streamer, the ship's speed was reduced for around 50 minutes to 3 and 2 kn, respectively.

Each active section comprises 16 hydrophon groups of 6.25 m length which are further subdivided into 5 subgroups of different length (Fig. 5). One of the subgroups is a high-resolution hydrophone with individual pre-amplifier. A programming module distributes the subgroups to 5 channels. As illustrated in Figure 5, every second 6.25 m long hydrophone subgroup was activated. They have even channel numbers from 2 to 48 on the streamer cable and were connected to BISON channels 1 to 24. Single hydrophones (streamer channels 97 to 108) were recorded on BISON channels 25 to 36.

MULTITRAK Bird Controller and System Control

At the end of every section a MULTITRAK Remote Unit (RU) was attached to the streamer. Each RU includes a depth and heading sensor as well as adjustable wings. The RUs are co-ordinated by the MULTITRAK controller in the seismic lab. Controller and RUs communicate via coils nested within the streamer and a twisted pair of wires within the deck cable. One of these wires had to be grounded to avoid transmission errors. Each shot trigger started a scan of water depth and heading (delay 0.5 s, duration 0.2 s). The actual position of the streamer is displayed on a monitor as depth or heading profile. All parameters are digitally stored on the controller PC together with shot number, date and time.

There are two options to manipulate the streamer depth. On way is to send an operating depth to the RUs which in most cases was $5 \pm 1.25$ m. The RUs try to force the streamer to the chosen depth by adjusting the wing angles accordingly. The second option is to set a constant wing angle which was sometimes advantageous for the distal RUs. Depth and wing angle statistics helped to select appropriate parameters.

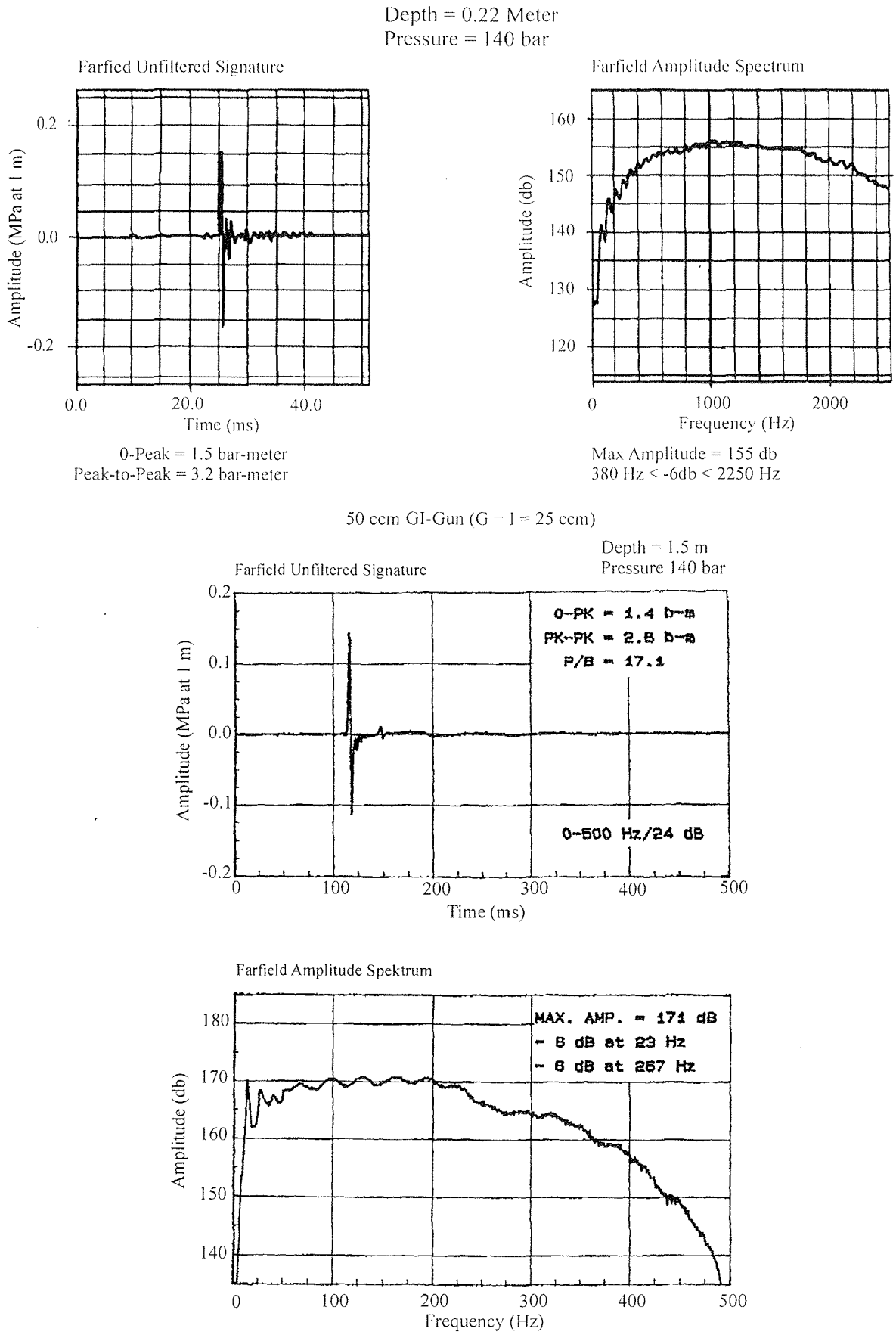


Figure 4 Source characteristics and frequency content of the S-15 Watergun (top) and the GI-Gun (bottom), measured under optimum conditions (from SODERA Gun Manuals).

| Subgroup | Length | Streamer channel (n=1..12) | Bison channel (n=1..12) |
|---|---|---|---|
| HG1 (HSG A/B/C/E) | 6.25 m | (n-1)*4+2 | (n-1)*2+1 |
| HG3 (HSG A/B/C/E) | 6.25 m | n*4 | n*2 |
| HG1 (HSG D = High-Res.) | 0.0 m | 96+n | 24+n |

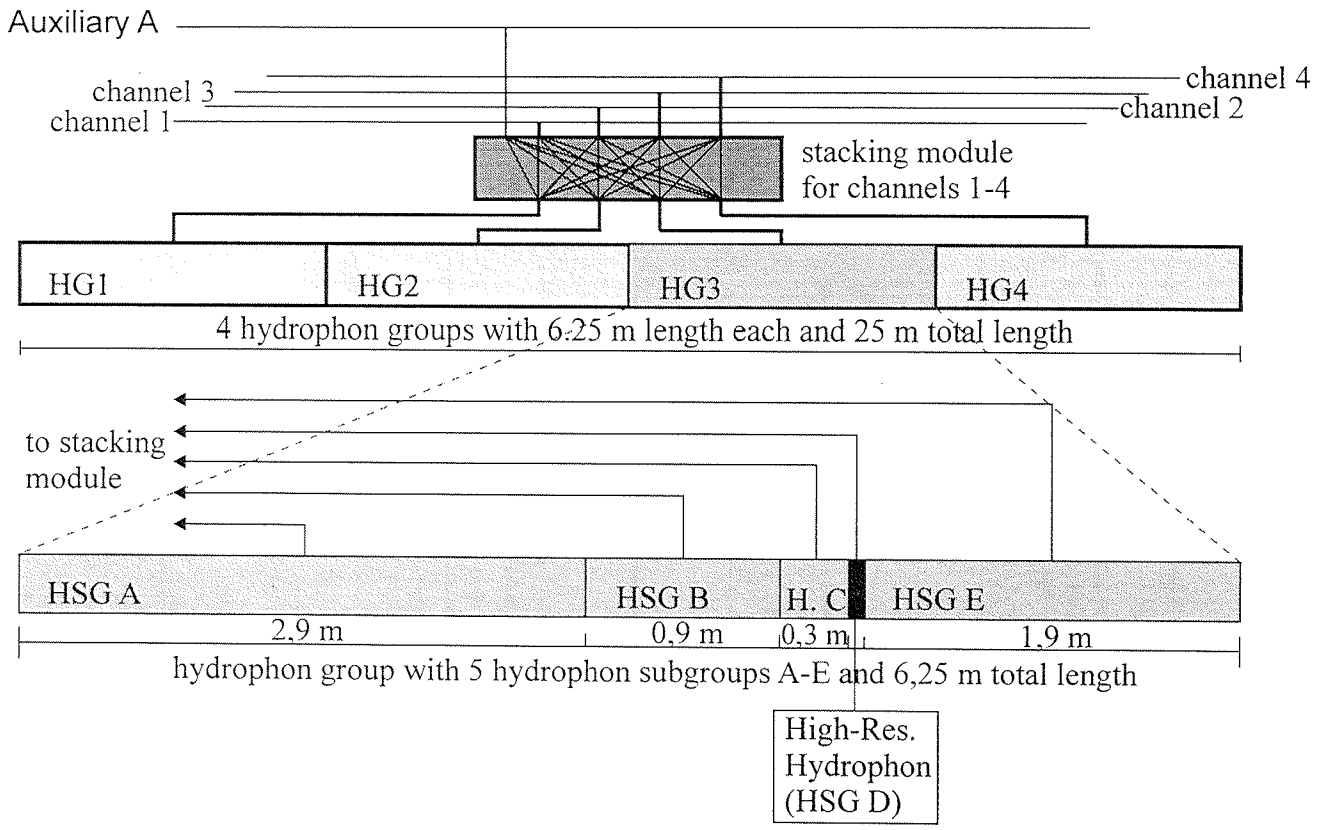


Figure 5 Hydrophon group and subgroup configuration of a 100 m long active streamer section and assignments of streamer to BISON recording channels.

Seismic sources, seismograph, MULTITRAK controller, on-line plotter and digital scope for the near field hydrophons were synchronized by a trigger unit. Because of too strong electromagnetic noise on the connecting line to an external GPS clock, an internal timer had to be used. The trigger output was a negative TTL signal for most devices.

Data Acquisition System

The recording unit includes a switchbox, a seismograph and a single channel recording unit for on-line plotting. The switchbox connects the streamer via a deck cable with the seismograph and allows the assignment and optional stacking of streamer hydrophone subgroups to individual recording channels. The configuration remained unchanged during the cruise and sorted the streamer channels such that hydrophone groups of the same length are available as a continuous series of channels (Fig. 5).

The 48 channel seismograph (BISON) was specially designed for the University of Bremen to perform a standard operation mode for very high-resolution seismic data. Except for line GeoB 97-001, where 48 channels were recorded, only 36 channels were activated to limit the data volume to the current maximum system capacity. The seismograph provides an on-line data display as well as on-line demultiplexing and storing in SEG-Y format. Analog filters were set to 8 Hz (low-cut) and 4000 Hz (high-cut). The sample rate was 0.125 ms for a recording length of 4000 ms. All channels were preamplified by a factor of 1000 (60 dB) to keep the signal within the optimum operation range. The data were stored on DLT cartridge tapes with 20 GByte uncompressed volume. The recording delay had to be adjusted according to the actual water depth. To limit the length of data gaps, the ship's speed was reduced to 3 kn for several minutes, while exchanging the storage media.

To achieve an immediate graphic information about the seismic data acquired and to store navigation data, a second recording system based on the ParaDigMA scheme with a HEWLETT PACKARD 3852 Data Acquisition Unit, a PC and a DESIGNJET 350 A1 roll paper plotter was set up. Unfortunately, an extremely high noise level on the signal lines made on-line plots impossible, except for line GeoB 97-006.

Data Processing

The total data volume collected during the cruise amounts to an equivalent of more than 2700 conventional 1/2" magnetic tapes. Main purpose of the onboard data processing was therefore to provide a quality control and preliminary overview of the seismic lines. Only a limited number of traces was hence selected from each tape and processed with Seismic Unix (SU) on a HEWLETT PACKARD Apollo 715 workstation.

The multichannel data were initially stored in demultiplexed SEG-Y format on tape. Accordingly, the onboard processing sequence started with a conversion to SU format. To speed up this operation, a program was written which also separated the Watergun

and GI-Gun data sets. From the GI-Gun data only the first 4 near offset traces of each shot, from the Watergun records only the first near offset trace were selected for further processing. The following list summarizes the complete onboard processing sequence applied to the data shown in this report.

- Conversion of demultiplexed SEG-Y to SU format.
- Sorting:
  Traces 1 to 4 (GI-Gun) and trace 1 (Watergun) of each shot were separated.
- Filtering:
  GI-Gun - bandpass 70 - 170 Hz, linear taper 40 - 70 Hz and 170 - 250 Hz;
  Watergun - bandpass 200 - 600 Hz, linear taper 100 - 200 Hz and 600 - 800 Hz.
- Resampling:
  GI-Gun - new sample rate 1 ms (originally 0.125 ms);
  Watergun - new sample rate 0.5 ms (originally 0.125 ms)
- Stacking:
  GI-Gun - brute stack of near offset traces 1 - 4 without statics or NMO correction;
  Watergun - no stacking.
- Plotting:
  All data were plotted using a linear time dependent gain. Polarity of GI-Gun waveforms was inverted before plotting.

## 4.3 Preliminary Results

### 4.3.1 Ceará Rise

The Ceará Rise, a northwest-southeast striking aseismic ridge (Kumar & Embley, 1977), rises about 2 km above the surrounding abyssal plains. The present survey illustrates quite well the asymmetric character of this structure (Fig. 6) with very steep (up to 9.6 degrees) southwestern flanks contrasting to smoother slopes on the northeastern side. Southwest of the rise, sedimentary sequences of up to 1300 ms TWT in thickness could be resolved. On top of the Ceará Rise signal penetration was limited to the uppermost about 300 - 600 ms TWT, but increases again towards the abyssal plain in the northeast (Fig. 6). This either reflects carbonate dissolution effects, or, more likely, results from an intensified influx of terrigenous material from the Amazon, as sedimentation rates generally appear to be higher in deeper waters.

At a later stage of processing the data will be carefully tied into the results of ODP Leg 154 (Curry, Shackleton, Richter et al., 1995). As a first approach, the seismic records were correlated to the three sedimentary units defined by Mountain & Curry (1995). These authors observed an about 1 km thick section consisting of lithogenic and biogenic deposits.

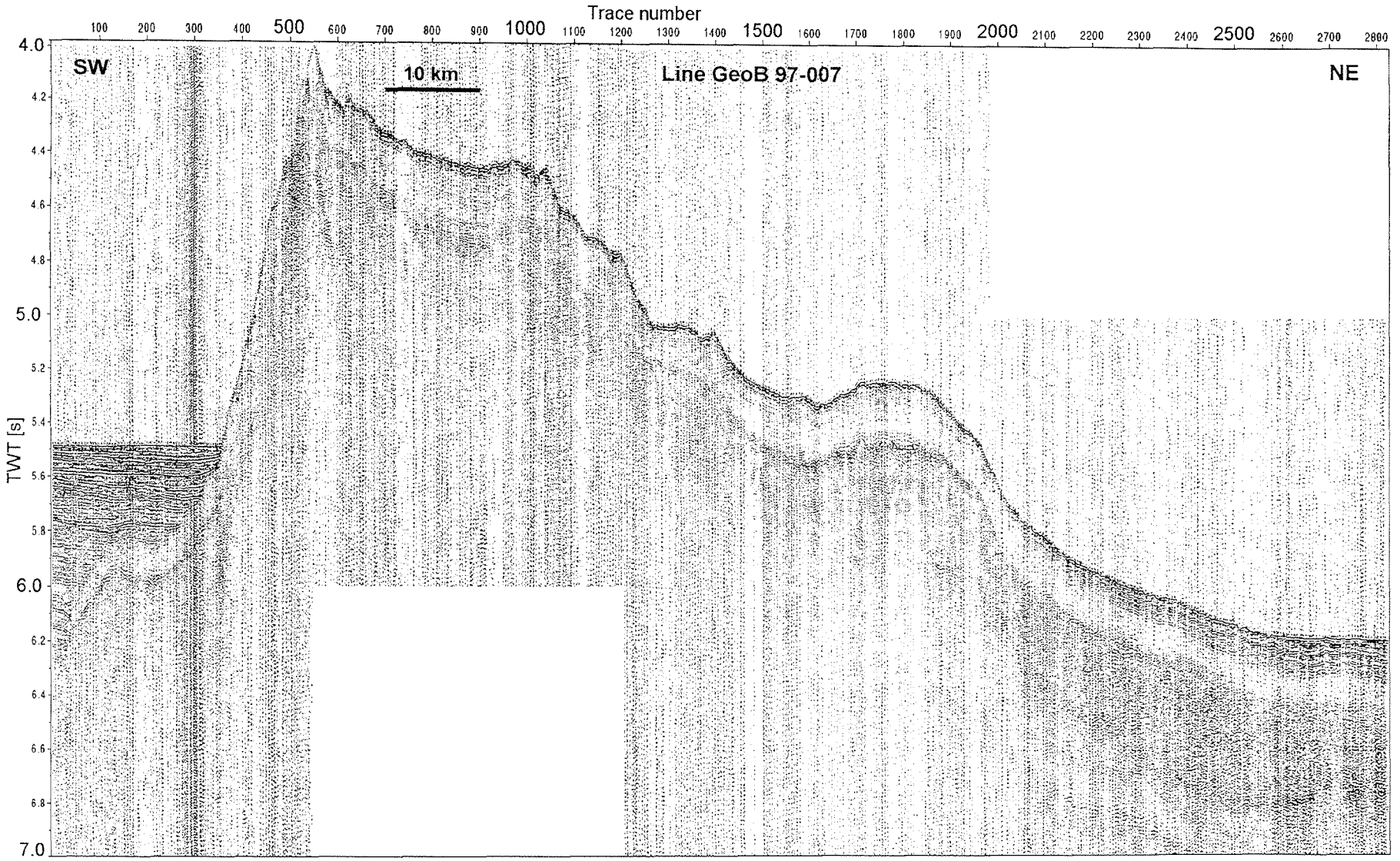


Figure 6 Multichannel seismic line GeoB 97-007 (GI-Gun) across the Ceará Rise. Stack of four near shot traces.

Unit 1 comprising the uppermost 100 - 250 ms TWT was very well covered by the present survey. It is characterized by continuous parallel internal reflections and can be further subdivided into two subunits. Reflector red of Mountain & Curry (1995) marks the transition from strong internal reflections above to a more transparent appearance below (Fig. 6). In a few places, e.g., shotpoint 900 in 4600 ms TWT of line GeoB 97-007, another strong reflector has be recognized, but could not be mapped on regional scale.

Unit 2 of Mountain & Curry (1995) can be clearly distinguished only in water depths of more than 5000 ms TWT on the northeastern slopes (Fig. 6). The upper parts of this unit show strong hummocky reflections which Mountain & Curry (1995) attributed to a depositional environment controlled by bottom currents. The transition to more transparent series 400 - 500 ms TWT below the unit's top is in good agreement with the depth of reflector yellow marking a change from small to large scale hummocks (Mountain & Curry, 1995).

Due to the lower energy of the seismic sources used in the present survey, Unit 3 of Mountain & Curry (1995) could not be resolved. A strong reflector on the southwestern flank of the Ceará Rise, which is downfaulted towards the Amazon Fan, was tentatively be correlated to reflector orange of Mountain & Curry (1995). In this area the fan deposits lap onto the base of the rise (Figs. 6 and 7).

Two PARASOUND profiles from the northeastern flanks of the Ceará Rise also exhibit a downslope increase in reflection amplitude and signal penetration. On the southern line (Fig. 8), which covers a depths interval between 4150 and 4500 m, penetrations expand from 20 to 50 m. The lowermost visible reflector at the upper end can be traced along the entire section. Its depth beneath sea floor varies from about 20 to >30 m. Likewise, the second line (Fig. 9) shows increasing penetrations in water depths between 3550 and 3950 m. These observations can be explained by a depth dependent influx of terrigenous sediments, transported as suspended material of turbiditic origin. Since the Ceará Rise acts as a barrier between the Amazon Fan and Pará Abyssal Plain, the suspension clouds must have traveled around the northwestern edge of the rise.

### 4.3.2 Distal Amazon Fan

The distal Amazon Fan is characterized by a thick pile of sedimentary sequences of which about 2000 ms TWT (2 km with $v_P$ = 2000 m/s) are resolved in the present data sets. The sedimentary layers thin towards the Ceará Rise and lap onto its downfaulted base (Figs. 7 and 10). They appear well stratified with the strongest reflections in the uppermost 300 ms TWT. This top unit shows indications of levees, e.g., at shotpoints 5000 and 5550 on line GeoB 97-006 and prograding series east of shotpoint 4600 suggesting a fairly recent active fan depocenter in this area (Fig. 10). A buried debris flow is found around shotpoint 600 in 5300 ms TWT depth on line GeoB 97-006.

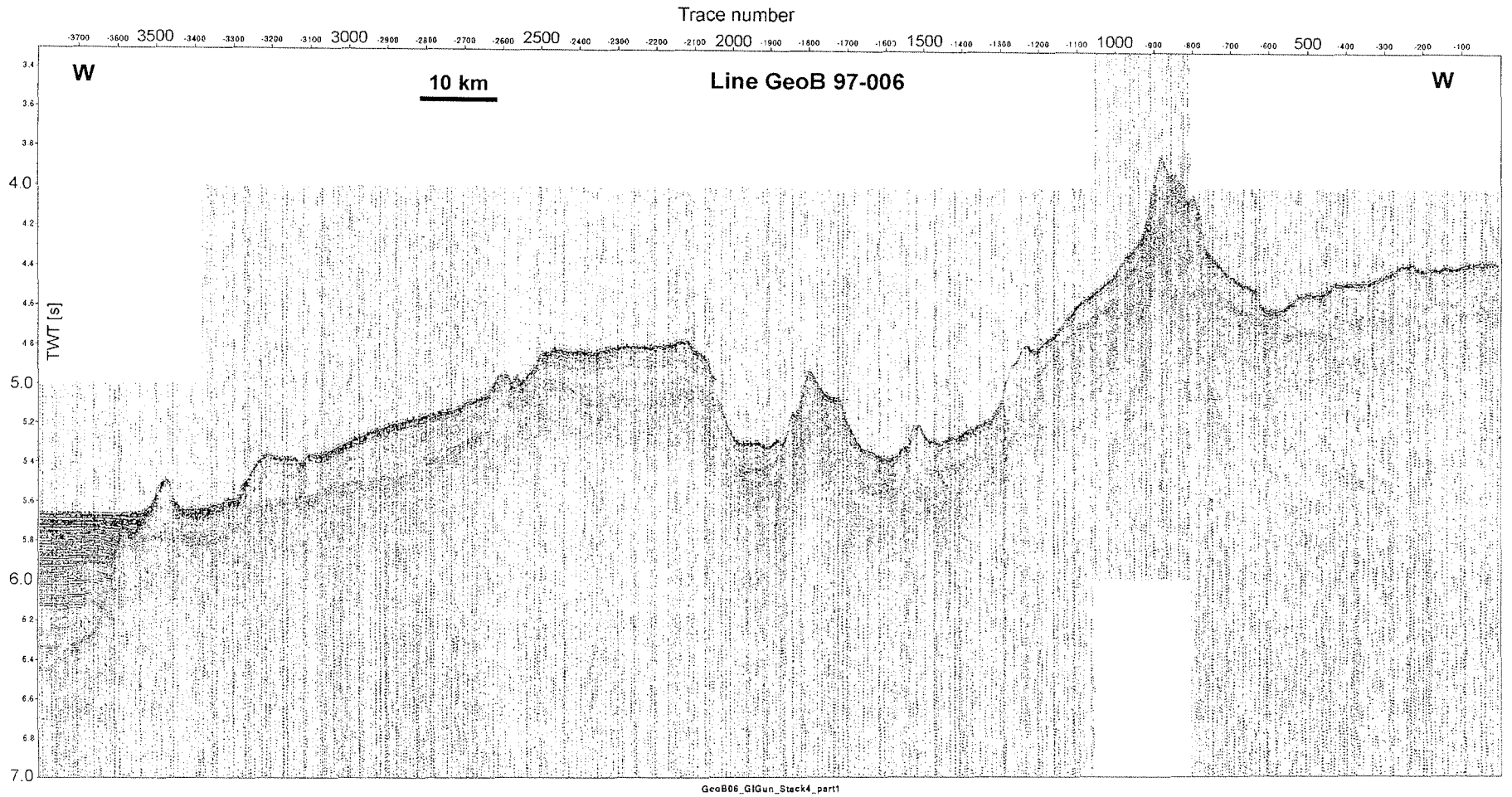


Figure 7 Eastern part of multichannel line GeoB 97-006 (GI-Gun) from the Ceará Rise to the southernmost distal Amazon Fan.

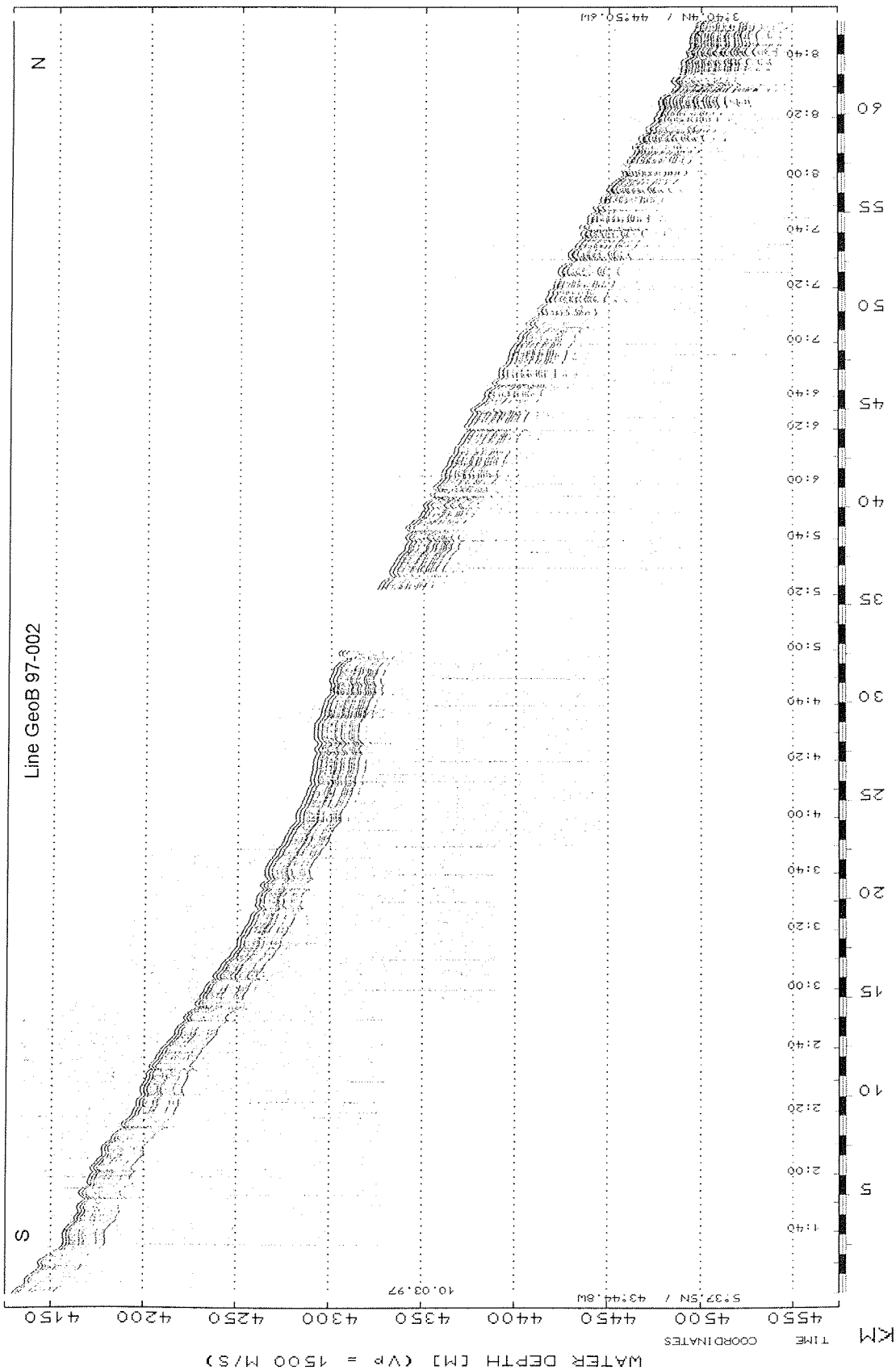


Figure 8 PARASOUND section along MCS line GeoB 97-002 on the northeastern flanks of the Ceará Rise. Reflection amplitude and penetration increase downslope indicating a variable influx of terrigenous material (see also Fig. 9).

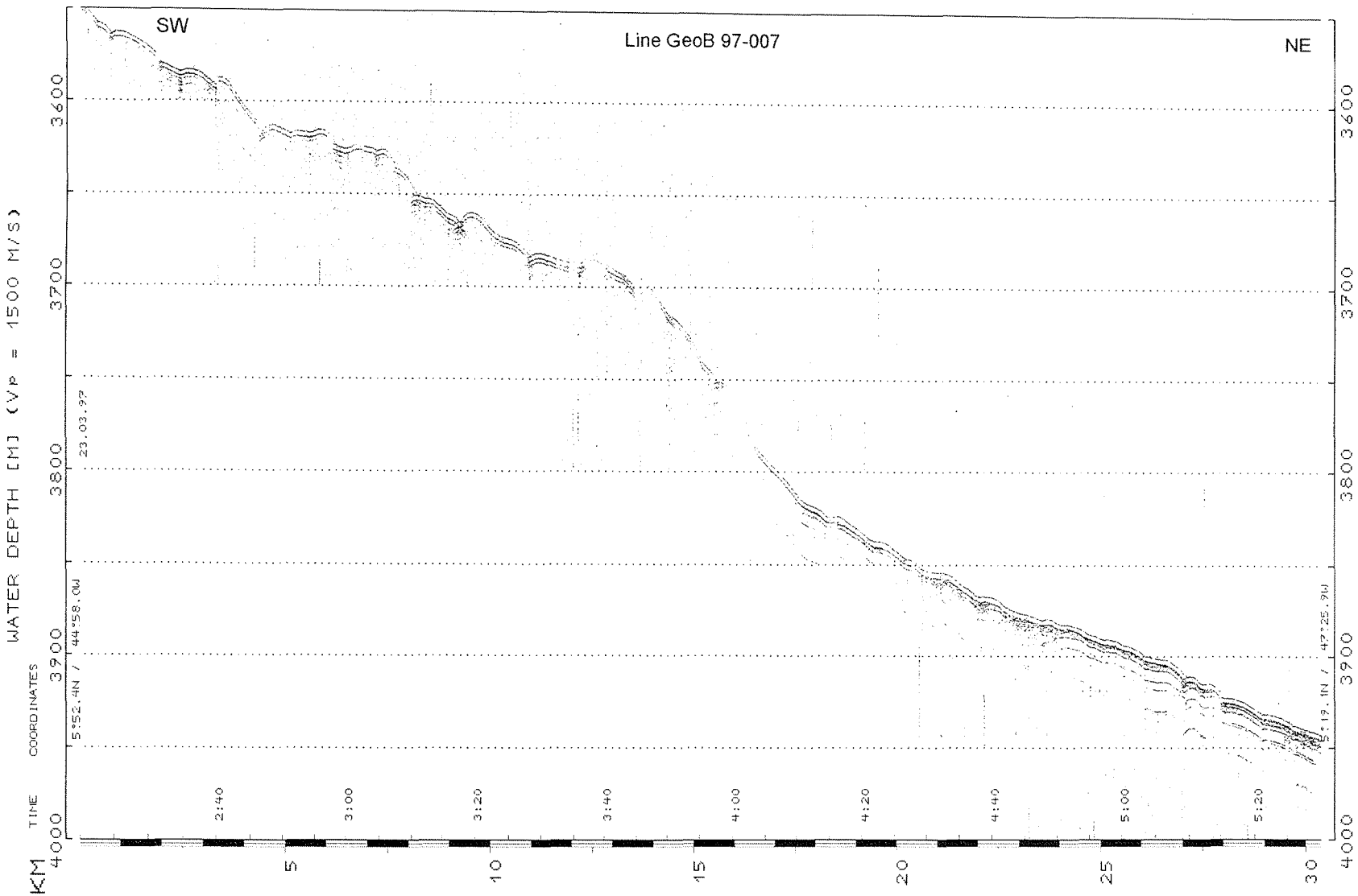


Figure 9 PARASOUND section along MCS line GeoB 97-007 on the northern flanks of the Ceará Rise. Reflection amplitude and penetration increase downslope indicating a variable influx of terrigenous material (see also Fig. 8).

The uppermost unit is underlain by an about 400 ms TWT thick sequence with a strong top reflector and moderate internal reflections. Amplitudes of the internal reflections increase to the east, where the reflectors terminate as top laps against the top reflector (Fig. 10) documenting an earlier eastward fan expansion. There is thus evidence for at least two major progradation phases.

Other remarkable features include a prominent reflector at 900 ms TWT and an about 100 ms TWT thick band of reflections in 2000 ms TWT which forms the base of the penetrated sedimentary series (Fig. 10). The 400 ms TWT thick reflection free zone between shotpoints 6300 and 6600 is tentatively interpreted as a slump.

The PARASOUND record along MCS line GeoB 97-001 (Fig. 11) shows the transition from near surface deposits of the southern and lower Amazon Fan to the Ceará Rise in water depths of around 4300 m. East of a more than 20 m deep erosive channel (central part of the profile) the about 4 m thick hemipelagic sediments vanish. The underlying fan deposits convert towards the rise from distinct subparallel layers in the west to a diffusely reflecting unit in the east. The rough sea floor topography and the presence of an erosive moat at the foot of the Ceará Rise flank indicate current controlled depositional processes.

Further to the north, where the slope of the Ceará Rise is less steep, the hemipelagic drape deposits are apparently not effected by bottom currents (Fig. 12, PARASOUND record along MCS line GeoB 97-007). Their lower boundary truncates underlying, divergent fan sediments striking out against a pinnacle, topped by a weak reflecting sediment sequence. The low reflection amplitudes indicate a reduced content of terrigenous components, owing to the elevated position. Towards the slopes of Ceará Rise reflection amplitudes of the wavy deposits decrease, presumably due to a decreasing influx of suspended material from the Amazon Fan.

### 4.3.3 Central and Southern Amazon Fan

The western end of MCS line GeoB 97-006 covers the southern Amazon Fan (Fig. 13). The profile strikes west - east almost perpendicular to the fan slope. Three interfingering seismic facies are identified, (1) semitransparent channel - levee systems (CLS), (2) weakly reflecting parallel layered units, and (3) high amplitude reflection sections.

Several CLSs of different dimensions can be discerned. High amplitude reflections beneath the crest of the systems represent channel-fill deposits. At the western end, weak parallel reflections onlap the levee flanks of the largest CLS. The hummocky surface of the CLS in the central part of the profile is caused by a high sinuosity of the meandering channel and the strike view orientation of the seismic line.

The distinct reflections in the eastern part are discontinuous and randomly oriented close to the CLS, they convert to continuous and subparallel reflections with increasing

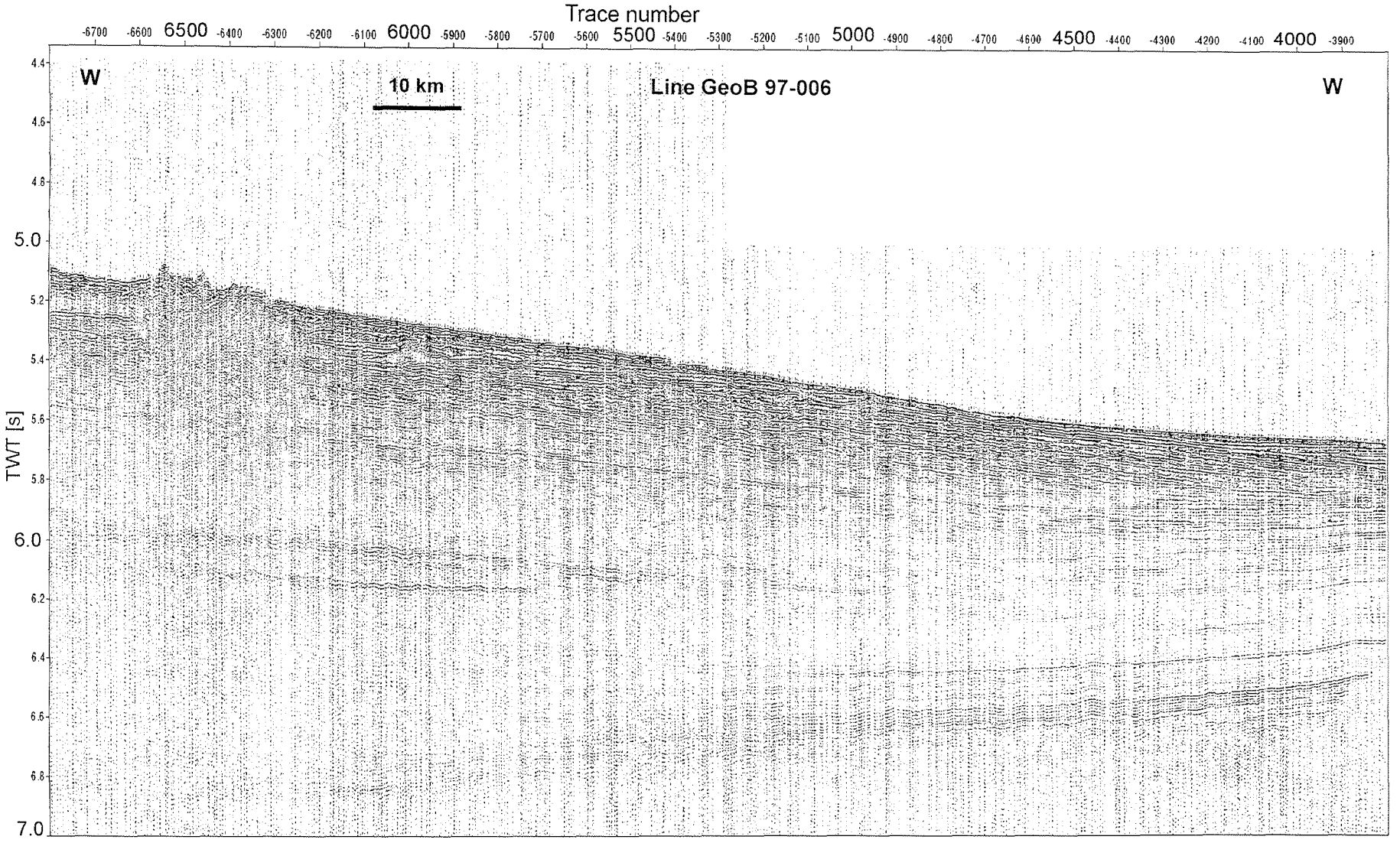


Figure 10 Middle part of multichannel seismic line GeoB 97-006 (GI-Gun) crossing the southern distal Amazon Fan. Thickness of sedimentary units increases upslope.

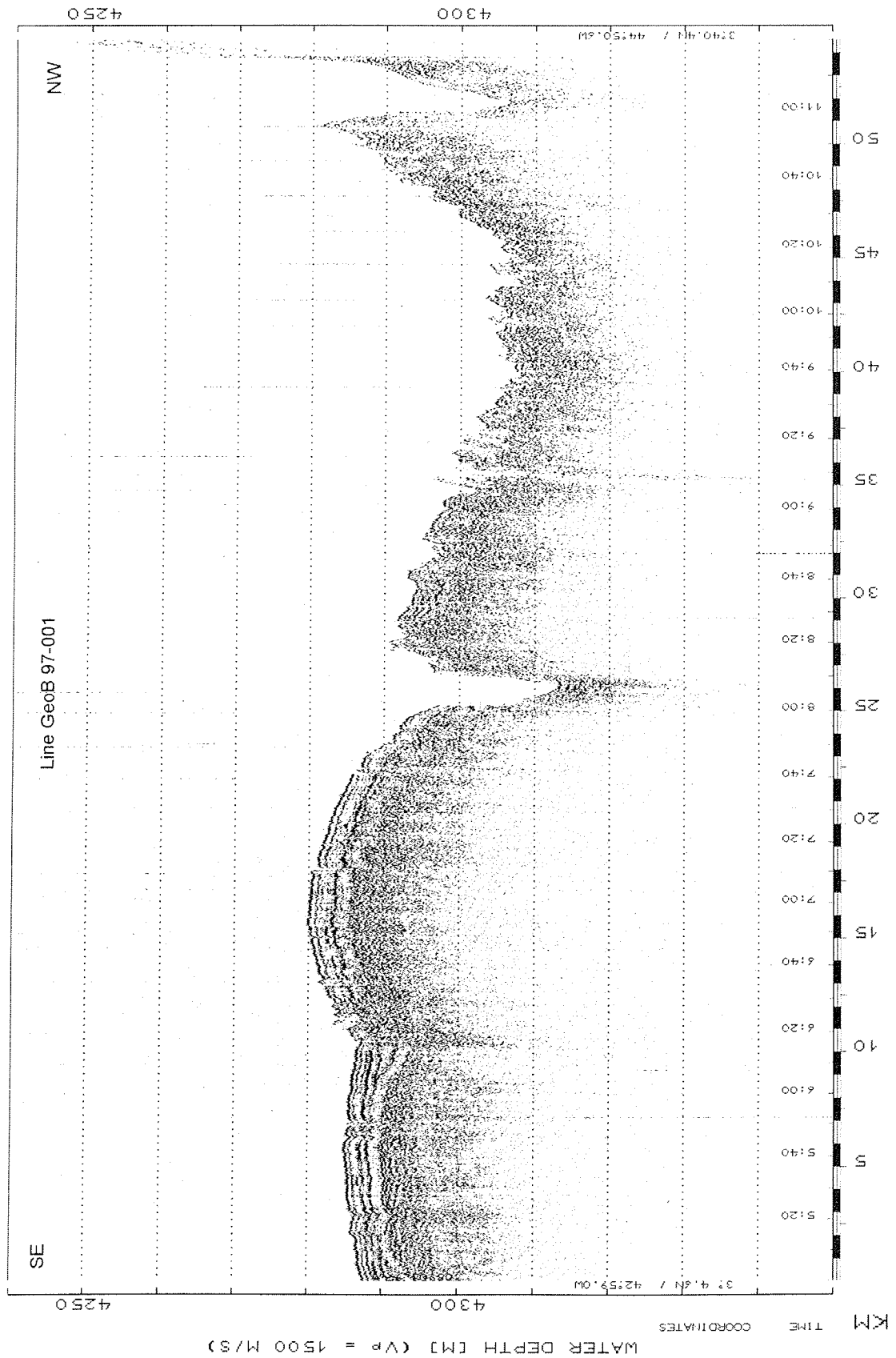


Figure 11 PARASOUND section along MCS line GeoB 97-001 in the distal southernmost Amazon Fan.

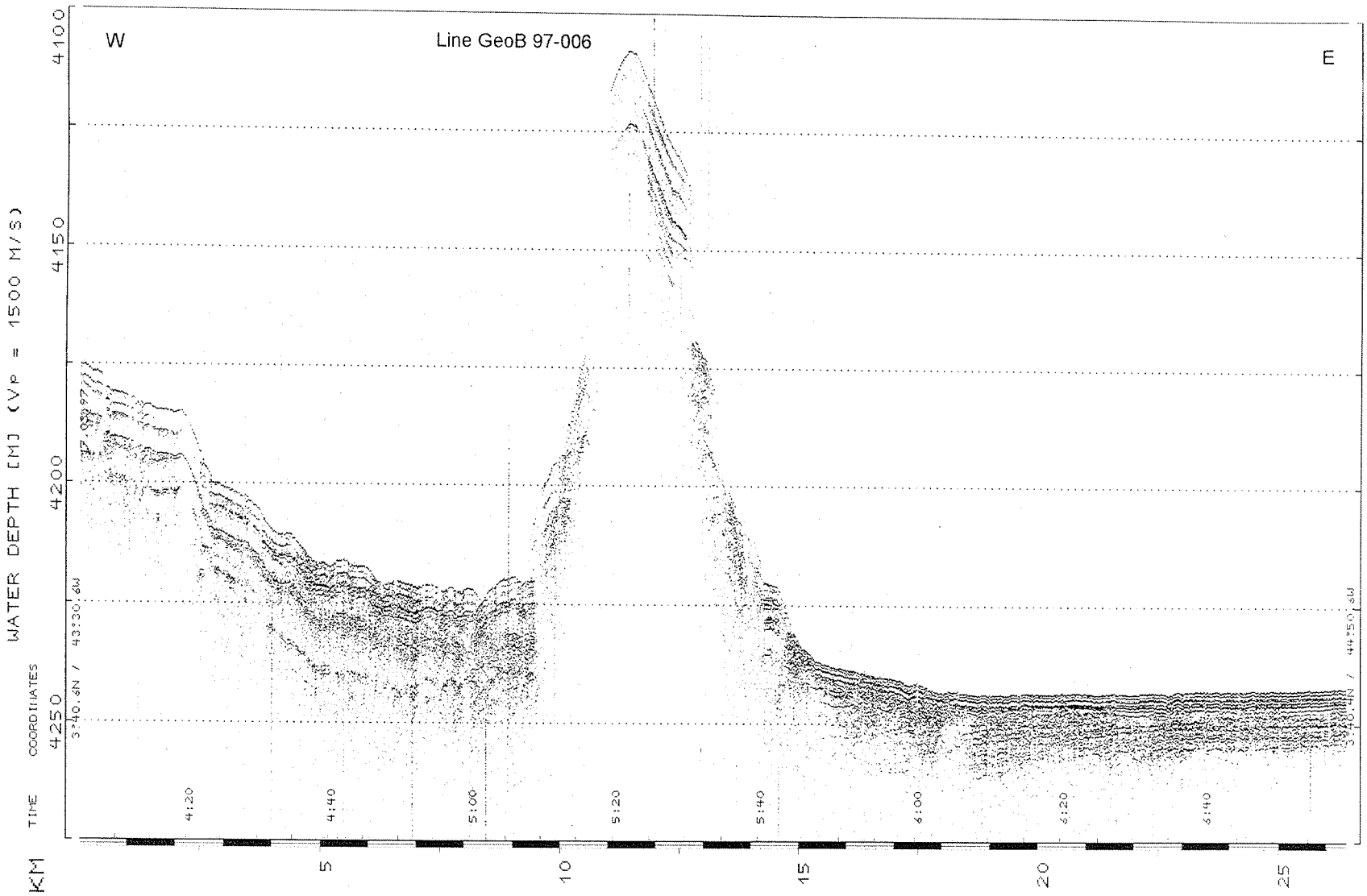


Figure 12 PARASOUND section along MCS line GeoB 97-006 at the foot of the Ceará Rise showing intervals of finer grained, hemipelagic deposits (left) and numerous coarser grained turbidites (right) separated by a sediment covered basement high.

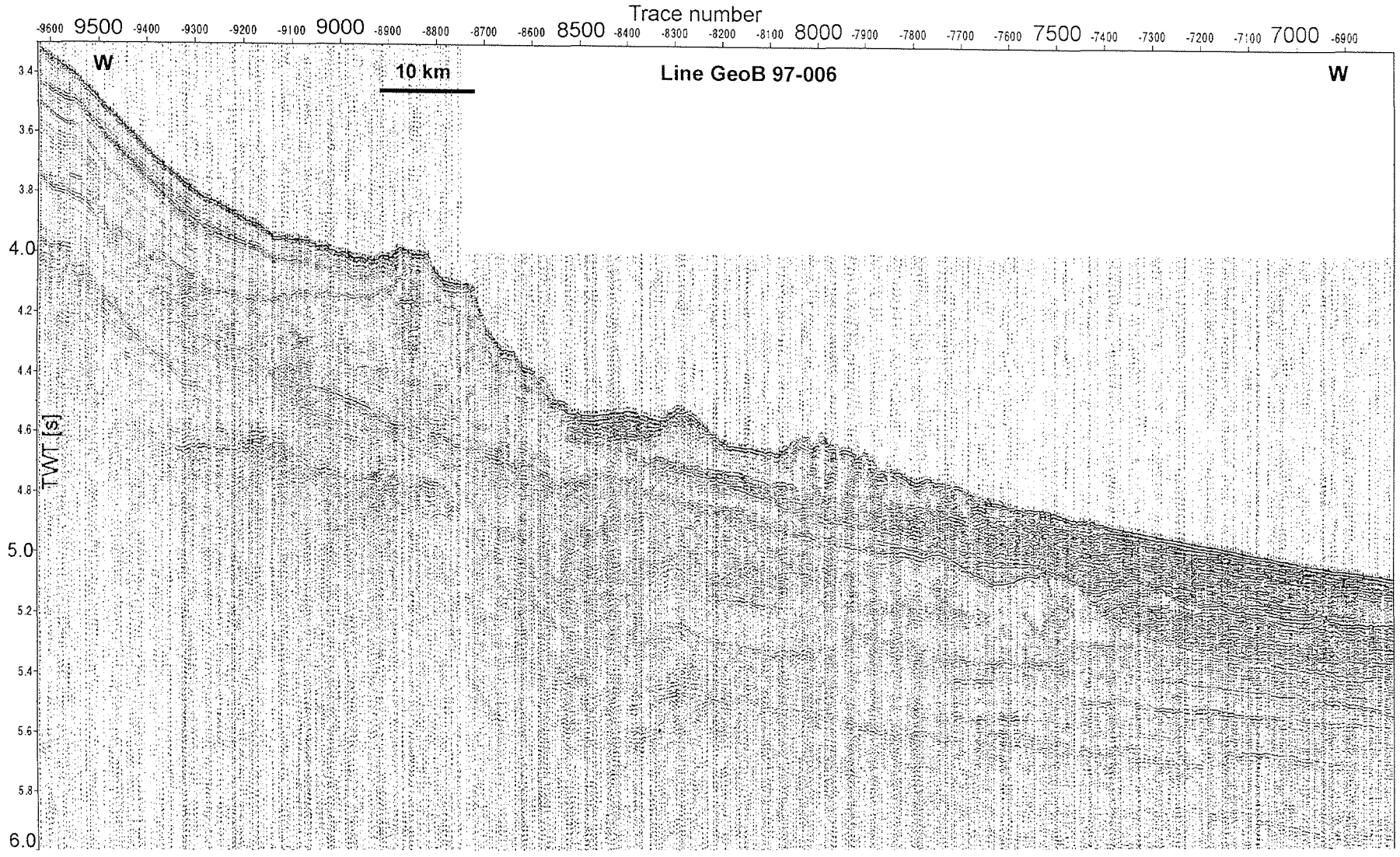


Figure 13 Western part of multichannel seismic line GeoB 97-006 (GI-Gun) at the transition between the proximal and distal Amazon Fan with buried and recently active channel - levee systems.

distance to the CLS. Some unconformities can be correlated to the base of CLSs, presumably representing the onset of CLS development during a late stage of sea level fall or lowstand.

The PARASOUND record of the upper 20 m of the sediments close to station GeoB 4409 on top of a distinctly meandering CLS (Fig. 14), reveals a semitransparent hemipelagic cover overlying fan deposits. Diffuse diffraction hyperbolae dominate the acoustic facies above the levee crest.

### 4.3.4 Amazon Channel

The youngest CLS of the Amazon Fan has been surveyed by 5 multichannel seismic lines, crossing both the active channel and adjacent ODP sites. The main purpose of these investigations was a correlation of the high-resolution seismic and digital echosounder data with published seismic records and the ODP core lithology.

Line GeoB 97-010 crossed ODP Sites 937 and 938, line GeoB 97-011 Site 939 and the CLS in the upper fan. The two subsequent lines (GeoB 97-012/-013) included traverses over the channel and ODP Sites 930, 940, 935 and 934 in the middle fan. The channel in the lower fan area adjacent ODP Sites 944 and 945 were surveyed with the last profile GeoB 97-014.

The watergun data from line GeoB 97-013 (Fig. 15) show the youngest CLS (Amazon Channel) bordered by the older Aqua Channel in the west and another older system to the east. Sea floor topography and sediment waves on the eastern flank of the main channel are resolved on a small scale owing to the high seismic source frequency. Channel fill deposits of the main channel form a parallel reflection series. High amplitude reflector packages (HARPs) within the levees beneath the levee crests of the main and eastern CLS clearly represent diffraction hyperbolae. The base of the CLSs are also characterized by HARPs.

### 4.3.5 Mid-Atlantic Ridge

On transect from the South American continental margin to the Canary Islands gravity cores have been taken from shallow water depth at mid-Atlantic Ridge near 17°N. PARASOUND records were used to identify appropriate coring stations. Figure 16 elucidates the difficulties encountered. The record is dominated by diffraction hyperbolae, only some of them of distinct shape (macrotopography). The microtopography causes a diffuse, prolonged echo, pretending penetration depths of 20 to 50 m. Core GeoB 4418, retrieved from 2720 m water depth near the northeastern end of the section, had but a length of around 4 m.

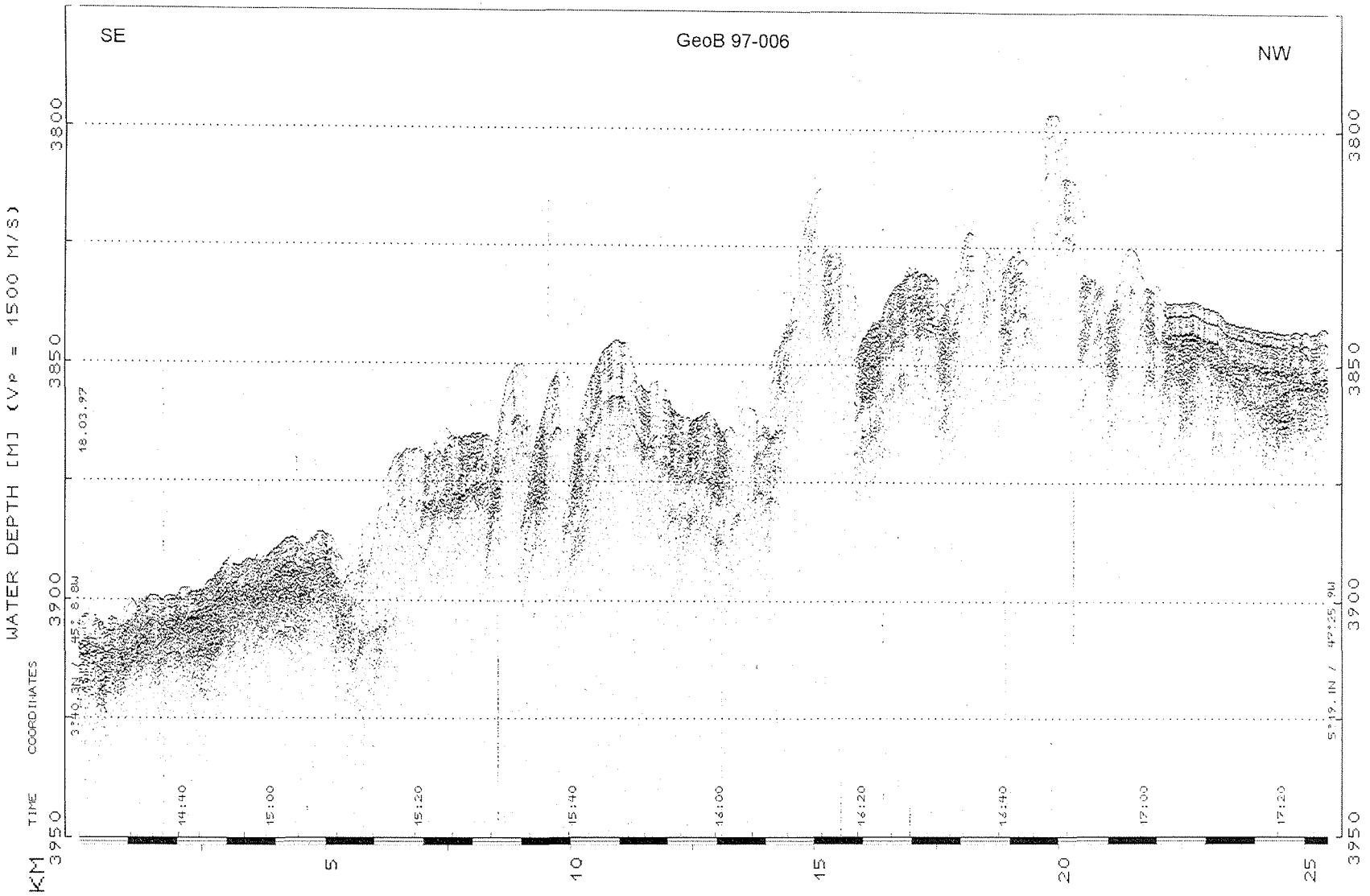


Figure 14 PARASOUND section along MCS line GeoB 97-006 on top of a meandering channel - levee systems in the Amazon Fan close to station GeoB 4409.

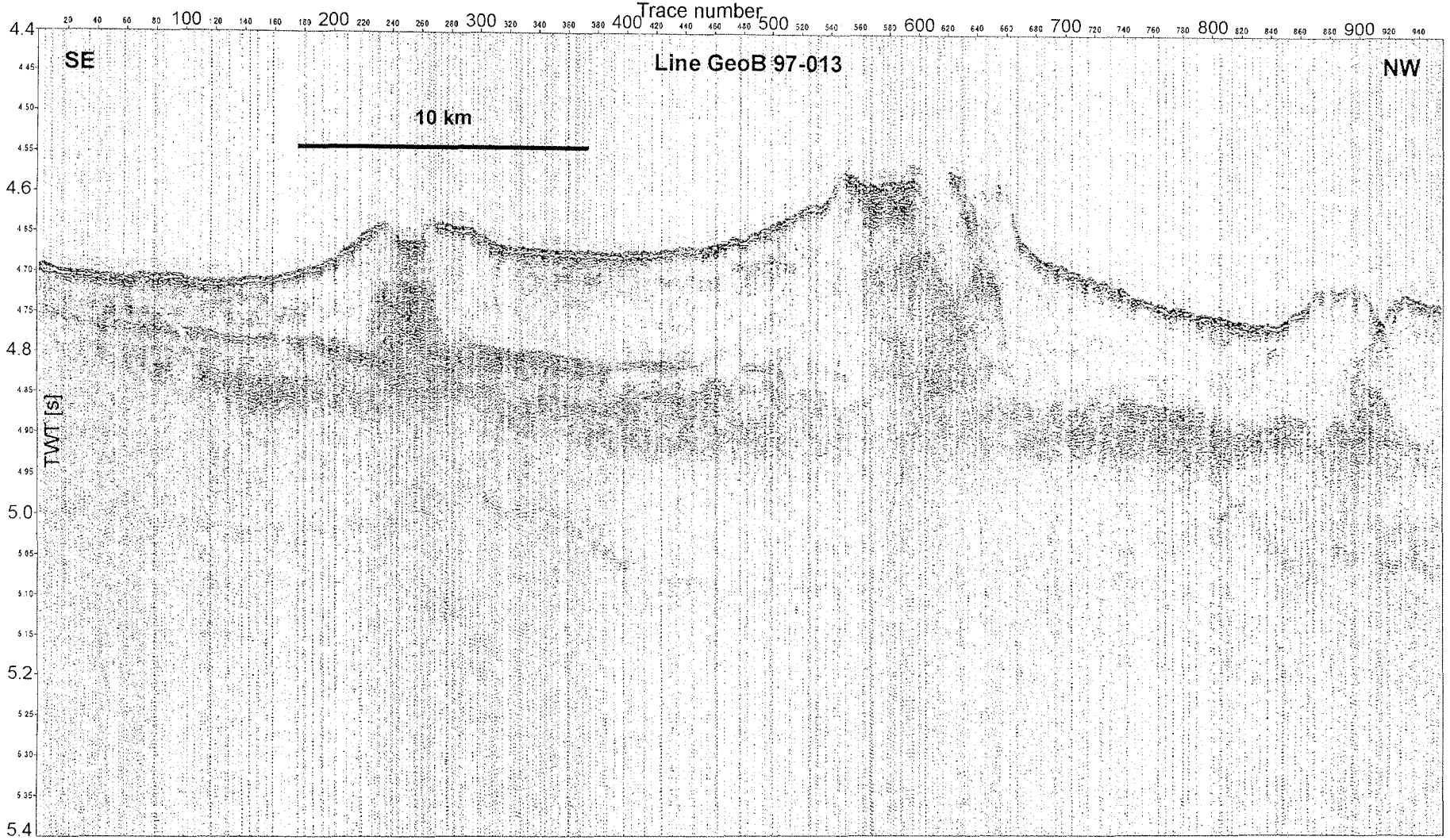


Figure 15 Section of multichannel seismic line GeoB 97-013 (Watergun, one channel) showing the recently active channel - levee systems in the central Amazon Fan bordered by the Aqua System to the west and an older, abandoned channel - levee system to the east.

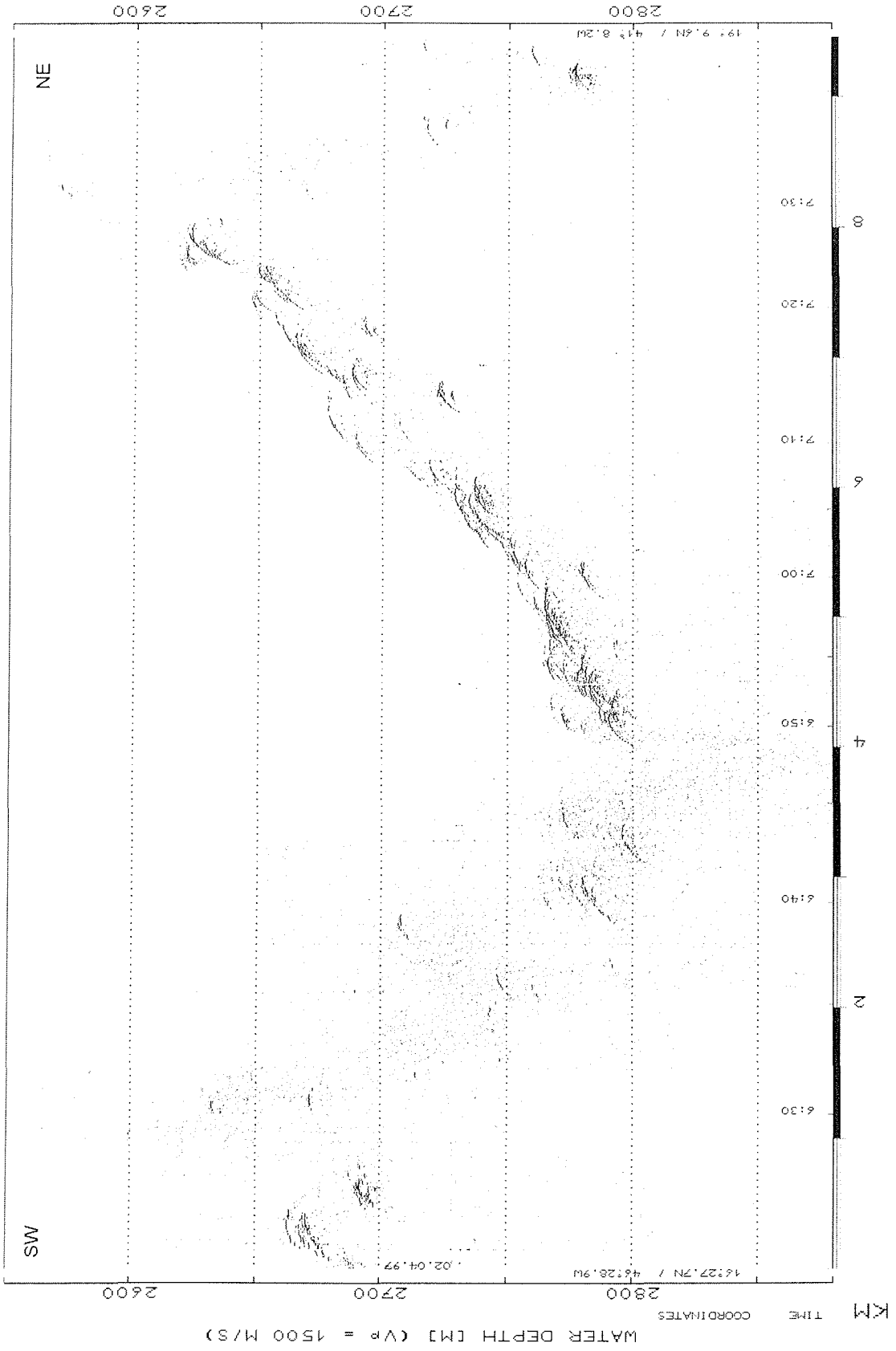


Figure 16 PARASOUND profile in the vicinity of station GeoB 4418 at the mid-Atlantic Ridge.

# 5 Sediment Sampling

*A. Benthien, H. Buschhoff, B. Donner, B. Dorschel, M. Giese, A. Meyer, B. Meyer-Schack, S. Mulitza, U. Rosiak, B. Schlünz, A. Vink*

The box corer, multicorer and gravity corer were used to recover surface and late Quaternary sediments at 24 stations on the Ceará Rise, in the Amazon Fan, on the continental slope off Guyana and at the mid-Atlantic Ridge near 17°N from water depths between about 2500 and 4600 m. Detailed information is summarized in the station list (Table 2).

## 5.1 Multicorer and Box Corer

The multicorer is designed to recover undisturbed surface sediment sections together with the overlying bottom water. The device deployed during Cruise M38/2 was equipped with 4 small and 8 large (6 and 10 cm inner diameter, respectively), 60 cm long plastic tubes. Typically 6 to 12 tubes were filled with more than 30 cm of sediment on the Ceará Rise and in the adjacent abyssal plains as well as in the Amazon Fan and on the Guyana continental slope. At the mid-Atlantic Ridge only 4 to 9 tubes recovered less than 20 cm of sediment (Table 3). The following standard sampling scheme was modified accordingly:

- 1 large tube was cut into 1 cm slices and frozen for organic carbon geochemistry,
- 1 large tube was cut into 1 cm slices for dinoflagellates analysis,
- 3 large tubes were cut into 1 cm slices to study the foraminiferal assemblages,
- 1 large tube was cut into 1 cm slices and frozen for sedimentological investigations and organic matter microscopy,
- 1 small tube was cut into 1 cm slices for rock magnetic analyses,
- a 1 cm surface sample of a small or large tube was preserved for granulometry, diatom and radiolaria investigations,
- pore waters of 1 small and 1 large tube were analyzed geochemically,
- 1 large and 2 small tubes were frozen as archive cores,
- 50 ml of bottom water were sampled for carbon and oxygen isotope analyses.

The box corer was used only at one station (GeoB 4420). After removal of the overlying water and measurement of the sediment temperature, the sediment surface has been photographed and sampled as follows:

- 400 $cm^2$ to study the foraminiferal assemblages were stained with rose bengal,
- 200 $cm^2$ for radiolaria analyses were stained with ethanol,
- 25 $cm^2$ for diatom investigations were stained with methanol,

Table 2 Station List METEOR Cruise M38/ 2.

| GeoB No. | Date 1997 | Time (UTC) | Device | Latitude (°N) | Longitude (°W) | Water Depth (m) | Core Length (cm) | Remarks |
|---|---|---|---|---|---|---|---|---|
| Ceará Rise | | | | | | | | |
| 4401-1 | 09.03. | 06:28 | KWS | 04°48.0' | 43°45.8' | 3400 | - | 15/15; 100, 50, 20, 10 m |
| 4401-2 | 09.03. | 07:47 | KWS | 04°48.0' | 43°45.8' | 3401 | - | 15/15; 2500, 2000, 1500, 1000, 800, 700, 600, 500, 400, 300, 250, 200, 150, 75, 3 m |
| 4401-3 | 09.03. | 10:09 | MC + CTD | 04°47.9' | 43°45.9' | 3396 | 33 | 8/4, 20 m pinger, 50 m CTD |
| 4401-4 | 09.03. | 13:11 | SL12 | 04°48.0' | 43°45.9' | 3397 | 695 | |
| 4401-5 | 09.03. | - | ELINOR | 04°45.6' | 43°45.5' | 3356 | - | released |
| 4401-6 | 09.03. | - | PROFILUR | 04°45.8' | 43°45.8' | 3355 | - | released |
| 4402-1 | 10.03. | 15:20 | KWS | 06°39.3' | 43°43.6' | 4638 | - | 15/15, 100, 50, 20, 10 m |
| 4402-2 | 10.03. | 16:37 | SL12 | 06°39.3' | 43°43.5' | 4637 | 822 | |
| 4402-3 | 10.03. | 19:20 | MC + CTD | 06°39.4' | 43°43.7' | 4641 | 35 | 6/4, 20 m pinger, 50 m CTD |
| 4403-1 | 11.03. | 02:18 | MC + CTD | 06°13.4' | 43°44.1' | 4503 | 34 | 3/4, 20 m pinger, 50 m CTD |
| 4403-2 | 11.03. | 06:17 | SL12 | 06°13.4' | 43°44.0' | 4505 | 844 | |
| 4404-1 | 11.03. | 10:34 | SL12 | 06°03.6' | 43°44.3' | 4402 | 710 | |
| 4404-2 | 11.03. | 13:41 | MC + CTD | 06°03.5' | 43°44.3' | 4397 | 34 | 8/4, 20 m pinger, 50 m CTD |
| 4405-1 | 11.03. | 18:07 | KWS | 05°54.5' | 43°44.5' | 4297 | - | 15/15 |
| 4405-2 | 11.03. | 19:34 | MC + CTD | 05°54.4' | 43°44.7' | 4300 | 34 | 3/4 |
| 4405-3 | 11.03 | 23:02 | SL12 | 5°54,5' | 43°44,5' | 4300 | 629 | at 60 cm depth ~ 20 cm sediment washed out between segments |
| 4405-4 | 12.03. | - | ELINOR | 04°45.2' | 43°47.2' | - | - | recovery failed |
| 4405-5 | 12.03. | - | PROFILUR | 04°45.2' | 43°47.2' | - | - | recovery failed |
| 4406-1 | 12.03. | 16:31 | SL12 | 05°05.6' | 43°45.3' | 3719 | 659 | |
| 4406-2 | 12.03. | 18:45 | MC + CTD | 05°05.4' | 43°45.7' | 3709 | 30 | 6/2 |

Table 2 continued

| GeoB No. | Date 1997 | Time (UTC) | Device | Latitude (°N) | Longitude (°W) | Water Depth (m) | Core Length (cm) | Remarks |
|---|---|---|---|---|---|---|---|---|
| 4406-3 | 12.03. | - | ELINOR | 04°45.6' | 43°47.6' | - | - | recovery failed |
| 4406-4 | 12.03. | - | PROFILUR | 04°45.6' | 43°47.6' | - | - | recovery failed |
| 4407-1 | 15.03. | 19:53 | SL12 | 03°49.4' | 41°37.3' | 3303 | 831 | geochemistry |
| 4407-2 | 15.03. | 21:55 | MC + CTD | 03°49.4' | 41°37.3' | 3306 | 32 | 5/4, 20 m pinger, 50 m CTD |
| 4407-3 | 16.03. | 00:49 | SL12 | 03°49.3' | 41°37.3' | 3306 | 753 | former GeoB site 1523 |
| 4407-4 | 16.03. | 02:07 | KWS | 03°49.5' | 41°36.8' | 3313 | - | 15/15; 100, 50, 20, 10 m |
| 4407-5 | 15.03. | 03:21 | KWS | 03°49.3' | 41°36.8' | 3312 | - | 15/15; 3000, 2000, 1500, 1000, 800, 700, 600, 500, 400, 300, 250, 200, 150, 75, 3 m |
| 4407-6 | 18.03. | - | PROFILUR | 04°37.9' | 44°45.0' | - | - | recovered |
| Amazon Fan | | | | | | | | |
| 4408-1 | 19.03. | 20:52 | KWS | 03°40.0' | 46°07.8' | 3457 | - | 15/15; 100, 50, 20, 10 m |
| 4408-2 | 19.03. | 21:47 | SL12 | 03°40.0' | 46°07.7' | 3466 | 652 | |
| 4408-3 | 19.03. | 23:56 | MC + CTD | 03°40.0' | 46°07.7' | 3466 | 33 | 6/2; 20 m pinger, 50 m CTD |
| 4409-0 | 20.03. | - | PROFILUR | 03°38.5' | 45°14.4' | - | - | released |
| 4409-1 | 20.03. | 10:11 | SL12 | 03°39.9' | 45°14.4' | 3847 | 525 | |
| 4409-2 | 20.03. | 12:29 | MC + CTD | 03°40.0' | 45°14.5' | 3846 | 32 | 4/4; 20 m pinger, 50 m CTD |
| 4409-3 | 20.03. | 16:01 | SL12 | 03°39.7' | 45°14.6' | 3855 | 631 | geochemistry |
| 4409-4 | 20.03. | - | PROFILUR | 03°37.0' | 45°16.5' | - | - | recovered |
| 4410-1 | 21.03. | 00:36 | KWS | 03°40.6' | 44°19.5' | 4156 | - | 15/15; 100, 50, 20, 10 m |
| 4410-2 | 21.03. | 01:41 | SL12 | 03°40.5' | 44°19.6' | 4156 | 736 | |
| 4410-3 | 21.03. | 04:18 | MC + CTD | 03°40.4' | 44°19.4' | 4158 | 33 | 4/2; 20 m pinger, 50 m CTD |

Table 2 continued

| GeoB No. | Date 1997 | Time (UTC) | Device | Latitude (°N) | Longitude (°W) | Water Depth (m) | Core Length (cm) | Remarks |
|---|---|---|---|---|---|---|---|---|
| Ceará Rise | | | | | | | | |
| 4411-1 | 23.03. | 23:13 | MC + CTD | 05°26.0' | 44°29.7' | 3298 | 33 | 4/2; 20 m pinger, 50 m CTD |
| 4411-2 | 24.03. | 02:49 | SL12 | 05°26.0' | 44°29.7' | 3295 | 686 | ~ 10 cm sediment washed out at 199 cm |
| 4412-0 | 24.03. | - | PROFILUR | 05°42.3' | 44°22.4' | - | - | released |
| 4412-1 | 24.03. | 06:42 | KWS | 05°43.4' | 44°21.6' | 3769 | - | 15/15; 100, 50, 20, 10 m |
| 4412-2 | 24.03. | 07:42 | SL12 | 05°43.4' | 44°21.6' | 3766 | 785 | |
| 4412-3 | 24.03. | 10:00 | MC + CTD | 05°43.4' | 44°21.6' | 3764 | 30 | 6/3; 20 m pinger, 50 m CTD |
| 4412-4 | 24.03. | - | PROFILUR | 05°41.6' | 44°23.7' | - | - | recovered |
| 4413-1 | 24.03. | 17:12 | MC + CTD | 06°05.2' | 44°11.6' | 4291 | 32 | 8/4; 20 m pinger, 50 m CTD |
| 4413-2 | 24.03. | 20:39 | SL12 | 06°05.1' | 44°11.5' | 4295 | 754 | |
| 4414-1 | 25.03. | 03:03 | SL12 | 05°56.7' | 44°55.5' | 3236 | 734 | |
| 4414-2 | 25.03. | 05:04 | MC + CTD | 05°56.9' | 44°55.5' | 3239 | 32 | 7/4; 20 m pinger, 50 m CTD |
| 4415-1 | 25.03. | 07:58 | KWS | 05°51.2' | 44°58.7' | 3586 | - | 15/15; 100, 50, 20, 10 m |
| 4415-2 | 25.03. | 09:15 | MC + CTD | 05°51.2' | 44°58.7' | 3584 | 33 | 8/4; 20 m pinger, 50 m CTD |
| 4415-3 | 25.03. | 12:11 | SL12 | 05°51.1' | 44°58.7' | 3584 | 711 | |
| 4416-1 | 25.03. | 15:21 | SL12 | 05°40.5' | 45°05.3' | 3901 | 301 | core tube broken |
| 4416-2 | 25.03. | 17:45 | MC + CTD | 05°40.5' | 45°05.3' | 3903 | 34 | |
| 4416-3 | 25.03. | 20:51 | SL8 | 05°40.5' | 45°05.3' | 3901 | 518 | |
| 4417-1 | 26.03. | - | PROFILUR | 05°08.7' | 46°33.6' | - | - | released |
| 4417-2 | 26.03. | 06:28 | KWS | 05°08.3' | 46°34.6' | 3512 | - | 15/15; 100, 50, 20, 10 |
| 4417-3 | 26.03 | 07:41 | KWS | 05°08.4' | 46°34.4' | 3511 | - | 15/15; 3000, 2000, 1500, 1000, 800, 700, 600, 500, 400, 300, 250, 200, 150, 75, 3 m |

Table 2 continued

| GeoB No. | Date 1997 | Time (UTC) | Device | Latitude (°N) | Longitude (°W) | Water Depth (m) | Core Length (cm) | Remarks |
|---|---|---|---|---|---|---|---|---|
| 4417-4 | 26.03. | 09:41 | SL8 | 05°08.3' | 46°34.5' | 3511 | 649 | |
| 4417-5 | 26.03. | 11:48 | MC + CTD | 05°08.3' | 46°34.5' | 3511 | 37 | 7/2; 20 m pinger, 50 m CTD |
| 4417-6 | 26.03. | 14:39 | SL8 | 05°08.2' | 46°34.5' | 3510 | 647 | geochemistry |
| 4417-7 | 26.03. | 17.09 | SL8 | 05°08.3' | 46°34.5' | 3510 | 549 | geochemistry |
| 4417-8 | 26.03. | - | PROFILUR | 05°08.7' | 46°33.7' | - | - | recovered |
| Guayana Continental Slope | | | | | | | | |
| 4418-1 | 29.03. | 23:08 | SL8 | 09°15.7' | 54°03.6' | 2499 | 711 | |
| 4418-2 | 30.03. | 00:44 | MC + CTD | 09°15,7' | 54°03.6' | 2490 | 34 | 7/2; 20 m pinger, 50 m CTD, no CTD data |
| 4418-3 | 30.03. | 04:30 | SL8 | 09°15.6' | 54°03.5' | 2495 | 700 | geochemistry |
| 4419-1 | 30.03. | - | PROFILUR | 09°40.2' | 54°15.5' | - | - | released |
| 4419-2 | 30.03. | 08:52 | KWS | 09°41.2' | 54°15.7' | 4486 | - | 15/15; 100, 50, 20, 10 m |
| 4419-3 | 30.03. | 10:03 | KWS | 09°40.9' | 54°15.5' | 4487 | - | 15/15; 3000, 2000, 1500, 1000, 800, 700, 600, 500, 400, 300, 200, 150, 75, 3 m |
| 4419-4 | 30.03. | 12:07 | SL8 | 09°40.9' | 54°15.4' | 4486 | 827 | sediment in weight |
| 4419-5 | 30.03. | 14:41 | MC + CTD | 09°40.7' | 54°15.5' | 4515 | 34 | 8/4; 20 m pinger, 50 m CTD |
| 4419-6 | 30.03. | 18:46 | SL12 | 09°40.4' | 54°15.2' | 4486 | 924 | |
| 4419-7 | 30.03. | - | PROFILUR | 09°37.5' | 54°15.8' | - | - | recovered |
| Mid-Atlantic Ridge | | | | | | | | |
| 4420-1 | 02.04. | 08:33 | MC + CTD | 16°28.3' | 46°27.8' | 2763 | 14 | 4/2; 20 m pinger, 50 m CTD |
| 4420-2 | 02.04. | 10:56 | SL8 | 16°28.4' | 46°27.8' | 2767 | 401 | |
| 4420-3 | 02.04. | 12:56 | GKG | 16°28.3' | 46°27.8' | 2767 | 40 | |
| 4421-1 | 02.04. | - | PROFILUR | 16°59.1' | 46°00.9' | - | - | released |

Table 2 continued

| GeoB No. | Date 1997 | Time (UTC) | Device | Latitude (°N) | Longitude (°W) | Water Depth (m) | Core Length (cm) | Remarks |
|---|---|---|---|---|---|---|---|---|
| 4421-2 | 02.04. | 20:13 | MC + CTD | 16°59.4' | 46°00.6' | 3176 | 20 | 7/2; 20 m pinger, 50 m CTD |
| 4421-3 | 02.04. | 22:52 | SL8 | 16:59.3' | 46°00.7' | 3184 | 343 | |
| 4421-4 | 02.04. | 23:57 | KWS | 16°59.8' | 46°00.6' | 3146 | - | 15/15; 100, 50, 20, 10 m |
| 4421-5 | 03.04 | 01:13 | KWS | 16°59.8' | 46°00.6' | 3146 | - | 15/15; 3000, 2000 1000, 900, 800, 700, 600, 500, 400, 300, 250, 200, 150, 75, 3 m |
| 4421-6 | 03.04. | | PROFILUR | 16°59.6' | 46°01.7' | - | - | recovered |
| 4422-1 | 03.04. | 08:43 | MC + CTD | 17°27.3' | 45°38.6' | 3851 | 17 | 4/2; 20 m pinger, 50 m CTD |
| 4422-2 | 03.04. | 13:14 | SL8 | 17°27.3' | 45°38.6' | 3867 | 427 | |
| 4423-1 | 03.04. | 19:37 | MC + CTD | 17°53.0' | 45°14.2' | 4172 | 16 | 0/4; 20 m pinger, 50 m CTD |
| 4423-2 | 03.04. | 22:56 | SL8 | 17°53.0' | 45°14.3' | 4187 | 736 | |
| 4423-3 | 04.04. | 01:22 | MC | 17°53.1' | 45°14.1' | 4189 | 15 | 3/2; 20 m pinger |
| 4424-1 | 04.04. | 11:14 | SL12 | 18°12.0' | 44°00.6' | 4778 | 940 | |
| 4424-2 | 04.04. | 13:54 | MC + CTD | 18°11.7' | 44°01.1' | 4779 | 11 | 4/2; 20 m pinger, 50 m CTD |

Equipment:

| | |
|---|---|
| CTD | CTD Profiler |
| ELINOR | Lander ELINOR |
| GKG | Box Corer (Großkastengreifer) |
| KWS | Multiple Water Sampler (Kranzwasserschöpfer) |
| MC | Multicorer (10 tubes) |
| PROFILUR | Lander PROFILUR |
| SL8 | Gravity Corer (Schwerelot), 8 m |
| SL12 | Gravity Corer (Schwerelot), 12 m |

Table 3 Multicorer sampling.

| Station GeoB No. | Water Depth (m) | Core Length (cm) | Recovery large/small tubes | Organic Geochemistry | Dinoflagellates | Foraminifers | Magnetics | Archive (frozen) | Pore Water Geochemistry | Bottom Water C-Isotopes, O-Isotopes |
|---|---|---|---|---|---|---|---|---|---|---|
| 4401-3 | 3399 | 33 | 8/4 | 2/0 | 1/0 | 3/1 | 0/1 | 1/1 | 4/0 | x |
| 4402-3 | 4639 | 35 | 6/4 | 1/0 | 1/0 | 3/0 | 0/1 | 0/2 | 1/1 | x |
| 4403-1 | 4504 | 34 | 3/4 | 1/0 | 0/1 | 2/1 | 0/1 | 0/1 | 0/0 | x |
| 4404-2 | 4398 | 34 | 8/4 | 2/0 | 1/0 | 3/0 | 0/1 | 1/2 | 1/1 | x |
| 4405-2 | 4300 | 34 | 3/4 | 1/0 | 0/0 | 1/2 | 0/1 | 0/1 | 1/0 | x |
| 4406-2 | 3700 | 30 | 6/2 | 1/0 | 0/0 | 3/0 | 0/1 | 1/0 | 1/1 | x |
| 4407-2 | 3303 | 32 | 5/4 | 1/0 | 1/0 | 2/2 | 0/1 | 0/0 | 1/1 | x |
| 4408-3 | 3468 | 33 | 6/2 | 1/0 | 1/0 | 2/1 | 0/1 | 1/0 | 1/1 | x |
| 4409-2 | 3856 | 32 | 4/4 | 1/0 | 1/0 | 1/2 | 0/1 | 0/1 | 2/1 | x |
| 4410-2 | 4157 | 33 | 4/2 | 1/0 | 1/0 | 2/0 | 0/1 | 0/1 | 0/0 | x |
| 4411-1 | 3300 | 33 | 4/2 | 1/0 | 1/0 | 2/0 | 0/1 | 0/1 | 0/0 | x |
| 4412-3 | 3767 | 30 | 6/3 | 1/0 | 1/0 | 2/0 | 0/1 | 0/1 | 2/1 | x |
| 4413-1 | 4295 | 32 | 8/4 | 2/0 | 1/0 | 2/1 | 0/1 | 3/2 | 0/0 | x |
| 4414-2 | 3245 | 32 | 7/4 | 2/0 | 1/0 | 2/1 | 0/1 | 2/2 | 0/0 | x |
| 4415-3 | 3584 | 33 | 8/4 | 2/0 | 1/0 | 2/2 | 1/0 | 2/2 | 0/0 | x |
| 4416-2 | 3902 | 34 | 8/2 | 2/0 | 0/0 | 2/0 | 0/1 | 3/0 | 1/1 | x |
| 4417-5 | 3510 | 37 | 7/2 | 2/0 | 1/0 | 2/0 | 0/1 | 1/0 | 1/1 | x |
| 4418-2 | 2490 | 34 | 7/2 | 2/0 | 1/0 | 3/0 | 0/1 | 1/0 | 0/1 | x |
| 4419-5 | 4515 | 34 | 8/4 | 2/0 | 1/1 | 2/0 | 0/1 | 1/1 | 2/1 | x |
| 4420-1 | 2763 | 14 | 4/2 | 1/0 | 1/0 | 1/1 | 0/1 | 0/0 | 1/1 | x |
| 4421-2 | 3176 | 20 | 7/2 | 1/0 | 1/0 | 2/1 | 0/1 | 1/0 | 2/1 | x |
| 4422-1 | 3851 | 17 | 4/2 | 1/0 | 1/0 | 2/0 | 0/1 | 0/1 | 0/0 | x |
| 4423-1 | 4172 | 16 | 0/4 | 0/0 | 0/1 | 0/0 | 0/0 | 0/3 | 0/0 | x |
| 4423-3 | 4189 | 15 | 3/2 | 1/0 | 1/0 | 1/1 | 0/1 | 0/0 | 0/0 | x |
| 4424-2 | 4779 | 11 | 4/2 | 1/0 | 1/0 | 2/0 | 0/1 | 0/1 | 0/0 | x |

- 25 $cm^2$ to study magnetic bacteria,
- 200 $cm^2$ for organic geochemistry were frozen at -27 °C,
- 1 syringe (10 ml) for clay mineral investigation,
- 1 sample (5 ml) for Thorium / Beryllium analysis.

Thereafter the front panel of the box corer was opened, the sediment cleaned, photographed and described. In addition to 3 archive cores (12 cm diameter) two series of 10 ml syringes were taken at 3 cm depth intervals, one for foraminiferal and one for organic geochemical analyses.

## 5.2 Gravity Cores

Some 210 m of sediments were recovered with the gravity corer during Cruise M38/2. Individual core lengths varied between 300 and 940 cm. All core liners have been marked with a straight line before use to retain a common azimuthal orientation of the core segments for paleomagnetic purposes. After recovery, the core liners were cut into 1 m long segments, sealed with caps at both ends and inscribed (Fig. 17).

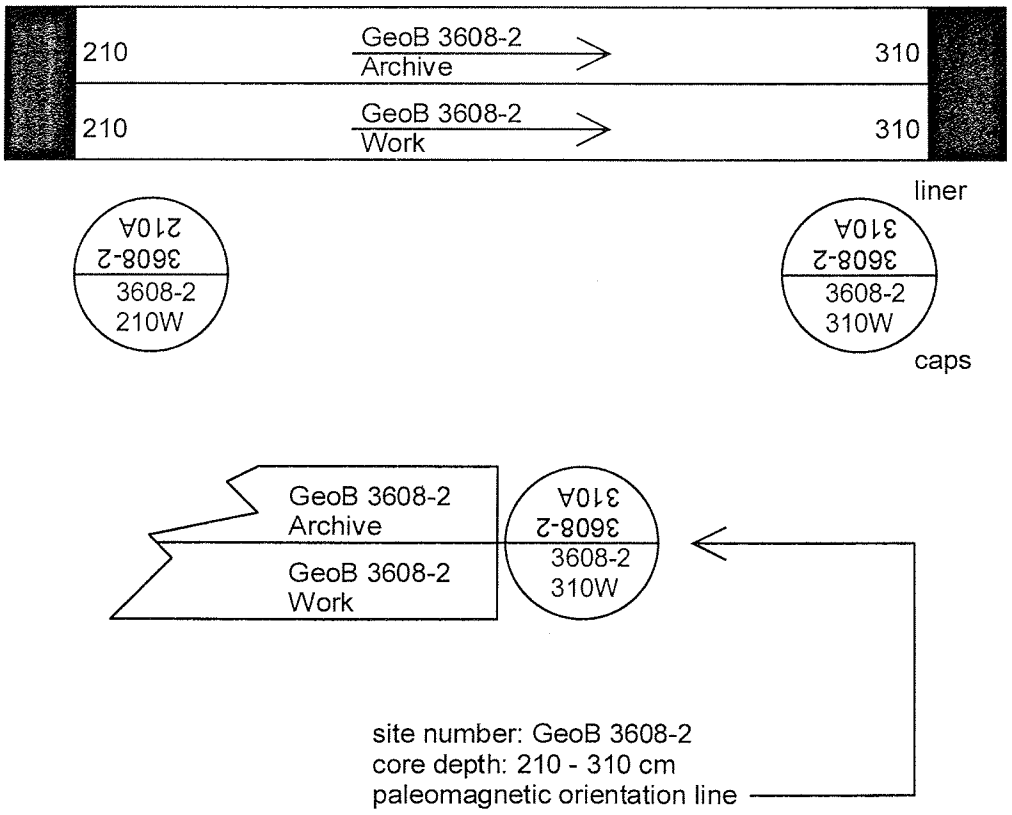


Figure 17 Inscription scheme of gravity core segments.

Table 4 Gravity core sampling.

| Station GeoB | Water Depth (m) | Core Length (cm) | Organic Geochemistry (10 ml) | Foraminifers (10 ml) | Paleomagnetics (7 ml) | Smear Slides |
|---|---|---|---|---|---|---|
| 4401-4 | 3397 | 695 | 139 | 139 | 136 | 18 |
| 4402-2 | 4638 | 823 | 165 | 165 | 162 | 15 |
| 4403-2 | 4505 | 850 | 170 | 170 | 164 | 18 |
| 4404-1 | 4402 | 712 | 142 | 142 | 144 | 20 |
| 4405-3 | 4300 | 629 | 126 | 126 | 125 | 18 |
| 4406-1 | 3719 | 659 | 132 | 132 | 129 | 14 |
| 4407-1 | 3303 | 831 | 166 | 166 | 166 | - |
| 4407-3 | 3306 | 761 | 152 | 152 | 149 | 19 |
| 4408-2 | 3466 | 660 | 132 | 132 | 128 | 10 |
| 4409-1 | 3847 | 531 | 106 | 106 | 100 | 8 |
| 4409-3 | 3855 | 631 | 126 | 126 | 125 | - |
| 4410-2 | 4156 | 747 | 149 | 149 | 134 | 11 |
| 4411-2 | 3395 | 687 | 137 | 137 | 135 | 9 |
| 4412-2 | 3766 | 785 | 157 | 157 | 156 | 13 |
| 4413-2 | 4295 | 770 | 154 | 154 | 148 | 17 |
| 4414-1 | 3236 | 737 | 147 | 147 | 146 | 14 |
| 4415-3 | 3584 | 713 | 143 | 143 | 142 | 13 |
| 4416-1 | 3901 | 313 | 63 | 63 | - | 4 |
| 4416-3 | 3901 | 519 | 104 | 104 | 102 | 4 |
| 4417-4 | 3511 | 648 | 130 | 130 | 130 | 9 |
| 4417-6 | 3510 | 647 | 129 | 129 | - | - |
| 4417-7 | 3510 | 549 | 110 | 110 | 100 | - |
| 4418-1 | 2499 | 712 | 142 | 142 | 138 | 12 |
| 4418-3 | 2495 | 700 | 140 | 140 | 135 | - |
| 4419-4 | 4486 | 827 | 165 | 165 | - | - |
| 4419-6 | 4486 | 925 | 185 | 185 | 180 | 10 |
| 4420-2 | 2767 | 499 | 100 | 100 | 96 | 4 |
| 4421-3 | 3184 | 343 | 69 | 69 | 68 | 5 |
| 4422-1 | 3867 | 427 | 85 | 85 | 81 | 4 |
| 4423-1 | 4187 | 736 | 147 | 147 | 127 | 12 |
| 4424-1 | 4779 | 944 | 189 | 189 | 94 | 9 |

Following shipboard whole-core geophysical measurements (Chapter 5.4), the segments have been cut along-core into a work and an archive half. Immediately after core opening, digital reflectance data were routinely recorded at 31 wavelengths in the visible light range (400 - 700 nm) on the archive halves using a hand-held MINOLTA CM-2002 spectrophotometer. Prior to every measurement of a core segment at 2 cm intervals the instrument was re-adjusted to white color reflectance by attaching a calibration cap. The sediment surfaces were carefully scraped to expose a fresh, clean plane and covered with a thin transparent plastic film to avoid any contamination. The data files

were transferred to a PC. A graphic representation of the percent reflectance at 3 selected wavelengths (450 nm [blue], 550 nm [green], and 700 nm [red]) is shown in Figures 18 to 41 for each core. Also on the archive halves the sediments were described and smear slide samples picked from representative horizons.

From the work half two parallel series of syringe samples (10 ccm) were collected at 5 cm depth intervals. They will be used for shore based measurements of physical properties and stable isotopes as well as for analyses of foraminiferal assemblages, mineralogy and organic geochemistry.

Work and an archive halves were then stored at +4 °C and also shipped to Bremen at this temperature. Cores for pore water analysis (indicated as 'geochemistry' in the station list [Table 2]) have been sampled as described in Chapter 5.5 and frozen afterwards.

## 5.3 Lithologic Core Summary

Figures 18 to 41 show preliminary lithologic summaries of the gravity core collection recovered during Cruise M38/2. They include visual descriptions of the representative lithologies and of special or unique layers, their color according to the MUNSELL soil color chart as well as sedimentary structures. Lithological data are primarily based on analyses of smear slides taken from distinctive horizons. Also displayed are color reflectance records of 3 wave lengths (450, 550, 700 nm) and core logs of different physical properties (see Chapter 5.4).

Ceará Rise and Adjacent Abyssal Plains (Coring Transects GeoB 4401-4 to 4407-3, GeoB 4411-2 to 4413-2, and GeoB 4414-1 to 4416-3

The first two coring profiles GeoB 4401 to 4407 and GeoB 4411 to 4413 extend from the summit region over eastern flanks of the Ceará Rise in water depths between 3300 and 4600 m. At all sites the uppermost 40 to 60 cm of sediments predominantly consist of brownish foram bearing nanno ooze characterized by high color reflectance. Thin dark brownish iron oxide horizons were encountered at their base. The correlation to core GeoB 1523-1 (METEOR Cruise M16/2; SCHULZ et al., 1991) suggests a Holocene age for this top layer. It covers terrigenous nanno and foram bearing clay sequences presumably deposited during isotope stages 2 to 4 and containing numerous small silty to sandy horizons in the cores from deeper waters. Their thickness increases from 2.5 m at 3400 m to about 6 at 4600 m water depth. The followingforam bearing nanno ooze, probably representing isotope stage 5, is thus found at progressively deeper core levels at greater water depths.

In clear contrast, the sediments retrieved on coring profile GeoB 4414 to 4416 over the western flanks of the Ceará Rise typically contain much higher amounts of terrigenous components. The concentration of terrigenous material notably increases below a 40 to 60 cm thick top layer of clayey nanno-foram ooze. Interbedded are organic rich

horizons with fragments of leafs and grass. A thick turbidite between 275 to 387 cm depth in core GeoB 4416-3 exhibits a conspicuous minimum in color reflectance.

Amazon Fan (Cores GeoB 4408-2, 4409-1, 4410-2, and 4417-4)

In the Amazon Deep Sea Fan 4 sediment cores were retrieved from water depths between 3500 and 4150 m. Core GeoB 4417-4 was taken in the central middle fan at the active channel - levee system, core GeoB 4410-2 in the eastern lower fan. Cores GeoB 4408-2 (at the former site GeoB 1514; METEOR Cruise M16/2; SCHULZ et al., 1991) and GeoB 4409-1 sampled the eastern middle fan. The uppermost 20 to 40 cm consist of hemipelagic, light yellowish brown clayey foram-nanno ooze showing highest color reflectance of the sediment series. At the base of this top section typically an iron oxide horizon occurs which is well known from previous investigations (cores GeoB 1511 to 1514; METEOR Cruise M16/2; SCHULZ et al., 1991; KASTEN, 1996 and ODP Leg 155; FLOOD et al., 1995). Below, the sediments change to terrigenous olive to dark greenish nannofossil mud. A smell of $H_2S$ was noticed in cores GeoB 4409-1 and 4410-2. Ikaite crystals were observed at 336 and 343 cm depth in core GeoB 4409-1, numerous specks of iron sulfide as well as organic rich spots ('Tiger-Look') throughout all cores. A sequence of three foram bearing layers was only encountered in core GeoB 4410-2 between 590 to 650 cm depth. The color reflection data indicate that core GeoB 4417-4 comprises no sediments older than the last glacial, core GeoB 4408-2 reaches the top of isotope stage 3, core GeoB 4409-1 into isotope stage 4, and core GeoB 4410-2 the top of isotope stage 6. According to these preliminary stratigraphic findings, sedimentation rates should be highest in the Amazon Fan as compared to the other working areas of Cruise M38/2.

Guyana Continental Slope (Cores GeoB 4418-1 and 4419-6)

The upper layer in both cores consists of light yellowish brown clay and foram bearing nannofossil ooze. Beneath, the color changes to olive gray and the silt content increases. At the boundary an iron oxide crust was found in core GeoB 4419-6. A fining upward sequence on top of core GeoB 4418-1 indicates a turbidite. Between 116 and 242 cm core depth a second large turbidite shows graded bedding of foram sand at the base to foram mud at the top. Some smaller turbidites also occur below 532 cm core depth. In relation to core GeoB 4418-1 foraminfera are relatively rare in core GeoB 4419-6. Small, cm sized turbidites are common throughout this core.

Mid-Atlantic Ridge (Coring Profile GeoB 4420-2 to 4424-1)

Core GeoB 4420-2 is almost entirely composed of nannofossil ooze with foraminifera and clay. Minor constituents are sponge spicules and quartz. Brown and yellow colors dominate. Limited bioturbation is evident in most parts of core. As no *G. menardii* could be found in the top layer, Holocene sediments may have been lost during the coring process. Color reflectance pattern as well as the occurrence of *G. menardii* indicate isotope stage 5 at around 200 cm core depth.

# Legend for stratigraphic columns

## Lithology

### one major component

*calcareous*

foraminiferal ooze

nannofossil ooze

sandy turbidite, (forams)

*siliceous*

siliceous ooze

diatom ooze

*terrigenous*

clay

mud

### mixtures

*calcareous*

nannofossil bearing foram ooze

foram-nannofossil ooze
nannofossil-foram ooze

foram bearing nannofossil ooze

*siliceous*

diatomaceous nannof. ooze
diatom bearing nannof. ooze

*terrigenous*

clayey nannofossil ooze
clay bearing nanno ooze

foram bearing clayey nannofossil ooze

nannofossil clay

### admixtures

*calcareous*

foram bearing

nannofossil bearing

*siliceous*

siliceous

diatom bearing

*terrigenous*

clay bearing

mud bearing

sand bearing

accessory mineral bearing

## Structures

**weakly bedded**

**bedded/laminated**

mm
cm dimension of bedding
dm

**scoured contact**

*S* **bioturbation (<30% of sediment)**

*SS* bioturbation (30-60% of sediment)

*SSS* **bioturbation (>60% of sediment)**

**fining upwards**

**coarsening upwards**

**graded bedding**

ww **wavy bedding**

## Fossils

**shells**

**shell fragments**

megafossil

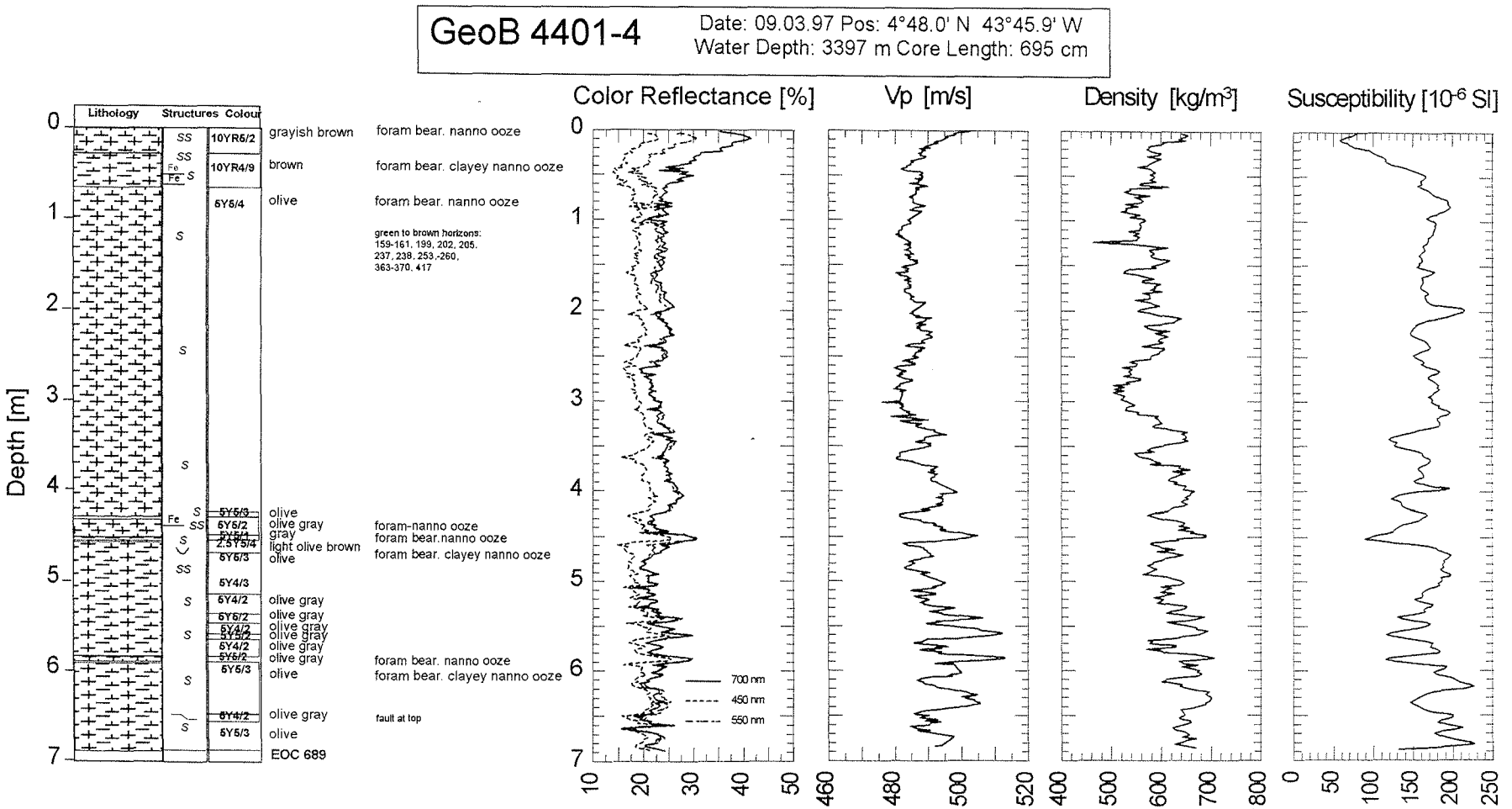


Figure 18 Gravity core 4401-4 - core description and physical property logs.

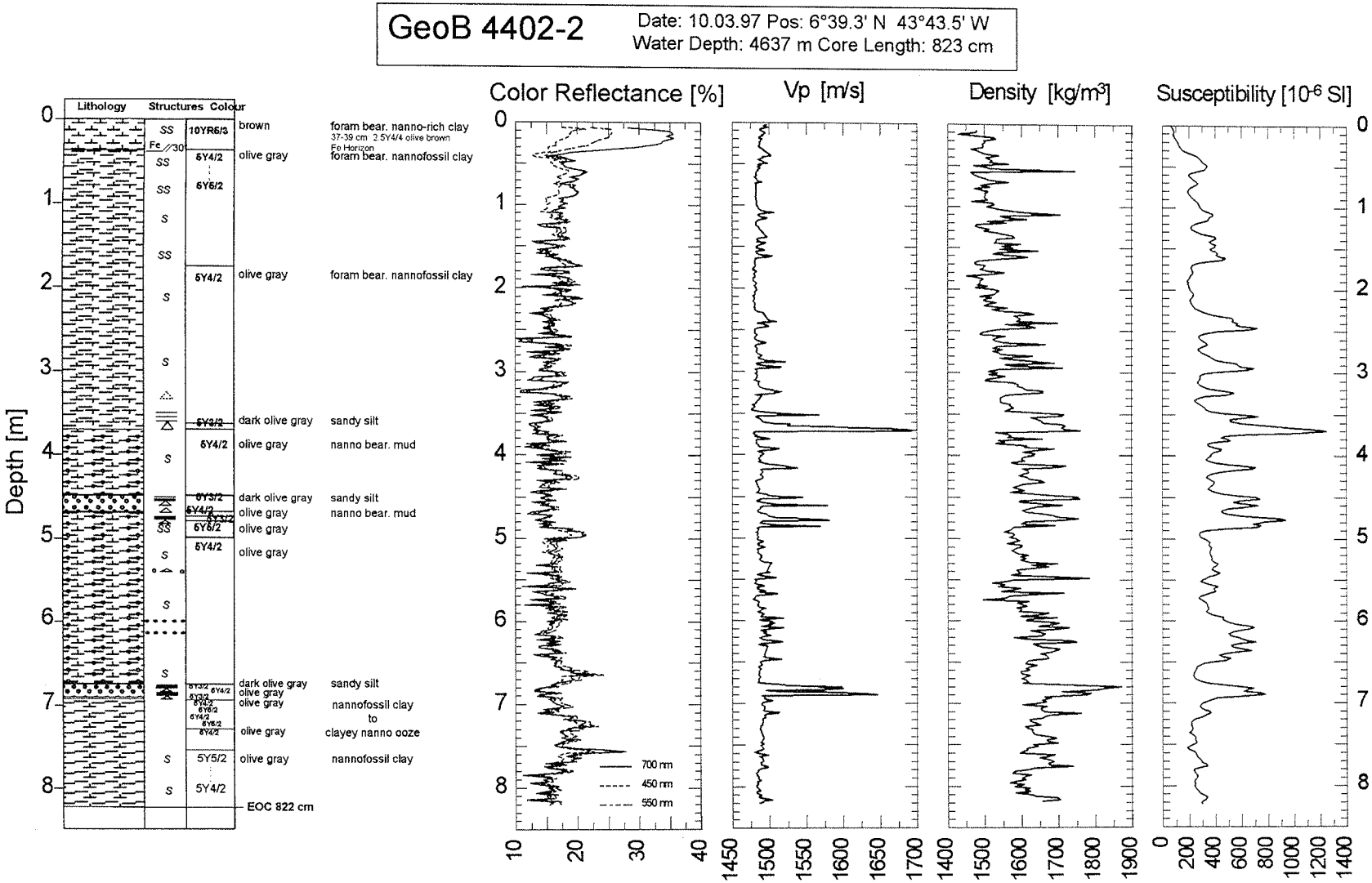


Figure 19 Gravity core 4402-2 - core description and physical property logs.

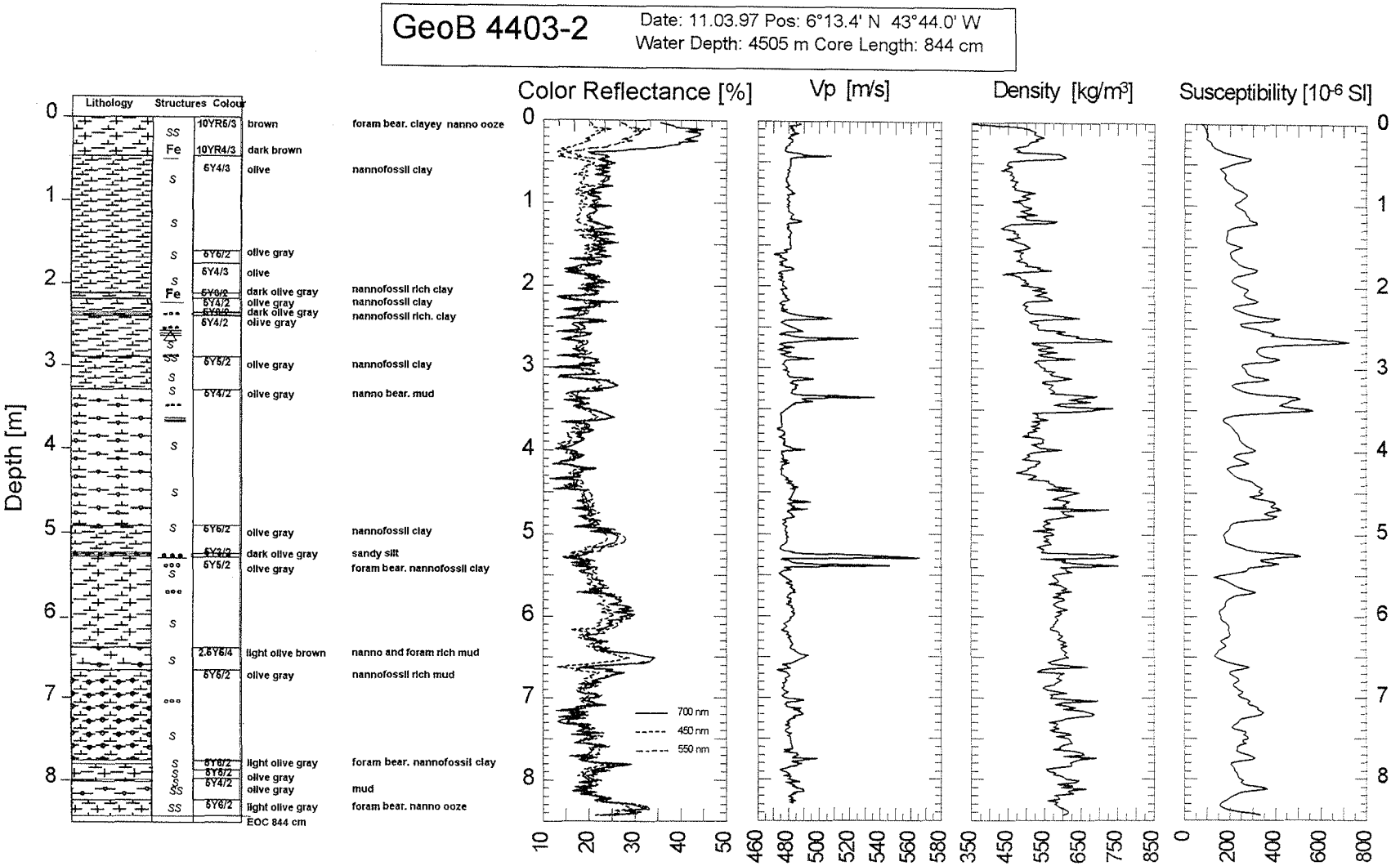


Figure 20 Gravity core 4403-2 - core description and physical property logs.

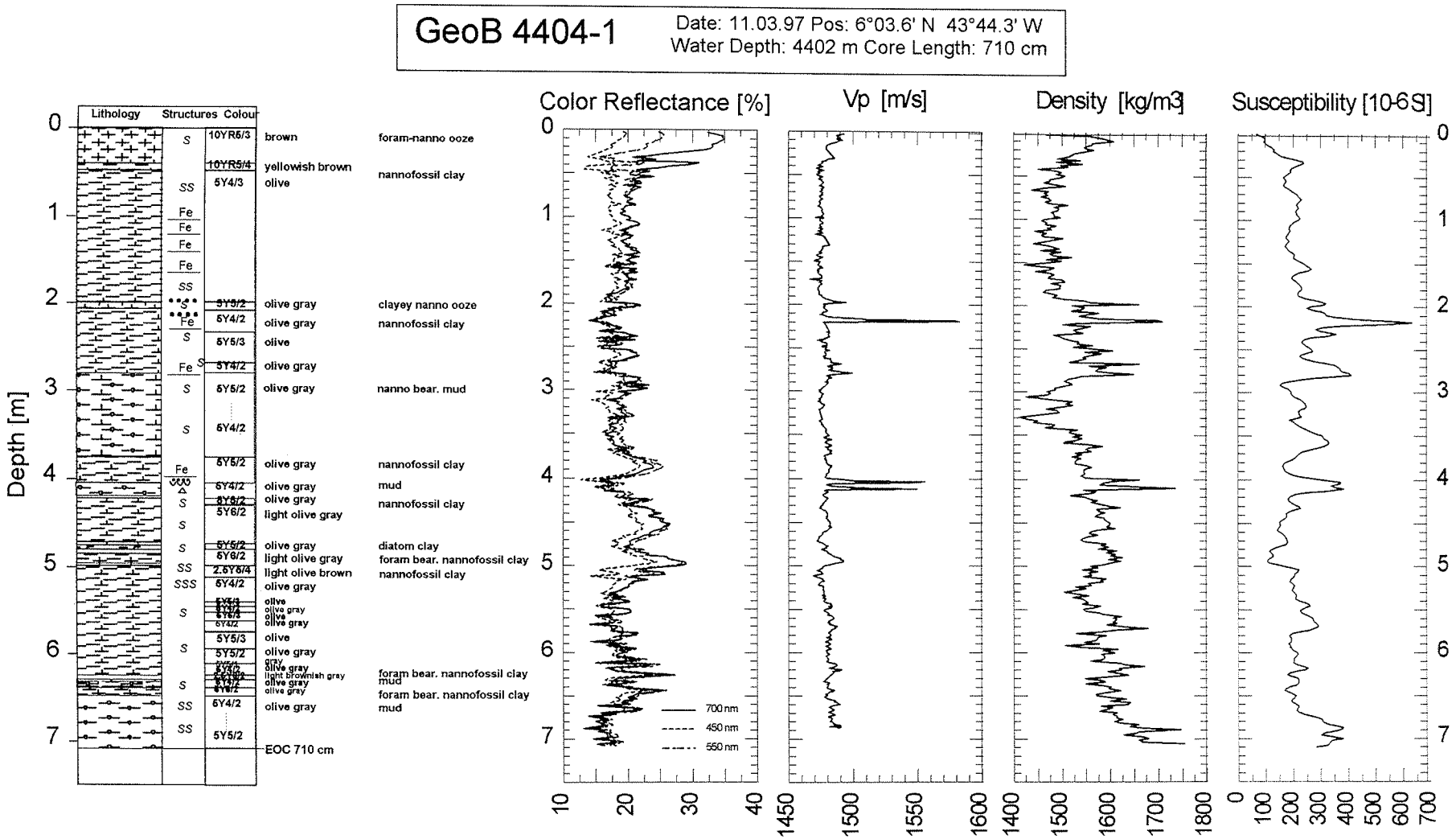


Figure 21 Gravity core 4404-1 - core description and physical property logs.

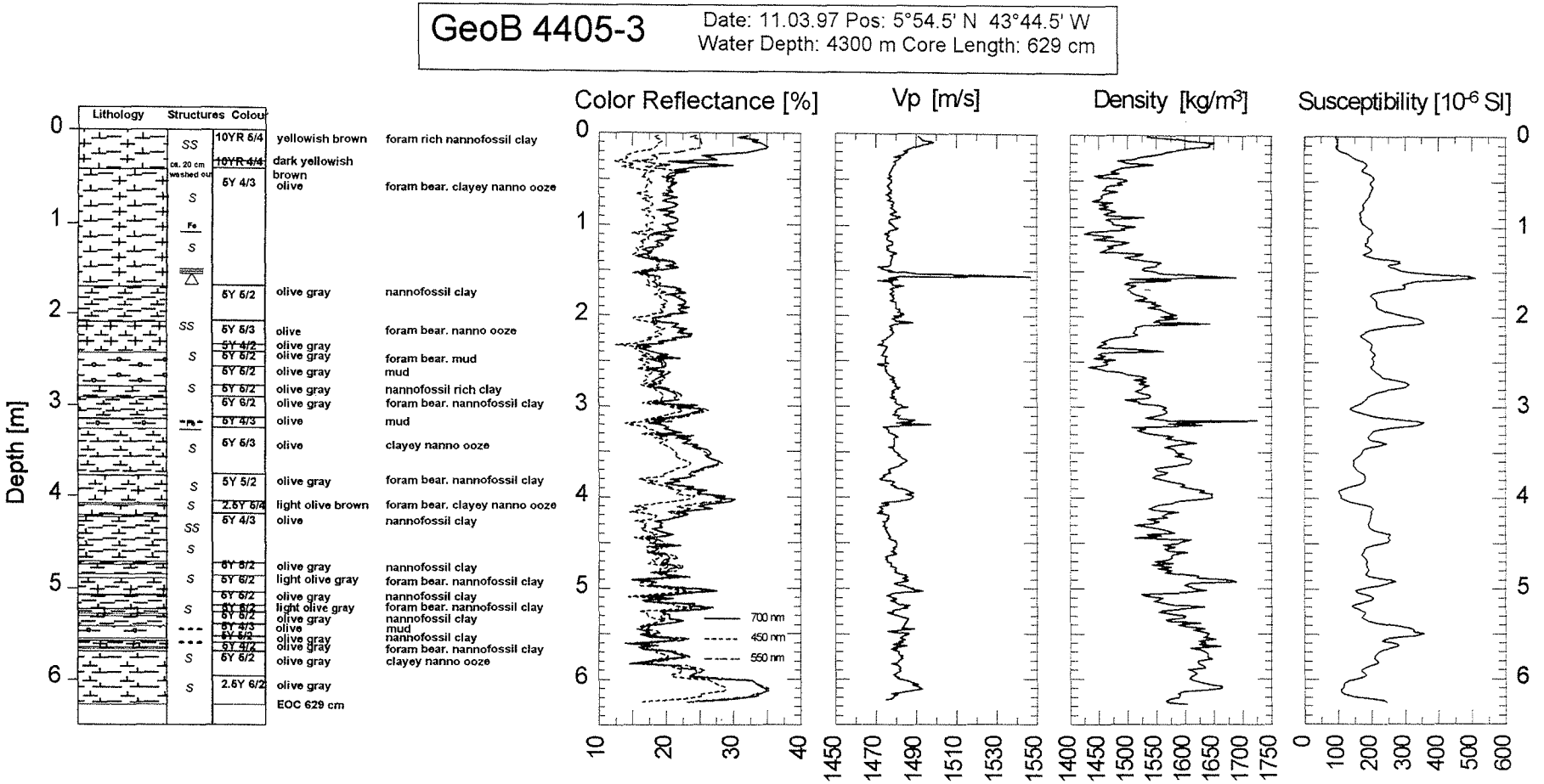


Figure 22 Gravity core 4405-3 - core description and physical property logs.

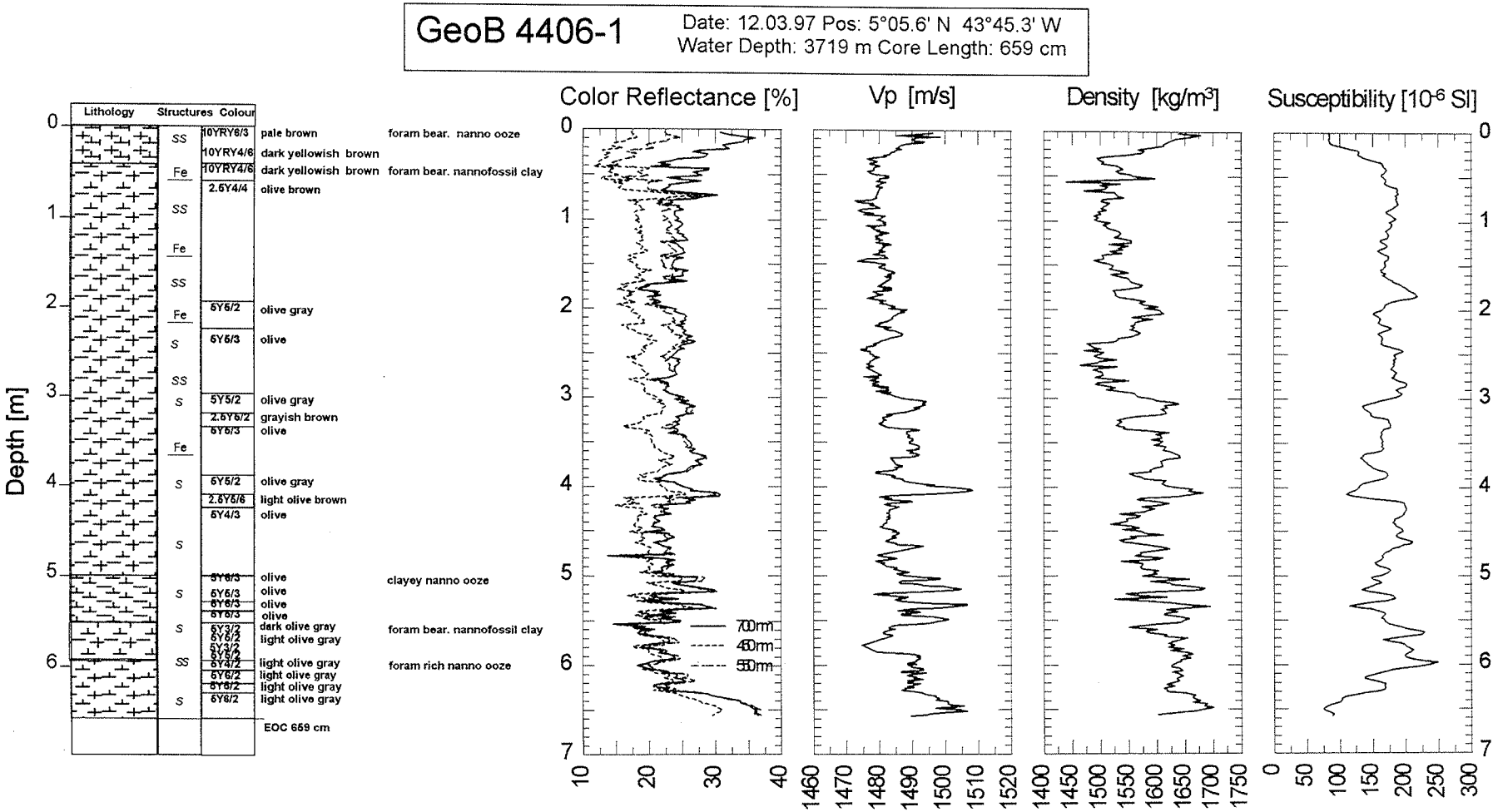


Figure 23 Gravity core 4406-1 - core description and physical property logs.

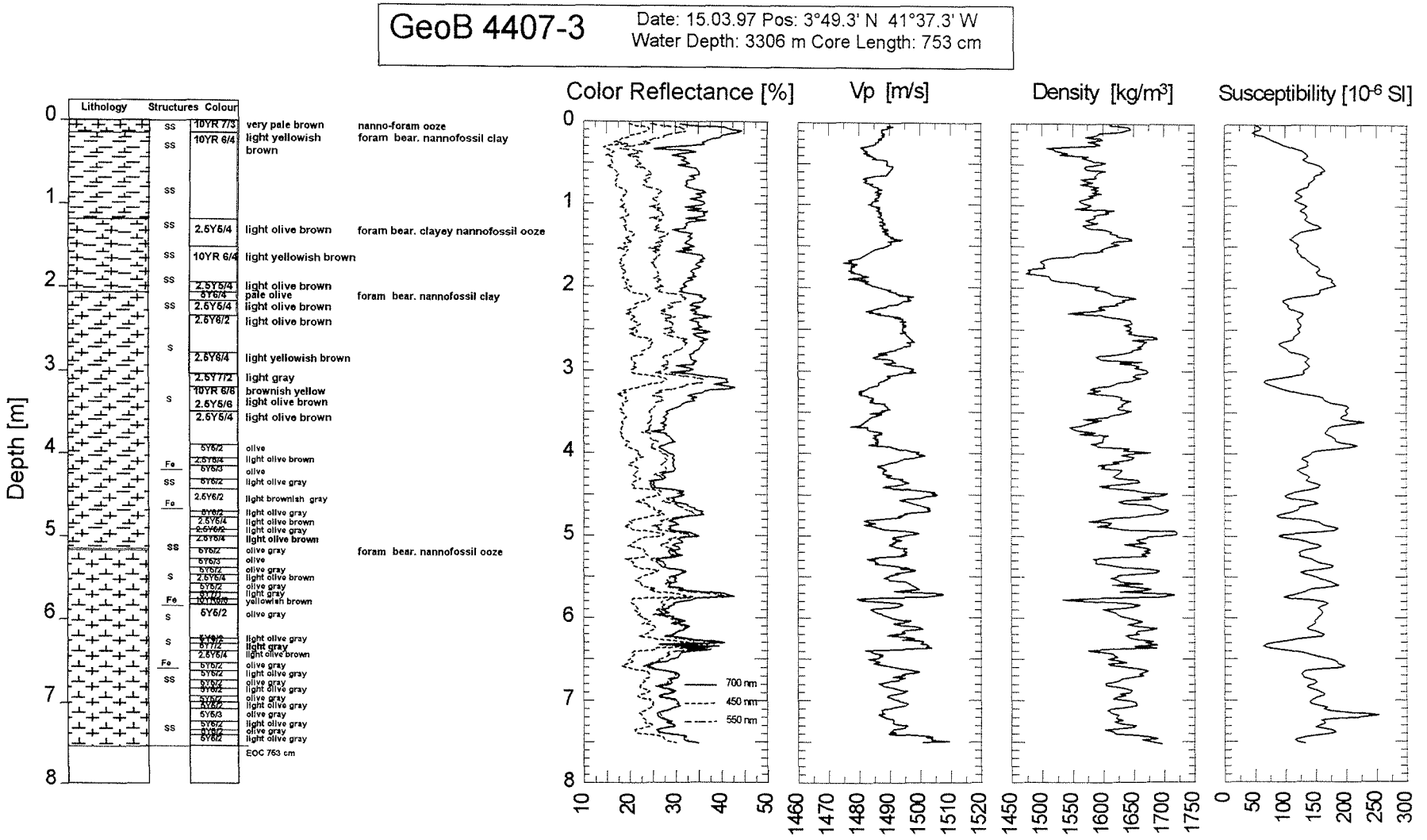


Figure 24 Gravity core 4407-3 - core description and physical property logs.

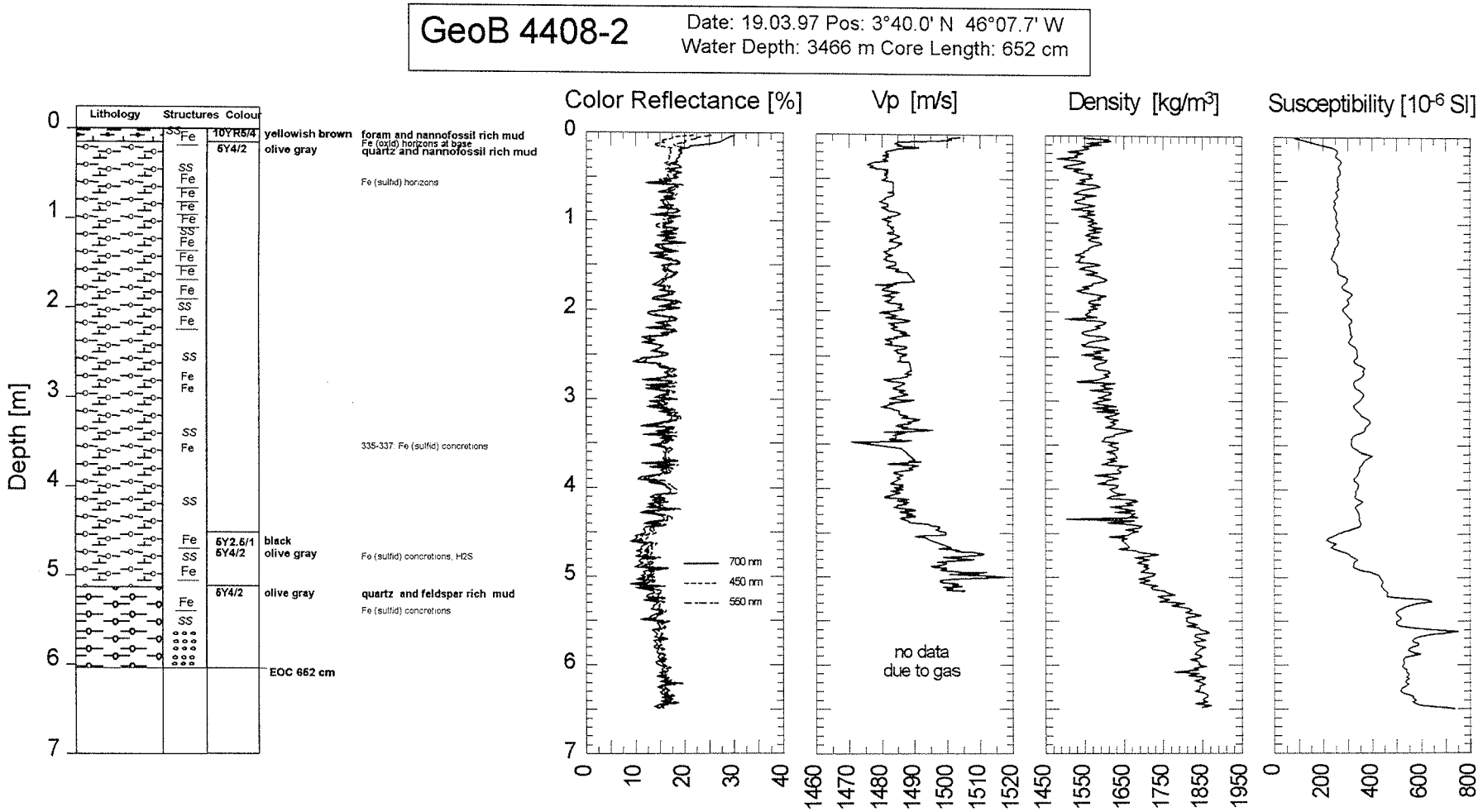


Figure 25 Gravity core 4408-2 - core description and physical property logs.

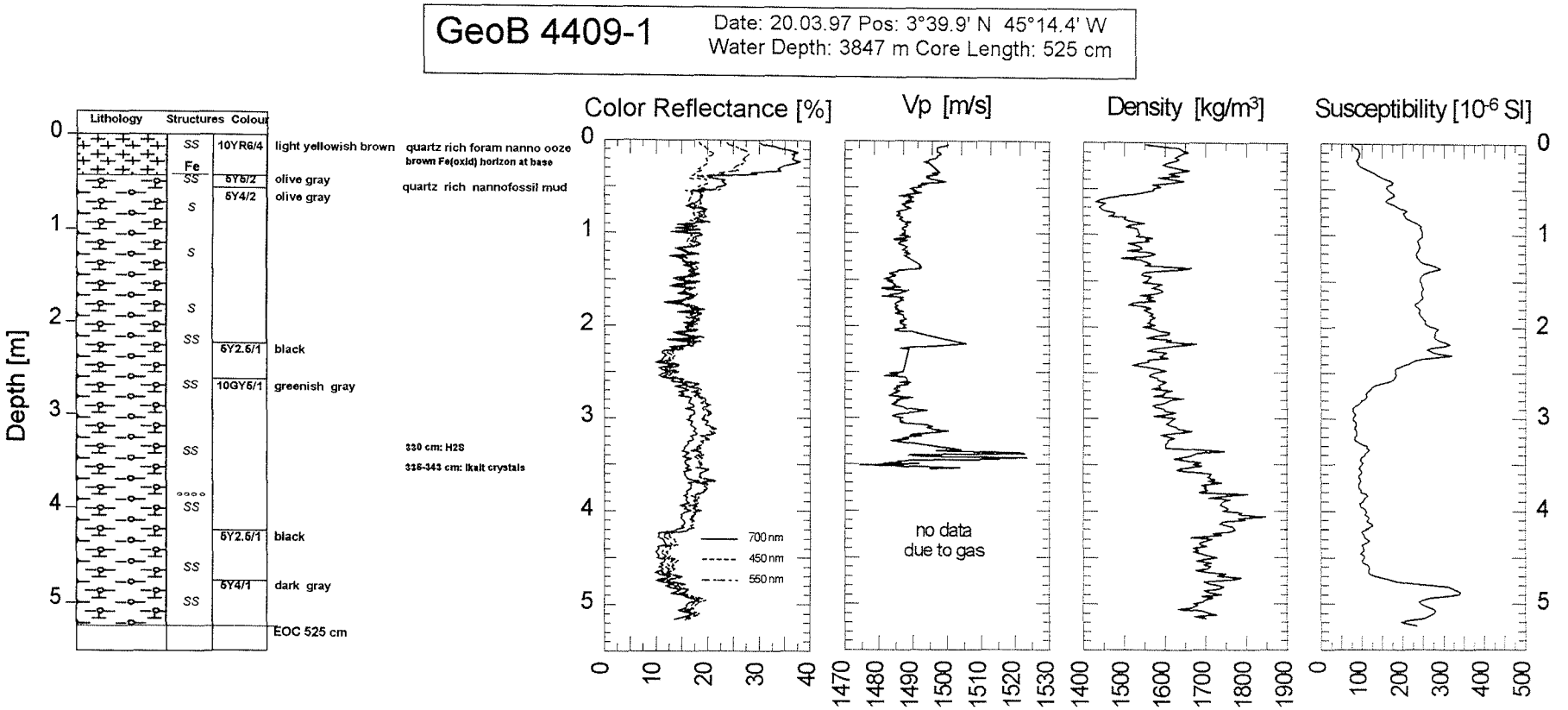


Figure 26 Gravity core 4409-1 - core description and physical property logs.

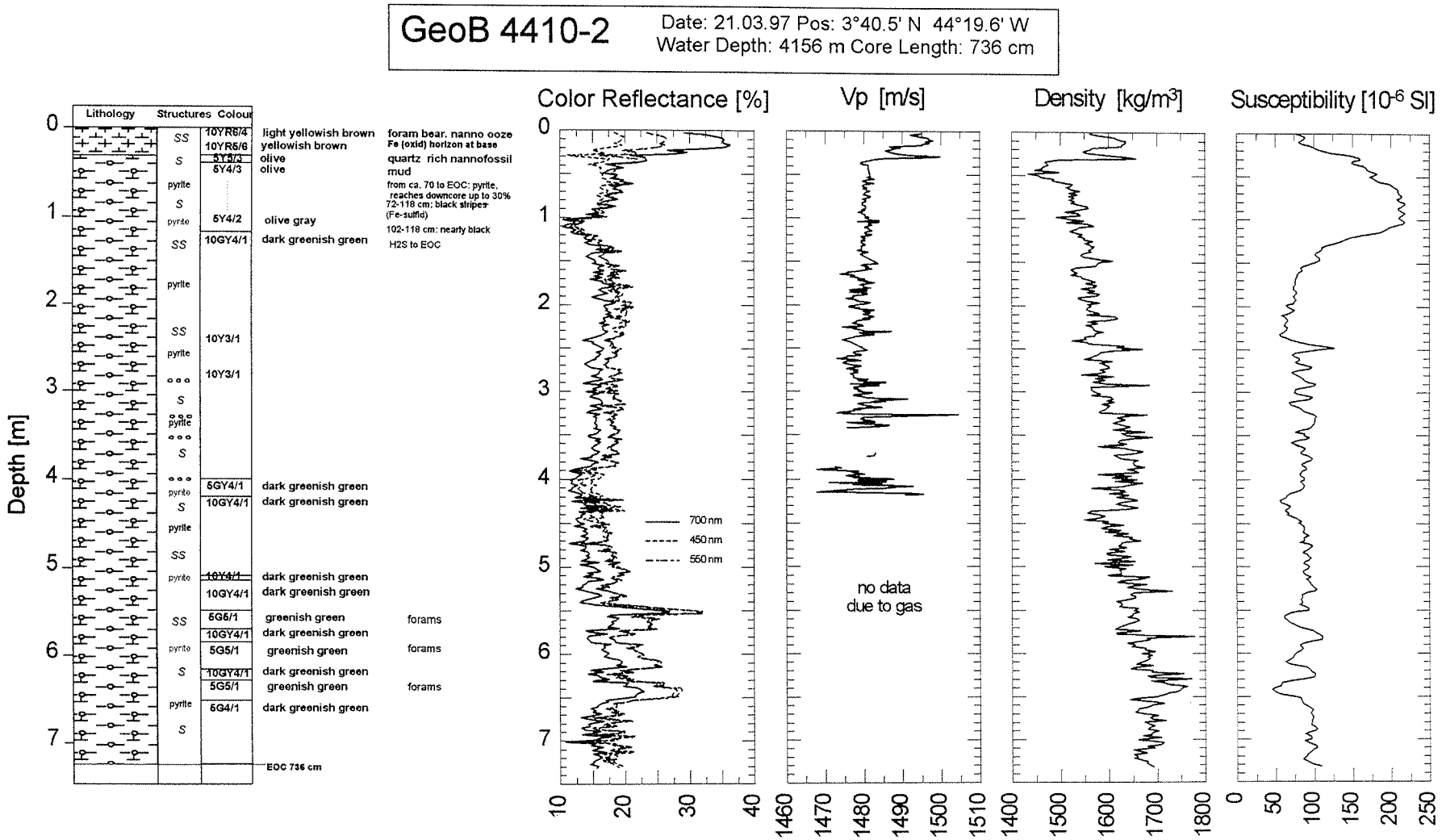


Figure 27 Gravity core 4410-2 - core description and physical property logs.

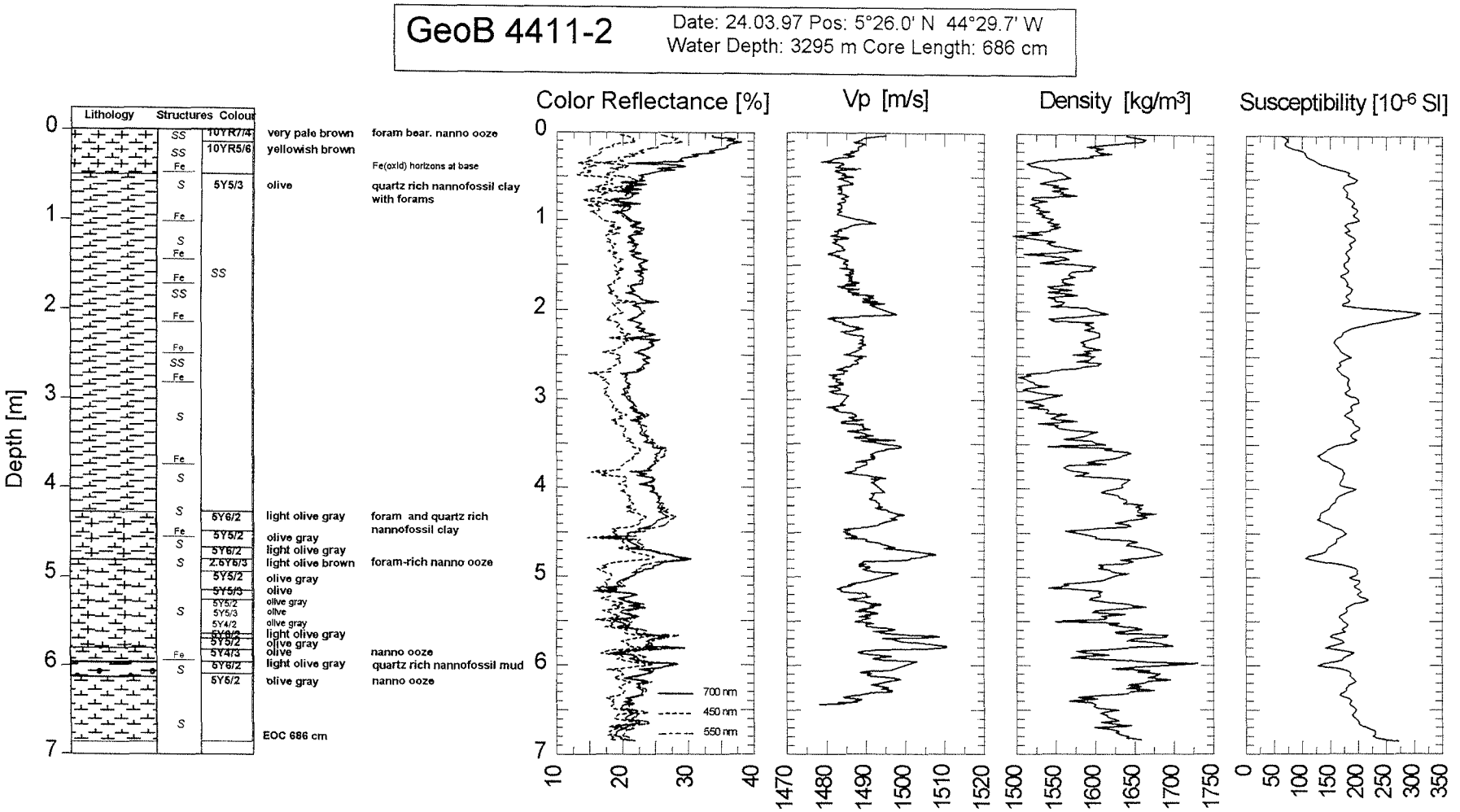


Figure 28 Gravity core 4411-2 - core description and physical property logs.

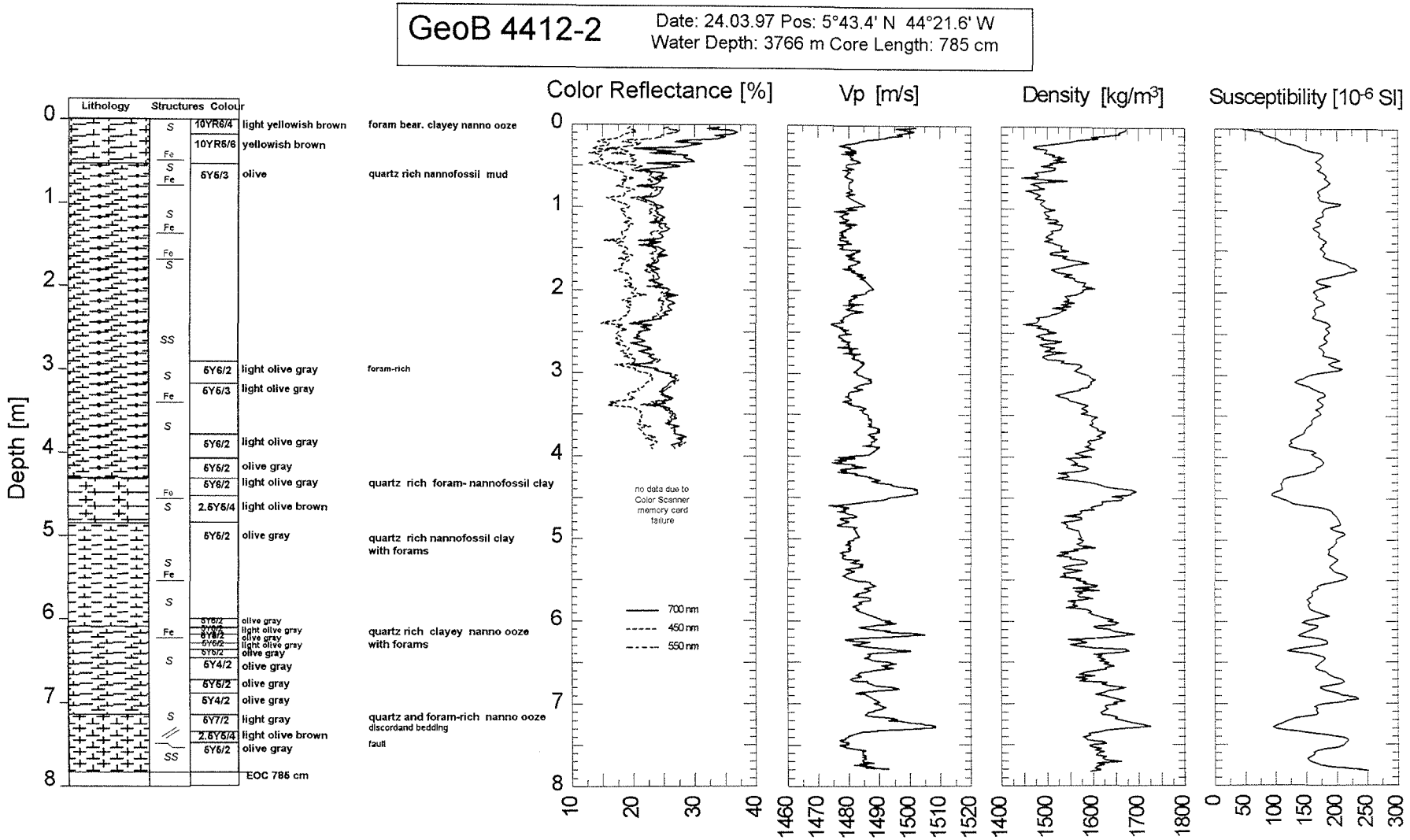


Figure 29 Gravity core 4412-2 - core description and physical property logs.

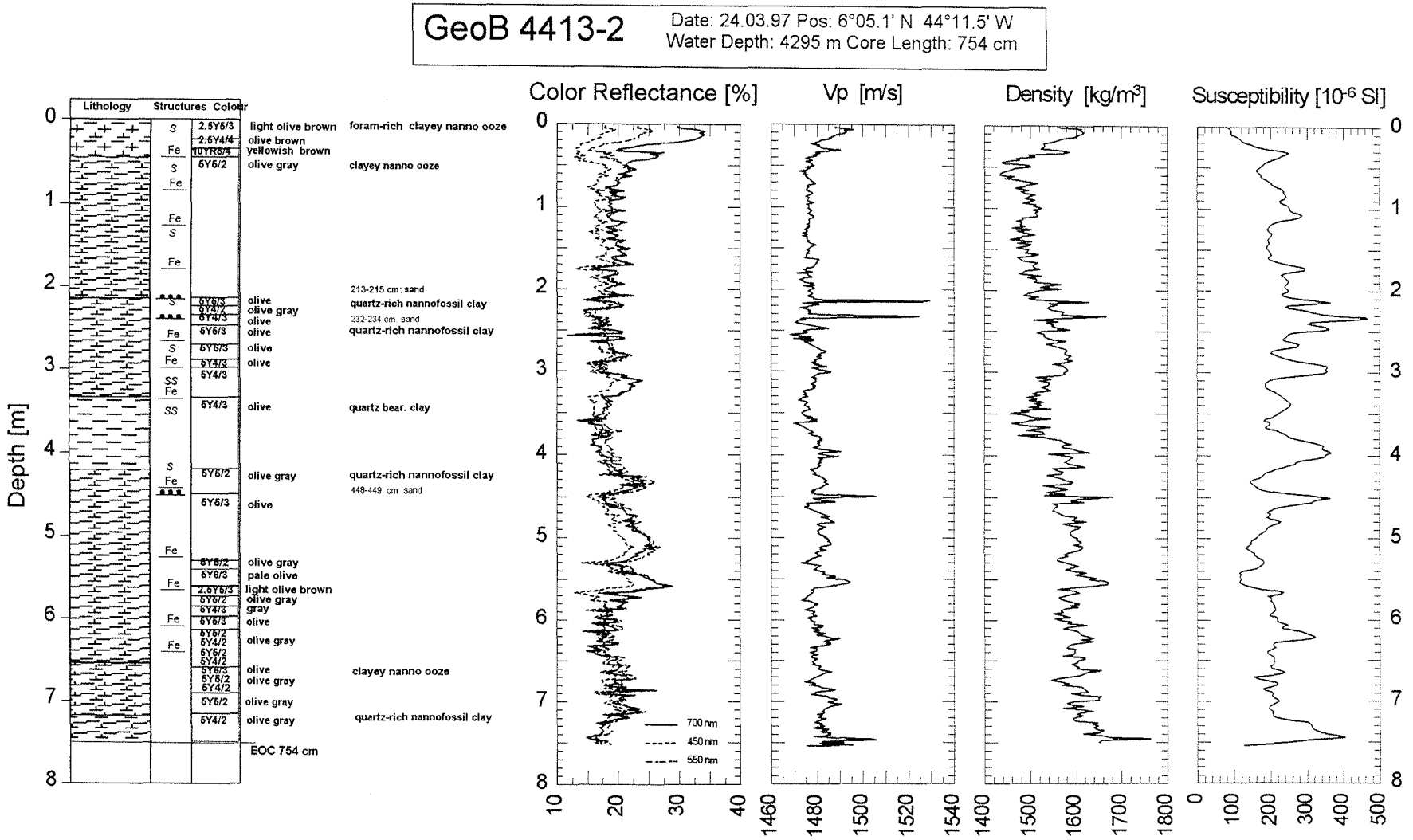


Figure 30 Gravity core 4413-2 - core description and physical property logs.

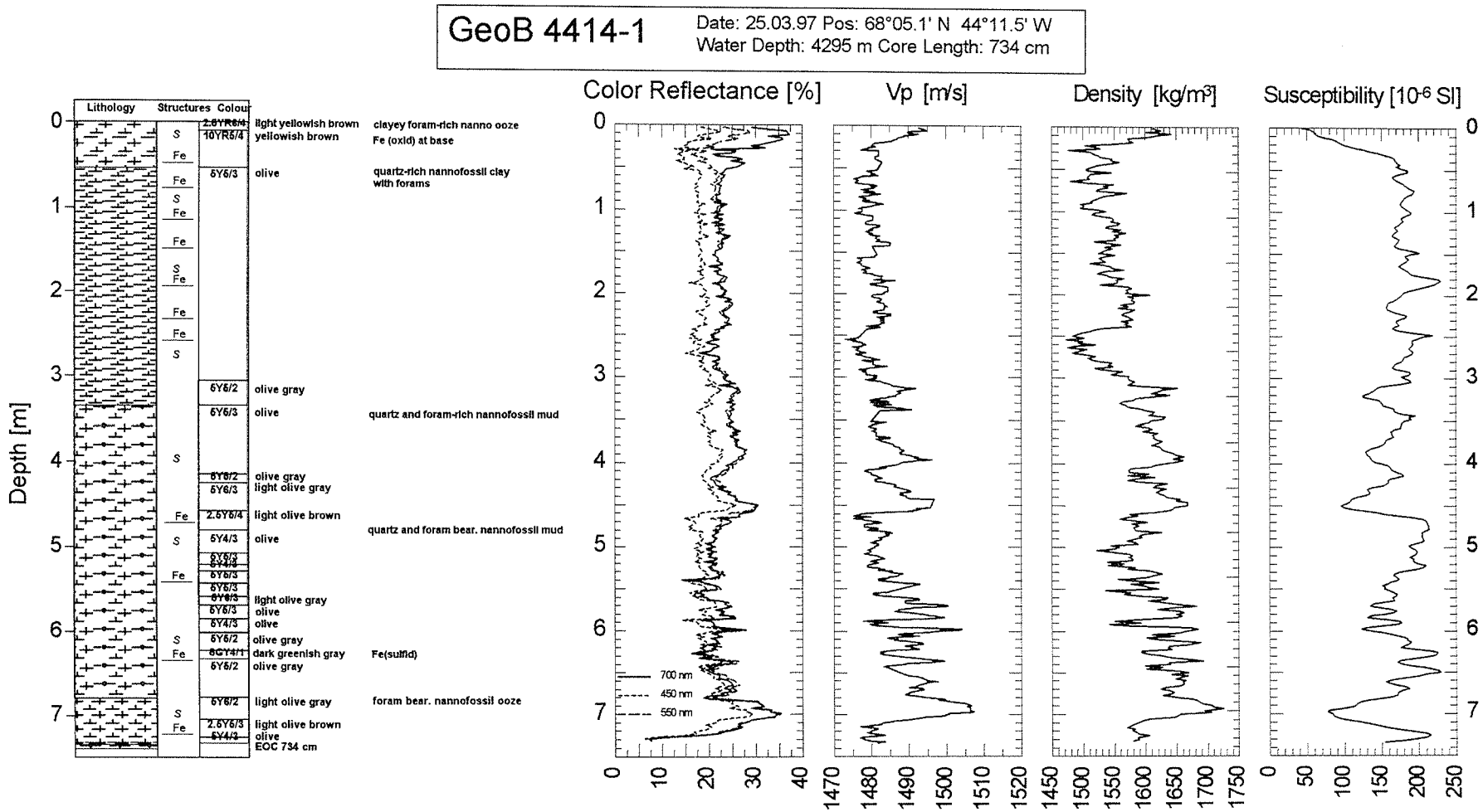


Figure 31 Gravity core 4414-1 - core description and physical property logs.

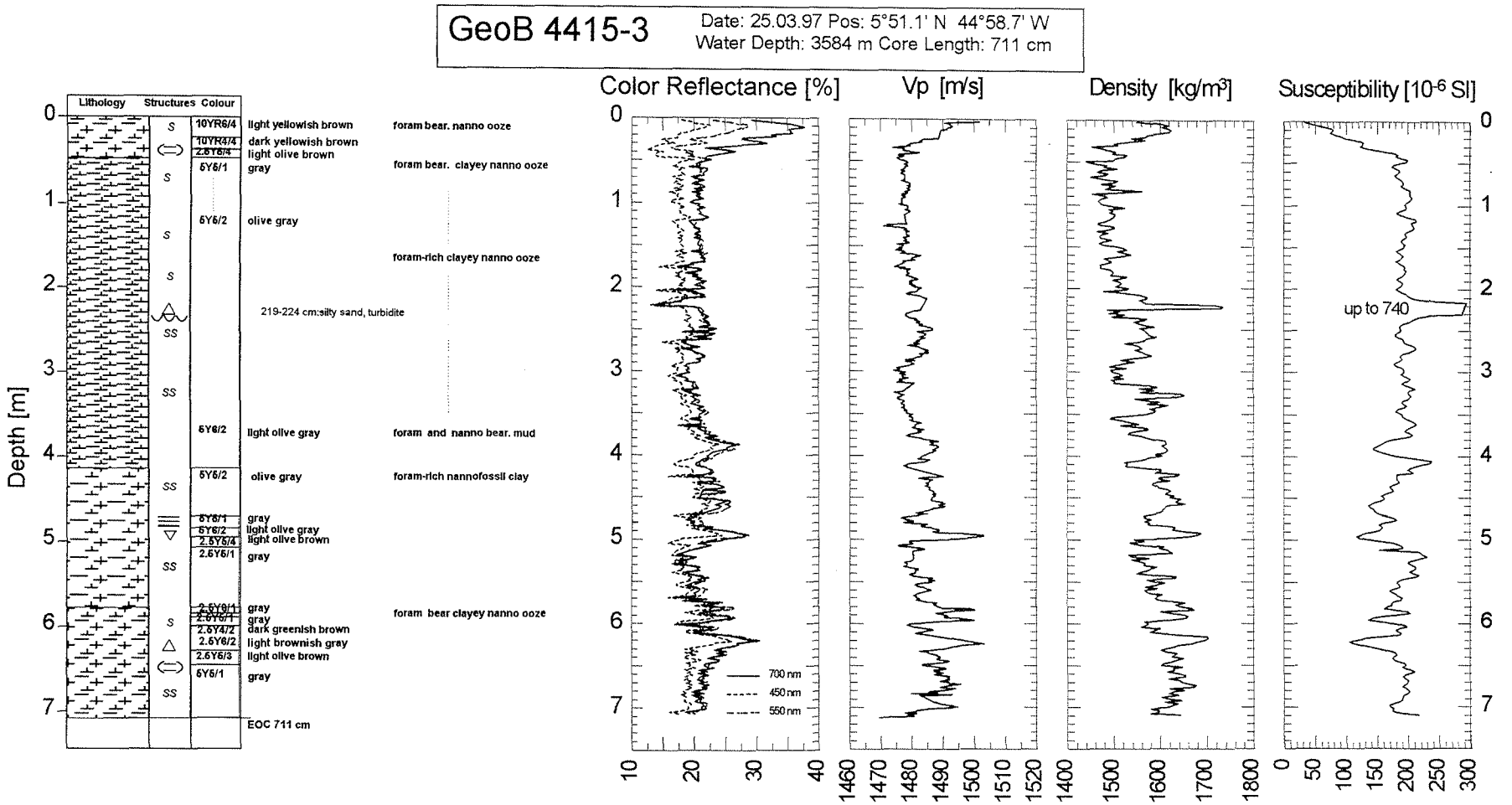


Figure 32 Gravity core 4415-3 - core description and physical property logs.

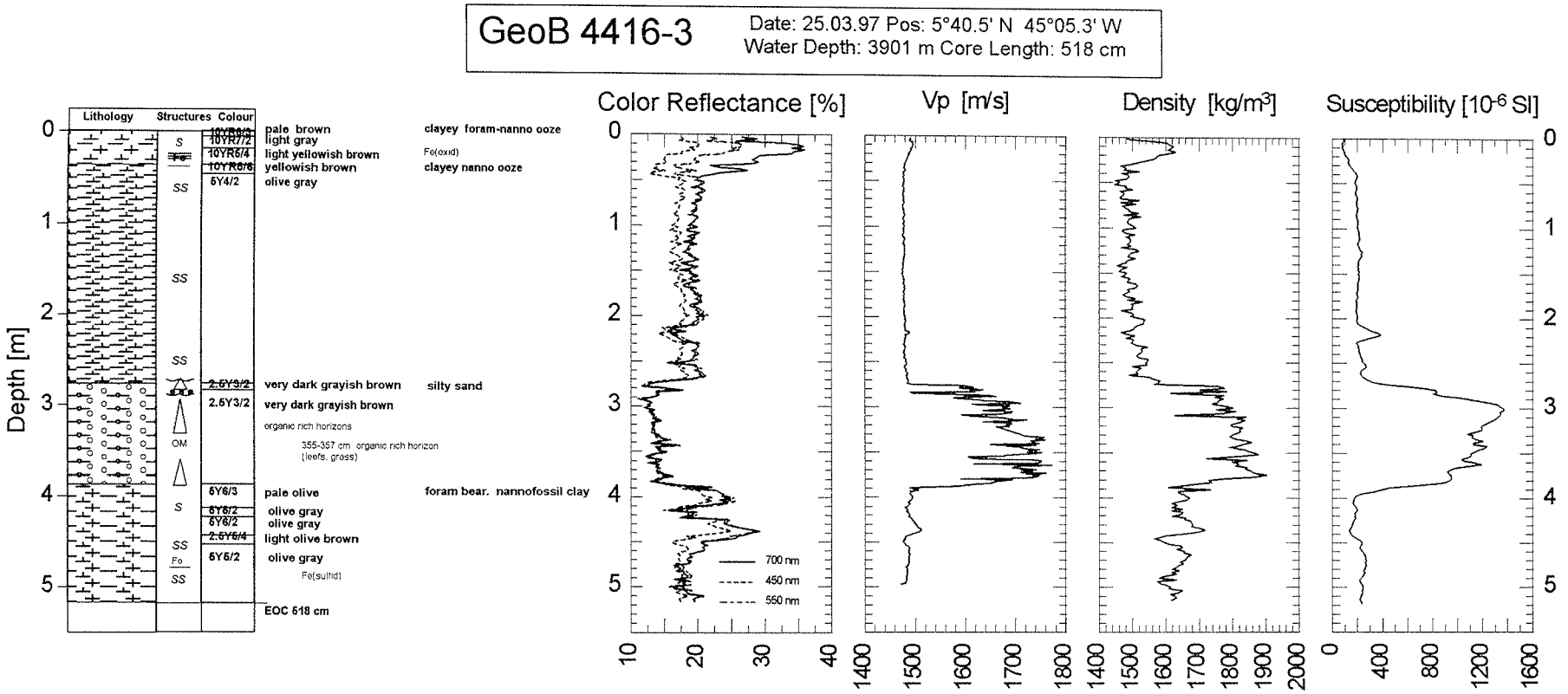


Figure 33 Gravity core 4416-3 - core description and physical property logs.

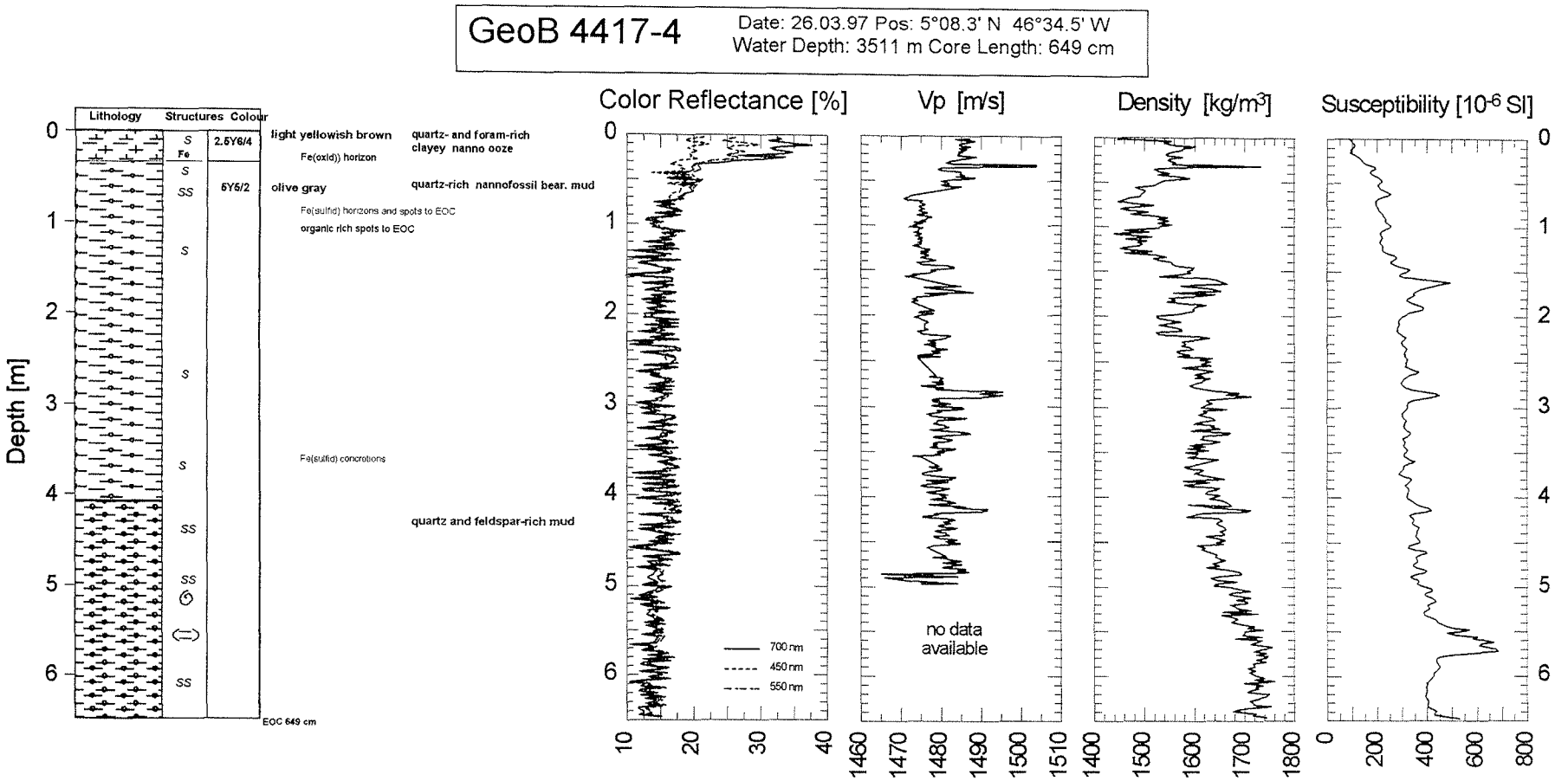


Figure 34 Gravity core 4417-4 - core description and physical property logs.

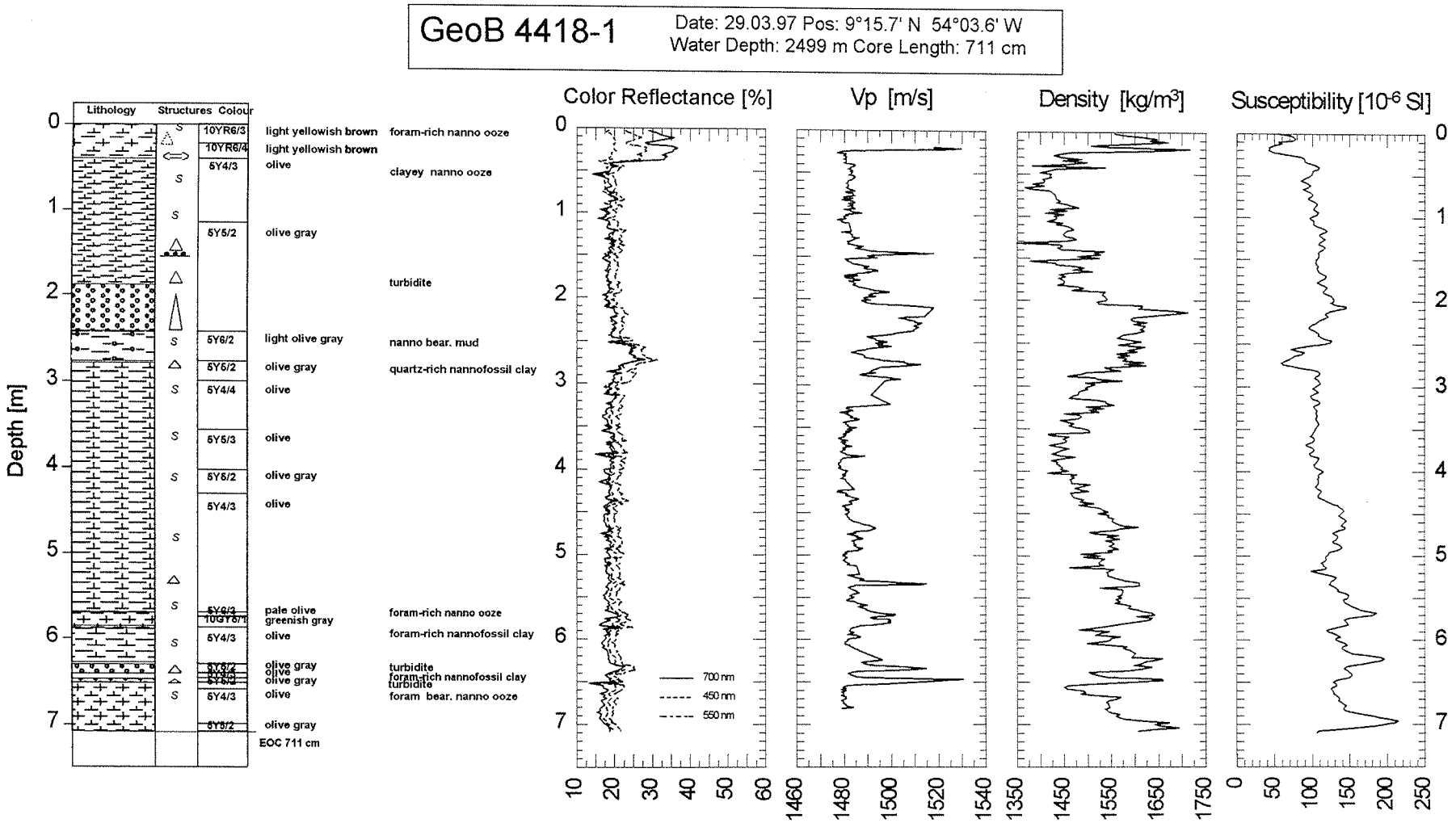


Figure 35 Gravity core 4418-1 - core description and physical property logs.

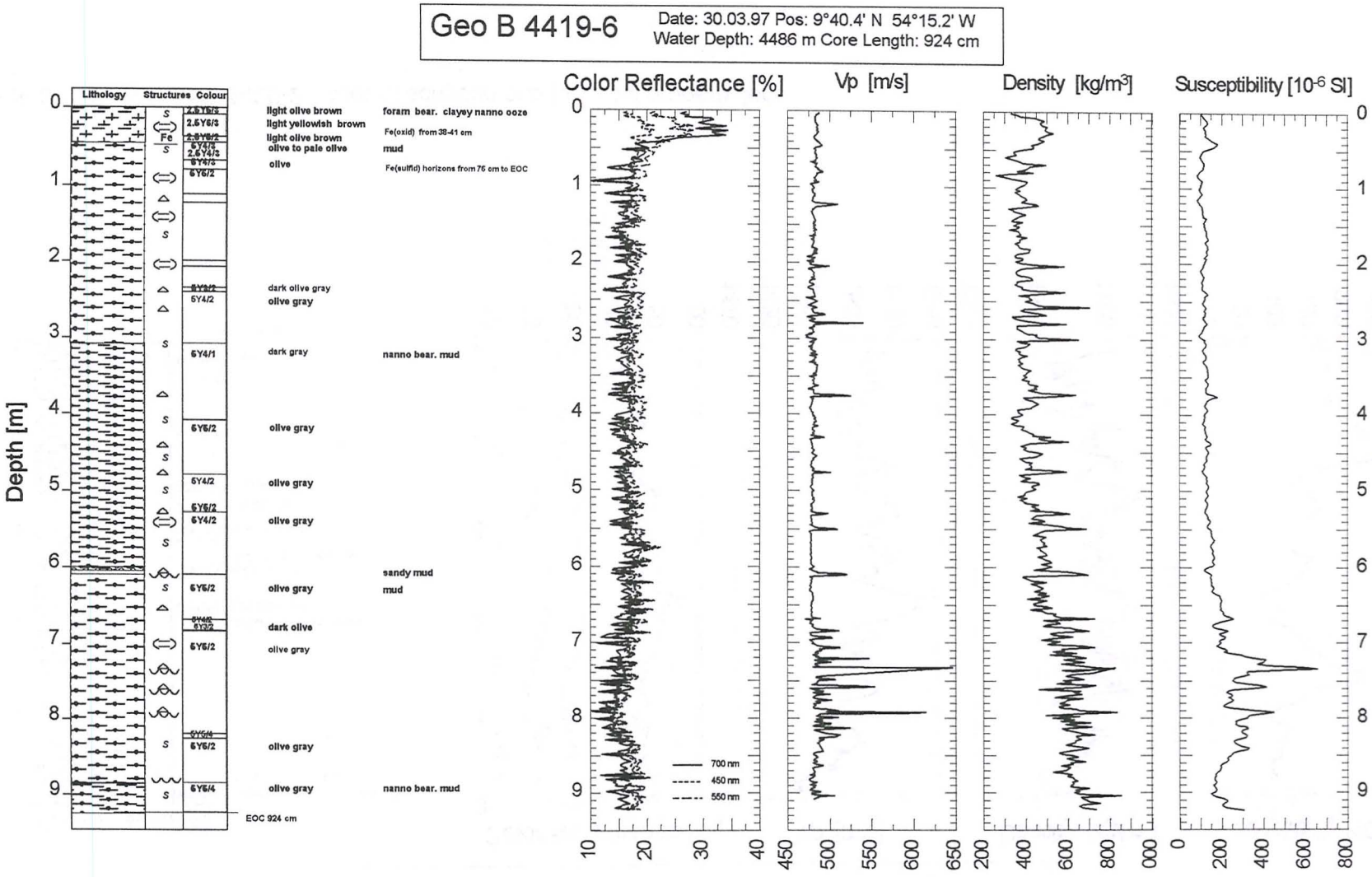


Figure 36 Gravity core 4419-6 - core description and physical property logs.

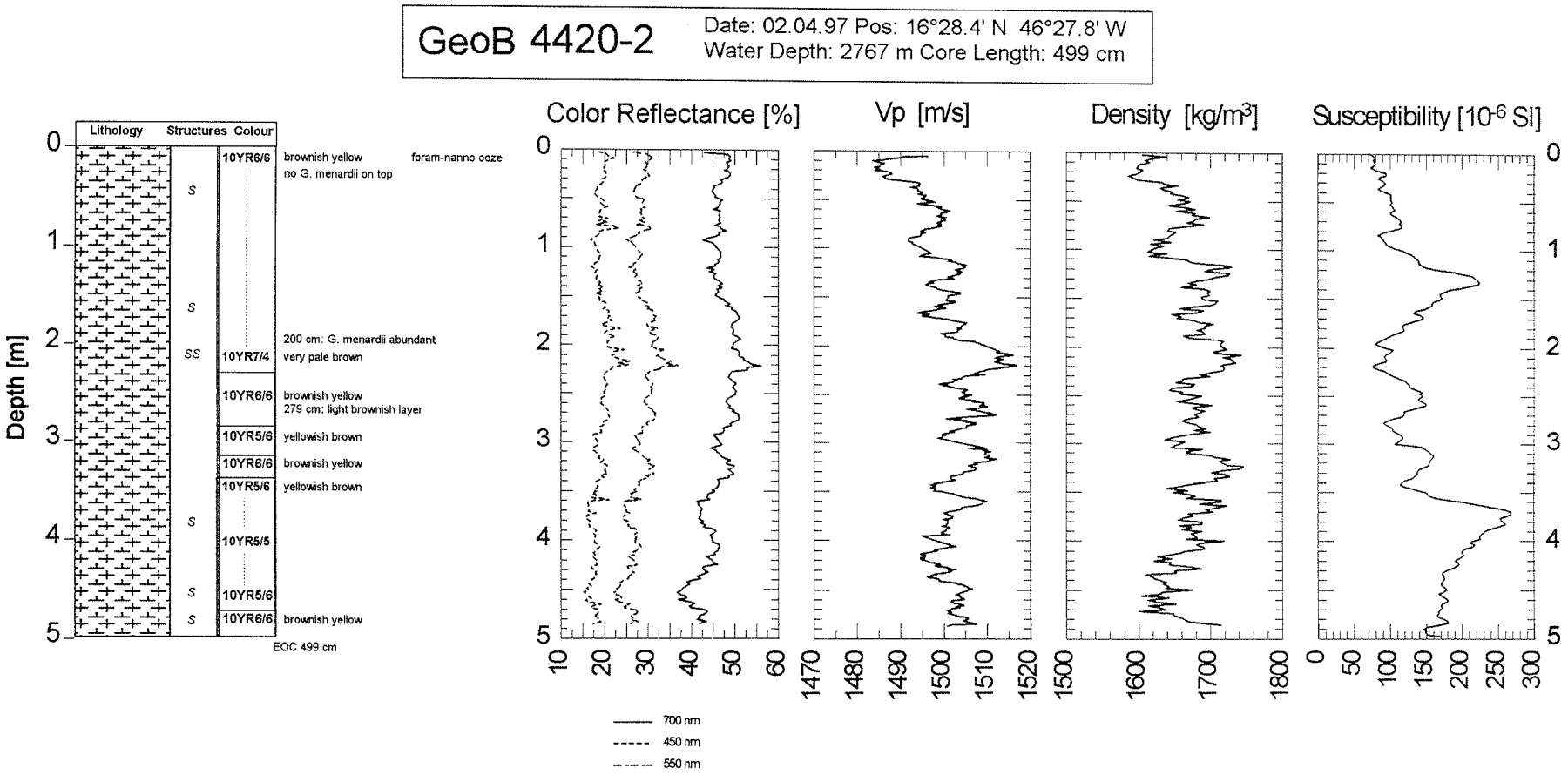


Figure 37 Gravity core 4420-2 - core description and physical property logs.

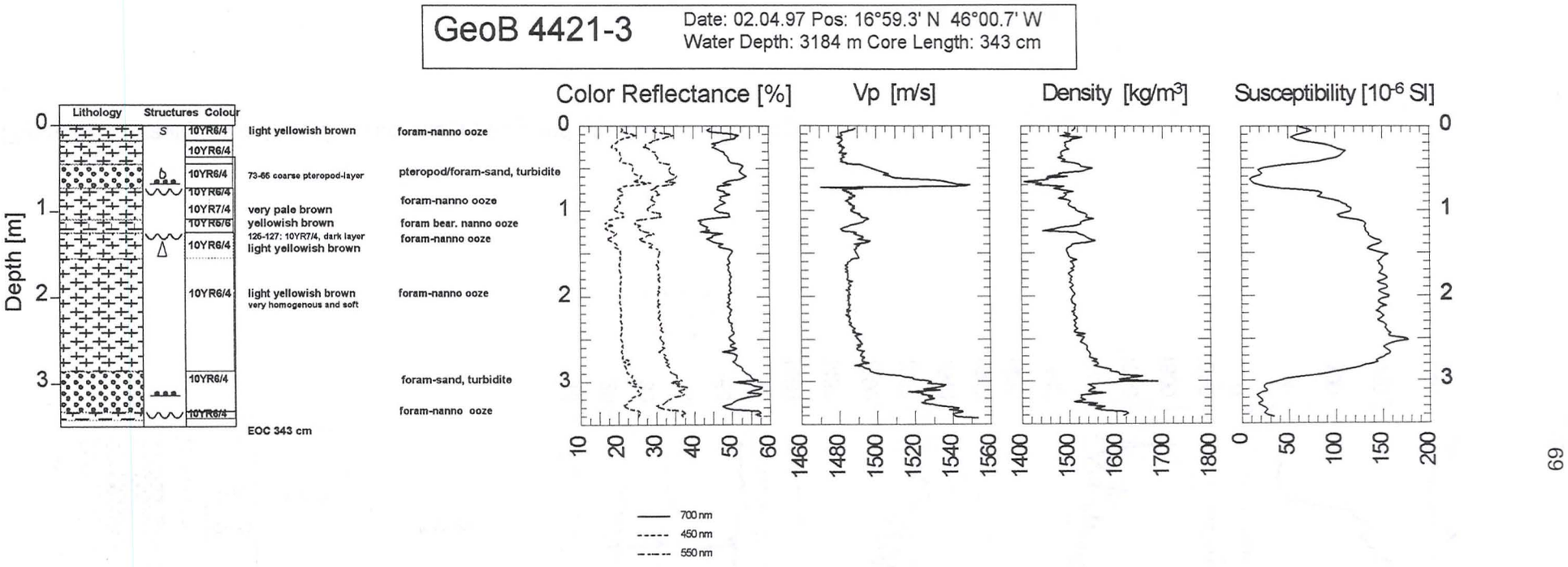


Figure 38 Gravity core 4421-3 - core description and physical property logs.

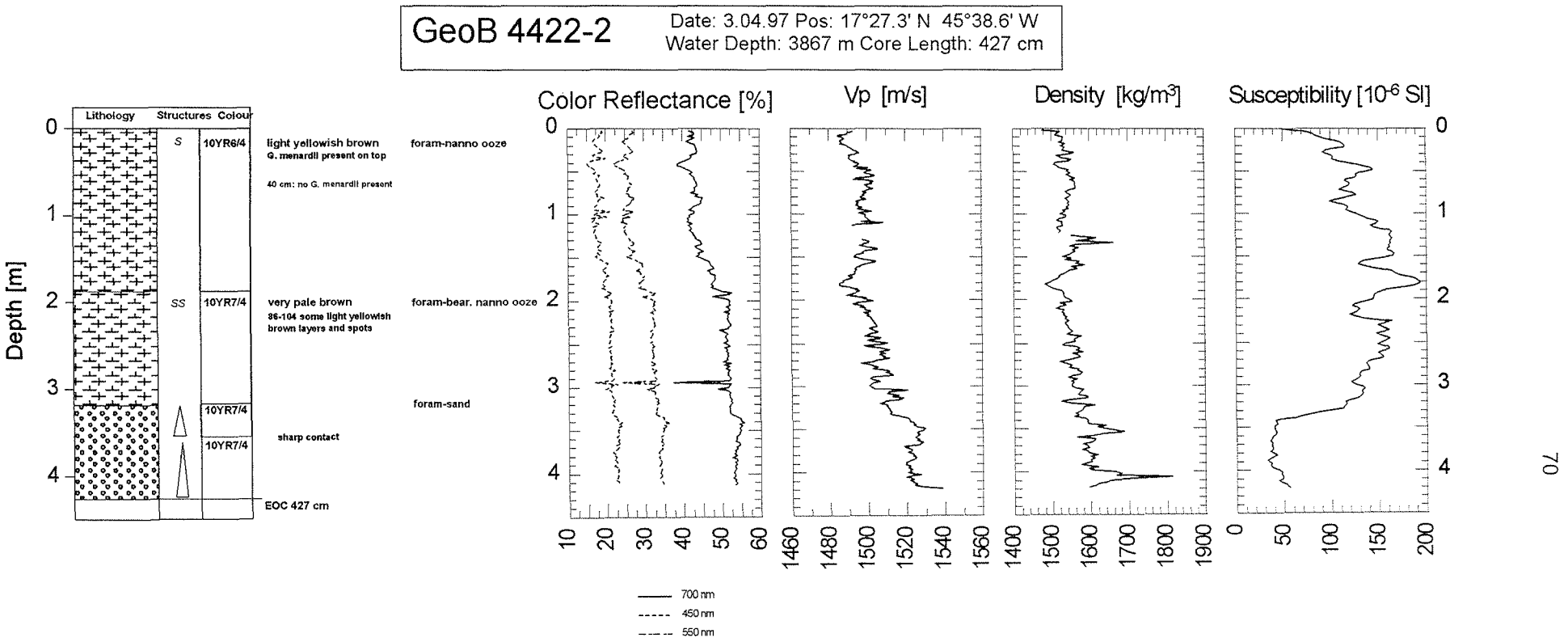


Figure 40 Gravity core 4423-2 - core description and physical property logs.

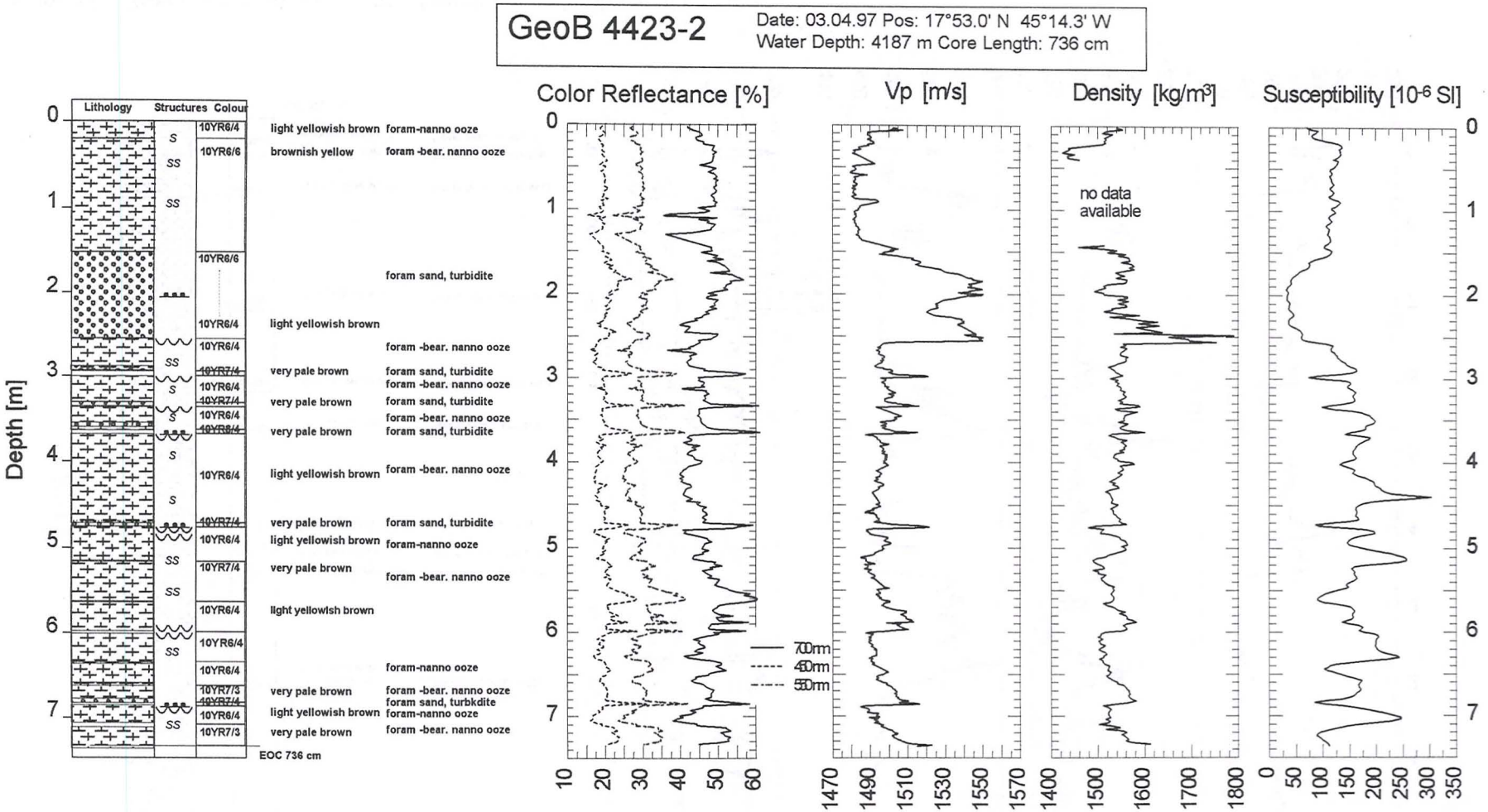


Figure 40 Gravity core 4423-2 - core description and physical property logs.

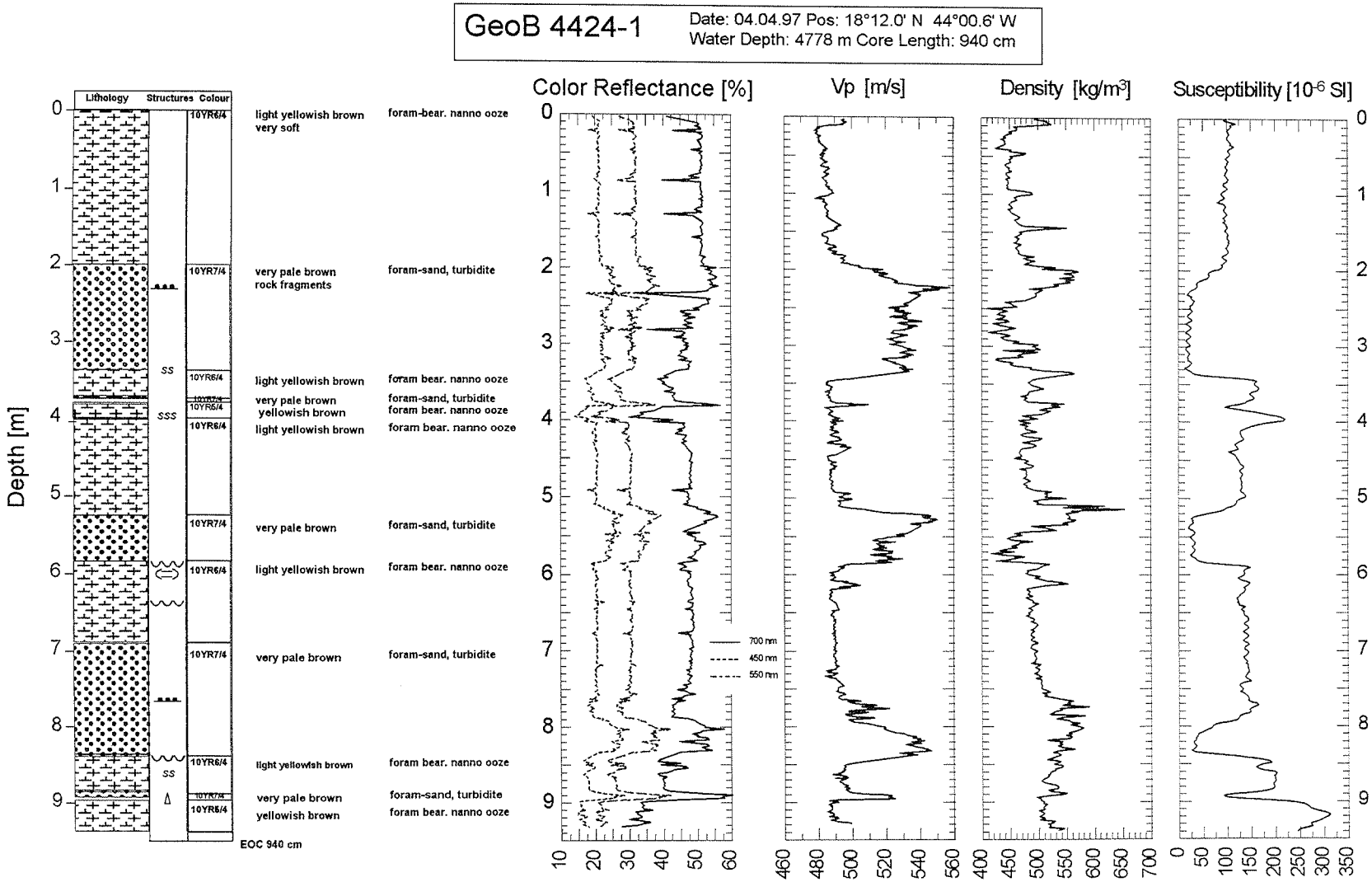


Figure 41 Gravity core 4424-1 - core description and physical property logs.

Turbidites of a few centimeters to more than a meter in thickness dominate the sedimentary columns of cores GeoB 4421-3 to 4424-1. They are characterized by yellowish brown foram sand, graded bedding and scoured contacts at the base. The top parts consist of very soft, homogenous foram bearing nanno ooze. Thickness and number of turbidites increase from site 4421 in shallowest to site 4424 in the deepest waters. The uppermost turbidite (200 - 339 cm) of core GeoB 4424-1 contains some rock fragments in. Abundant *discoasters* in cores GeoB 4423-2 and 4424-1 indicate sediments older than Pleistocene.

## 5.4 Physical Properties Studies

*T. Frederichs, C. Hilgenfeldt, A. Schmidt*

The complete sediment series recovered during METEOR Cruise M38/2 with the gravity corer were subject to laboratory geophysical studies. Shipboard measurements on the segmented cores routinely comprised three basic physical parameters:

- compressional (p-) wave velocity $v_p$,
- electric resistivity $R_s$ (as a measure of density and porosity), and,
- magnetic volume susceptibility $\kappa$.

These properties are closely related to lithology and grain size of the sediments and provide high-resolution core logs (spacing 1 cm for p-wave velocity, 2 cm for electric resistivity and magnetic volume susceptibility) available prior to all other detailed investigations. In addition, oriented samples for subsequent shore based rock and paleomagnetic studies were taken at typically 5 cm intervals.

### 5.4.1 Physical Background and Experimental Techniques

The experimental set ups for the shipboard measurements were basically identical to those of previous cruises. Their descriptions are therefore kept brief here. A more detailed treatment of the experimental procedures are given in WEFER et al. (1991) for $R_s$ and SCHULZ et al. (1991) for $v_p$.

*P-Wave Velocity*

The p-wave velocity $v_p$ is derived from digitally processed ultrasonic transmission seismograms recorded perpendicular to the core axis with a fully automated logging system. First arrivals are picked using a cross-correlation algorithm based on the 'zero-offset' signal of the piezoelectric wheel probes. Combined with the core diameter d, the travel time of the first arrivals t yields a p-wave velocity profile with an accuracy of 1 to 2 m/s

$$v_p = (d - d_L) / (t - t_0 - t_L)$$

where $d_L$ is the thickness of the liner walls, $t_L$ the travel time through the liner walls and $t_0$ the 'zero-offset' travel time.

Following SCHULTHEISS & McPHAIL (1989), a temperature calibration of $v_p$ is effected using the equation

$$v_{20} = v_T + 3 \cdot (20 - T)$$

where $v_{20}$ is the p-wave velocity at 20 °C and T the temperature (in °C) of the core segment when logged. Simultaneously, the maximum peak-to-peak amplitudes of the transmission seismograms are evaluated to estimate attenuation variations along the sediment core. P-wave profiles can be used for locating strong as well as fine-scale lithological changes, e.g., turbidite layers or gradual changes in the sand, silt or clay content.

*Electrical Resistivity, Porosity, and Density*

The electrical sediment resistivity $R_s$ was determined using a handhold sensor with a miniaturized four-electrodes-in-line ('Wenner') configuration (electrode spacing: 4 mm). A rectangular alternating current signal is fed to the sediment about 1 cm below the split core surface by the two outer electrodes. Assuming a homogeneously conducting medium, the potential difference at the inner two electrodes will be directly proportional to the sediment resistivity $R_s$. An integrated fast resistance thermometer simultaneously provides data for a temperature correction.

According to the empirical ARCHIE's equation, the ratio of sediment resistivity $R_s$ and pore water resistivity $R_w$ can be approximated by a power function of porosity $\phi$

$$R_s/R_w = k \cdot \phi^{-m}$$

Following a recommendation by BOYCE (1968), suitable for sea water saturated clay-rich sediments, values of 1.30 and 1.45 were used for the constants k and m, respectively. The calculated porosity $\phi$ is subsequently converted to wet bulk density $\rho_{wet}$ using the equation (BOYCE, 1976)

$$\rho_{wet} = \phi \cdot \rho_f + (1 - \phi) \cdot \rho_m$$

with a pore water density $\rho_f$ of 1030 kg/m$^3$ and a matrix density $\rho_m$ of 2670 kg/m$^3$. For the sake of an unbiased uniform treatment of all cores, these empirical coefficients were not adapted to individual sediment lithologies at this stage. Nevertheless, at least relative density changes should be well documented.

*Magnetic Volume Susceptibility*

The magnetic volume susceptibility $\kappa$ is defined by the equations

$$B = \mu_0 \cdot \mu_r \cdot H = \mu_0 \cdot (1 + \kappa) \cdot H = \mu_0 \cdot H + \mu_0 \cdot \kappa \cdot H = B_0 + M$$

with the magnetic induction B, the absolute and relative permeabilities $\mu_0$ and $\mu_r$, the magnetizing field H, the magnetic volume susceptibility $\kappa$ and the volume magnetization M. As can be seen from the third term, $\kappa$ is a dimensionless physical quantity. It records the amount to which a material is magnetized by an external magnetic field.

For marine sediments the magnetic susceptibility may vary from an absolute minimum value of around $-15 \cdot 10^{-6}$ (diamagnetic minerals such as pure carbonate or silicate) to a maximum of some $10.000 \cdot 10^{-6}$ for basaltic debris rich in (titano-) magnetite. In most cases $\kappa$ is primarily determined by the concentration of ferrimagnetic minerals, while paramagnetic matrix components such as clays are of minor importance. High magnetic susceptibilities indicate high concentrations of lithogenic compounds / high iron (bio-)mineraliztion or low carbonate / opal productivity and vice versa. This relation may serve for the mutual correlation of sedimentary sequences which were deposited under similar global or regional conditions.

The measuring equipment consists of a commercial BARTINGTON M.S.2 susceptibility meter with a 125 mm loop sensor and a non-magnetic core conveyor system. Due to the sensor's size, its sensitivity extents over a core interval of about 8 cm. Consequently, sharp susceptibility changes in the sediment column will appear smoothed in the $\kappa$ core log and, e.g., thin layers such as ashes cannot appropriately be resolved by whole-core susceptibility measurement.

### 5.4.2 Shipboard Results

*Sampling Sites and Recovery*

The gravity coring program of Cruise M38/2 concentrated primarily on the Ceará Rise and adjacent abyssal plains covering the area of about 3 to 6°N and 41 to 45°W. Sediments were retrieved from the summit region (cores GeoB 4401-4, 4406-1 and 4407-3) and from the eastern (cores GeoB 4402-2, 4403-2, 4404-1, 4405-3, 4411-2, 4412-2, and 4413-2) and western flanks (cores GeoB 4414-1, 4415-3, 4416-1, and 4416-3). Further coring activities included the Amazon Fan (cores GeoB 4408-2, 4409-1, 4410-2 and 4417-4), the continental slope off Guyana (cores GeoB 4418-1 and 4419-4 / -6) and the mid-Atlantic Ridge near 17°N (cores GeoB 4420-2, 4421-3, 4422-2, 4423-2, and 4424-1).

Cores GeoB 4401-4, 4406-1, 4405-3, 4404-1, 4403-2, and 4402-2 make up a bathymetric transect from 3397 down to 4637 m water depth over the north-eastern slope of the Ceará Rise into the Pará Abyssal Plain including ODP Sites 928 and 929 (Leg 154). This coring strategy particularly aimed at documenting the effects of calcite dissolution and was repeated about 30 nm to the west starting at 3295 and ending at 4295 m a water depth (cores GeoB 4411-2, 4412-2, and 4413-2). The series of cores GeoB 4414-1, 4415-3, 4416-1, and 4416-3 are the counterparts on the south-western flank (3236 to 3901 m water depth) towards the Ceará Abyssal Plain. With core GeoB 4407-3 the former GeoB location 1523 of METEOR Cruise M16/2 (1991) was

resampled on the south-eastern top of the Ceará Rise. Cores GeoB 4410-2, 4409-1, and 4408-2 located along about 6 N connect the Ceará Abyssal Plain to the Amazon Fan realm which was further sampled in 3511 m water depth (core GeoB 4417-4) at location GeoB 1514 of the 1991 METEOR Cruise M16/2. Cores GeoB 4418-1, 4419-4, and 4419-6 were recovered on the continental slope off Guyana (about 9°N, 54°W) at 2499 and 4486 m water depth, respectively and are to supplement sediment materials collected during the 1996 METEOR Cruise M34/4. In the last working area on the mid-Atlantic Ridge (about 16 to 17°N and 44 to 46°W) cores GeoB 4420-2, 4421-3, 4422-2, 4423-2, and 4424-1 were retrieved from water depths between 2767 and 4778 m along a transect running in NE direction, oblique to the ridge axis.

The recovery varied between 301 (core GeoB 4416-1) and 940 cm (core GeoB 4424-1). A total of 26 sediment cores with a cumulative length of 176 m was investigated (see upper part of Figure 42).

*General Results*

The general characteristics of the physical properties are compiled in the lower part of Figure 42. Dots mark the mean values of compressional wave velocity, density and magnetic susceptibility for the individual cores, vertical bars denote their standard deviations. Each diagram is divided into six sections according to the six working areas, separating data sets from the western flank of the Ceará Rise (CR West), its summit region (CR Top) and eastern flank (CR East), the Amazon Fan (AF), the Guyana Continental Slope (GCS) and the mid-Atlantic Ridge (MAR).

The average p-wave velocities ranging from 1477 to 1526 m/s are relatively uniform throughout all sites, except for core GeoB 4416-3. The velocity data show no obvious trends in relation to water depth nor specific regional distinctions.

Overall, average densities (1481 to 1669 kg/m$^3$) parallel the results of p-wave velocity measurements, their variabilities are slightly more pronounced, however. A rather poorly developed trend of decreasing average densities with greater water depths in the sediments from the top region of the Ceará Rise (1619 to 1575 kg/m$^3$), the Amazon Fan (1650 to 1611 kg/m$^3$) and the Guyana Continental Slope (1520 to 1481 kg/m$^3$) is much enhanced (1669 to 1492 kg/m$^3$) at the mid-Atlantic Ridge. On both flanks of the Ceará Rise average densities varying from 1480 to 1526 kg/m$^3$ exhibit no consistent relationship to water depth.

Mean susceptibilities, ranging from 98 to 367·10$^{-6}$ SI for the entire core collection, rise with increasing water depths in top region and on the eastern flank of the Ceará Rise, while in the Amazon Fan just an opposite trend is observed. For the other working areas no such unequivocal relationship between susceptibility and water depth could be observed.

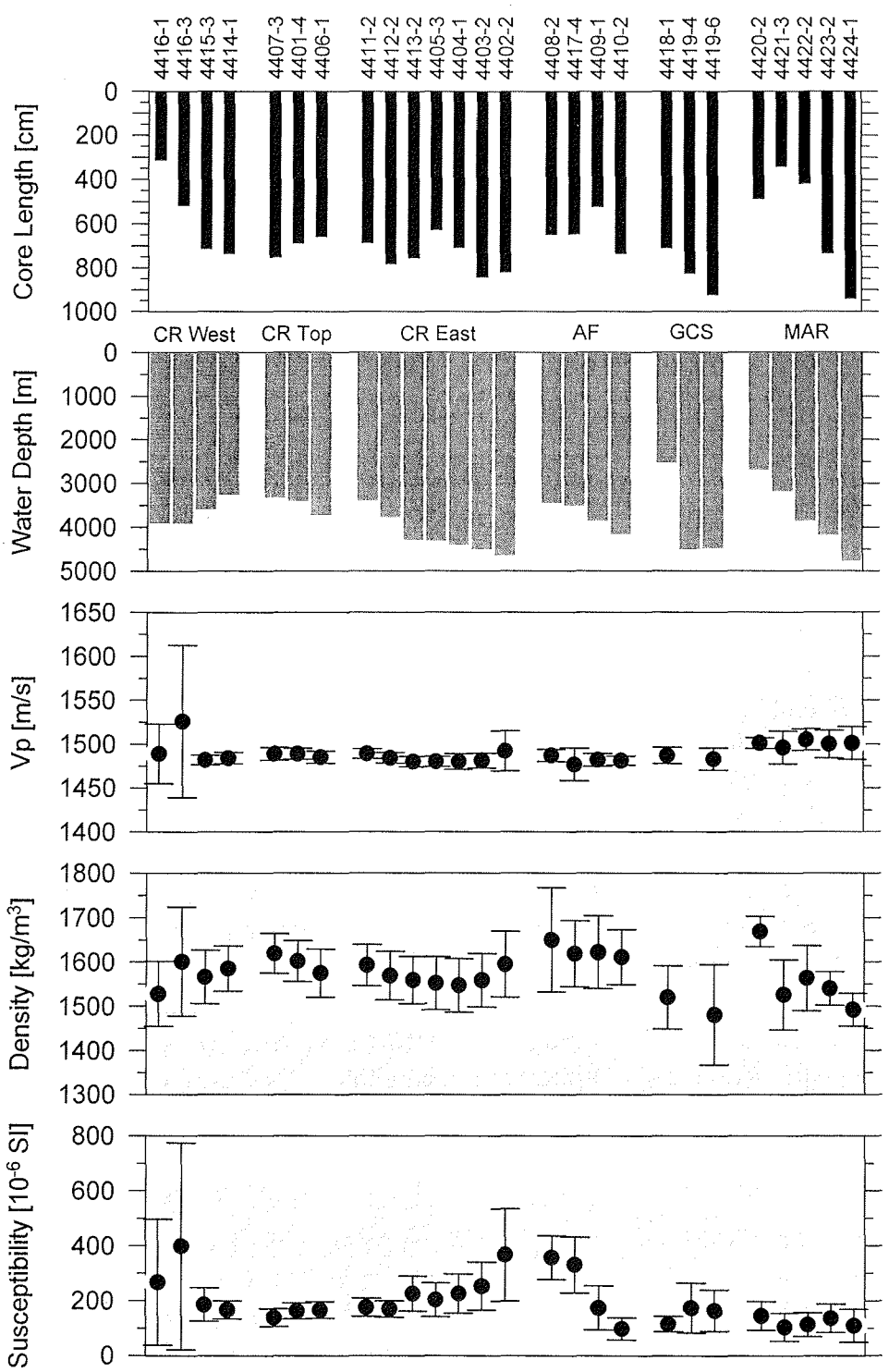


Figure 42 Mean compressional wave velocities, densities and magnetic susceptibilities of cores GeoB 4401-4 through 4424-1 as compared to variations in water depth at the sampling sites and core recovery. The vertical bars denote standard deviations. Data sets are classified according to the six working areas, the western flank of the Ceará Rise (CR West), its summit region (CR Top) and eastern flank (CR East) as well as the Amazon Fan (AF), Guyana Continental Slope (GCS) and mid-Atlantic Ridge (MAR).

Physical property logs for the individual cores are shown in Figures 18 to 41 together with the visual core descriptions.

*Special Features*

Ceará Rise Summit Region (Cores GeoB 4401-4, 4406-1 and 4407-3)

Mean p-wave velocities between 1485 and 1489 m/s and mean densities of 1575 to 1619 kg/m$^3$ were encountered. Magnetic susceptibilities range from 139 to 166·10$^{-6}$ SI. Site to site correlations of the physical property core logs are quite obvious and can be extended to the western and eastern flanks. The locations provide excellent climatically controlled susceptibility records indicating sedimentation rates between 3 and 5 cm/kyr.

Ceará Rise Eastern Flank (Cores GeoB 4402-2, 4403-2, 4404-1, 4405-1, 4411-2, 4412-2 and 4413-2)

Sediments from water depths above 4000 m (cores GeoB 4411-2 and 4412-2) show the same climatically induced susceptibility patterns as those from the top of the Ceará Rise. Their mean p-wave velocities range from 1484 to 1489 m/s, densities from 1569 to 1593 kg/m$^3$ and magnetic susceptibilities from 170 to 176·10$^{-6}$ SI. Below 4000 m water depth (cores GeoB 4402-2, 4403-2, 4404-1, 4405-1, and 4413-2), the number of interlayered turbidites increases considerably. For some of them a straightforward correlation over several sites seems plausible. While mean p-wave velocities (1480 to 1492 m/s) and densities (1547 to 1595 kg/m$^3$) are not affected, turbidites typically produce maxima in the magnetic susceptibility logs and mean values increase to between 203 and 267·10$^{-6}$ SI. A possible explanation for this phenomenon could be a diagenetic formation of magnetite or alternatively a relatively enhanced deposition of ore components in proximal turbiditic deposits. The age model developed for the Ceará Rise summit region can entirely be transferred to the eastern flank sediments by correlating characteristic variations in the magnetic susceptibility logs. Due to the progressively more abundant turbidites, the apparent sedimentation rate rises from around 4 cm/kyr (Site GeoB 4405) to about 7 cm/kyr (Site GeoB 4402) with increasing water depth.

Ceará Rise Western Flank (Cores GeoB 4414-1, 4415-3, 4416-1 and 4416-3)

In sediments from shallow water depth on the western flank of the Ceará Rise (cores GeoB 4414-1 and 4415-3) the average p-wave velocity amounts to around 1483 m/s. Wet bulk densities range from 1566 to 1585 kg/m$^3$, magnetic susceptibilities from 167 and 186·10$^{-6}$ SI and their variations can easily be matched in both core logs. The most prominent feature in cores GeoB 4416-1 and 4416-3 is an about 1 m thick turbidite below 270 cm core depth. Close to its base all three physical properties reach their maximum values, p-wave velocity rises to 1750 m/s, density to 1900 kg/m$^3$ and magnetic susceptibility to almost 1400·10$^{-6}$ SI which is seven times higher than the mean for the remaining core. Unlike this positive correlation between p-wave velocity and magnetic susceptibility within the turbidite, there are also horizons with an inverse relationship between the two parameters (e.g., at 620 cm in core GeoB 4415-3). In cores GeoB 4414-1 and 4415-3 from shallower water depth significantly thinner turbidites

were encountered. Their down-core variations of magnetic susceptibility are thus predominantly climatically induced. Sedimentation rates of about 4 to 5 cm/kyr slightly increase with greater water depth.

Amazon Fan (Cores GeoB 4408-2, 4409-1, 4410-2 and 4417-4)

In their deeper parts the sediment cores from the Amazon Fan contained variable amounts of methane. Acoustic measurements were often not possible in these sections because of insufficient signal amplitudes as degassing of methane and formation of gas bubbles due to pressure release strongly attenuate sound transmission. Where acoustic measurements could be performed mean p-wave velocities range between 1477 and 1489 m/s. Wet bulk densities vary from to 1611 to 1650 m/kg$^3$, magnetic susceptibilities from 98 to 357·10$^{-6}$ SI. Cores from water depths of 3400 to 3500 m (GeoB 4408-2, 4417-4) exhibit significantly higher susceptibilities as compared to those from deeper waters. This depletion in magnetic constituents with greater water depth should reflect the reduced deposition of terrigenous material with increasing distance to the continental shelf. Core to core correlations based on magnetic susceptibility variations confirm this trend as they indicate distinctly higher sedimentation rates in cores from shallow water depth. The approximately linear down-core increase of density observed in all four cores suggests a quite strong compaction of the sediments resulting from exceptionally high overall deposition rates.

Guyana Continental Slope (Cores GeoB 4418-1, 4419-4 and 4419-6)

Sediments from the outer margin of the Guyana Plateau yield mean p-wave velocities of 1483 to 1487 m/s, densities of 1481 to 1520 kg/m$^3$ and magnetic susceptibilities of 116 to 174·10$^{-6}$ SI. At shallow water depth (core GeoB 4418-1, 2499 m) only a few thin turbidites occur and density variations are fairly cyclic. In deeper water (core GeoB 4419-4, 4419-6, and 4486 m) the deposits are characterized by numerous turbidites, particularly in the lower sections of the cores resulting in increased densities and p-wave velocities. Similar as in the cores from the deeper Ceará Rise realm, the turbidites display again elevated susceptibilities. The cyclic density variations are replaced by down-core compaction, especially in the lowest part of the cores, where the turbiditic layers dominate.

Mid-Atlantic Ridge (Cores GeoB 4420-2, 4431-3, 4422-2, 4423-2 and 4424-1)

For the mid-Atlantic Ridge sediment series no obvious core to core correlations could be established based on physical properties. Mean p-wave velocities (1496 to 1505 m/s) and magnetic susceptibilities (109 to 145·10$^{-6}$ SI) show only moderate variations and no dependence on water depth. In contrast to sediments from the Ceará Rise, p-wave velocities and magnetic susceptibilities are inversely correlated. In the cores from deeper waters the cyclic pattern in magnetic susceptibility as in core GeoB 4420-2 (2767 m) is interrupted by layers of about constant low as well as high susceptibilities. In general, mean wet bulk densities decrease with greater water depth from 1669 (core GeoB 4420-2) to 1492 kg/m$^3$ (core GeoB 4424-1).

## 5.5 Pore Water Chemistry

*K. Enneking, C. Hensen, S. Hinrichs, S. Kasten*

Main objectives of the geochemical investigations during Cruise M38/2 included

- a study of early diagenetic mineralization processes of organic matter in marine sedimentary deposits by quantifying diffusive pore water fluxes. The pore water concentration profiles of nutrients in near surface sediments supplement the existing data base for the western equatorial Atlantic Ocean and are used to calculate and model the diffusive fluxes across the sediment/water interface on a regional scale. Subsequent detailed analyses will be performed at the University of Bremen in the scope of the German JGOFS program.

- a resampling of station GeoB 1523 (METEOR Cruise M16/2, 1991) on the Ceará Rise to determine relevant pore water constituents and thereby complementing already available high-resolution solid phase data sets for this site. The pore water measurements together with additional analyses of fresh sediment material should give conclusive evidence for the origin and mode of formation of characteristic solid phase element enrichments discovered at glacial/interglacial transitions in these deposits.

- the recovery of gravity cores from the Amazon Fan - including a resampling of the former station GeoB 1514 - to examine deeper, anoxic layers for methane and to probe the sediment solid phase under argon atmosphere. These data and samples are lacking for the gravity cores taken in the Amazon Fan during Meteor Cruise M16/2 in 1991. They are intended to prove that sulphate reduction taking place in a narrow sub-bottom depth interval between 5 and 6 m is essentially driven by anaerobic methane oxidation. Furthermore, analyses of the deep-sea fan sediments aim at evaluating the potential of climatically induced non-steady-state depositional conditions to modify the solid phase record. The Amazon Fan experienced such a distinct change in sedimentary environment during the Pleistocene/Holocene transition. Detailed solid phase examinations including acid digestions as well as mineralogical and physical studies will be performed at the University of Bremen.

### 5.5.1 Methods

In order to prevent a warming of the sediments, all cores were transferred to a cooling room immediately after recovery and maintained at a temperature of 2 - 4 °C.

The multicorer cores were processed directly after they had been retrieved. From the bottom water samples were taken for pH and Eh measurements and for nutrient analysis. The remaining bottom water was carefully removed by means of a siphon to avoid any disturbance of the sediment surface. During subsequent cutting of the core

into slices for pressure filtration, pH and Eh have been determined at 0.5 cm intervals. Density and porosity of the sediments were obtained from electrical conductivity and temperature measurements (see Chapter 5.4) performed on a second core of the same cast.

The gravity cores have been cut into 1 m segments on deck. At locations, where methane was expected to be present, syringe samples were immediately taken from every cut segment surface. Higher resolution sampling for methane analysis was carried out in the cooling laboratory. Via openings in the core liners syringe samples of 5 ml sediment were taken every 10 - 20 cm and injected into 50 ml septum vials containing 20 ml of sea water. After closing and shaking, methane becomes enriched in the head space of the vial. Parallel to the sampling for methane analysis, $H_2S$ was determined by means of a needle electrode and a reference electrode.

Within a few days after their recovery the gravity cores have been cut lengthwise into two halves. On the working halves pH and Eh were determined and sediment samples taken every 20 cm for pressure filtration. At same intervals conductivity and temperature were measured on the archive halves as well as solid phase samples taken afterwards kept in gas-tight glass bottles under argon atmosphere. The storage temperature for all sediments was -20 °C to avoid dissimilatory oxidation.

All work on opened cores was done in a glove box under argon atmosphere. For pressure filtration Teflon- and PE-squeezers were operated with argon at a pressure gradually increased to 5 bar. The pore water was retrieved through 0.2 µm cellulose acetate or polyamide membrane filters. Depending on porosity and compressibility of the sediments, the amount of pore water recovered varied between 5 and 20 ml.

The following parameters have been determined on board:

- Eh, pH, electrical conductivity and temperature were measured by means of electrodes before the sediment structure was disturbed by any sampling.
- For nitrate and phosphate standard photometrical methods were employed using an autoanalyser.
- Ammonium was obtained from conductivity measurements after extruding $NH_3$ with sodium hydroxide into HCl.
- Alkalinity was calculated from a volumetric titration of 1.5 ml subsamples with 0.01 or 0.05 M HCl, respectively.
- For photometrical iron analyses 1 ml subsamples were taken within the glove box and immediately complexed with 50 µl of Ferrospectral.
- $SO_4^{2-}$ and $Cl^-$ were determined by ion chromatography of pore water diluted 1:20 with deionized water.
- Fluoride was measured with an ion sensitive electrode.
- For $H_2S$ a similar potentiometrical technique was utilized. The ion sensitive needle electrode and reference electrode were calibrated by adding $Na_2S$ to oxygen free

'Sørensen' buffer solutions with different pH. This method is suitable for $H_2S$ concentrations below 100µmol/l.

- To quantify methane 25 µl of the gas accumulated in the headspace of a vial as described above were analyzed in a gas chromatograph. Preliminary methane contents calculated here from the concentrations measured assume a uniform porosity of 0.6 in all gravity cores.

The remaining pore water was acidified with $HNO_{3\ (suprapure)}$ to a pH of 2 for storing and subsequent determination of cations by ICP-AES and AAS. All pore water samples are preserved at 4 °C until further analyses in shore based laboratories.

### 5.5.2 Shipboard Results

During Cruise M38/2 sediments from a total of 15 stations were examined geochemically, including 4 gravity cores and 15 multicorers.

At all these stations nitrate and phosphate pore water profiles (Figs. 43 and 44) indicate low mineralization rates of organic matter in the top sediments reflecting the overall oligotrophic conditions in surface waters of the working areas. Following a slight increase to depth, nitrate concentrations remain on an about constant level in the multicorer cores. The onset of denitrification is only observed in multicorer cores at stations GeoB 4409, 4417, 4418, and 4419 (Figs. 43a, b). Pore water concentration profiles depicted in Figure 44 show a limited flux of phosphate into the bottom water. At several locations, the topmost phosphate concentrations would even suggest a flux of phosphate into the sediment. This, however, is attributed to result from the sampling procedure.

The pore water concentration profiles determined for gravity core GeoB 4407-1 (Fig. 45) - which resampled the previous GeoB location 1523 - reveal similar geochemical conditions as cores GeoB 1505 and 1508 also recovered during METEOR Cruise M16/2 in 1991. Denitrification is confined to the upper 1.5 m of the sediment column. The phosphate profile indicates both a diffusive flux into the bottom water and a solid phase fixation between 4 and 4.5 m core depth. At this level alkalinity shows a distinct decrease. It seems likely therefore that the consumption of both constituents is linked to the precipitation of carbonates. Iron is present in pore water below about 2.7 m indicating the reduction of iron (hydr)oxides. The level of reoxidation of reduced iron is identified between 2.7 and 3 m.

The two cores GeoB 4409-3 and 4417-7 (former GeoB location 1514) recovered from the Amazon Fan show the typical stratigraphy of this sedimentary setting. The topmost layers consist of pelagic foraminiferal ooze. These calcareous deposits are separated from the underlying late glacial terrigenous clays and silts by a diagenetic rust-colored, iron-rich crust which should approximately mark the Pleistocene/Holocene boundary. The lower sections of the cores are characterized by abundant authigenic

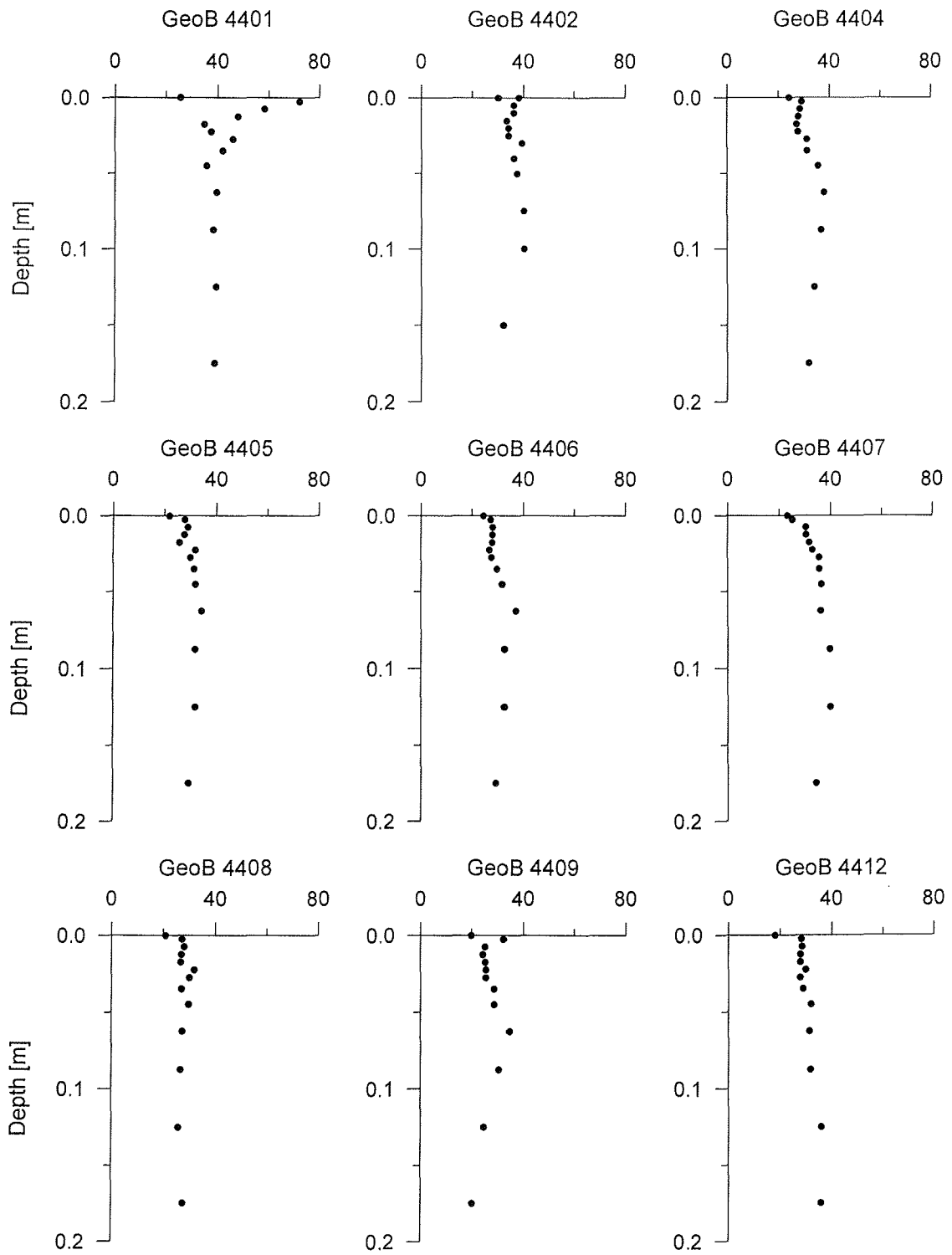


Figure 43a Pore water concentration profiles of nitrate (µmol/l) in the multicorers.

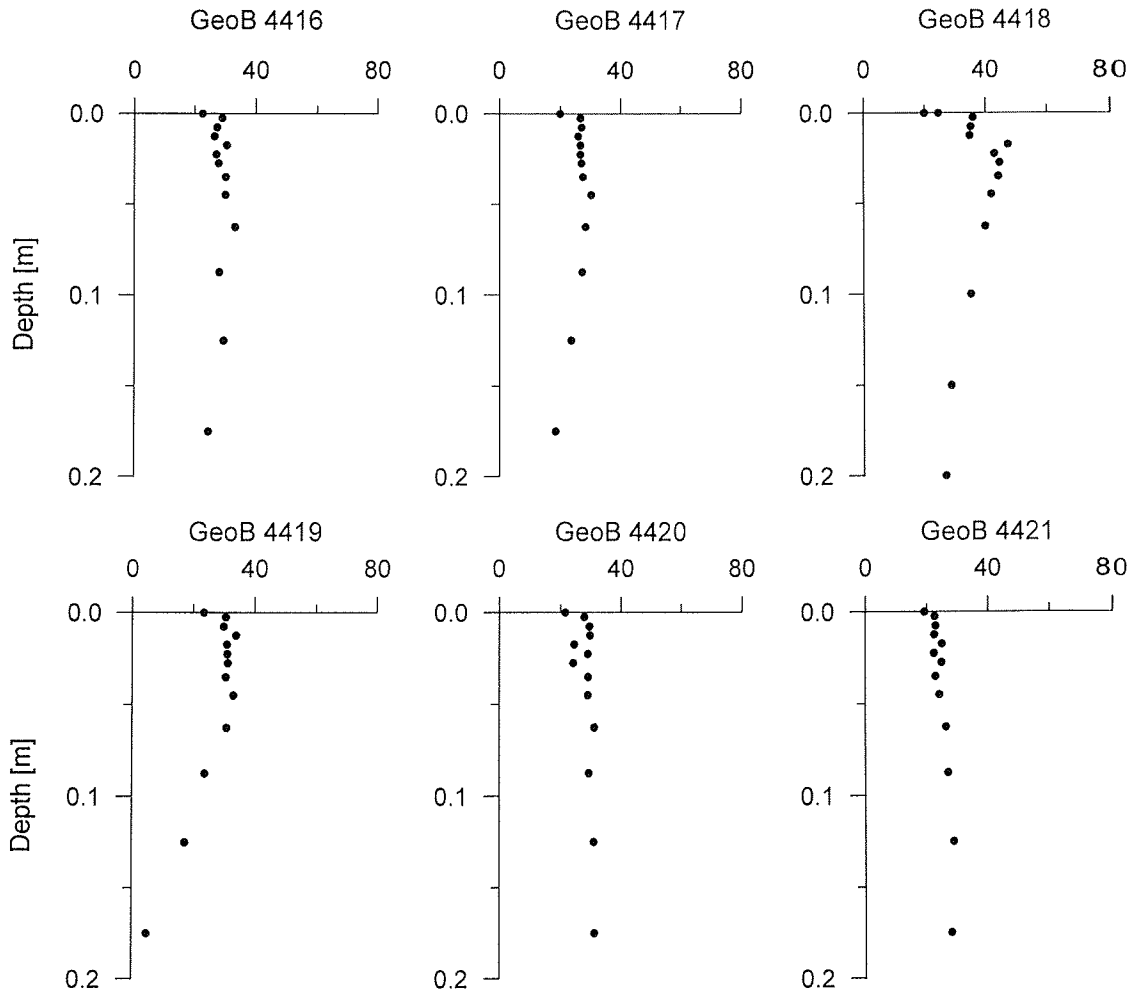


Figure 43b Pore water concentration profiles of nitrate (µmol/l) in the multicorers.

iron sulfide minerals. Pore water constituents analyzed on board reveal similar geochemical features in both cores (Figs. 46 and 47). Sulphate decreases linearly from the bottom water down to core depths of 5.7 m (core GeoB 4409-3) and 3.9 m (core GeoB 4417-7), respectively. These zones of sulphate reduction coincide with the interval in which methane diffusing upwards from greater sediment depth is consumed (Fig. 48). The distinct methane/sulphate relationship clearly documents that deep sulphate reduction in the Amazon Fan sediments is not driven by the degradation of organic matter but by an anaerobic oxidation of upward diffusing methane. The pore water profiles of ammonium, which display no significant gradient change within this reaction zone, further substantiate this interpretation. Preliminary evaluations of the diffusive fluxes of methane and sulphate into the reaction zone indicate a complete reduction of sulphate by methane at both sites. A comparison of the pore water profiles of the two cores with those from stations off Namibia, where anaerobic methane oxidation takes place at significant rates, shows striking differences in the phosphate con-

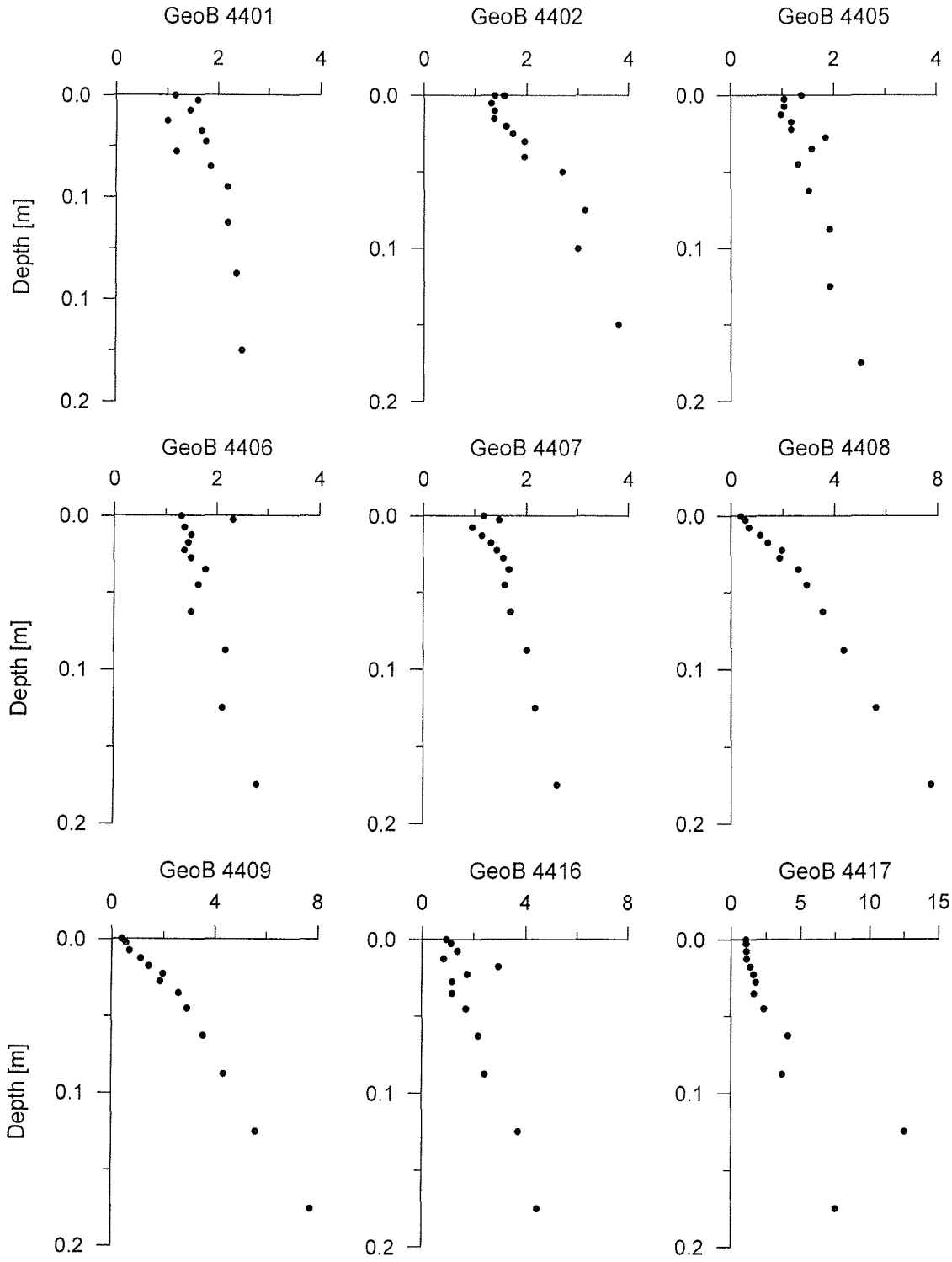


Figure 44 Pore water concentration profiles of phosphate (µmol/l) in the multicorers.

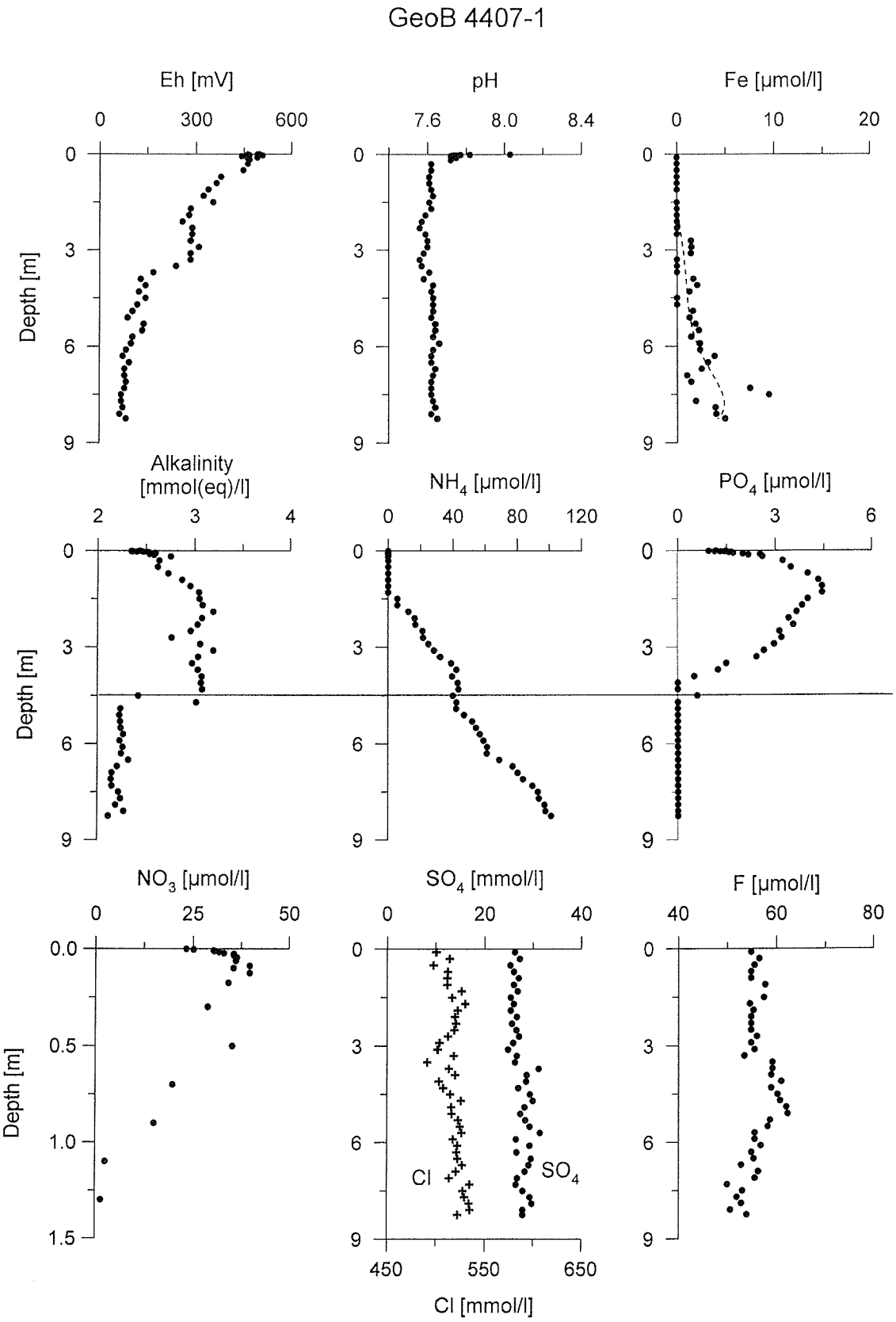


Figure 45 Pore water concentration profiles in gravity core GeoB 4407-1.

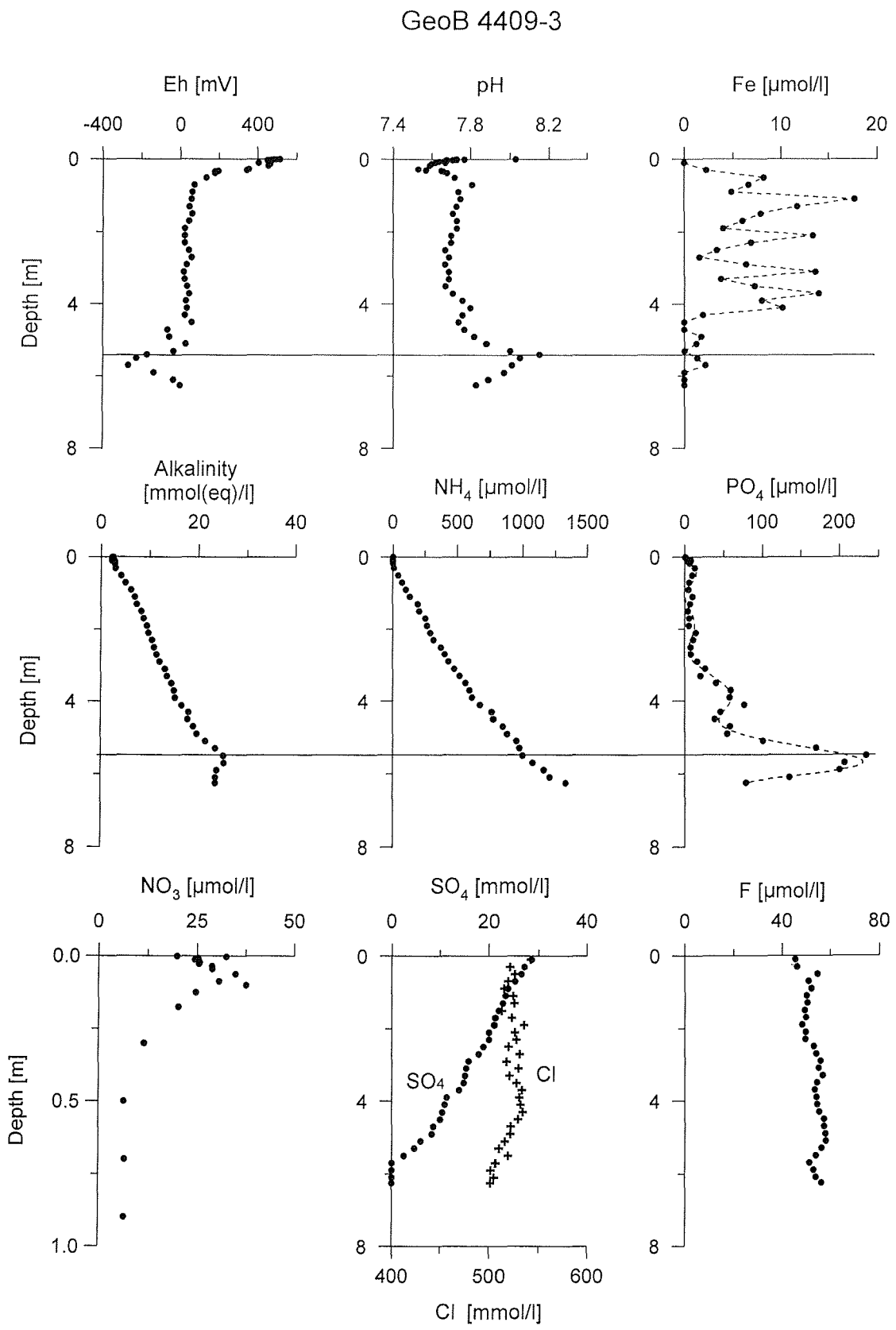


Figure 46 Pore water concentration profiles in gravity core GeoB 4409-3.

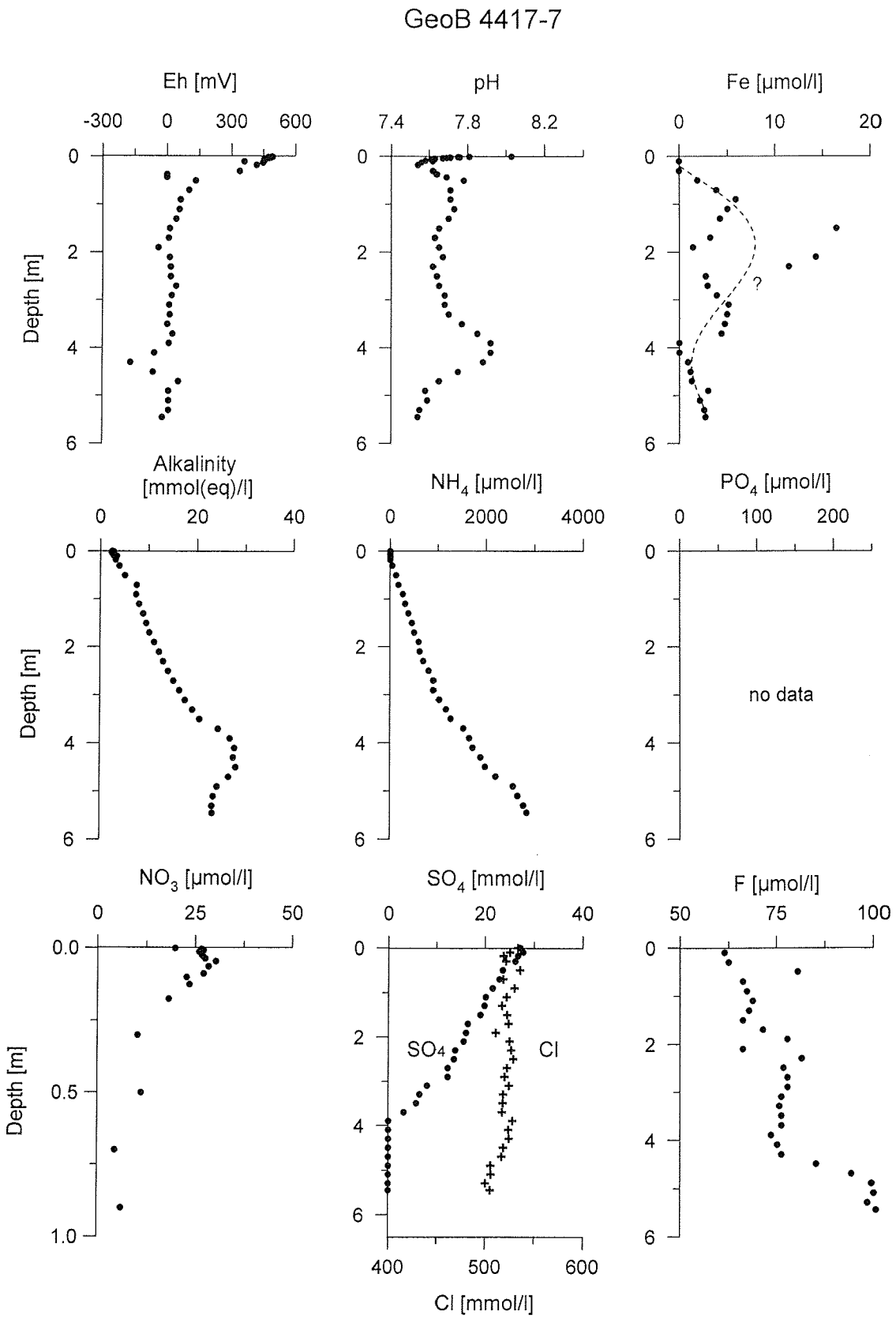


Figure 47 Pore water concentration profiles in gravity core GeoB 4417-7.

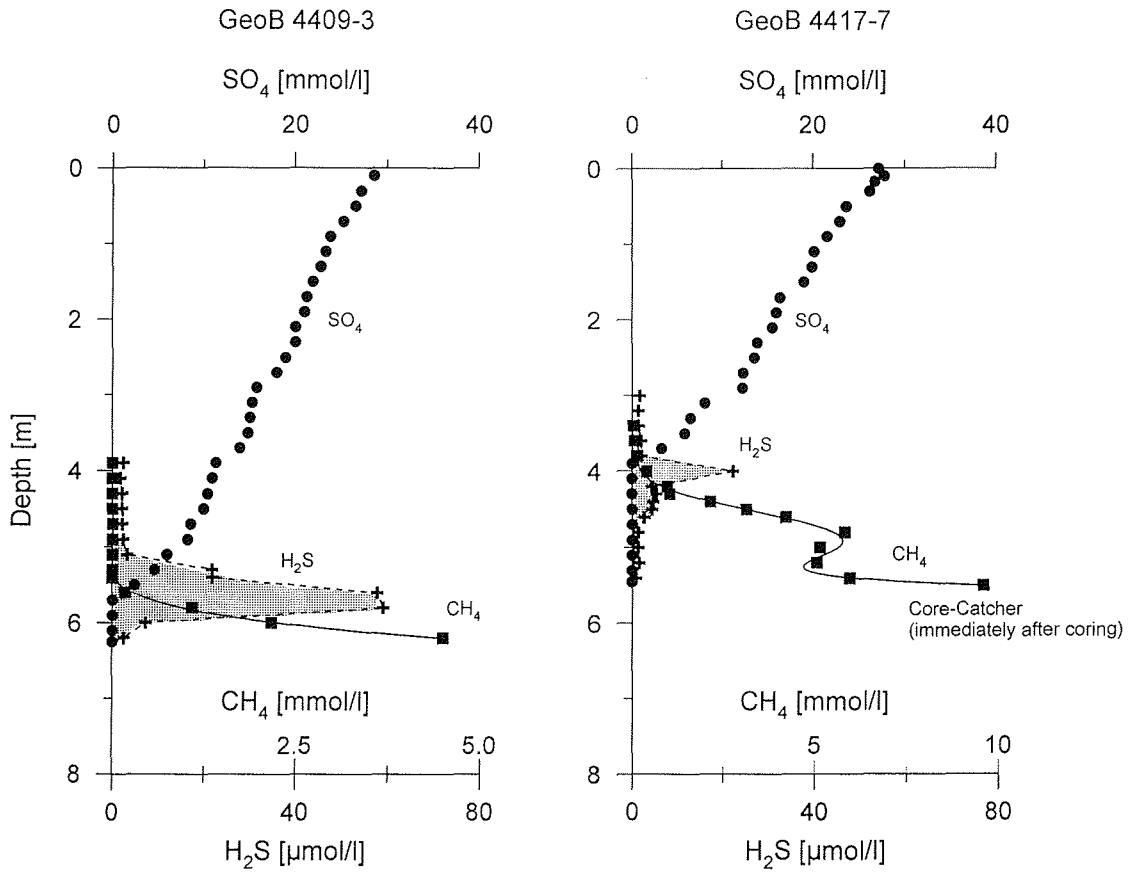


Figure 48 Comparison of pore water concentration profiles of sulphate, $H_2S$ and methane in gravity cores GeoB 4409-3 and GeoB 4417-7.

centration profiles. While off Namibia phosphate and ammonium concentrations follow a similar trend, discrete phosphate peaks occur within the methane/sulphate transition zone of the Amazon Fan sediments. This finding is ascribed to the higher amount of reactive iron in the latter deposits. Where dissolved sulphate is completely reduced and iron removed as sulfides, the phosphate concentrations decrease rapidly, suggesting that available reduced iron precipitates as iron phosphate. Millimeter-sized nodules of vivianite found below the methane/sulphate transition zone in ODP cores recovered from the Amazon Fan during Leg 155 further support this interpretation.

In core GeoB 4409-3 the methane concentration decreases from about 5 mmol/l at the bottom of the core to zero within the methane/sulphate transition zone at around 5.7 m core depth. Core GeoB 4417-7 reaches deeper beneath the methane/sulphate transition zone and methane concentrations in the lower part of the core scatter around 5 mmol/l which is close to the saturation concentration of methane at 1 atm. A methane concentration of almost 10 mmol/l in the sample taken from the core catcher immediately after retrieval of this core suggests that large amounts of methane have already degassed prior to the routine sampling in the cooling room. Particularly sensitive needle electrode measurements revealed a distinct zone of free $H_2S$ which could not be

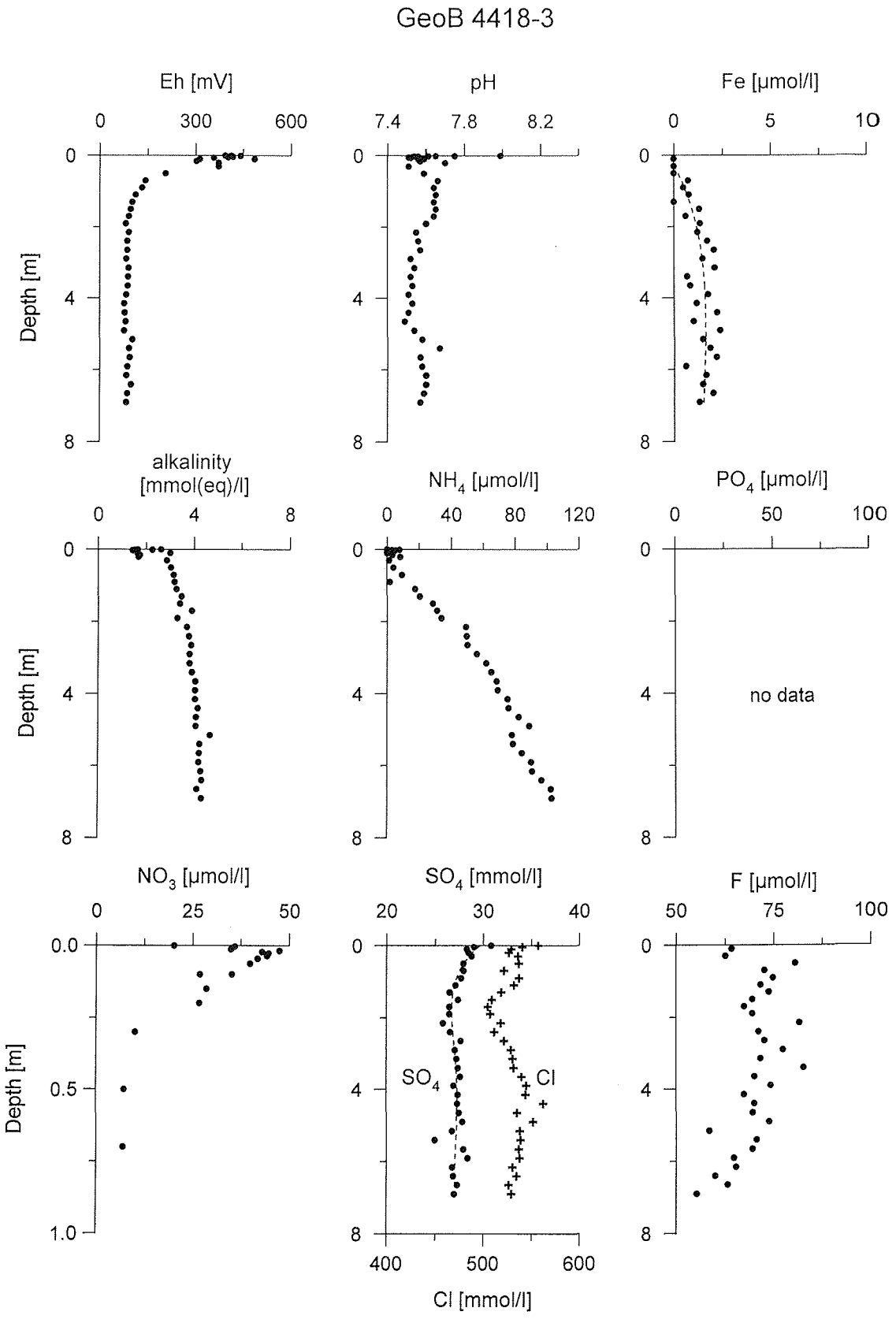


Figure 49 Pore water concentration profiles in gravity core GeoB 4418-3.

documented so far. Maximum $H_2S$ concentrations amounting to 60 µmol/l in core GeoB 4409-3 and 25 µmol/l in core GeoB 4417-7 were found in the methane/ sulphate transition zones (Fig. 48). The higher concentrations of $H_2S$ found in core GeoB 4409-3 may be due to a depositional regime of less reactive iron than at site GeoB 4417 closer to the Amazon River mouth, where an influx of high amounts of detrital iron (hydr)oxides appears more likely. The presence of reduced iron leads to an efficient removal of any $H_2S$ from pore water by precipitation of iron sulfides.

Below the methane/sulphate transition zone the sediment structures are unusually disturbed. In these depth intervals the chloride pore water concentrations decrease slightly (Figs. 46 and 47). A possible explanation for both phenomena could be a melting of methane hydrates previously present *in situ*.

Core GeoB 4418-3 (Fig. 49) recovered from the upper slope of the Guyana Plateau consists of a foraminiferal sequence on top of several meters of silts and clays with numerous interlayered turbidites. The transition at about 35 cm core depth is characterized by a distinct color change and Eh reduction from around 400 to a constant level of approximately 100 mV. At this depth denitrification is more or less completed. Below the color change, iron is present in pore water at a uniform concentration of 2 µmol/l. The pore water profiles of alkalinity and ammonium increase slightly down-core indicating low biomineralization activity in deeper sediment layers. The sulphate concentration profile displays an about linear decrease in the upper 1.5 meters to around 26 mmol/l. This might reflect a near surface sulphate reduction driven by the degradation of organic matter which is usually not observed in deep-sea deposits.

# 6 Plankton Sampling

*H. Buschhoff, B. Donner, A. Meyer, B. Meyer-Schack, S. Mulitza, A. Vink*

## 6.1 Dinoflagellate Investigations

Dinoflagellates are unicellular, biflagellated green algae, forming a major constituent of the marine phytoplankton. With the exception of the calcareous walled vegetative coccoid *Thoracosphaera heimii* most dinoflagellates undergo two important stages in their life cycle, one as a motile cellulosic vegetative thecate stage and the other as a resting cyst stage in which the cysts are usually organic walled but may also, in a few cases, be calcareous ('calcispheres'). Studies of the calcareous dinoflagellate cysts and their corresponding thecae, including the vegetative coccoid *Th. heimii*, are of special interest at the University of Bremen; focusing primarily on the complex and interacting relationships between recent species associations in the South Atlantic and environmental parameters such as temperature, salinity, light, nutrient supply, effects of hydrodynamic current systems, etc. Understanding of these interactions is extremely important for the interpretation of fossil dinoflagellate cyst assemblages in the sedimentary record which can be greatly applicable as a proxy in paleoceanography and paleoenvironmental modeling. In order to improve our knowledge on the geographic and vertical distribution of individual species and to attempt culturing them for future experimentation, phytoplankton samples were collected during the cruise from variable depths of the water column, ranging from surface waters down to 100 m depth (dinoflagellates show a variable depth distribution but are generally found within tens of meters below the water surface as most are photosynthetic).

Surface water samples were acquired from a depth of about 2.5 m three times a day using the ship's membrane pump (7 - 11; 12 - 16 and 17 - 20 board time; see Table 5). The water was continuously passed over a 100 µm filter to remove the zooplankton as much as possible and then filtered over a 10 µm gauze, thereby acquiring the 10 - 100 µm organic matter fraction in a 1 l collecting vessel. Filtered down to 150 ml using a 5 µm polycarbonate filter and a vacuum pump system, the samples were subsequently scanned for living vegetative thecate dinoflagellates, calcareous dinoflagellate cysts and the vegetative coccoid *Th. heimii*. Individual specimens have been isolated and placed in mixtures of sterile polyterene Cell Wells™ containing different types of culture media (f/2 35 ‰, K 35 ‰) and 0.2 µm filtered sea water (ratio about 1:1). In this way, attempts were made at culturing calcareous cyst producing dinoflagellates under on board conditions using the local day/night cycle at temperatures between 20 and 25 °C. Germination experiments and further routine culturing of these dinoflagellates aimed at investigating various aspects of ecology, productivity, life cycles, biomineralization processes and systematics will be carried out at the University of Bremen. After analysis, the water samples were stored, together with their filters, in 250 ml Nalgene polycarbonate flasks and fixated with 3 - 4 % formaldehyde. For transportation, the samples were kept in the dark at 4 °C.

Table 5 Surface water samples taken for dinoflagellate analyses.

| Date Sample No. | Start / End of Filtration (UTC) | Latitude (°N) at Start / End of Filtration | Longitude (°W) at Start / End of Filtration | Water Depth (m) | Salinity (‰) | Water Temperature (°C) |
|---|---|---|---|---|---|---|
| 07.03.a | 10:11 | 01°48.7' | 42°16.5' | 4345 | 35.69 | 27.3 |
| | 13:46 | 01°59.0' | 42°28.7' | | | |
| 07.03.b | 15:09 | 02°04.8' | 42°32.1' | 4322 | 35.69 | 27.4 |
| | 19:10 | 02°22.8' | 42°40.2' | | | |
| 07.03.c | 20:08 | 02°27.3' | 42°42.3' | 4309 | 35.70 | 27.4 |
| | 23:05 | 02°40.1' | 42°47.9' | | | |
| 08.03.a | 08:00 | 03°16.7' | 43°04.3' | 4296 | 35.62 | 27.2 |
| | 11:46 | 03°32.8' | 43°11.7' | | | |
| 08.03.b | 15:08 | 03°48.2' | 43°18.6' | 3778 | 35.69 | 27.3 |
| | 19:31 | 04°07.8' | 43°27.4' | | | |
| 08.03.c | 19:55 | 04°09.7' | 43°28.1' | 3064 | 35.70 | 27.3 |
| | 22:30 | 04°21.2' | 43°33.4' | | | |
| 09.03.c | 20:20 | 05°08.8' | 43°45.3' | 3754 | 35.82 | 27.0 |
| | 23:02 | 05°24.6' | 43°45.0' | | | |
| 10.03.a | 08:12 | 06°09.0' | 43°44.2' | 4466 | 35.94 | 26.8 |
| | 11:44 | 06°25.2' | 43°43.8' | | | |
| 11.03.a | 09:30 | 06°03.5' | 43°44.4' | 4399 | 35.94 | 26.8 |
| | 13:00 | 06°03.6' | 43°44.1' | | | |
| 12.03.a | 09:08 | 04°45.2' | 43°46.1' | ~3400 | 35.65 | 27.1 |
| | 13:05 | 04°45.2' | 43°46.1' | | | |
| 13.03.a | 09:01 | 05°03.9' | 43°23.8' | 3942 | 35.73 | 27.0 |
| | 13:04 | 05°15.0' | 43°08.6' | | | |
| 13.03.b | 14:00 | 05°17.7' | 43°04.8' | 4340 | 35.56 | 27.0 |
| | 18:02 | 05°23.8' | 42°56.3' | | | |
| 13.03.c | 19:00 | 05°20.9' | 43°00.3' | 4470 | 35.62 | 27.0 |
| | 22:00 | 05°13.5' | 43°10.4' | | | |
| 14.03.a | 09:11 | 05°31.3' | 42°45.9' | 4682 | 35.82 | 26.9 |
| | 13:03 | 05°42.3' | 42°30.7' | | | |
| 14.03.b | 13:59 | 05°44.9' | 42°26.9' | 4692 | 36.00 | 26.9 |
| | 17:55 | 05°37.6' | 42°18.5' | | | |
| 14.03.c | 19:00 | 05°32.4' | 42°18.2' | 4326 | 35.76 | 27.0 |
| | 21:41 | 05°19.1' | 42°16.9' | | | |
| 15.03.a | 09:07 | 04°25.6' | 42°02.9' | 4013 | 35.68 | 27.3 |
| | 11:33 | 04°15.5' | 41°55.8' | | | |
| 15.03.b | 13:56 | 04°05.5' | 41°48.7' | 3514 | 35.98 | 27.4 |
| | 17:57 | 03°48.9' | 41°37.0' | | | |
| 16.03.a | 09:08 | 03°48.1' | 41°53.5' | 3393 | 35.77 | 27.3 |
| | 12:58 | 03°46.4' | 42°12.9' | | | |
| 16.03.b | 14:11 | 03°46.0' | 42°19.4' | 3604 | 35.59 | 27.3 |
| | 18:00 | 03°44.4' | 42°39.9' | | | |
| 16.03.c | 19:02 | 03°43.9' | 42°45.4' | 3965 | 35.59 | 27.3 |
| | 22:37 | 03°42.3' | 43°03.5' | | | |
| 17.03.a | 09:55 | 03°40.4' | 43°59.1' | 4221 | 35.70 | 27.3 |
| | 12:02 | 03°40.3' | 44°09.7' | | | |
| 17.03.b | 14:02 | 03°40.4' | 44°20.0' | 4154 | 35.74 | 27.3 |
| | 17:51 | 03°40.4' | 44°40.1' | | | |
| 18.03.a | 09:01 | 04°37.6' | 44°44.9' | 4067 | 35.73 | 27.1 |
| | 12:53 | 03°57.6' | 45°01.6' | | | |
| 18.03.b | 13:58 | 03°45.7' | 45°06.6' | 3919 | 35.85 | 27.2 |
| | 17:49 | 03°40.0' | 45°23.8' | | | |

Table 5 continued

| Date Sample No. | Start / End of Filtration (UTC) | Latitude (°N) at Start / End of Filtration | Longitude (°W) at Start / End of Filtration | Water Depth (m) | Salinity (‰) | Water Temperature (°C) |
|---|---|---|---|---|---|---|
| 18.03.c | 19:00 | 03°40.0' | 45°29.2' | 3794 | 35.88 | 27.2 |
| | 21:49 | 03°39.9' | 45°43.5' | | | |
| 19.03.a | 09:09 | 03°40.0' | 46°38.4' | 3000 | 35.89 | 27.0 |
| | 12:51 | 03°40.0' | 46°56.8' | | | |
| 19.03.b | 14:01 | 03°39.2' | 47°02.0' | 2416 | 35.96 | 27.1 |
| | 18:04 | 03°37.1' | 46°26.1' | | | |
| 20.03.c | 19:15 | 03°37.1' | 45°04.4' | 3927 | 35.75 | 27.2 |
| | 21:56 | 03°37.3' | 44°39.2' | | | |
| 21.03.a | 09:05 | 04°00.9' | 44°25.0' | 4129 | 35.60 | 27.1 |
| | 13:01 | 03°39.7' | 44°35.9' | | | |
| 21.03.b | 14:03 | 04°50.1' | 44°38.8' | 4104 | 35.59 | 27.0 |
| | 17:55 | 05°12.7' | 44°35.8' | | | |
| 21.03.c | 19:02 | 05°18.0' | 44°33.4' | | 35.70 | 27.0 |
| | 21:55 | 05°31.8' | 44°26.8' | | | |
| 22.03.a | 09:13 | 06°24.3' | 44°02.7' | 4633 | 36.01 | 26.9 |
| | 12:54 | 06°30.0' | 44°11.9' | | | |
| 22.03.b | 13:57 | 06°30.0' | 44°17.1' | 4591 | 35.77 | 26.8 |
| | 17:58 | 06°28.3' | 44°36.1' | | | |
| 22.03.c | 19:00 | 06°24.0' | 44°38.7' | 4394 | 35.78 | 26.9 |
| | 21:55 | 06°11.3' | 44°46.4' | | | |
| 23.03.b | 13:58 | 05°00.3' | 45°29.9' | 3933 | 35.74 | 27.0 |
| | 18:04 | 05°11.3' | 45°04.0' | | | |
| 23.03.c | 18:59 | 05°14.4' | 44°56.8' | 4053 | 35.62 | 26.9 |
| | 21:57 | 05°25.0' | 44°32.2' | | | |
| 26.03.c | 18:22 | 05°08.6' | 46°34.2' | 3512 | 35.94 | 27.1 |
| | 22:09 | 04°38.1' | 46°56.4' | | | |
| 27.03.a | 09:05 | 04°48.6' | 47°42.3' | 2862 | 36.06 | 27.1 |
| | 12:53 | 05°04.9' | 47°33.7' | | | |
| 27.03.b | 13:57 | 05°09.7' | 47°31.2' | 3246 | 36.11 | 27.2 |
| | 17:59 | 05°24.7' | 47°32.1' | | | |
| 27.03.c | 18:55 | 05°26.6' | 47°35.9' | 3492 | 36.14 | 27.4 |
| | 22:02 | 05°33.2' | 47°48.9' | | | |
| 28.03.a | 09:15 | 06°56.9' | 47°54.1' | 4107 | 35.50 | 26.4 |
| | 12:59 | 07°01.5' | 48°14.0' | | | |
| 28.03.b | 13:57 | 07°06.2' | 48°23.9' | 4159 | 35.44 | 26.4 |
| | 17:55 | 07°26.3' | 49°05.9' | | | |
| 28.03.c | 18:57 | 07°31.5' | 49°16.8' | 4274 | 35.79 | 26.3 |
| | 21:56 | 07°46.5' | 49°47.9' | | | |
| 29.03.a | 09:23 | 08°42.3' | 51°49.5' | 4661 | 35.20 | 26.3 |
| | 13:04 | 08°52.4' | 52°29.9' | | | |
| 29.03.b | 14:05 | 08°55.4' | 52°41.9' | 4607 | 35.56 | 26.5 |
| | 18:19 | 09°07.4' | 53°29.8' | | | |
| 29.03.c | 19:48 | 09°11.6' | 53°46.8' | 4293 | 35.72 | 26.8 |
| | 21:55 | 09°17.7' | 54°06.3' | | | |
| 31.03.a | 09:10 | 11°03.7' | 52°37.3' | 4920 | 36.12 | 25.8 |
| | 12:58 | 11°31.1' | 52°06.1' | | | |
| 31.03.b | 13:59 | 11°38.4' | 51°57.8' | 4966 | 36.13 | 25.8 |
| | 17:58 | 12°07.2' | 51°24.8' | | | |
| 31.03.c | 19:19 | 12°17.1' | 51°13.5' | 5027 | 36.08 | 25.8 |
| | 21:57 | 12°35.9' | 50°51.8' | | | |

Table 5 continued

| Date Sample No. | Start / End of Filtration (UTC) | Latitude (°N) at Start / End of Filtration | Longitude (°W) at Start / End of Filtration | Water Depth (m) | Salinity (‰) | Water Temperature (°C) |
|---|---|---|---|---|---|---|
| 01.04.a | 09:14 | 13°57.2' | 49°18.4' | | 36.25 | 25.2 |
| | 12:56 | 14°22.2' | 48°49.6' | | | |
| 01.04.b | 15:48 | 14°43.6' | 48°24.7' | 3390 | 36.15 | 25.5 |
| | 17:59 | 15°00.0' | 48°05.8' | | | |
| 01.04.c | 19:00 | 15°07.6' | 47°56.9' | 3880 | 36.34 | 25.1 |
| | 21:56 | 15°29.6' | 47°31.5' | | | |
| 04.04.c | 19:20 | 18°21.6' | 43°29.1' | 4523 | 36.93 | 24.3 |
| | 21:57 | 18°31.6' | 42°59.9' | | | |
| 05.04.a | 09:12 | 19°14.2' | 40°54.5' | 4716 | 37.08 | 23.6 |
| | 13:28 | 19°30.1' | 40°06.0' | | | |
| 05.04.b | 13:57 | 19°32.0' | 40°02.4' | | 37.03 | 23.7 |
| | 17:58 | 19°47.3' | 39°17.0' | | | |
| 05.04.c | 18:49 | 19°50.5' | 39°07.3' | 5140 | 37.26 | 24.2 |
| | 21:48 | 20°01.6' | 38°34.8' | | | |
| 06.04.a | 08:11 | 20°40.4' | 36°39.7' | 5749 | 36.93 | 23.4 |
| | 11:50 | 20°53.6' | 36°00.5' | | | |
| 06.04.b | 12:56 | 20°57.6' | 35°48.7' | 4851 | 37.22 | 22.9 |
| | 16:58 | 21°13.0' | 35°02.9' | | | |
| 06.04.c | 18:03 | 21°17.2' | 34°50.3' | 5772 | 37.19 | 23.2 |
| | 20:59 | 21°28.3' | 34°17.2' | | | |
| 07.04.a | 08:09 | 22°10.2' | 32°11.5' | 5051 | 37.31 | 22.6 |
| | 11:59 | 22°23.5' | 31°30.9' | | | |
| 07.04.b | 13:01 | 22°27.1' | 31°20.3' | 4815 | 37.24 | 22.6 |
| | 17:07 | 22°43.0' | 30°32.5' | | | |
| 07.04.c | 18:18 | 22°47.4' | 30°19.1' | 5280 | 37.37 | 22.3 |
| | 21:05 | 22°58.2' | 29°46.5' | | | |
| 08.04.a | 07:17 | 23°36.5' | 27°50.7' | 5570 | 37.29 | 22.1 |
| | 10:57 | 23°50.2' | 27°08.7' | | | |
| 08.04.b | 12:01 | 23°54.2' | 26°56.6' | 5448 | 37.34 | 21.7 |
| | 15:59 | 24°09.0' | 26°12.0' | | | |
| 08.04.c | 17:29 | 24°14.4' | 25°55.4' | 5322 | | 21.8 |
| | 20:03 | 24°23.7' | 25°27.0' | | | |
| 09.04.a | 07:12 | 25°06.2' | 23°17.0' | 4976 | 37.10 | 21.3 |
| | 10:15 | 25°17.8' | 22°41.0' | | | |
| 09.04.b | 12:06 | 25°24.1' | 22°21.9' | 4851 | 37.11 | 20.9 |
| | 16:01 | 25°35.2' | 21°48.1' | | | |
| 09.04.c | 17:01 | 25°37.7' | 21°40.4' | 4666 | 37.09 | 20.9 |
| | 19:56 | 25°46.2' | 21°14.0' | | | |
| 10.04.a | 07:11 | 26°20.0' | 19°29.8' | 4212 | 36.95 | 20.4 |
| | 11:02 | 26°31.6' | 18°54.3' | | | |
| 10.04.b | 12:05 | 26°34.5' | 18°44.5' | 3663 | 36.95 | 20.6 |
| | 15:59 | 26°46.5' | 18°07.8' | | | |

Table 6 Water samples taken for dinoflagellate analyses from 10 l Niskin bottles.

| Station No. | Date/ Time (UTC) | Water Depth (m) | Volume of Water Filtered (l) | Latitude (°N) | Longitude (°W) | Salinity (‰) | Water Temperature (°C) |
|---|---|---|---|---|---|---|---|
| 4401-1 | | | | | | | |
| 10 m | 09.03. | 3402 | 38.8 | 04°48.0' | 43°45.9' | 35.8 | 27.1 |
| 20 m | 06:30 | | 40.0 | | | 35.8 | 27.1 |
| 50 m | | | 25.1 | | | 35.8 | 27.0 |
| 100 m | | | 24.8 | | | 36.0 | 26.6 |
| 4401-2 | | | | | | | |
| 75 m | 09.03. | 3402 | 9.4 | 04°48.0' | 43°45.9' | 35.9 | 27.0 |
| 150 m | 06:55 | | 9.2 | | | 35.6 | 15.0 |
| 4402-1 | | | | | | | |
| 10 m | 10.03. | 4638 | 37.6 | 06°39.3' | 43°43.5' | 35.9 | 26.9 |
| 20 m | 15:21 | | 38.5 | | | 35.9 | 26.9 |
| 50 m | | | 38.1 | | | 35.9 | 26.9 |
| 100 m | | | 30.5 | | | 36.2 | 26.8 |
| 4405-1 | | | | | | | |
| 10 m | 11.03. | 4297 | 39.4 | 05°54.5' | 43°44.4' | 35.8 | 27.0 |
| 20 m | 18:03 | | 39.0 | | | 35.9 | 26.9 |
| 50 m | | | 37.0 | | | 35.9 | 26.8 |
| 100 m | | | 29.5 | | | 36.0 | 26.8 |
| 4407-4 | | | | | | | |
| 10 m | 16.03. | 3314 | 39.3 | 03°49.4' | 41°36.8' | 36.0 | 27.6 |
| 20 m | 02:05 | | 39.3 | | | 36.0 | 27.6 |
| 50 m | | | 39.4 | | | 35.9 | 27.5 |
| 100 m | | | 29.3 | | | 36.0 | 26.0 |
| 4408-1 | | | | | | | |
| 10 m | 19.03. | 3471 | 39.5 | 03°39.9' | 46°07.8' | 35.9 | 27.2 |
| 20 m | 20:49 | | 38.7 | | | 35.9 | 27.2 |
| 50 m | | | 39.4 | | | 35.8 | 27.0 |
| 100 m | | | 28.8 | | | 36.4 | 22.7 |
| 4410-1 | | | | | | | |
| 10 m | 21.03. | 4157 | 38.8 | 03°40.6' | 44°19.5' | 35.6 | 27.3 |
| 20 m | 00:34 | | 39.0 | | | 35.7 | 27.3 |
| 50 m | | | 39.8 | | | 35.7 | 27.4 |
| 100 m | | | 29.0 | | | 36.0 | 27.1 |
| 4412-1 | | | | | | | |
| 10 m | 24.03. | 3765 | 38.9 | 05°43.4' | 44°21.6' | 35.7 | 27.0 |
| 20 m | 06:39 | | 39.1 | | | 35.7 | 27.0 |
| 50 m | | | 40.3 | | | 35.8 | 27.0 |
| 100 m | | | 30.0 | | | 36.4 | 23.5 |
| 4415-1 | | | | | | | |
| 10 m | 25.03. | 3585 | 39.3 | 05°51.2' | 44°58.6' | 36.0 | 27.0 |
| 20 m | 07:55 | | 39.5 | | | 36.0 | 27.0 |
| 50 m | | | 39.5 | | | 35.8 | 27.0 |
| 100 m | | | 30.1 | | | 36.2 | 26.8 |

Table 6 continued

| Station No. | Date/ Time (UTC) | Water Depth (m) | Volume of Water Filtered (l) | Latitude (°N) | Longitude (°W) | Salinity (‰) | Water Temperature (°C) |
|---|---|---|---|---|---|---|---|
| 4417-2 | | | | | | | |
| 10 m | 26.03. | 3513 | 38.2 | 05°08.3' | 46°34.6' | 36.0 | 27.0 |
| 20 m | 06:25 | | 37.7 | | | 36.0 | 27.0 |
| 50 m | | | 35.2 | | | 36.2 | 27.2 |
| 100 m | | | 27.6 | | | 36.3 | 26.3 |
| 4419-2 | | | | | | | |
| 10 m | 30.03. | 4486 | 39.5 | 09°41.2' | 54°15.8' | 36.1 | 26.9 |
| 20 m | 08:49 | | 39.4 | | | 36.1 | 26.9 |
| 50 m | | | 39.8 | | | 36.1 | 26.9 |
| 100 m | | | 29.2 | | | 36.8 | 26.2 |
| 4421-4 | | | | | | | |
| 10 m | 02.04. | 3192 | 36.7 | 16°59.8' | 46°00.7' | 36.8 | 24.8 |
| 20 m | 23:52 | | 37.3 | | | 36.8 | 24.5 |
| 50 m | | | 37.7 | | | 36.9 | 24.4 |
| 100 m | | | 27.7 | | | 37.2 | 23.6 |
| 4421-5 | 03.04. | | | | | | |
| 150 m | 00:16 | 3192 | 8.1 | 16°59.8' | 46°00.7' | 36.9 | 20.5 |

In addition to acquiring surface water samples, approximately 40 l of sea water was collected at 10, 20, 50, 100 m (occasionally at 75 and 150 m) water depth using a rosette. Samples were taken at 11 stations (positions and depths are listed in Table 6). In general, four 10 l Niskin bottles were filled at each depth. The obtained sea water was passed over a 100 µm mesh sieve and filtered with 5 µm polycarbonate filters using a vacuum pump system. The samples were reduced to a volume of 150 ml and subsequently treated in a similar manner as the surface samples acquired from the membrane pump. All stored samples will be further analyzed at the University of Bremen, mainly through Scanning Electron Microscopy (SEM), in order to provide more information on the composition, regional geographic distribution, vertical distribution and possibly the diurnal variations in the vertical distribution of dinoflagellate communities in the upper 100 m of the western equatorial South Atlantic Ocean in the Amazon Fan and Ceará Rise area.

Motile vegetative thecate dinoflagellate stages and calcareous resting cysts have been observed in every sample taken. Thecae and cysts were generally very abundant in surface water samples, but were found in significantly lower quantities in the 10 - 100 m samples. The predominant calcareous dinoflagellates, generally present in all working areas and at all sampled depths, were *'Sphaerodinella' albatrosiana*, *'Sphaerodinella' tuberosa* and the vegetative coccoid *Th. heimii*. The cyst *Orthopithonella granifera* was found selectively in very low concentrations, showing higher abundance in the surface waters between about 8 to 10°N and 51.5 to 54.5°W, where water

temperature (<26.8 °C) and salinity (<35.5 ‰) is slightly lower than in the Amazon Fan area, and the influence of the North Equatorial Current is more intense. *Rhabdothorax sp.* was only observed in two surface water samples in the mid-Atlantic Ridge region. Organic walled dinoflagellate cysts were only very rarely detected. No obvious differences were noticed in cyst composition and quantity between samples taken at different times of the day. Approximately 260 specimens of calcareous dinoflagellate cysts have been isolated for cultivation on board and, in due time, for experimentation at the University of Bremen. The cells containing these cysts were scanned at regular intervals, in order to register when excystment and reproduction had occurred. Those specimens which produced a sufficient number of new cysts and motile stages were transferred to small, sterile bottles for transportation to Bremen.

## 6.2 Sampling for Chlorophyll-a Analyses

For the determination of chlorophyll-a concentrations in surface waters, 0.5 l of sea water was collected three times a day from the ships clean sea water pump system (inlet at 3.5 m water depth). Sampling locations are listed in Table 7. The water was filtered through glass fiber filters and frozen at -20 °C. Chlorophyll-a measurements by means of photometry will be carried out at the University of Bremen.

## 6.3 Sampling for Diatom Analyses

To investigate the diatom assemblages in tropical surface waters marine plankton material was sampled during the entire cruise (Table 8). The shipboard sea water pump was used to filter between 0.35 and 2.5 $m^3$ of water through a 20 µm mesh net each day. The plankton was washed into plastic jugs and stored at 4 °C.

## 6.4 Planktic Foraminifera Investigations

To obtain information about the stable isotope compositions of living planktic foraminifera and their relation to the regional hydrography, plankton samples were collected daily from 3.5 m water depth using the ship's emergency pump system. A plankton net (70 µm mesh size) was tied on the main deck with the firehose discharging directly into the net for several hours (Table 9). Planktic foraminifera larger than 150 µm were picked immediately from wet samples, measured with a reticule, washed with freshwater and ethanol and finally dried and stored in Fema cells for shore based stable isotope analyses. Additionally, a 50 ml water sample was taken at the end of each coring transect. Figure 50 shows the latitudinal distribution of identified species. The diversity was generally low around the equator, where only *Globigerinoides sacculifer*, *G. ruber*, *Globorotalia menardii* and *Neogloboquadrina dutertrei* have been observed. This group was abundant in most all of the samples. Between 4 and 6°N, the foraminiferal assem-

Table 7 Sampling for chlorophyll-a analyses.

| No. | Date | Time | Latitude (°N) | Longitude (°W) | Water Depth (m) | Temperature (°C) |
|---|---|---|---|---|---|---|
| 155 | 07.03. | 19:12 | 2°23.4' | 42°40.3' | 4308 | 27.4 |
| 156 | 07.03. | 19:12 | 2°23.4' | 42°40.3' | 4308 | 27.4 |
| 157 | 08.03. | 10:56 | 3°29.3' | 43°09.0' | 4286 | 27.2 |
| 158 | 08.03. | 10:56 | 3°29.3' | 43°09.0' | 4286 | 27.2 |
| 159 | 08.03. | 15:01 | 3°47.7' | 43°18.3' | 3770 | 27.3 |
| 160 | 08.03. | 15:01 | 3°47.7' | 43°18.3' | 3770 | 27.3 |
| 161 | 08.03. | 20:23 | 4°11.8' | 43°29.1' | 3034 | 27.3 |
| 162 | 08.03. | 20:23 | 4°11.8' | 43°29.1' | 3034 | 27.3 |
| 163 | 09.03. | 10:05 | 4°47.9' | 43°45.8' | 3398 | 27.1 |
| 164 | 09.03. | 10:05 | 4°47.9' | 43°45.8' | 3398 | 27.1 |
| 165 | 09.03. | 21:28 | 5°14.6' | 43°45.2' | 3819 | 27.0 |
| 166 | 09.03. | 21:28 | 5°14.6' | 43°45.2' | 3819 | 27.0 |
| 167 | 10.03. | 10:53 | 6°21.4' | 43°43.9' | 4534 | 26.8 |
| 168 | 10.03. | 10:53 | 6°21.4' | 43°43.9' | 4534 | 26.8 |
| 169 | 10.03. | 15:39 | 6°39.4' | 43°43.6' | 4639 | 26.9 |
| 170 | 10.03. | 15:39 | 6°39.4' | 43°43.6' | 4639 | 26.9 |
| 171 | 11.03. | 15:33 | 6°03.4' | 43°44.3' | 4395 | 26.9 |
| 172 | 11.03. | 15:33 | 6°03.4' | 43°44.3' | 4395 | 26.9 |
| 173 | 12.03. | 10:18 | 4°45.3' | 43°46.1' | - | 27.0 |
| 174 | 12.03. | 10:18 | 4°45.3' | 43°46.1' | - | 27.0 |
| 175 | 12.03. | 15:56 | 5°05.5' | 43°45.3' | 3718 | 27.1 |
| 176 | 12.03. | 15:56 | 5°05.5' | 43°45.3' | 3718 | 27.1 |
| 177 | 13.03. | 10:15 | 5°07.0' | 43°19.4' | 4041 | 27.0 |
| 178 | 13.03. | 10:15 | 5°07.0' | 43°19.4' | 4041 | 27.0 |
| 179 | 13.03. | 15:24 | 5°20.8' | 43°00.5' | 4460 | 27.0 |
| 180 | 13.03. | 15:24 | 5°20.8' | 43°00.5' | 4460 | 27.0 |
| 181 | 14.03. | 10:33 | 5°35.1' | 42°40.6' | 4688 | 26.9 |
| 182 | 14.03. | 10:33 | 5°35.1' | 42°40.6' | 4688 | 26.9 |
| 183 | 14.03. | 16:16 | 5°45.9' | 42°19.7' | 4689 | 26.9 |
| 184 | 14.03. | 16:16 | 5°45.9' | 42°19.7' | 4689 | 26.9 |
| 185 | 15.03. | 10:15 | 4°21.9' | 41°39.6' | 3790 | 27.3 |
| 186 | 15.03. | 10:15 | 4°21.9' | 41°39.6' | 3790 | 27.3 |
| 187 | 15.03. | 15:14 | 4°00.4' | 41°45.0' | 3479 | 27.5 |
| 188 | 15.03. | 15:14 | 4°00.4' | 41°45.0' | 3479 | 27.5 |
| 189 | 15.03. | 19:08 | 3°49.2' | 41°37.5' | 3302 | 27.5 |
| 190 | 15.03. | 19:08 | 3°49.2' | 41°37.5' | 3302 | 27.5 |
| 191 | 16.03. | 10:26 | 3°47.7' | 41°59.9' | 3355 | 27.2 |
| 192 | 16.03. | 10:26 | 3°47.7' | 41°59.9' | 3355 | 27.2 |
| 193 | 16.03. | 16:07 | 3°45.2' | 42°29.8' | 3895 | 27.3 |
| 194 | 16.03. | 16:07 | 3°45.2' | 42°29.8' | 3895 | 27.3 |
| 195 | 17.03. | 08:30 | 3°40.6' | 44°01.8' | 4215 | 27.3 |
| 196 | 17.03. | 08:30 | 3°40.6' | 44°01.8' | 4215 | 27.3 |
| 197 | 17.03. | 14:45 | 3°40.4' | 44°34.6' | 3910 | 27.4 |
| 198 | 17.03. | 14:45 | 3°40.4' | 44°34.6' | 3910 | 27.4 |
| 199 | 17.03. | 19:09 | 3°40.5' | 44°46.6' | 3848 | 27.3 |
| 200 | 17.03. | 19:09 | 3°40.5' | 44°46.6' | 3848 | 27.3 |
| 201 | 18.03. | 10:40 | 4°22.6' | 44°51.0' | 4017 | 27.2 |
| 202 | 18.03. | 10:40 | 4°22.6' | 44°51.0' | 4017 | 27.2 |
| 203 | 18.03. | 15:14 | 3°39.9' | 45°11.7' | 3888 | 27.2 |
| 204 | 18.03. | 15:14 | 3°39.9' | 45°11.7' | 3888 | 27.2 |

Table 7 continued

| No. | Date | Time | Latitude (°N) | Longitude (°W) | Water Depth (m) | Temperature (°C) |
|---|---|---|---|---|---|---|
| 205 | 18.03. | 20:37 | 3°40.0' | 45°37.5' | 3740 | 27.2 |
| 206 | 18.03. | 20:37 | 3°40.0' | 45°37.5' | 3740 | 27.2 |
| 207 | 19.03. | 10:57 | 3°39.9' | 46°47.2' | 2873 | 27.0 |
| 208 | 19.03. | 10:57 | 3°39.9' | 46°47.2' | 2873 | 27.0 |
| 209 | 19.03. | 19:16 | 3°36.9' | 46°16.5' | 3323 | 27.1 |
| 210 | 19.03. | 19:16 | 3°36.9' | 46°16.5' | 3323 | 27.1 |
| 211 | 20.03. | 10:08 | 3°39.9' | 45°14.4' | 3844 | 27.2 |
| 212 | 20.03. | 10:08 | 3°39.9' | 45°14.4' | 3844 | 27.2 |
| 213 | 21.03. | 10:15 | 4°10.4' | 44°27.7' | 4114 | 27.1 |
| 214 | 21.03. | 10:15 | 4°10.4' | 44°27.7' | 4114 | 27.1 |
| 215 | 21.03. | 14:17 | 4°52.5' | 44°39.5' | 4103 | 27.0 |
| 216 | 21.03. | 14:17 | 4°52.5' | 44°39.5' | 4103 | 27.0 |
| 217 | 21.03. | 19:01 | 5°17.9' | 44°33.5' | 2841 | 27.0 |
| 218 | 21.03. | 19:01 | 5°17.9' | 44°33.5' | 2841 | 27.0 |
| 219 | 22.03. | 10:22 | 6°29.3' | 44°00.3' | 4637 | 26.9 |
| 220 | 22.03. | 10:22 | 6°29.3' | 44°00.3' | 4637 | 26.9 |
| 221 | 22.03. | 16:56 | 6°29.9' | 44°31.9' | 4508 | 26.9 |
| 222 | 22.03. | 16:56 | 6°29.9' | 44°31.9' | 4508 | 26.9 |
| 223 | 23.03. | 11:30 | 5°11.3' | 45°23.1' | 3969 | 26.9 |
| 224 | 23.03. | 11:30 | 5°11.3' | 45°23.1' | 3969 | 26.9 |
| 225 | 23.03. | 15:41 | 5°02.2' | 45°24.1' | 3945 | 27.0 |
| 226 | 23.03. | 15:41 | 5°02.2' | 45°24.1' | 3945 | 27.0 |
| 227 | 23.03. | 21:41 | 5°23.8' | 44°34.6' | 3240 | 26.9 |
| 228 | 23.03. | 21:41 | 5°23.8' | 44°34.6' | 3240 | 26.9 |
| 229 | 24.03. | 11:00 | 5°43.3' | 44°21.6' | 3766 | 26.9 |
| 230 | 24.03. | 11:00 | 5°43.3' | 44°21.6' | 3766 | 26.9 |
| 231 | 24.03. | 16:10 | 6°05.2' | 44°11.2' | 4293 | 26.9 |
| 232 | 24.03. | 16:10 | 6°05.2' | 44°11.2' | 4293 | 26.9 |
| 233 | 25.03. | 08:00 | 5°51.2' | 44°58.7' | 3587 | 26.9 |
| 234 | 25.03. | 08:00 | 5°51.2' | 44°58.7' | 3587 | 26.9 |
| 235 | 25.03. | 17:24 | 5°40.5' | 45°05.3' | 3903 | 27.0 |
| 236 | 25.03. | 17:24 | 5°40.5' | 45°05.3' | 3903 | 27.0 |
| 237 | 26.03. | 10:19 | 5°08.3' | 46°34.6' | 3512 | 26.9 |
| 238 | 26.03. | 10:19 | 5°08.3' | 46°34.6' | 3512 | 26.9 |
| 239 | 26.03. | 22:22 | 4°36.3' | 46°57.8' | 3144 | 27.1 |
| 240 | 26.03. | 22:22 | 4°36.3' | 46°57.8' | 3144 | 27.1 |
| 241 | 27.03. | 10:17 | 4°53.5' | 47°39.6' | 3025 | 27.1 |
| 242 | 27.03. | 10:17 | 4°53.5' | 47°39.6' | 3025 | 27.1 |
| 243 | 27.03. | 16:36 | 5°21.6' | 47°25.9' | 3512 | 27.1 |
| 244 | 27.03. | 16:36 | 5°21.6' | 47°25.9' | 3512 | 27.1 |
| 245 | 27.03. | 22:20 | 5°33.9' | 47°50.3' | 3556 | 27.3 |
| 246 | 27.03. | 22:20 | 5°33.9' | 47°50.3' | 3556 | 27.3 |
| 247 | 28.03. | 10:50 | 6°57.7' | 48°02.3' | 4120 | 26.4 |
| 248 | 28.03. | 10:50 | 6°57.7' | 48°02.3' | 4120 | 26.4 |
| 249 | 29.03. | 12:48 | 8°51.9' | 52°27.3' | 4616 | 26.3 |
| 250 | 29.03. | 12:48 | 8°51.9' | 52°27.3' | 4616 | 26.3 |
| 251 | 29.03. | 16:17 | 9°01.7' | 53°06.9' | 4595 | 26.4 |
| 252 | 29.03. | 16:17 | 9°01.7' | 53°06.9' | 4595 | 26.4 |
| 253 | 29.03. | 22:26 | 9°15.6' | 54°03.8' | 2506 | 27.2 |
| 254 | 29.03. | 22:26 | 9°15.6' | 54°03.8' | 2506 | 27.2 |

Table 7 continued

| No. | Date | Time | Latitude (°N) | Longitude (°W) | Water Depth (m) | Temperature (°C) |
|---|---|---|---|---|---|---|
| 255 | 30.03. | 09:15 | 9°40.9' | 54°15.4' | 4488 | 26.8 |
| 256 | 30.03. | 09:15 | 9°40.9' | 54°15.4' | 4488 | 26.8 |
| 257 | 31.03. | 10:20 | 11°11.9' | 52°27.9' | 4932 | 25.7 |
| 258 | 31.03. | 10:20 | 11°11.9' | 52°27.9' | 4932 | 25.7 |
| 259 | 31.03. | 15:13 | 11°47.4' | 51°47.4' | 4977 | 25.7 |
| 260 | 31.03. | 15:13 | 11°47.4' | 51°47.4' | 4977 | 25.7 |
| 261 | 31.03. | 23:33 | 12°47.3' | 50°38.9' | 4976 | 25.7 |
| 262 | 31.03. | 23:33 | 12°47.3' | 50°38.9' | 4976 | 25.7 |
| 263 | 01.04. | 10:33 | 14°06.9' | 49°07.1' | 4987 | 25.1 |
| 264 | 01.04. | 10:33 | 14°06.9' | 49°07.1' | 4987 | 25.1 |
| 265 | 01.04. | 16:30 | 14°48.8' | 48°18.7' | 3522 | 25.6 |
| 266 | 01.04. | 16:30 | 14°48.8' | 48°18.7' | 3522 | 25.6 |
| 267 | 01.04. | 21:24 | 15°25.3' | 47°36.3' | 4633 | - |
| 268 | 01.04. | 21:24 | 15°25.3' | 47°36.3' | 4633 | - |
| 269 | 02.04. | 10:27 | 16°28.3' | 46°27.8" | 2774 | 24.7 |
| 270 | 02.04. | 10:27 | 16°28.3' | 46°27.8' | 2774 | 24.7 |
| 271 | 02.04. | 22:16 | 16°59.9' | 46°00.5' | 3214 | 24.6 |
| 272 | 02.04. | 22:16 | 16°59.9' | 46°00.5' | 3214 | 24.6 |
| 273 | 03.04. | 10:11 | 17°27.3' | 45°38.6' | 3864 | 24.5 |
| 274 | 03.04. | 10:11 | 17°27.3' | 45°38.6' | 3864 | 24.5 |
| 275 | 03.04. | 19:00 | 17°53.0' | 45°14.2' | 4189 | 24.6 |
| 276 | 03.04. | 19:00 | 17°53.0' | 45°14.2' | 4189 | 24.6 |
| 277 | 04.04. | 08:30 | 18°12.1' | 44°00.6' | 4775 | 24.2 |
| 278 | 04.04. | 08:30 | 18°12.1' | 44°00.6' | 4775 | 24.2 |
| 279 | 04.04. | 21:57 | 18°31.5' | 42°59.8' | 4874 | 24.3 |
| 280 | 04.04. | 21:57 | 18°31.5' | 42°59.8' | 4874 | 24.3 |
| 281 | 05.04. | 10:29 | 19°19.0' | 40°40.4' | 5106 | 23.7 |
| 282 | 05.04. | 10:29 | 19°19.0' | 40°40.4' | 5106 | 23.7 |
| 283 | 05.04. | 16:12 | 19°40.6' | 39°36.8' | - | 23.8 |
| 284 | 05.04. | 16:12 | 19°40.6' | 39°36.8' | - | 23.8 |
| 285 | 06.04. | 09:00 | 20°47.0' | 36°19.9' | 5505 | 22.8 |
| 286 | 06.04. | 09:00 | 20°47.0' | 36°19.9' | 5505 | 22.8 |
| 287 | 06.04. | 14:41 | 21°04.2' | 35°28.9' | 5595 | 23.5 |
| 288 | 06.04. | 14:41 | 21°04.2' | 35°28.9' | 5595 | 23.5 |
| 289 | 06.04. | 21:15 | 21°29.4' | 34°13.9' | 5318 | 23.2 |
| 290 | 06.04. | 21:15 | 21°29.4' | 34°13.9' | 5318 | 23.2 |
| 291 | 07.04. | 09:15 | 22°14.2' | 31°59.4' | 5053 | 22.5 |
| 292 | 07.04. | 09:15 | 22°14.2' | 31°59.4' | 5053 | 22.5 |
| 293 | 07.04. | 14:12 | 22°31.6' | 31°06.6' | 5051 | 22.6 |
| 294 | 07.04. | 14:12 | 22°31.6' | 31°06.6' | 5051 | 22.6 |
| 295 | 07.04. | 21:47 | 23°00.9' | 29°38.2' | 5646 | 22.3 |
| 296 | 07.04. | 21:47 | 23°00.9' | 29°38.2' | 5646 | 22.3 |
| 297 | 08.04. | 07:58 | 23°39.0' | 27°43.0' | 5545 | 22.2 |
| 298 | 08.04. | 07:58 | 23°39.0' | 27°43.0' | 5545 | 22.2 |
| 299 | 08.04. | 14:00 | 24°01.5' | 26°34.9' | 5404 | 22.2 |
| 300 | 08.04. | 14:00 | 24°01.5' | 26°34.9' | 5404 | 22.2 |
| 301 | 09.04. | 08:42 | 22°59.9' | 22°59.9' | 4935 | 21.1 |
| 302 | 09.04. | 08:42 | 22°59.9' | 22°59.9' | 4935 | 21.1 |

Table 8 Sampling for diatom analyses.

| No | Date | Time* (UTC) | Latitude* (°N) | Longitude* (°W) | Water Temperature* (°C) | Water Clock* |
|---|---|---|---|---|---|---|
| 11 | 07.03. | 11:28 | 01°51.9' | 42°20.2' | 27.3 | 674.66 |
| | | 19:04 | 02°22.3' | 42°40.0' | 27.4 | 675.37 |
| 12 | 08.03. | 10:27 | 03°27.1' | 43°09.0' | 27.2 | 675.37 |
| | | 18:59 | 04°05.7' | 43°26.4' | 27.4 | 676.46 |
| 13 | 09.03. | 10:10 | 04°47.9' | 43°45.9' | 27.1 | 676.46 |
| | | 20:43 | 05°10.3' | 43°45.3' | 27.0 | 677.46 |
| 14 | 10.03. | 10:20 | 06°18.8' | 43°44.0' | 26.8 | 677.46 |
| | | - | - | - | - | 679.46 |
| 15 | 11.03. | 09:46 | 06°03.5' | 43°44.3' | 26.8 | 679.46 |
| | | 18:04 | 05°54.5' | 43°44.3' | 26.9 | 680.83 |
| 16 | 12.03. | 10:09 | 04°45.3' | 43°46.1' | 27.1 | 680.83 |
| | | 21:45 | 04°59.0' | 43°46.6' | 27.2 | 681.83 |
| 17 | 13.03. | 10:02 | 05°06.5' | 43°20.2' | 27.0 | 681.83 |
| | | 21:40 | 05°14.4' | 43°09.3' | 27.1 | 682.60 |
| 18 | 14.03. | 10:04 | 05°33.7' | 43°42.5' | 26.9 | 682.60 |
| | | 21:39 | 05°19.3' | 42°17.0' | 27.1 | 683.33 |
| 19 | 15.03. | 10:05 | 04°21.6' | 41°59.9' | 27.3 | 683.33 |
| | | 23:01 | 03°49.5' | 41°37.3' | 27.4 | 684.47 |
| 20 | 16.03. | 11:13 | 03°47.3' | 42°03.8' | 27.3 | 684.47 |
| | | 20:21 | 03°43.4' | 42°52.0' | 27.4 | 685.10 |
| 21 | 17.03. | 13:09 | 03°40.4' | 44°15.5' | 27.3 | 685.70 |
| | | 22:01 | 03°43.4' | 45°00.3' | 27.2 | 686.91 |
| 22 | 18.03. | 10:05 | 04°29.2' | 44°48.4' | 27.2 | 686.91 |
| | | 22:01 | 03°40.0' | 45°37.6' | 27.2 | 688.37 |
| 23 | 19.03. | 12:37 | 03°40.0' | 46°55.7' | 27.1 | 688.37 |
| | | 20:12 | 03°36.9' | 46°08.8' | 27.1 | 689.38 |
| 24 | 20.03. | 08:30 | 03°39.9' | 45°14.4' | 27.1 | 689.38 |
| | | 20:15 | 03°37.2' | 44°55.1' | 27.2 | 690.06 |
| 25 | 21.03. | 08:00 | 04°09.8' | 44°27.6' | 27.1 | 690.06 |
| | | 21:10 | 05°28.2' | 44°28.7' | 27.0 | 690.80 |
| 26 | 22/23. | 09:54 | 06°27.3' | 44°01.2' | 26.9 | 690.80 |
| | 03. | 11:57 | 05°09.7' | 45°24.1' | 26.9 | 691.15 |
| 27 | 23.03. | 12:27 | 05°07.6' | 45°25.4' | 26.9 | 691.15 |
| | | 23:51 | 05°26.1' | 44°29.7' | 26.7 | 691.83 |
| 28 | 24.03. | 09:00 | 05°43.3' | 44°21.7' | 26.9 | 691.83 |
| | | - | - | - | - | 692.83 |
| 29 | 25.03. | 08:15 | 05°51.2' | 44°58.6' | 26.9 | 692.85 |
| | | 22:56 | 05°36.7' | 45°15.8' | 26.9 | 693.45 |
| 30 | 26.03. | 10:27 | 05°08.3' | 46°34.5' | 26.9 | 693.45 |
| | | 22:32 | 04°34.5' | 46°58.9' | 27.0 | 693.91 |
| 31 | 27.03. | 10:09 | 04°53.0' | 47°39.9' | 27.1 | 693.91 |
| | | 20:12 | 05°29.2' | 47°41.1' | 27.4 | 695.06 |
| 32 | 28.03. | 10:41 | 06°57.6' | 48°01.5' | 26.4 | 695.06 |
| | | 20:31 | 07°39.2' | 49°32.8' | - | 696.57 |
| 33 | 29.03. | 11:26 | 08°48.0' | 52°12.1' | 26.3 | 696.57 |
| | | 23:34 | 09°15.7' | 54°09.6' | 27.1 | 697.23 |
| 34 | 31.03. | 10:23 | 11°12.3' | 52°27.5' | 25.7 | 697.23 |
| | | - | - | - | - | 698.24 |

Table 8 continued

| No | Date | Time* (UTC) | Latitude* (°N) | Longitude* (°W) | Water Temperature* (°C) | Water Clock* |
|---|---|---|---|---|---|---|
| 35 | 01.04 | 10:43 | 14°08.1' | 49°05.7' | 25.1 | 698.24 |
| | | 22:33 | 15°34.2' | 47°26.0' | 25.0 | 699.06 |
| 36 | 02.04 | 10:17 | 16°28.3' | 46°27.7' | 24.7 | 699.06 |
| | | 23:25 | 16°59.3' | 46°00.5' | 24.6 | 699.74 |
| 37 | 03./04 | 10:24 | 17°27.3' | 45°38.6' | 24.5 | 699.94 |
| | .04. | 00:48 | 17°53.0' | 45°14.1' | 24.5 | 700.44 |
| 38 | 04.04. | 10:15 | 18°12.0' | 44°00.5' | 24.2 | 700.44 |
| | | 21:27 | 18°29.7' | 43°05.6' | 24.2 | 701.02 |
| 39 | 05.04. | 10:24 | 19°18.8' | 40°41.2' | 23.7 | 701.02 |
| | | 24:00 | 20°10.1' | 38°09.7' | 23.4 | 702.00 |
| 40 | 06.04. | 10:00 | 20°47.1' | 36°19.7' | 22.8 | 702.00 |
| | | 21:03 | 21°28.7' | 34°16.2' | 23.1 | 703.04 |
| 41 | 07.04. | 09:19 | 22°14.0' | 31°59.8' | 22.5 | 703.04 |
| | | 19:09 | 22°50.7' | 30°09.1' | 22.4 | 705.55 |

*) at start / end of pumping

Table 9 Sampling for planktic foraminifera analyses.

| Sample No. | Date 1997 | Local Time* | Latitude* (°N) | Longitude* (°W) | Water Temperature* (°C) | Salinity* (‰) | Water Sample |
|---|---|---|---|---|---|---|---|
| FP 26 | 07.03. | 08:55 | 01°50.7' | 42°18.8' | 27.3 | 35.72 | x |
| | | 12:13 | 02°00.8' | 42°30.3' | 27.5 | 35.69 | |
| FP 27 | 08.03. | 08:35 | 03°27.6' | 43°09.3' | 27.2 | 35.69 | x |
| | | 14:13 | 03°52.9' | 43°20.6' | 27.5 | 35.69 | |
| FP 28 | 09.03. | 08:20 | 04°47.9' | 43°45.8' | 27.1 | 35.76 | - |
| | | 14:50 | 04°45.5' | 43°45.5' | 27.2 | 35.74 | |
| FP 29 | 10.03. | 09:35 | 06°24.6' | 43°43.8' | 26.8 | 35.95 | - |
| | | 14:30 | 06°39.3' | 43°43.6' | 26.9 | 35.74 | |
| FP 30 | 11.03. | 13:20 | 06°03.4' | 43°44.3' | 26.9 | 35.95 | - |
| | | 18:00 | 05°54.5' | 43°44.7' | 26.9 | 35.92 | |
| FP 31 | 12.03. | 09:40 | 04°45.1' | 43°46.0' | 27.1 | 35.67 | x |
| | | 15:20 | 05°05.6' | 43°45.3' | 26.9 | | |
| FP 32 | 13.03. | 09:00 | 05°09.1' | 43°16.6' | 27.0 | 35.69 | x |
| | | 17:00 | 05°20.8' | 43°00.4' | 27.0 | - | |
| FP 33 | 14.03. | 08:45 | 05°35.7' | 42°39.7' | 26.9 | 35.90 | x |
| | | 16:00 | 05°47.3' | 42°48.1' | - | - | |
| FP 34 | 15.03. | 08:20 | 04°20.4' | 41°59.1' | 27.3 | 35.74 | x |
| | | 15:20 | 03°50.6' | 41°38.2' | 27.4 | 35.88 | |
| FP 35 | 16.03. | 08:05 | 03°47.7' | 41°58.2' | 27.2 | 35.69 | x |
| | | 14:00 | 03°45.1' | 42°30.4' | 27.3 | 35.57 | |
| FP 36 | 17.03. | 08:15 | 03°40.5' | 44°00.8' | 27.3 | 35.71 | x |
| | | 14:00 | 03°40.4' | 44°30.1' | 27.4 | 35.77 | |
| FP 37 | 18.03. | 08:35 | 04°23.5' | 44°50.8' | 27.3 | 35.74 | x |
| | | 13:40 | 03°40.0' | 45°14.0' | 27.3 | 35.87 | |

Table 9 continued

| Sample No. | Date 1997 | Local Time* | Latitude* (°N) | Longitude* (°W) | Water Temperature* (°C) | Salinity* (‰) | Water Sample |
|---|---|---|---|---|---|---|---|
| FP 38 | 19.03. | 08:05 | 03°40.0' | 46°43.0' | 27.1 | 35.90 | x |
| | | 13:15 | 03°36.4' | 46°50.7' | 27.2 | 35.93 | |
| FP 39 | 20.03. | 08:15 | 03°39.9' | 45°14.4' | 27.1 | 35.84 | x |
| | | 13:45 | 03°39.7' | 45°14.4' | 27.2 | 35.83 | |
| FP 40 | 21.03. | 07:30 | 04°03.7' | 44°25.8' | 27.1 | 35.64 | x |
| | | 13:50 | 05°03.1' | 44°49.3' | 27.0 | 35.59 | |
| FP 41 | 22.03. | 08:15 | 06°28.9' | 44°00.4' | 26.9 | 36.03 | x |
| | | 13:50 | 06°29.9' | 44°26.2' | 26.9 | 35.79 | |
| FP 42 | 23.03. | 09:15 | 05°11.6' | 44°22.9' | 26.9 | 35.73 | x |
| | | 15:30 | 05°11.6' | 45°03.2' | 26.9 | 35.61 | |
| FP 43 | 24.03. | 09:00 | 05°43.3' | 44°21.7' | 26.9 | 35.75 | x |
| | | 14:00 | 06°05.1' | 44°11.5' | 27.0 | 35.85 | |
| FP 44 | 25.03. | 08:15 | 05°51.2' | 44°58.6' | 26.9 | 35.83 | x |
| | | 13:15 | 05°40.5' | 45°05.3' | 26.9 | 35.82 | |
| FP 45 | 26.03. | 14:00 | 05°08.3' | 46°34.5' | 27.1 | 35.96 | - |
| | | 20:00 | 04°39.8' | 45°55.2' | 27.0 | - | |
| FP 46 | 27.03. | 08:00 | 04°52.8' | 47°39.9' | 27.1 | 36.06 | x |
| | | 15:30 | 05°23.2' | 47°29.0' | 27.0 | 36.14 | |
| FP 47 | 28.03. | 09:20 | 06°57.9' | 48°05.7' | 26.4 | 35.48 | x |
| | | 15:00 | 07°16.6' | 48°45.5' | 26.8 | 35.59 | |
| FP 48 | 29.03. | 08:30 | 08°45.6' | 52°02.3' | 26.4 | 35.14 | x |
| | | 15:30 | 09°05.2' | 53°20.7' | 26.6 | 35.32 | |
| FP 49 | 30.03. | 08:45 | 09°40.9' | 54°15.4' | 26.8 | 35.89 | x |
| | | 14:30 | 09°40.7' | 54°15.5' | 27.0 | 35.89 | |
| FP 50 | 31.03. | 08:00 | 11°10.6' | 52°29.4' | 25.7 | 36.10 | x |
| | | 15:30 | 12°04.3' | 51°28.1' | 25.9 | 36.09 | |
| FP 51 | 01.04. | 08:00 | 14°07.7' | 49°06.2' | 25.1 | 36.28 | x |
| | | 16:00 | 15°02.2' | 48°03.1' | 25.3 | 36.20 | |
| FP 52 | 02.04. | 09:15 | 16°28.3' | 46°27.7' | 24.7 | 36.48 | x |
| | | 16:30 | 16°59.9' | 46°00.3' | 24.8 | 36.72 | |
| FP 53 | 03.04. | 08:30 | 17°27.3' | 45°38.6' | 24.5 | 36.90 | x |
| | | 18:30 | 17°53.0' | 45°14.2' | 24.6 | 36.82 | |
| FP 54 | 04.04. | 08:30 | 18°12.1' | 44°00.6' | 24.2 | 36.80 | x |
| | | 20:00 | 18°32.4' | 42°57.2' | 24.2 | 36.90 | |
| FP 55 | 05.04. | 08:00 | 19°18.0' | 40°43.5' | 23.7 | 36.99 | - |
| | | 20:00 | 20°02.6' | 38°31.7' | 23.7 | 37.01 | |
| FP 56 | 06.04. | 08:15 | 20°44.6' | 36°27.3' | 22.8 | 37.33 | x |
| | | 20:00 | 21°28.3' | 34°17.0' | - | - | |
| FP 57 | 07.04. | 09:00 | 22°17.1' | 31°50.7' | 22.8 | 37.14 | x |
| | | 20:30 | 22°59.7' | 29°41.9' | 22.3 | 37.37 | |
| FP 58 | 08.04. | 08:30 | 23°41.3' | 27°36.1' | 22.2 | 37.29 | x |
| | | 22.25 | 24°25.1' | 25°22.6' | 22.0 | 37.21 | |

*) at start / end of pumping

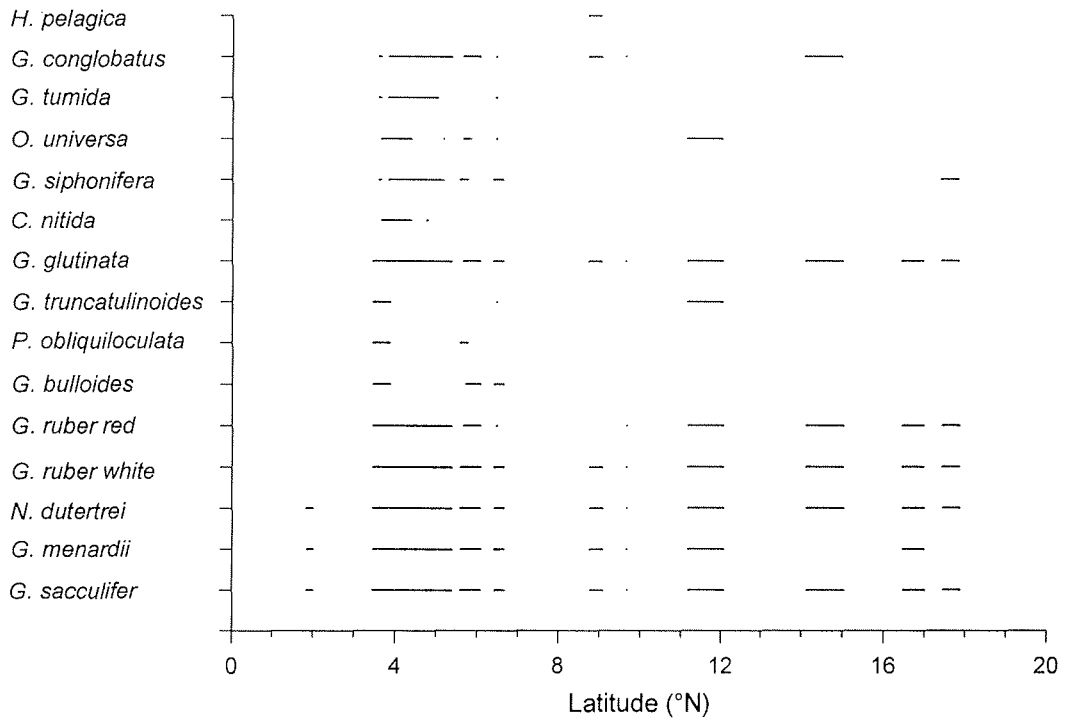


Figure 50 Latitudinal distribution of identified planktic foraminifera species.

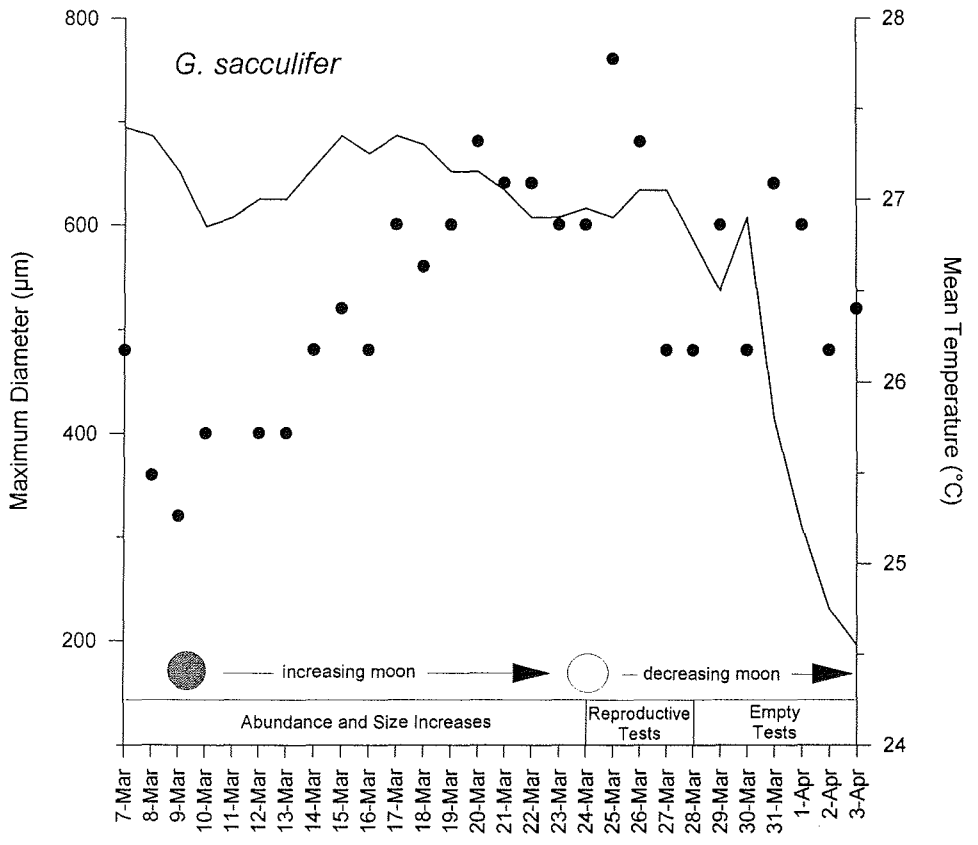


Figure 51 Monthly size cycle of *Globigerinoides sacculifer.*

blage is characterized by a higher diversity (*Globigerina bulloides*, *Globorotalia tumida, Globigerinita. glutinata* and *Pulleniatina. obliquiloculata*). North of 6°N diversity and abundance decreased again.

*G. sacculifer* revealed a pronounced monthly cycle in abundance and size. Figure 51 shows maximum diameters measured along the longest axis together with mean water temperatures and moon phases during Cruise M38/2. Smallest diameters and lowest abundance were encountered with the new moon at the beginning of the cruise. During increasing moon, maximum diameters of the *G. sacculifer* population reached around 800 µm. As the size, abundance was at a maximum around full moon. Tests in the reproductive stage (emerging cytoplasm at the primary aperture) were observed from full moon until four days after this date. Five days after full moon, the abundance of large adult specimens drastically decreased. A considerable proportion of empty tests was observed in the respective samples. Stable isotope analyses on the collected planktic foraminifera assemblages will provide new insights about the role of the ontogenetic cycle for this important parameters.

## 6.5 Water Sampling

*M. Giese, A. Meyer, S. Mulitza, A. Vink*

At 16 stations a rosette with 15 10 l Niskin bottles was deployed to collect sea water. Depending on the regional hydrography, samples were taken between 3 and 3000 m water depth (see station list, Table2). Immediately after recovery the sea water was siphoned into three 50 ml glass bottles for stable isotope analyses. To prevent any biological activity, two water samples for $\delta^{13}C$ measurements were poisoned with 1 ml saturated HgCl solution. A 5 ml scintillation cup was provided to the geochemistry group for shipboard nutrient determinations. All samples for shore based studies were stored at 4 °C. The remaining sea water was filled into plastic jugs and filtered fordino-flagellate investigations (see Chapter 6.1).

# 7 CTD Profiling

*B. Donner*

A self-contained SEABIRD SBE 19 CTD profiler equipped with a conductivity-temperature-depth sensor, an oxygen probe and a CHELSEA fluorometer for chlorophyll-a measurements was deployed at every station to determine the water column stratification. Prior to the cruise all sensors have been calibrated by the manufacturer. The instrument was attached to the cable 50 m above the multicorer. Full parameter sets were taken at 0.5 sec intervals both during downcast and upcast.

In the different working areas from the Amazon Fan, the Ceará Rise and adjacent abyssal plains, to the Guyana continental margin and mid-Atlantic Ridge CTD profiles comprised water depths between 3200 and 4900 m. Immediately after each deployment the records were transferred to a PC, the downcast data averaged and displayed in standard plots. All but one cast (station GeoB 4418) have been successful. Repeatedly, the CHELSEA fluorometer did not register or went out of range at greater water depths. As the chlorophyll-a concentrations are negligible below 200 to 300 m, this was a very minor drawback.

Amazon Fan (Stations GeoB 4408 to 4410 and 4417)

As an example for the Amazon Fan CTD profiles Figure 52 shows the results at site GeoB 4408. The salinities range only from 34.4 to 36.4 ‰ reflection the freshwater inflow from the Amazon River. The chlorophyll-a maximum extends from 100 to 150 m, the oxygen minimum zone from 200 to 1300 m water depth. At the deepest reaching site GeoB 4410 Antarctic Bottom water (AABW) is identified below 4100 m by lower temperature (around 1 °C) and a lower oxygen contents than the overlying North Atlantic Deep Water (NADW).

Ceará Rise and Adjacent Abyssal Plains (Stations GeoB 4401 to 4407, GeoB 4411 to 4413 and GeoB 4414 to 4416

On the Ceará Rise as well as on its eastern slopes to the Pará Abyssal Plain the influence of the Amazon River is still apparent in the salinity ranges which don't exceed 36.4 ‰. The slope stations are characterized by a relatively high oxygen maximum at 300 to 400 m water depth. This maximum is not detected at sites on top of the rise. It documents the better ventilated NADW masses coming from the northeast and reaching the eastern flanks but not the in the summit region of the Ceará Rise. Beneath 4500 m water depth AABW was identified under the NADW by decreasing temperature, oxygen and salinity. Typical CTD profiles for sites on the rise (station GeoB 4406) and flanks (station GeoB 4403) are shown in Figures 53 and 54, respectively.

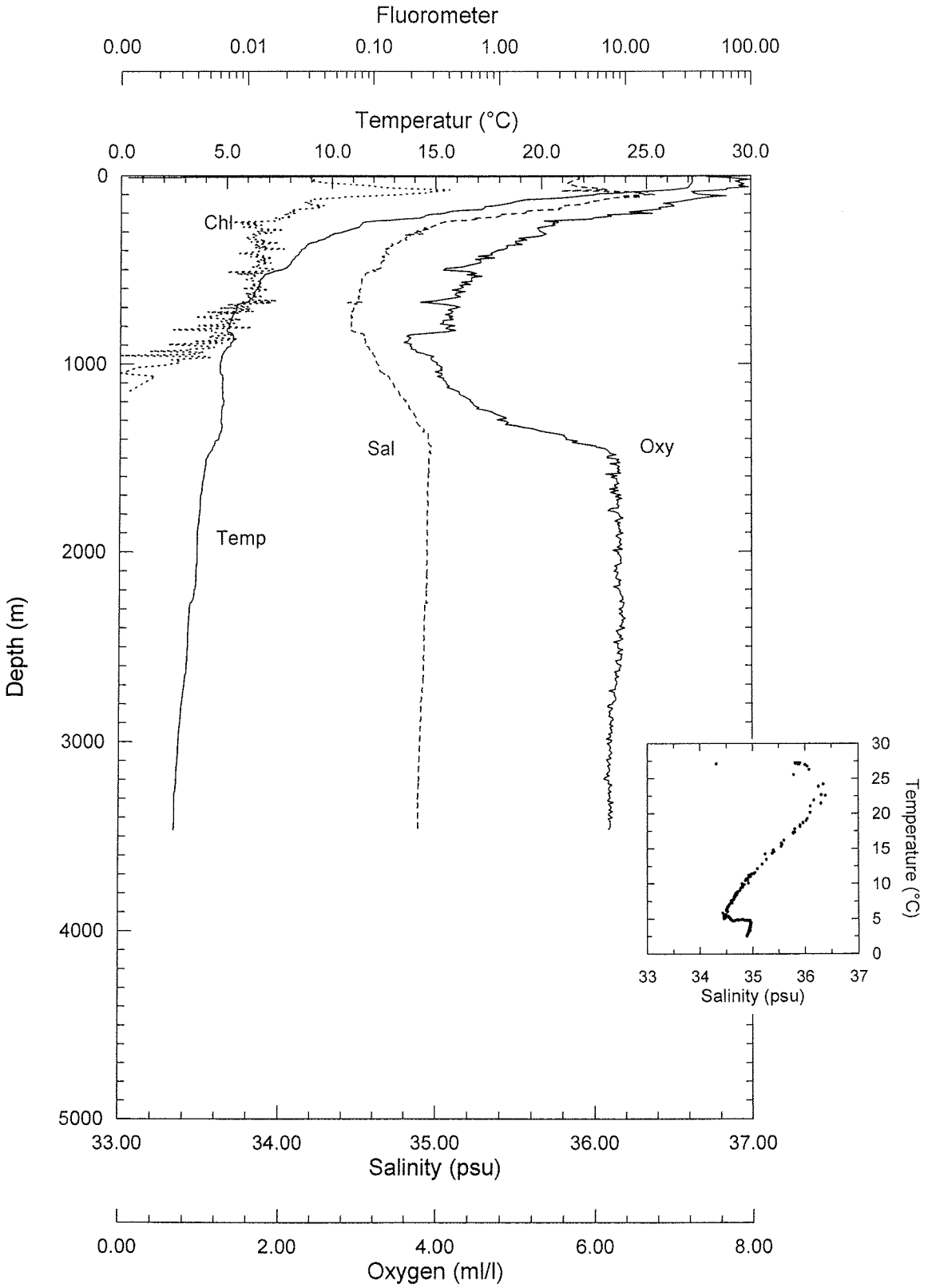


Figure 52 Station GeoB 4408 (03°40.0'N / 46°07.8'W) - CTD profile.

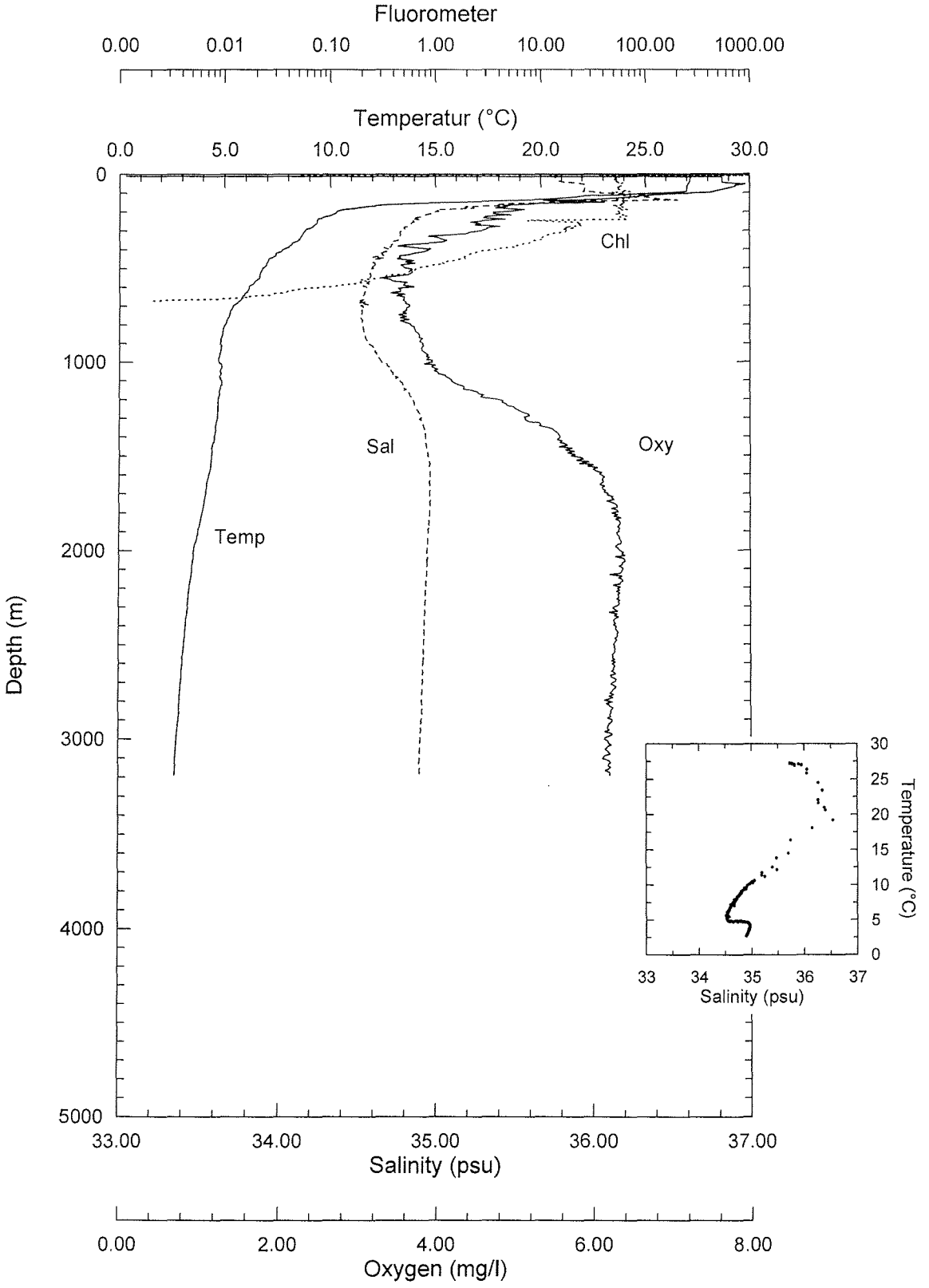


Figure 53 Station GeoB 4406 (05°05.6'N / 43°45.4'W) - CTD profile.

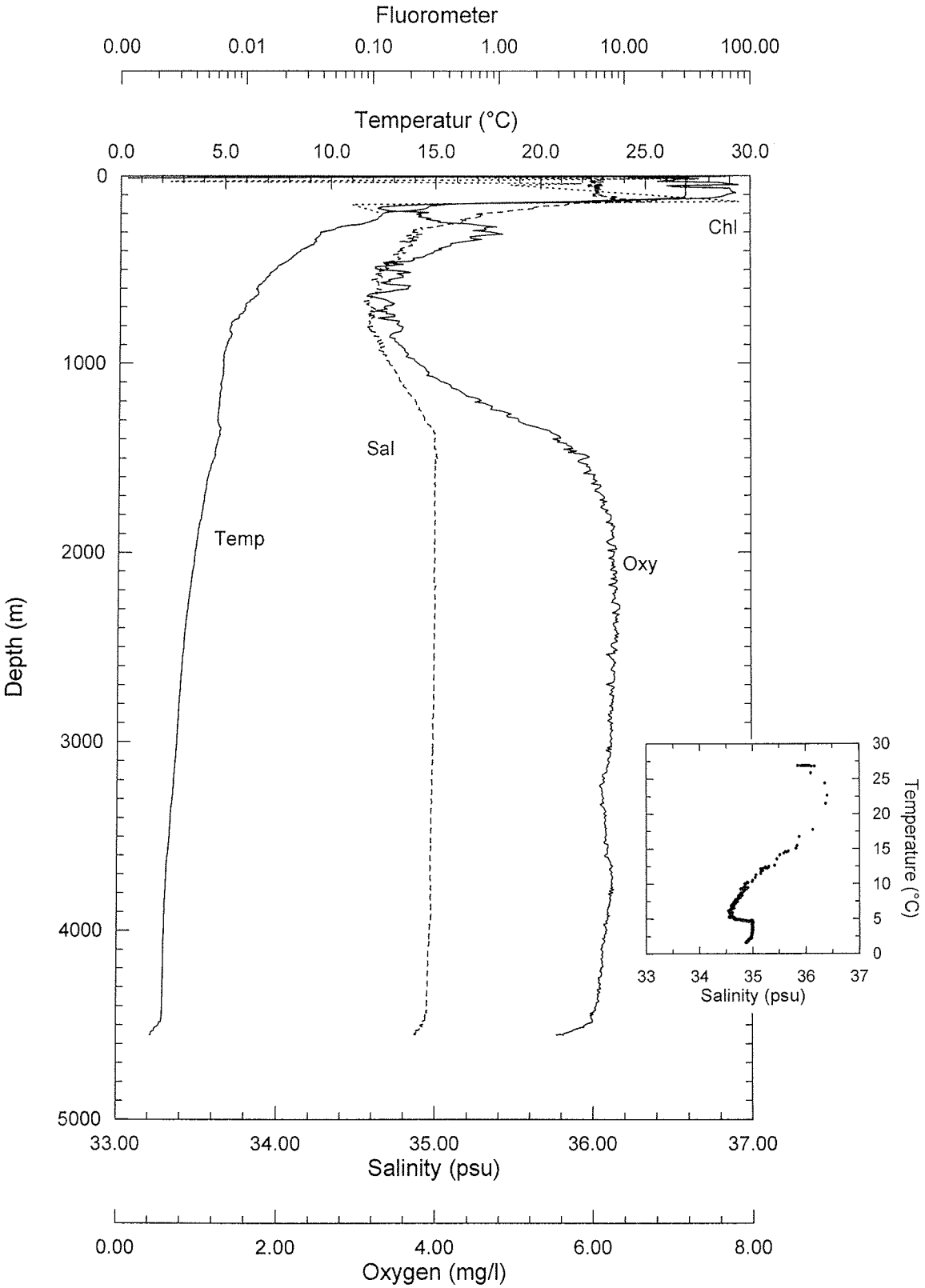


Figure 54 Station GeoB 4403 (06°13.4'N / 43°44.1'W) - CTD profile.

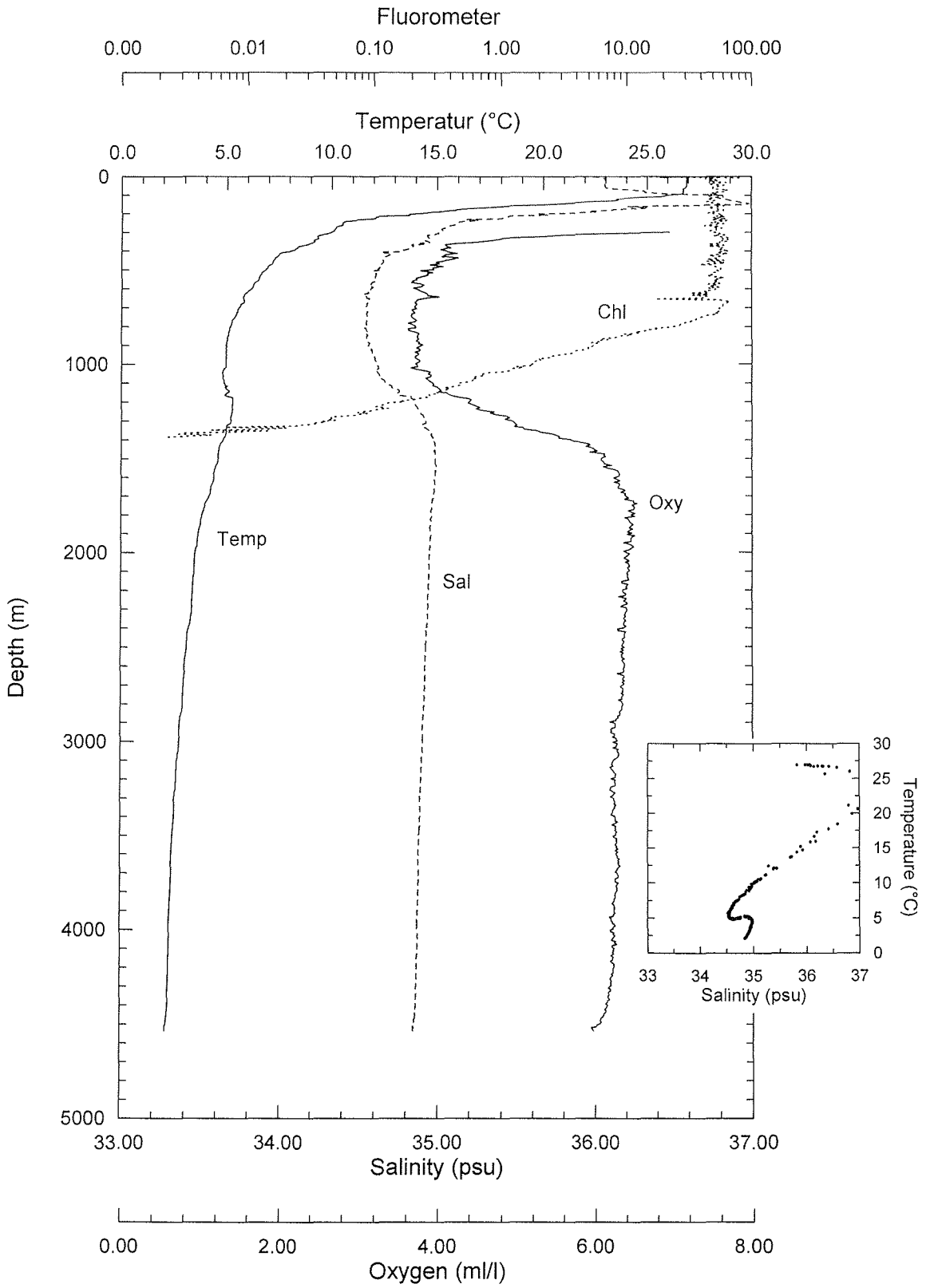


Figure 55 Station GeoB 4419 (09°41.0'N / 54°15.7'W) - CTD profile.

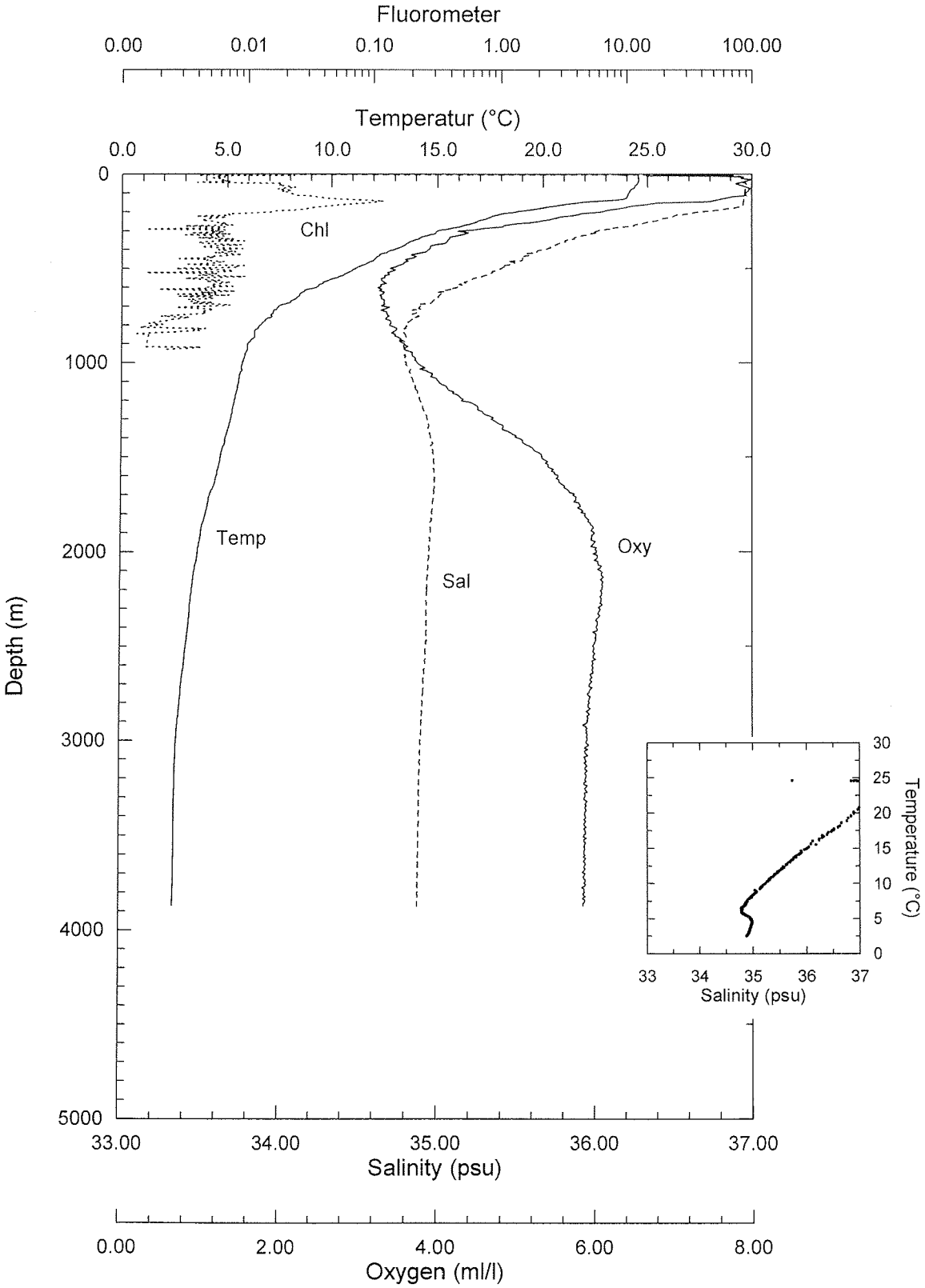


Figure 56 Station GeoB 4422 (17°27.3'N / 45°38.6'W) - CTD profile.

Guyana Continental Margin (Stations GeoB 4418 and 4419).

Salinities reaching 37 ‰ in the surface waters clearly show a different oceanographic regime than at stations influenced by the Amazon discharge. Chlorophyll-a data recorded to 700 m water depth at station GeoB 4419 (Fig. 55) suggest a failure of the sensor.

Mid-Atlantic Ridge (Stations GeoB 4420 to 4424)

Figure 56 (site GeoB 4422) shows an example of the CTD profiles recorded at the mid-Atlantic Ridge near 17°N.The temperature and salinity decrease in the upper water column is smoother than at the previous sites close to the South American continent. Salinities of the surface and subsurface layers exceed 37 ‰. The chlorophyll-a maximum is found between 150 and 200 m water depth. A broad thermocline extending from about 200 to 800 m indicates typical subtropical conditions. NADW can definitely be distinguished, while no trace of AABW was detected to 4800 m water depth at station GeoB 4424.

## 8 Lander Deployments

*O. Holby, S. Meyer, F. Wenzhöfer*

As listed below, a free falling *in situ* chamber lander system (Elinor) and a free falling *in situ* profiling lander system (Profilur) have been deployed during Cruise M38/2. Also indicated are laboratory studies that include incubations of and oxygen profiles in sediment cores recovered with the multicorer.

Table 10 Cruise M38/2 lander deployments and supplementary laboratory analyses.

| Station | Elinor | Profilur | Type | Laboratory |
|---|---|---|---|---|
| GeoB 4401 | X | X | N | X |
| GeoB 4407 | - | - | - | X |
| GeoB 4409 | - | X | S | X |
| GeoB 4412 | - | X | VS | X |
| GeoB 4417 | - | X | VS | X |
| GeoB 4419 | - | X | S | X |
| GeoB 4421 | - | X | VS | X |

N - normal, S - short, VS - very short deployment time (see text for details)

The pre-programmed free falling lander system Elinor is designed to *in situ* incubate a sediment surface of 900 $cm^2$ with preferably 10 to 15 cm overlying water. The water inside the chamber is normally stirred with eight revolutions per minute to create a diffusive boundary layer of about 0.7 mm. Mineralization processes are studied by measuring the total flux of oxygen from the overlying water into the sediment and fluxes of mineralization products between the sediment and the overlying water. Unfortunately, lander Elinor has been lost during the first deployment. Possible scenarios could be that glass spheres imploded or the lander has surfaced, but its satellite transmitter was broken.

The pre-programmed free falling lander system Profilur is designed to acquire oxygen, pH and carbonate profiles *in situ* at the sea floor with a depth resolution of 25 to 200 µm. The lander carries five electrodes to determine the diffusive flux of oxygen, three pH electrodes and two carbonate electrodes penetrating the surface sediment to about 10 cm depth. A 5 l water sample is collected 50 cm above the sediment for calibration of the electrodes and chemical analyses of the bottom water. A camera system documents the sampled sediment surface. During this cruise, the profiling lander was for the first time equipped with a new optrode device allowing to measure oxygen penetration down to 55 cm into the sediment with a depth resolution of 100 µm.

The pH profiles enable to identify various biogeochemical processes in the sediment. On basis of carbonate concentration, pH data and the saturation state obtained from the bottom water sample, calcite dissolution can be calculated. The duration of the deployments listed above (Table 10) reads as follows: normal deployment - all

parameters were measured over the full lengths of all profiles; short deployment - there was insufficient time to measure carbonate and the profiles are limited in length; very short deployment - there was just enough time to activate the optrode unit.

Both landers may also be used for temperature, pressure, oxygen and pH (Profilur) profiling through the water column as they descend or/and ascend (Profilur). Combining their *in situ* results gives a good opportunity to study exchange rates in undisturbed sediments and especially uptake processes of oxygen. The *in situ* analyses were supplemented by measurements on sediment cores recovered with the multicorer and incubated under near *in situ* conditions. A comparison of the lander and laboratory data provides basic information about the degree of disturbance caused by retrieving the sediment from the sea floor.

## 8.1 Preliminary Results

A typical oxygen measurement performed by Profilur at station GeoB 4419 is shown in Figure 57. The oxygen concentration profile recorded in the water column during

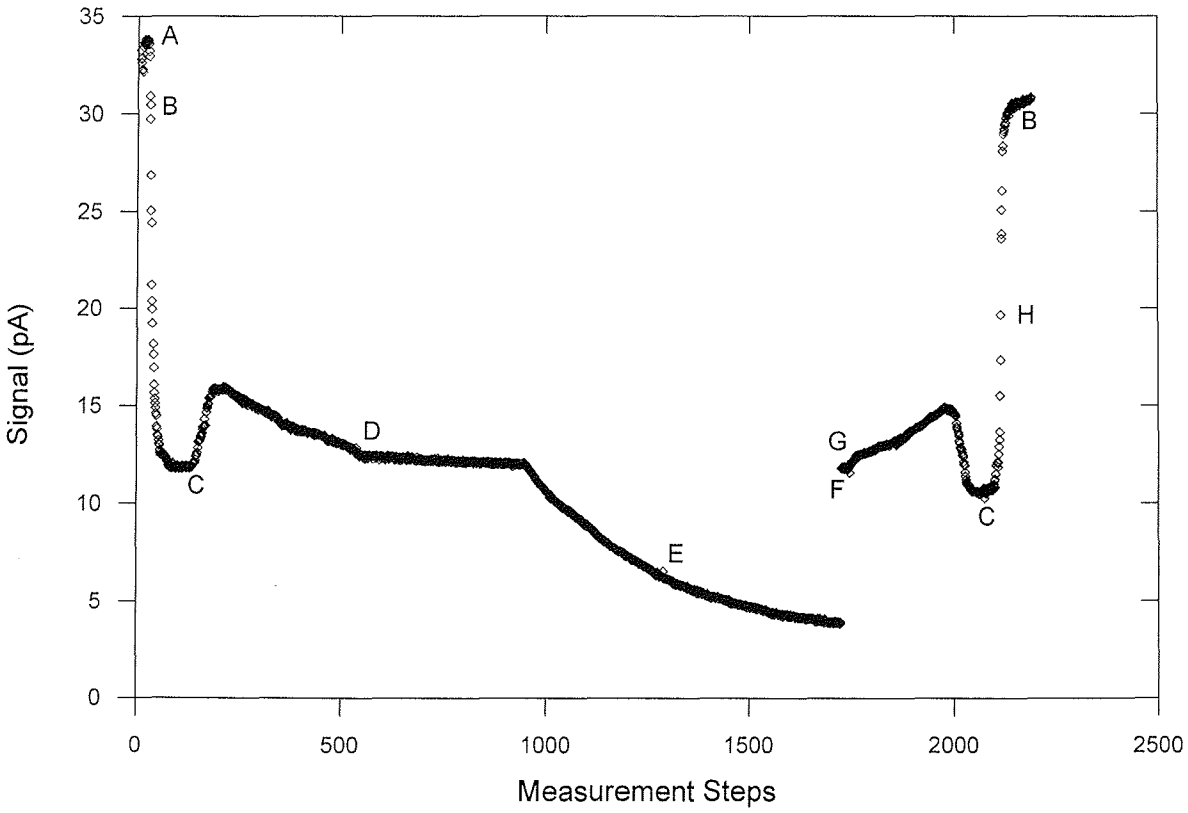


Figure 57 Oxygen measurements at station GeoB 4419. A - Profilur standing on deck, B - over-saturated surface water, C - oxygen minimum in about 400 to 1100 m water depth, D - Profilur has landed, E - oxygen profile in the sediment, F - re-calibration of the electrodes, G - burn wire release, H - oxygen measurements in the water column during ascent.

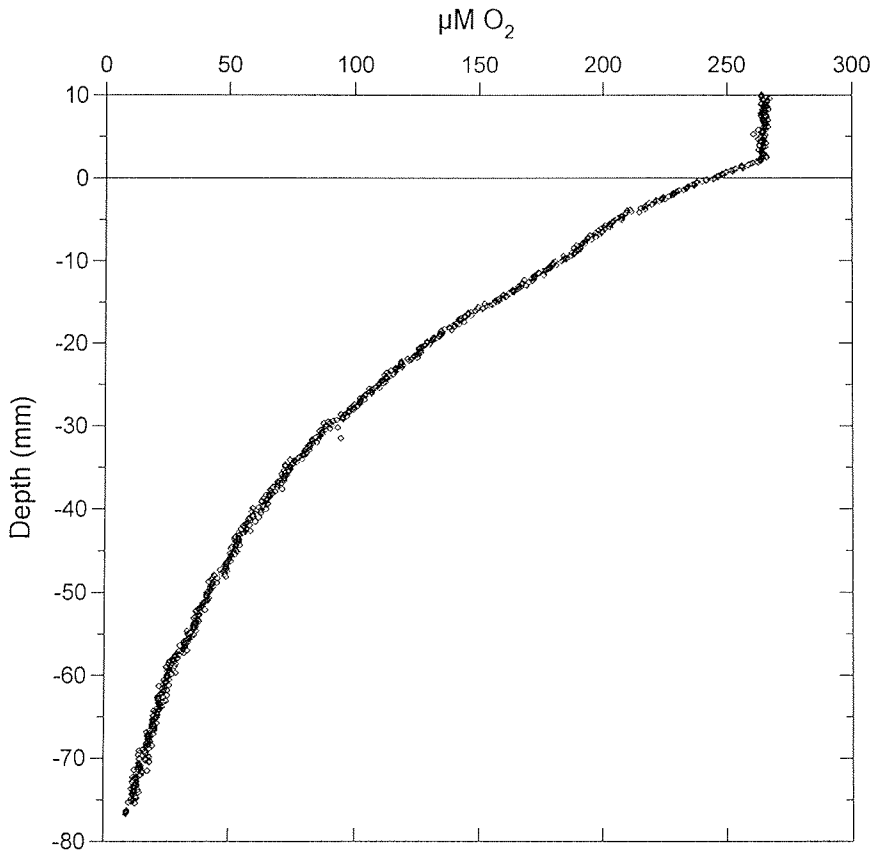


Figure 58 Oxygen profile in the sediment at station GeoB 4419 measured by Profilur.

descent and ascent of the lander reveals a minimum zone from about 400 to 1100 m water depth. The electrodes are sensitive to temperature changes, during this deployment they were equilibrated for 3 °C. The data in the upper parts of the water column, where the temperature is considerable higher, have to be re-calibrated therefore, their general trend is correct, however. The *in situ* sediment oxygen profile at station GeoB 4419 presented in Figure 58 indicates a diffusive boundary layer of about 1 mm thickness and a diffusive oxygen flux into the sediment of around 0.8 mmol/$m^2$ d. The new optrode system for deeper oxygen penetration profiles was successfully tested *in situ*.

## 9 ESTOC Station

At noon of April 12, FS METEOR sailed from Las Palmas to the European Station for Time-Series in the Ocean, Canary Islands (ESTOC). The joint Spanish and German research program there comprises monthly sampling routines since 1994. Twenty scientists from institutions in Germany, the Canary Islands and Scotland (Table 11) embarked on this 2 day's journey to cover the ESTOC experimental work for the month of April 1997.

Table 11 Participants of the M38/2 ESTOC cruise.

| Name | Research Field | Institution |
|---|---|---|
| Adolph, Kerstin | Particle Flux | GeoB |
| Cianca, Andres | Nutrients, $O_2$, Chl | ICCM |
| Escanez, Jose | Nutrients | IEO |
| Fraas, Gerd | Trace Metals | PhysB |
| Godoy, Juana | $O_2$-Incubation | ICCM |
| González-Dávila, Melchor | $CO_2$-System | ULPGC |
| Heinze, Katrin | Bio-Optics | UO |
| Hernández-Brito, Joaquin | Trace Metals | ULPGC |
| Koy, Uwe | CTD | IfMK |
| Kukolka, Florian | Trace Metals | PhysB |
| Lopez-Laatzen, Federico | CTD | IEO |
| Luzardo, Francisco | Nutrients, $O_2$, Chl | ICCM |
| Neuer, Susanne | Particle Flux | GeoB |
| Otto, Sabine | Trace Metals | ChemB |
| Ramos, Sergio | Nutrients, $O_2$, Chl | ICCM |
| Santana-Casiano, J. Magdalena | $CO_2$-System | ULPGC |
| Steffen, Soenke | DOC | UHH |
| Stewart, Iain | Foraminifera | UE |
| Torres-Lopez, Silvia | CTD | IEO |
| Villagarcia, Marimar | Nutrients, $O_2$, Chl | ICCM |

| | |
|---|---|
| ChemB | Fachbereich Biologie/Chemie, Universität Bremen |
| GeoB | Fachbereich Geowissenschaften, Universität Bremen |
| ICCM | Instituto Canario de Ciencias Marinas, Telde, Gran Canaria |
| IEO | Instituto Español de Oceanografia, Santa Cruz, Tenerife |
| IfMK | Institut für Meereskunde, Kiel |
| PhysB | Fachbereich Physik/Elektrotechnik, Universität Bremen |
| UE | University of Edinburgh |
| UHH | Universität Hamburg |
| ULPGC | University of Las Palmas |
| UO | Universität Oldenburg |

Table 12 ESTOC station list.

| Date | Latitude (N) Longitude (W) | Depth (m) | Profile | Time Start | Instrument | Depth (m) | Sampling Depth (m) | Remarks |
|---|---|---|---|---|---|---|---|---|
| 12.04. | 28°34.7' / 15°26.0' | 3565 | 1 | 14:34 | CTD FSI | 200 | 200 | trace metals ULPGC, alkalinity, pH |
| 12.04. | 29°09.9' / 15°30.8' | 3615 | | 19:19 | PIT | | | deployment |
| 12.04. | 29°10.0' / 15°30.0' | 3613 | 2 | 21:00 | CTD FSI | 300 | 200, 125, 100, 75, 50, 25, 10 | taxonomic pigments, POC |
| 12.04. | 29°10.1' / 15°30.3' | 3613 | 3 | 22:15 | CTD FSI | 25 | 25 | dilution experiment |
| 12.04. | 29°10.0' / 15°30.5' | 3613 | 4 | 23:10 | CTD FSI | 50 | 50 | dilution experiment |
| 13.04. | 29°10.6' / 15°30.6' | 3613 | 5 | 00:45 | CTD FSI | 3000 | 1500, 1300, 1200, 1000 | trace metals ULPGC, DOC, isotopes, nutrients IEO, ICCM, alkalinity, pH, $O_2$ |
| 13.04. | 29°10.8' / 15°30.4' | 3614 | 6 | 03:59 | CTD FSI | 3050 | - | |
| 13.04. | 29°10.4' /15°30.4' | 3614 | 7 | 06:11 | GoFlo | 3614 | 3585, 3575, 3550, 3500, 3400, 3200 | trace metals ULPGC, ChemB, nutrients, $O_2$, He/$H_3$ |
| | | | | | Pumps | | 3535, 3220, 2600, 1000, 700 | |
| 13.04. | 29°10.3' / 15°31.3' | 3614 | 8 | 11:33 | CTD FSI | 614 | 200,150, 125, 100, 75, 65,50, 40, 30, 25, 10, 0 | trace metal ULPGC, DOC, isotopes, nano nutrients IEO, nutrients, chl, alkalinity, pH, $O_2$ ICCM, IEO |
| 13.04. | 29°10.3' / 15°32.0' | 3614 | 9 | 13:23 | HN | 100 | | |
| 13.04. | 29°10.5' / 15°32.5' | 3614 | 10 | 14:14 | CTD FSI | 200 | 200, 150, 100, 50, 25, 10 | He/$H_3$ |
| 13.04. | 29°10.8' / 15°32.7' | 3616 | 11 | 15:12 | GoFlo | 2520 | 2500, 2000, 1800, 800, 300 | trace metals ULPGC, ChemB, DOC, isotopes, nutrients ICCM, alkalinity, pH, $O_2$ ICCM, IEO, He/$H_3$ |
| 13.04. | 29°11.2' / 15°32.9' | 3616 | 12 | 19:48 | CTD SIS | 1020 | | |
| 13.04. | 29°09.7' / 15°32.7' | 3616 | | 21:35 | PIT | | | recovery |

CTD - CTD profiler, PIT - particle interceptor trap, HN - hand net;
nutrients - nitrate, nitrite, phosphate, ammonium, total nitrogen, total phosphate; nano nutrients - nanomolar concentrations of nutrients;
DOC - dissolved organic carbon; POC - particulate organic carbon

In addition to measurements of water column parameters which are regularly monitored such as conductivity, temperature, oxygen, nutrients, chlorophyll, trace metals, stable isotopes and dissolved inorganic carbon this cruise offered the opportunity for a number of supplementary investigations. They included continuous underway profiling of $CO_2$, collection of trace metals with GoFlos and particle pumps, water column sampling for dissolved organic carbon (DOC), nanomolar concentrations of nutrients, particulate organic carbon (POC), foraminifera and taxonomic pigments. Moreover, a productivity experiment based on dilution and oxygen changes was performed, a free-floating trap array deployed and the new IEO CTD/Rosette system tested (Table 12). Overall, the cruise has been very successful as it brought together many more scientists at one time to ESTOC than usually possible to carry out measurements that in the future will be implemented in the standard ESTOC program.

Underway from Las Palmas to the ESTOC station temperature profiles were recorded with Expandable Bathythermographs (XBTs) at 28°20.0'N / 15°23.4'W, 28°40.0'N / 15°27.0'W, 28°50.0'N / 15°27.7'W, 29°00.0'N / 15°28.9'W and 29°10.0'N / 15°30.0'W.

## 9.1 Sampling and *in situ* Determination of Dissolved Aluminium

*J. J. Hernández-Brito and M. D. Gelado-Caballero*

Aluminium distributions in central East Atlantic waters show a great variability and marked latitudinal gradients from east to west (Gelado-Caballero et al., 1996). Various major features of the area affect the aluminium biogeochemical characteristics such as an elevated aeolian dust influx from the Sahara Desert, proximity (150 - 200 km) to upwelling systems and mesoscale island effects in the course of the Canary Current. The study of Al variations along these gradients and at a fixed station will provide a better understanding of the physical and biogeochemical processes controlling the mesoscale regional distribution of aluminium.

The main objectives of the cruise were

- to record spring profiles of dissolved aluminium at the ESTOC station (Hernández-Brito et al., 1996),
- to determine high-resolution profiles of dissolved aluminium in the surface (200 m) and deeper layers (400 m) at the ESTOC station,
- an intercalibration of electrochemical and spectrophotometrical methods to measure dissolved aluminium.

The water sampling was performed with silicone rubber coated Niskin bottles. The containers were cleaned before deployment using standard procedures in trace metal experiments, the samples taken and manipulated wearing plastic gloves to avoid contaminations. One part of the samples was measured on board, the other stored in

250 ml polyethylene bottles and immediately frozen until shore based analysis. Go-flo bottles were used to sample sea water for the intercalibration study.

On board, dissolved aluminium was determined with the High Performance Adsorptive Cathodic Stripping Voltametry method (HPACSV; Hernández-Brito et al., 1994). Samples were prepared in teflon cups of a polarographic cell containing 10 ml of water, 2 µl 10-6 M DASA and 0.01 M BES. The adsorption potential (-0.9 V) was applied to the working electrode while stirring the solution for 40 s and let it settle for 5 s. The scanning started at -0.9 V and terminated at -1.4 V running a staircase modulation with a rate of 30 V/s and a pulse height of 5 mV. The DASA Al-peak appears at about -1.25 V. A standard was added to quantify the absolute aluminium concentration. The analyses were carried out on a clean bench (class-100) to avoid contaminations by dust particles.

## 9.2 Collection of Planktic Foraminifera for DNA Analysis

*I. Stewart*

Planktic foraminifera were collected from about 5 m depth by pumping sea water from METEORS' fire hose system through a 70 micron mesh net. The plankton net was also lowered to a depth of 100 m before being raised to the surface, a method found to be more successful since the samples remained relatively intact. Collection details are summarized in Tables 13 and 14.

The foraminifera were identified and the majority of specimens individually crushed in 30 µl of lysis buffer to protect the DNA from enzymatic action. The remaining specimens have been placed in a small volume of sea water, all specimens then labelled and frozen at -20 °C. The foraminifera frozen in sea water were taken to the laboratory for a full DNA extraction. One sample pumped from 5 m was preserved to examine the foraminiferal tests under an electron microscope.

The foraminifera from the surface collection tended to be small and immature, while specimens from the depth collection typically were larger and more mature. This is not surprising since in the later stages of a foraminifers' life cycle they sink from near the surface to the thermocline, where they reproduce. The species found were *Globigerinoides ruber* (pink and white forms), *Globigerinella siphonifera, Globigerinita glutinata, Globorotalia truncatulinoides and Orbulina universa.* Other species included a *Globigerina bulloides / Globigerina falconensis* morphotype as well as some individuals which could not be positively identified. The use of DNA analysis will allow a more accurate species list to be compiled once the sequences can be compared to a DNA database. An interesting finding was that the species *Turborotalita humilis,* most common during Cruise M37/2, now appeared extremely scarce. This highlights the season-

ality of some species of planktic foraminifera. A total of 48 individual specimens were taken for analysis.

Table 13 Planktic foraminifera pump collection data.

| Date | Pump Time Start | Position | Pump Time Stop | Position |
|---|---|---|---|---|
| 12.04. | 14:55 | 28°32'N / 15°25'W | 21.30 | 29°09'N / 15°30'W |
| 13.04. | 7:30 | 29°10'N / 15°30'W | 19.30 | 29°10'N / 15°30'W |

Table 14 Planktic foraminifera depth collection data.

| Date | Time of Collection | Time at 100 m | Position | Depth Range (m) |
|---|---|---|---|---|
| 13.04. | 14:00 - 14:15 | 2 min | 29°10'N / 15°30'W | 100 - 0 |

## 9.3 Carbonate System in the Canary Islands Area

*M. González Dávila, J. M. Santana Casiano*

Underway from Gran Canaria to the ESTOC station and back to Gran Canaria, $CO_2$ partial pressure ($pCO_2$) was continuously monitored with an infrared analyzer together with total alkalinity and pH (25 °C) using high-precision potentiometric alkalinity and pH systems.

Partial $CO_2$, pH and alkalinity data are useful in assessing the regional extent of different water masses. Based on the interdependence between various properties, regulating processes and their relationships to oceanographic environments can be identified. In the surface and intermediate waters total $CO_2$ concentrations, normalized to 35 ‰ salinity were linearly related to water temperature. Due to photosynthesis highest pH was found in the surface waters (upper 100 m) and oxidation of organic material resulted in a decrease to further depth. The minimum at about 800 m coincided with a maximum in $pCO_2$. The pH increase as well as higher normalized alkalinities in deep waters were associated with the dissolution of $CaCO_3$. Normalized total $CO_2$ in the surface layer amounted to about 1.980 mmol/kg. In deeper waters $\Sigma CO_2$ increased due to the oxidation of organic material. Precipitation or formation of solid $CaCO_3$ in the surface waters and dissolution of solid $CaCO_3$ in deep waters is a very important process in transferring $CO_2$ to depth. The saturation levels in the Canary Islands area have been found to be 3500 m for calcite and 2500 m for aragonite.

The salinity distribution and pH characteristics at ESTOC are clearly related. Salinity profiles indicate the presence of North Atlantic Central Waters (NACW) from 100 to

800 - 1000 m. The slight maximum at 1200 m is the signature of Mediterranean Overflow Water (MOW). A diagram of pH25 in total proton scale (mol/kg sea water) versus salinity shows the influence of MOW in higher pH and also the NACW and North Eastern Atlantic Deep Water (NEADW) water masses.

Partial $CO_2$ variations at ESTOC depend on temperature and biological effects. Over 25 hours, the sea water concentrations were between 15 and 20 µmol/mol lower on average than the equilibrium to air (367 µmol/mol). The results suggest that the ESTOC area tends to gain $CO_2$ from the atmosphere during the night until noon, while in the afternoon and mainly from 5 to 6 pm equilibrium is attained between air and sea water $CO_2$. In late winter and early spring upwelling reduces the regional absorption of $CO_2$ by the ocean. Using wind speed and environmental conditions air - sea $CO_2$ exchange will be modelled.

To evaluate the relevance of the Canary Islands area in the global carbon cycle, additional studies of seasonal variabilities in $CO_2$ fluxes will include continuous $pCO_2$ measurements and discrete carbonate parameters at ESTOC.

## 9.4 Particle Flux and Plankton Biomass

*S. Neuer*

Particle flux in the ESTOC region is subject to seasonal and short-term variability due to varying productivity and hydrographic conditions. Experiments with moored particle traps at ESTOC showed that a large portion of the deep particle flux originates from lateral influx. It is therefore important to quantify the particulate carbon flux directly beneath the euphotic zone. Ideally, these sinking flux determinations need to be supplemented by measurements of the standing stock and production rates of the plankton community.

Two types particle interceptor traps (PIT) were deployed to 200 and 220 m water depth (Fig. 59) from April 12, 19:19 until April 13, 21:35 to study the particle flux below the euphotic zone. The traps have been attached to a surface spar with ARGOS transmitter, flash and Radar reflector. The main buoyancy was installed in about 30 m depth to avoid the wind induced Ekman layer. The CLS ARGOS service traced the trap array.

To quantify the plankton community in the euphotic zone during the trap deployment, water samples were taken for chlorophyll, taxonomically characteristic pigments (analyzed with High Pressure Liquid Chromatography, HPLC) and POC (particulate organic carbon), and passed through GF/F filters. Chlorophyll was determined immediately after returning to Gran Canaria as acetone extract using a Turner AU 10 fluorometer, POC and HPLC samples were frozen until analysis at Bremen University.

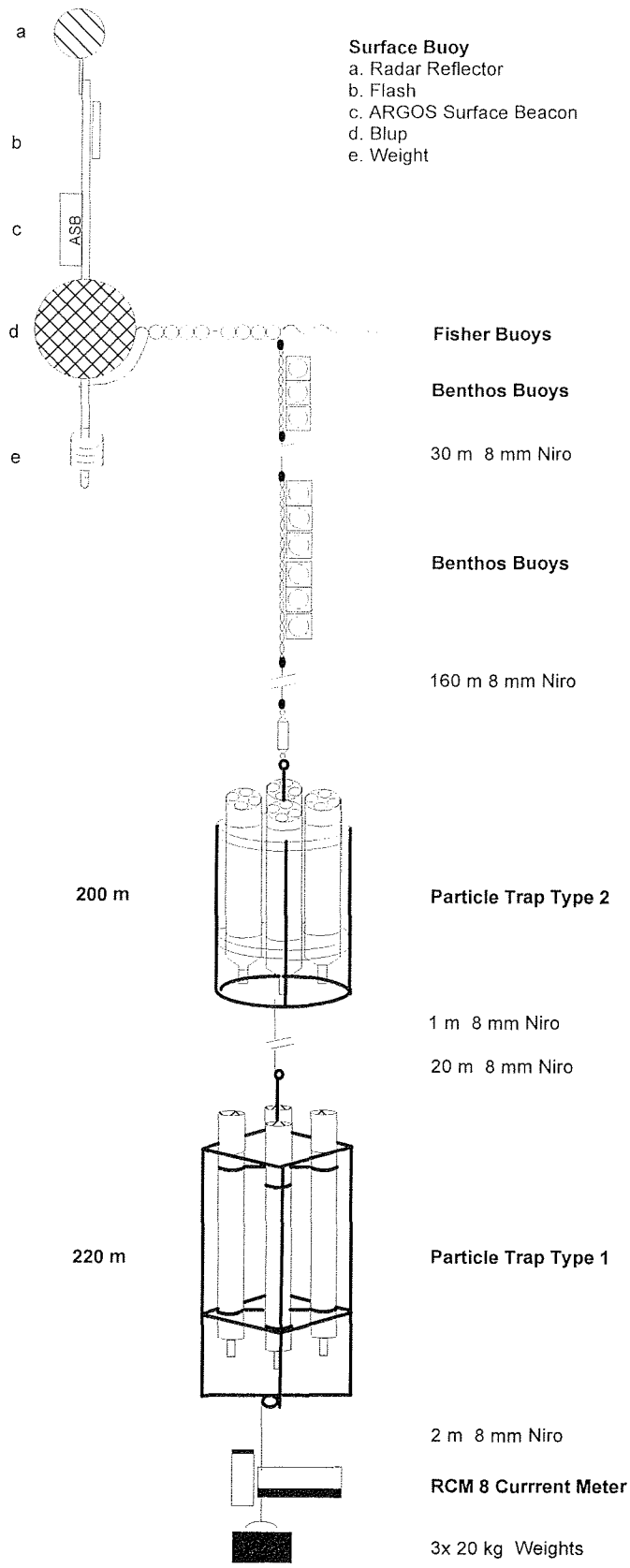


Figure 59 Surface floating particle interceptor trap.

During the deployment of the particle trap dilution experiments and incubations which monitored the change of oxygen were performed to determine phytoplankton growth and microzooplankton grazing rates under close to *in situ* conditions. The dilution experiments used water from 25 and 50 m depth collected at the beginning of the particle trap deployment period. The incubations were carried out on deck with neutral density screens to simulate *in situ* light conditions.

## 9.5 Marine Chemistry

*S. Otto, F. Kukolka*

In marine biogeochemical cycling particle - water interactions are key mechanism for the distribution of chemical elements. Uptake by particulate matter and its subsequent sinking (scavenging) has major control on the chemical composition of sea water and maintains the concentrations of many elements in the oceans rather low. Particulate materials comprise (a) suspended particulate matter (SPM) consisting of almost non-sinkable biogenic and terrigenic detritus with a large surface to volume ratio and (b) relatively fast sinking particles as found in sediment traps responsible for the vertical transport to the ocean floor. A comparison of the composition and distribution of trace elements in dissolved and different particulate phases should provide important clues on transport and sorption as well as on the general geochemical bearing of these elements in the ocean. As part of the CANIGO project the vertical distribution of trace metals in dissolved, suspended and particulate form in the water column is examined at the ESTOC station and compared to their abundances in surface sediments.

During this cruise intermediate and bottom waters were sampled for dissolved trace metals and suspended particulate matter to supplement data sets acquired at ESTOC station on recent METEOR cruises (M37/2a and M38/1). Samples have been collected by means of GoFlo bottles and filtrations using special *in situ* pumps attached to a non-metallic wire. To avoid contaminations, clean sampling techniques were rigorously applied and sample processing was done inside a clean bench. Two casts recovered five *in situ* pump samples and six water samples each. Dissolved trace element samples were filtered through cleaned 0.4 µm polycarbonate filters and acidified for storage, SPM was accumulate onto filters of identical material and kept frozen until shore based analysis. Samples for total dissolvable aluminum have also been frozen for analyses at Bremen University using a fluorescence method.

In addition to trace metal sampling, water samples were taken for nutrients and oxygen. Only oxygen was analyzed on board by titration using the Winkler method.

## 10 References

BOYCE, R.E., 1968. Electrical resistivity of modern marine sediments from the Bering Sea. J. Geophys. Res. 73, 4759-4766.

BOYCE, R.E., 1976. Sound velocity - density parameters of sediment and rock from DSDP Drill Sites 315 - 318 on the Line Islands Chain, Manihiki Plateau, and Tuamotu Ridge in the Pacific Ocean. In: Schlanger, S.O., E.D. Jackson et al., Init. Repts. DSDP 33, 695-728.

CURRY, W.B., N.J. SHACKLETON, C. RICHTER et al., 1995. Proc. ODP, Init. Repts., 154. College Station, Ocean Drilling Program.

FLOOD, R.D., D.J.W. PIPER, A. KLAUS et al., 1995. Proc. ODP, Init. Repts., 15%. College Station, Ocean Drilling Program.

GELADO-CABALLERO M.D., J.J. HERNANDEZ-BRITO, M.E. TORRES-PADRON, J.A. HERRERA-MELIAN & J. PEREZ, 1996. Aluminium distributions in central East Atlantic waters (Canary Islands). Mar. Chem. 51: 359-372.

HERNANDEZ-BRITO J.J., M.D. GELADO-CABALLERO, J. PEREZ & J.A. HERRERA-MELIAN, 1994. Fast determination of aluminum reactive to 1.2-dihydroxyanthra-quinone-3-sulfonic acid in sea water. Analyst 119: 1593-1597.

HERNANDEZ-BRITO J.J., O. LLINAS-GONZALEZ, M.J. RUEDA-LOPEZ & M.D GELADO-CABALLERO, 1997. Annual variations of aluminium at the ESTOC station (Canary Islands). in prep.

KASTEN, S., 1996. Early diagenetic metal enrichments in marine sediments as documents of nonsteady-state depositional conditions. Berichte, Fachbereich Geowissenschaften, Universität Bremen 82, 1118 p.

KUMAR N. & R.W. EMBLEY, 1977. Evolution and origin of the Ceará Rise: an aseismic rise in the western equatorial Atlantic. Geol. Soc. Am. Bull. 88: 683-694.

MOUNTAIN G.S. & W.B. CURRY, 1995. Cruise Ew9209: Site survey for Leg 154. In: Curry, W.B, N.J. Shackleton, C. Richter et al., 1995. Proc. ODP, Init. Repts., 154. College Station, Ocean Drilling Program, 39-52.

SCHULTHEISS, P.J. & S.D. McPHAIL, 1989. An automated p-wave logger for recording fine-scale compressional wave velocity structures in sediments. In: W. Ruddiman, M. Sarnthein et al., Proc. ODP, Sci. Results 108, 407-413.

SCHULZ, H.D. et al., 1991. Bericht und erste Ergebnisse der METEOR-Fahrt M16/2. Berichte, Fachbereich Geowissenschaften, Universität Bremen 19, 149 p.

WEFER, G. et al., 1991. Bericht und erste Ergebnisse über die METEOR-Fahrt M 16/1. Berichte, Fachbereich Geowissenschaften, Universität Bremen 18, 120 p.

## 11 Acknowledgements

The scientific party aboard R/V METEOR during Leg 2 of Cruise No. 38 gratefully acknowledges the friendly cooperation and efficient technical assistance of Captain Kull, his officers and crew who substantially contributed to the overall scientific success of this expedition.

We also appreciate the most valuable help of the Leitstelle METEOR, Hamburg in the planning and realization of the cruise.

The work was funded by the Deutsche Forschungsgemeinschaft within the scope of the Sonderforschungsbereich 261 at Bremen University.

## Publications of this Series

**No. 1** **Wefer, G., E. Suess und Fahrtteilnehmer**
Bericht über die POLARSTERN-Fahrt ANT IV/2, Rio de Janeiro - Punta Arenas, 06.11. - 01.12.1985. 60 p., 1986.

**No. 2** **Hoffmann, G.**
Holozänstratigraphie und Küstenlinienverlagerung an der andalusischen Mittelmeerküste. 173 p., 1988. (out of print)

**No. 3** **Wefer, G. und Fahrtteilnehmer**
Bericht über die METEOR-Fahrt M 6/6, Libreville - Las Palmas, 18.02. - 23.03.1988. 97 p., 1988.

**No. 4** **Wefer, G., G.F. Lutze, T.J. Müller, O. Pfannkuche, W. Schenke, G. Siedler, W. Zenk**
Kurzbericht über die METEOR-Expedition Nr. 6, Hamburg - Hamburg, 28.10.1987 - 19.05.1988. 29 p., 1988. (out of print)

**No. 5** **Fischer, G.**
Stabile Kohlenstoff-Isotope in partikulärer organischer Substanz aus dem Südpolarmeer (Atlantischer Sektor). 161 p., 1989.

**No. 6** **Berger, W.H. und G. Wefer**
Partikelfluß und Kohlenstoffkreislauf im Ozean. Workshop am 3./4. Juli 1989 in Bremen. Bericht und Kurzfassungen. 57 p., 1989.

**No. 7** **Wefer, G. und Fahrtteilnehmer**
Bericht über die METEOR-Fahrt M 9/4, Dakar - Santa Cruz, 19.02. - 16.03.1989. 103 p., 1989.

**No. 8** **Kölling, M.**
Modellierung geochemischer Prozesse im Sickerwasser und Grundwasser. 135 p., 1990.

**No. 9** **Heinze, P.-M.**
Das Auftriebsgeschehen vor Peru im Spätquartär. 204 p., 1990. (out of print)

**No. 10** **Willems, H., G. Wefer, M. Rinski, B. Donner, H.-J. Bellmann, L. Eißmann, A. Müller, B.W. Flemming, H.-C. Höfle, J. Merkt, H. Streif, G. Hertweck, H. Kuntze, J. Schwaar, W. Schäfer, M.-G. Schulz, F. Grube, B. Menke**
Beiträge zur Geologie und Paläontologie Norddeutschlands. Exkursionsführer. 202 p., 1990.

**No. 11** **Wefer, G. und Fahrtteilnehmer**
Bericht über die METEOR-Fahrt M 12/1, Kapstadt - Funchal, 13.03. - 14.04.1990. 66 p., 1990.

**No. 12** **Dahmke, A., H.D. Schulz, A. Kölling, F. Kracht, A. Lücke**
Schwermetallspuren und geochemische Gleichgewichte zwischen Porenlösung und Sediment im Wesermündungsgebiet. 121 p., 1991.

**No. 13** **Rostek, F.**
Physikalische Strukturen von Tiefseesedimenten des Südatlantiks und ihre Erfassung in Echolotregistrierungen. 209 p., 1991.

**No. 14** **Baumann, M.**
Die Ablagerung von Tschernobyl-Radiocäsium in der Norwegischen See und in der Nordsee. 133 p., 1991.

**No. 15** **Kölling, A.**
Frühdiagenetische Prozesse und Stoff-Flüsse in marinen und ästuarinen Sedimenten. 140 p., 1991.

**No. 16** **SFB 261**
1. Kolloquium des Sonderforschungsbereichs 261 der Universität Bremen: Der Südatlantik im Spätquartär - Rekonstruktion von Stoffhaushalt und Stromsystemen. Kurzfassungen der Vorträge und Poster. 66 p., 1991.

**No. 17** **Pätzold, J., T. Bickert, L. Brück, C. Gaedicke, K. Heidland, G. Meinecke, S. Mulitza**
Bericht und erste Ergebnisse über die METEOR-Fahrt M 15/2, Rio de Janeiro - Vitória, 18.01. - 07.02.1991. 46 p., 1993.

**No. 18** **Wefer, G. und Fahrtteilnehmer**
Bericht und erste Ergebnisse über die METEOR-Fahrt M 16/1, Pointe Noire - Recife, 27.03. - 25.04.1991. 120 p., 1991.

**No. 19** **Schulz, H.D. und Fahrtteilnehmer**
Bericht und erste Ergebnisse über die METEOR-Fahrt M 16/2, Recife - Belem, 28.04. - 20.05.1991. 149 p., 1991.

**No. 20** **Berner, H.**
Mechanismen der Sedimentbildung in der Fram-Straße, im Arktischen Ozean und in der Norwegischen See. 167 p., 1991.

**No. 21** **Schneider, R.**
Spätquartäre Produktivitätsänderungen im östlichen Angola-Becken: Reaktion auf Variationen im Passat-Monsun-Windsystem und in der Advektion des Benguela-Küstenstroms. 198 p., 1991. (out of print)

**No. 22** **Hebbeln, D.**
Spätquartäre Stratigraphie und Paläozeanographie in der Fram-Straße. 174 p., 1991.

**No. 23** **Lücke, A.**
Umsetzungsprozesse organischer Substanz während der Frühdiagenese in ästuarinen Sedimenten. 137 p., 1991.

**No. 24** **Wefer, G. und Fahrtteilnehmer**
Bericht und erste Ergebnisse der METEOR-Fahrt M 20/1, Bremen - Abidjan, 18.11. - 22.12.1991. 74 p., 1992.

**No. 25** **Schulz, H.D. und Fahrtteilnehmer**
Bericht und erste Ergebnisse der METEOR-Fahrt M 20/2, Abidjan - Dakar, 27.12.1991 - 03.02.1992. 173 p., 1992.

**No. 26** **Gingele, F.**
Zur klimaabhängigen Bildung biogener und terrigener Sedimente und ihrer Veränderung durch die Frühdiagenese im zentralen und östlichen Südatlantik. 202 p., 1992.

**No. 27** **Bickert, T.**
Rekonstruktion der spätquartären Bodenwasserzirkulation im östlichen Südatlantik über stabile Isotope benthischer Foraminiferen. 205 p., 1992. (out of press)

**No. 28** **Schmidt, H.**
Der Benguela-Strom im Bereich des Walfisch-Rückens im Spätquartär. 172 p., 1992.

**No. 29** **Meinecke, G.**
Spätquartäre Oberflächenwassertemperaturen im östlichen äquatorialen Atlantik. 181 p., 1992.

**No. 30** **Bathmann, U., U. Bleil, A. Dahmke, P. Müller, A. Nehrkorn, E.-M. Nöthig, M. Olesch, J. Pätzold, H.D. Schulz, V. Smetacek, V. Spieß, G. Wefer, H. Willems**
Bericht des Graduierten Kollegs "Stoff-Flüsse in marinen Geosystemen". Berichtszeitraum Oktober 1990 - Dezember 1992. 396 p., 1992.

**No. 31** **Damm, E.**
Frühdiagenetische Verteilung von Schwermetallen in Schlicksedimenten der westlichen Ostsee. 115 p., 1992.

**No. 32** **Antia, E.E.**
Sedimentology, Morphodynamics and Facies Association of a Mesotidal Barrier Island Shoreface (Spiekeroog, Southern North Sea). 370 p., 1993.

**No. 33** **Duinker, J. und G. Wefer**
Bericht über den 1. JGOFS-Workshop. 1./2. Dezember 1992 in Bremen. 83 p., 1993.

**No. 34** **Kasten, S.**
Die Verteilung von Schwermetallen in den Sedimenten eines stadtbremischen Hafenbeckens. 103 p., 1993.

**No. 35** **Spieß, V.**
Digitale Sedimentographie. Neue Wege zu einer hochauflösenden Akustostratigraphie. 199 p., 1993.

**No. 36** **Schinzel, U.**
Laborversuche zu frühdiagenetischen Reaktionen von Eisen (III)- Oxidhydraten in marinen Sedimenten. 189 p., 1993.

**No. 37** **Sieger, R.**
CoTAM - ein Modell zur Modellierung des Schwermetalltransports in Grundwasserleitern. 56 p., 1993. (out of print)

**No. 38** **Willems, H.**
Geowissenschaftliche Untersuchungen im Tethys-Himalaya. 183 p., 1993.

**No. 39** **Hamer, K.**
Entwicklung von Laborversuchen als Grundlage für die Modellierung des Transportverhaltens von Arsenat, Blei, Cadmium und Kupfer in wassergesättigten Säulen. 147 p., 1993.

**No. 40** **Sieger, R.**
Modellierung des Stofftransports in porösen Medien unter Ankopplung kinetisch gesteuerter Sorptions- und Redoxprozesse sowie thermischer Gleichgewichte. 158 p., 1993.

**No. 41** **Thießen, W.**
Magnetische Eigenschaften von Sedimenten des östlichen Südatlantiks und ihre paläozeanographische Relevanz. 170 p., 1993.

**No. 42** **Spieß, V. und Fahrtteilnehmer**
Report and Preliminary Results of METEOR Cruise M 23/1, Cape Town - Rio de Janeiro, 04.02. - 25.02.1993. 139 p., 1994.

**No. 43** **Bleil, U. und Fahrtteilnehmer**
Report and Preliminary Results of METEOR Cruise M 23/2, Rio de Janeiro - Recife, 27.02. - 19.03.1993. 133 p., 1994.

**No. 44** **Wefer, G. und Fahrtteilnehmer**
Report and Preliminary Results of METEOR Cruise M 23/3, Recife - Las Palmas, 21.03. - 12.04.1993. 71 p., 1994.

**No. 45** **Giese, M. und G. Wefer**
Bericht über den 2. JGOFS-Workshop. 18./19. November 1993 in Bremen. 93 p., 1994.

**No. 46** **Balzer, W. und Fahrtteilnehmer**
Report and Preliminary Results of METEOR Cruise M 22/1, Hamburg - Recife, 22.09. - 21.10.1992. 24 p., 1994.

**No. 47** **Stax, R.**
Zyklische Sedimentation von organischem Kohlenstoff in der Japan See: Anzeiger für Änderungen von Paläozeanographie und Paläoklima im Spätkänozoikum. 150 p., 1994.

**No. 48** **Skowronek, F.**
Frühdiagenetische Stoff-Flüsse gelöster Schwermetalle an der Oberfläche von Sedimenten des Weser Ästuares. 107 p., 1994.

**No. 49** **Dersch-Hansmann, M.**
Zur Klimaentwicklung in Ostasien während der letzten 5 Millionen Jahre: Terrigener Sedimenteintrag in die Japan See (ODP Leg 128). 149 p., 1994.

**No. 50** **Zabel, M.**
Frühdiagenetische Stoff-Flüsse in Oberflächen-Sedimenten des äquatorialen und östlichen Südatlantik. 129 p., 1994.

**No. 51** **Bleil, U. und Fahrtteilnehmer**
Report and Preliminary Results of SONNE Cruise SO 86, Buenos Aires - Cape Town, 22.04. - 31.05.1993. 116 p., 1994.

**No. 52** **Symposium - The South Atlantic: Present and Past Circulation**
Bremen, Germany, 15-19 August 1994. Abstracts. 167 p., 1994.

**No. 53** **Kretzmann, U. B.**
$^{57}$Fe-Mössbauer-Spektroskopie an Sedimenten - Möglichkeiten und Grenzen. 183 p., 1994.

**No. 54** **Bachmann, M.**
Die Karbonatrampe von Organjá im oberen Oberapt und unterem Unteralb (NE-Spanien, Prov. Lerida): Fazies, Zyklo- und Sequenzstratigraphie. 147 p., 1994.

**No. 55** **Kemle-von Mücke, S.**
Oberflächenwasserstruktur und -zirkulation des Südostatlantiks im Spätquartär. 151 p., 1994.

**No. 56** **Petermann, H.**
Magnetotaktische Bakterien und ihre Magnetosome in Oberflächensedimenten des Südatlantiks. 134 p., 1994.

**No. 57** **Mulitza, S.**
Spätquartäre Variationen der oberflächennahen Hydrographie im westlichen äquatorialen Atlantik. 97 p., 1994.

**No. 58** **Segl, M. und Fahrtteilnehmer**
Report and Preliminary Results of METEOR Cruise M 29/1, Buenos Aires - Montevideo, 17.06. - 13.07.1994. 94 p., 1994.

**No. 59** **Bleil, U. und Fahrtteilnehmer**
Report and Preliminary Results of METEOR Cruise M 29/2, Montevideo - Rio de Janeiro, 15.07. - 08.08.1994. 153 p., 1994.

**No. 60** **Henrich, R. und Fahrtteilnehmer**
Report and Preliminary Results of METEOR Cruise M 29/3, Rio de Janeiro - Las Palmas, 11.08. - 05.09.1994. (in prep.)

**No. 61** **Sagemann, J.**
Saisonale Variationen von Porenwasserprofilen, Nährstoff-Flüssen und Reaktionen in intertidalen Sedimenten des Weser-Ästuars. 108 p., 1994.

**No. 62** **Giese, M. und G. Wefer**
Bericht über den 3. JGOFS-Workshop. 5./6. Dezember 1994 in Bremen. 84 p., 1995.

**No. 63** **Mann, U.**
Genese kretazischer Schwarzschiefer in Kolumbien: Globale vs. regionale / lokale Prozesse. 153 p., 1995.

**No. 64** **Willems, H., X. Wan, J. Yin, L. Dongdui, G. Liu, S. Dürr, K.-U. Gräfe**
The Mesozoic development of the N-Indian passive margin and of the Xigaze Forearc Basin in southern Tibet, China. - Excursion Guide to IGCP 362 Working Group Meeting "Integrated Stratigraphy". 113 p., 1995.

**No. 65** **Hünken, U.**
Liefergebiets-Charakterisierung proterozoischer Goldseifen in Ghana anhand von Fluideinschluß-Untersuchungen. 270 p., 1995.

**Nr. 66** **Nyandwi, N.**
The Nature of the Sediment Distribution Patterns in the Spiekeroog Backbarrier Area, the East Frisian Islands. 162 p., 1995.

**No. 67** **Isenbeck-Schröter, M.**
Transportverhalten von Schwermetallkationen und Oxoanionen - Laborversuche in Säulen und ihre Modellierung. 182 p., 1995.

**No. 68** **Hebbeln, D. und Fahrtteilnehmer**
Cruise Report of R/V SONNE Cruise 102, Valparaiso - Valparaiso, 09.05. - 28.06.1995. 126 p., 1995.

**No. 69** **Willems, H., U. Bathmann, U. Bleil, T. v. Dobeneck, K. Herterich, B.B. Jørgensen, E.-M. Nöthig, M. Olesch, J. Pätzold, H.D. Schulz, V. Smetacek, V. Spieß, G. Wefer**
Bericht des Graduierten-Kollegs "Stoff-Flüsse in marinen Geosystemen". Berichtszeitraum Januar 1993 - Dezember 1995. 45 & 468 p., 1995.

**No. 70** **Giese, M. und G. Wefer**
Bericht über den 4. JGOFS-Workshop. 20./21. November 1995 in Bremen. 60 p., 1996.

**No. 71** **Meggers, H.**
Pliozän-quartäre Karbonatsedimentation und Paläozeanographie des Nordatlantiks und des Europäischen Nordmeeres - Hinweise aus planktischen Foraminiferengemeinschaften. 143 p., 1996. (out of press)

**No. 72** **Teske, A.**
Phylogenetische und ökologische Untersuchungen an Bakterien des oxidativen und reduktiven marinen Schwefelkreislaufs mittels ribosomaler RNA. 220 p., 1996.

**No. 73** **Andersen, N.**
Biogeochemische Charakterisierung von Sinkstoffen und Sedimenten aus ostatlantischen Produktions-Systemen mit Hilfe von Biomarkern. 215 p., 1996.

**No. 74** **Treppke, U.**
Saisonalität im Diatomeen- und Silikoflagellatenfluß im östlichen tropischen und subtropischen Atlantik. 200 p., 1996.

**No. 75** **Schüring, J.**
Die Verwendung von Steinkohlebergematerialien im Deponiebau im Hinblick auf die Pyritverwitterung und die Eignung als geochemische Barriere. 110 p., 1996.

**No. 76** **Pätzold, J. und Fahrtteilnehmer**
Report and Preliminary Results of R/V VICTOR HENSEN Cruise JOPS II, Leg 6, Fortaleza - Recife, 10.03. - 26.03.1995 and Leg 8, Vitória - Vitória, 10.04. - 23.04.1995. 87 p., 1996.

**No. 77** **Bleil, U. und Fahrtteilnehmer**
Report and Preliminary Results of METEOR Cruise M 34/1, Cape Town - Walvis Bay, 03.01. - 26.01.1996. 129 p., 1996.

**No. 78** **Schulz, H.D. und Fahrtteilnehmer**
Report and Preliminary Results of METEOR Cruise M 34/2, Walvis Bay - Walvis Bay, 29.01.-18.02.1996. 133 p., 1996

**No. 79** **Wefer, G. und Fahrtteilnehmer**
Report and Preliminary Results of METEOR Cruise M 34/3, Walvis Bay - Recife, 21.02.-17.03.1996. 168 p., 1996.

**No. 80** **Fischer, G. und Fahrtteilnehmer**
Report and Preliminary Results of METEOR Cruise M 34/4, Recife - Bridgetown, 19.03.-05.04.1996. 105 p., 1996.

**No. 81** **Kulbrok, F.**
Biostratigraphie, Fazies und Sequenzstratigraphie einer Karbonatrampe in den Schichten der Oberkreide und des Alttertiärs Nordost-Ägyptens (Eastern Desert, N'Golf von Suez, Sinai). 153 p., 1996.

**No. 82** **Kasten, S.**
Early Diagenetic Metal Enrichments in Marine Sediments as Documents of Nonsteady-State Depositional Conditions. 118 p., 1996.

**No. 83** **Holmes, M.E.**
Reconstruction of Surface Ocean Nitrate Utilization in the Southeast Atlantic Ocean Based on Stable Nitrogen Isotopes. 113 p., 1996.

**No. 84** **Rühlemann, C.**
Akkumulation von Carbonat und organischem Kohlenstoff im tropischen Atlantik: Spätquartäre Produktivitäts-Variationen und ihre Steuerungsmechanismen. 139 p., 1996.

**No. 85** **Ratmeyer, V.**
Reconstruction of Surface Ocean Nitrate Utilization in the Southeast Atlantic Ocean Based on Stable Nitrogen Isotopes. 113 p., 1996.

**No. 86** **Cepek, M.**
Zeitliche und räumliche Variationen von Coccolithophoriden-Gemeinschaften im subtropischen Ost-Atlantik: Untersuchungen an Plankton, Sinkstoffen und Sedimenten. 156 p., 1996.

**No. 87** **Otto, S.**
Die Bedeutung von gelöstem organischen Kohlenstoff (DOC) für den Kohlenstoffffluß im Ozean. 150 p., 1996.

**No. 88** **Hensen, C.**
Frühdiagenetische Prozesse und Quantifizierung benthischer Stoff-Flüsse in Oberflächensedimenten des Südatlantiks. 132 p., 1996.

**No. 89** **Giese, M. und G. Wefer**
Bericht über den 5. JGOFS-Workshop. 27./28. November 1996 in Bremen. 73 p., 1997.

**No. 90** **Wefer, G. und Fahrtteilnehmer**
Report and Preliminary Results of METEOR Cruise M 37/1, Lisbon - Las Palmas, 04.-23.12.1996. 79 p., 1997.

**No. 91** **Isenbeck-Schröter, M., E. Bedbur, M. Kofod, B. König, G. Mattheß**
Occurrence of Pesticide Residues in Water - Assessment of the Current Situation in Selected EU Countries. 65 p., 1997.

**No. 92** **Kühn, M.**
Geochemische Folgereaktionen bei der hydrogeothermalen Energiegewinnung. 129 p., 1997.

**No. 93** **Determann, S. und K. Herterich**
JGOFS-A6 "Daten und Modelle": Sammlung JGOFS relevanter Modelle in Deutschland. 26 p., 1997.

**No. 94** **Fischer, G. und Fahrtteilnehmer**

Report and Preliminary Results of METEOR Cruise M 38/1, Las Palmas - Recife, 25.01. - 01.03.1997. (in prep.)